HAL
open science

Caractérisation des nanomédecines pour la clinique : développement de méthodes évaluant les interactions nanoparticules-protéines plasmatiques pour une application en contrôle qualité

Jean-Baptiste Coty

To cite this version:

Jean-Baptiste Coty. Caractérisation des nanomédecines pour la clinique : développement de méthodes évaluant les interactions nanoparticules-protéines plasmatiques pour une application en contrôle qualité. Biotechnologie. Université Paris Saclay (COmUE), 2017. Français. NNT : 2017SACLS432 . tel-01953458

HAL Id: tel-01953458

https://theses.hal.science/tel-01953458

Submitted on 13 Dec 2018

HAL is a multi-disciplinary open access archive for the deposit and dissemination of scientific research documents, whether they are published or not. The documents may come from teaching and research institutions in France or abroad, or from public or private research centers.

L'archive ouverte pluridisciplinaire **HAL**, est destinée au dépôt et à la diffusion de documents scientifiques de niveau recherche, publiés ou non, émanant des établissements d'enseignement et de recherche français ou étrangers, des laboratoires publics ou privés.

université PARIS-SACLAY

NNT : 2017SACLS432

Thèse de doctorat

université PARIS-SACLAY

ÉCOLE DOCTORALE
Innovation thérapeutique : du fondamental à l'appliqué

UNIVERSITÉ PARIS SUD
Comprendre le monde, construire l'avenir

Caractérisation des nanomédecines pour la clinique : développement de méthodes évaluant les interactions nanoparticules-protéines plasmatiques pour une application en contrôle qualité

-

Nanomedicine characterization for the clinics: development of methods evaluating the interactions nanoparticles-plasmatic proteins for a quality control purpose

Thèse de doctorat de l'Université Paris-Saclay
préparée à l'Université Paris Sud
Institut Galien Paris Sud
Faculté de Pharmacie de Chatenay-Malabry

École doctorale n°569
Innovation thérapeutique : du fondamental à l'appliqué
Spécialité de doctorat: Pharmacotechnie et Physico-chimie Pharmaceutique,

Thèse présentée et soutenue à Chatenay-Malabry, le 12 décembre 2017, par

Jean-Baptiste COTY

Composition du Jury :

Moein Moghimi
Professeur, Newcastle University – Institute of Cellular Medicine — Rapporteur

Jérémie Pourchez
DR, Ecole Nationale Supérieure des Mines de Saint-Etienne – Centre Ingénierie et Santé — Rapporteur

Patrick Couvreur
Professeur, Université Paris-Sud – Institut Galien Paris-Sud — Président

Catherine Passirani-Malleret
Professeur, Université d'Angers – INSERM U1066-CNRS 6021 — Examinateur

Boris Vauzeilles
DR, Institut de Chimie Moléculaire et des Matériaux d'Orsay — Examinateur

Christine Vauthier
DR, Université Paris-Sud – Institut Galien Paris-Sud — Directeur de thèse

« Je ne cherche pas à connaître les réponses,
je cherche à comprendre les questions. »

Confucius

A la mémoire de ma marraine Isabelle, mon parrain Francis, partis trop tôt.

Remerciements

Au-delà des aspects purement scientifiques, ces trois années de thèse resteront marquées par la rencontre de nombreuses personnes, qui ont contribués, chacun à leur façon, à mon aventure de doctorant. Je tiens à les remercier içi.

Je remercie d'abord le Professeur Elias Fattal, pour m'avoir accueilli au sein de l'Institut Galien Paris Sud pour la réalisation de mon doctorat ainsi que les Professeurs Marc Pallardy et Christian Poüs, successivement directeurs de l'école doctorale 569 au cours de ces trois années.

Je tiens à remercier le Professeur Gilles Ponchel, responsable de l'équipe 6 de l'Institut Galien Paris Sud, où j'ai eu la chance d'effectuer cette thèse. Merci pour l'accueil au sein de l'équipe ainsi que pour les discussions sur des sujets divers et variés que nous avons pu avoir lors de mes passages dans la « maison mère » de l'équipe 6.

J'aimerai particulièrement remercier le Dr. Christine Vauthier, pour son accompagnement en tant que directeur de thèse pendant ces trois années. Un grand merci pour le savoir que vous avez pu me transmettre mais aussi pour votre gentillesse, disponibilité et bienveillance qui m'ont permis d'évoluer sereinement au cours de cette thèse. Enfin, merci pour la confiance que vous m'avez accordé depuis le premier jour.

Je remercie les personnes qui ont accepté de composer mon jury de thèse. Merci au Dr. Jérémie Pourchez, rapporteur de la thèse également impliqué depuis le comité de mi-thèse. Many thanks to Pr. Moein Moghimi for accepting to report my PhD work and for coming from England for my defense. Merci aux Professeurs Patrick Couvreur et Catherine Passirani-Malleret, ainsi qu'au Dr. Boris Vauzeilles pour leur implication en tant que jury examinateurs.

Remerciements à BPI France, pour le soutien financier qui a permis la réalisation de ce projet ainsi qu'à tous les membres du consortium NICE : CEA-Leti, DBI Amatsi Nanobiotix et Onxeo. Merci plus particulièrement à Christelle Zandanel, Sophary Seng, Anne-Claude Couffin, Véronique Mourier et Mathieu Germain.

Merci beaucoup au Dr. Fanny Varenne, pour les nombreuses discussions et travaux réalisés ensemble, ainsi que pour les moments partagés de la vie du bureau B309 et de l'équipe 6.

Grand merci au Professeur Claire Smadja pour sa gentillesse et son implication dans le projet d'électrophorèse capillaire. Au Dr. Isabelle Lepotier pour m'avoir également aidé dans ce projet. Merci également au Pr. Myiam Taverna, pour son accueil dans son laboratoire tout au long de mes expériences de CE.

Merci beaucoup à Magali Noiray pour son implication dans les études SPR et la confiance qu'elle a pu me donner au long de ces études.

Merci à Jean-Jacques Vachon pour son aide et sa compréhension lors de l'élaboration de dispositifs plus ou moins exotiques.

Merci au Docteur Anouar Benmalek pour l'aide qu'il a pu m'apporter dans les études statistiques.

Merci aux étudiants qui ont travaillé avec moi et m'ont aidé dans l'avancement des travaux de thèse. Grand merci à Olfa Garsaa pour son sérieux, sa coopération et son implication dans la réalisation des études de CE. Merci à Laurie Ladet et Mélanie Daniel qui ont également pu m'aider dans divers travaux.

Je voudrais ensuite saluer les différentes personnes avec qui j'ai pu échanger et apprendre, au sein de l'Institut Galien et des laboratoires de la Faculté de Pharmacie de Chatenay-Malabry. Merci :

Au Dr. Kawthar Bouchemal, pour sa gentillesse et ses conseils au sein de l'équipe 6.

Au Dr. François-Xavier Legrand pour les discussions quotidiennes et les études que nous avons pu faire ensemble.

Aux Dr. Simona Mura, Thuy Tran-Maignan, Gillian Barratt, Nicolas Huang, Nicolas Tsapis et Vincent Faivre pour leur sympathie et l'aide qu'ils ont pu m'apporter.

A Mesdames Sylvie Zemmour, Dominique Martin, Marie-Claude Amnella, Fathia Hamza et Patricia Livet pour leur aide et leur accompagnement dans toutes les démarches administratives.

A Céline Boursier, pour son aide dans les études protéomiques.

A Delphine Courilleau pour son aide et son accueil au sein de la platforme de l'IPSIT.

Ensuite, je tiens à remercier tous les étudiants avec qui j'ai pu échanger et passer de bons moments dans l'unité au cours de ces trois années.

Tout d'abord, les amis de la tour B, pour les discussions quotidiennes, l'entraide au labo ainsi que nos soirées culinaires : Julien, Marline et Xiao.

Aux membres de l'équipe 6, bien qu'éloignés géographiquement toujours proches pour échanger et s'entraider. Particulièrement à Any, Raul, Herman, Sarah, Henrique. Ainsi qu'aux aux autres personnes de l'équipe que j'ai été heureux de connaitre : Sofiane, Zanou, Fabiola, Pierre-Louis, Sophia, Tiphany, Zeeshan.

Merci à ma deuxième équipe, l'équipe 4, que j'ai beaucoup côtoyé pendant mes études en CE. Merci pour leur aide quotidienne et pour les bons moments qu'on a pu passer ensemble. Merci Corentin, Jeanne, Coralie, Cédric, Nacéra, Duc, Minh et les autres membres de l'équipe que j'ai pu cottoyer dans les labos.

Les amis de la tour D5, en particulier mes amies de la cuvée 2017 : Claire, Elise, Mathilde et Sophie, ainsi que Marion, Dunja, Felix, Alexandre, Amine, Gianpiero, Tanguy et tant d'autres avec qui j'ai pu converser lors d'un Friday beer. Ce fut un plaisir de partager ces 3 années avec vous.

J’adresse également une mention spéciale de remerciements à tous les amis « Do Brazil » que j’ai pu rencontrer pendant mon séjour dans les laboratoires de Chatenay Malabry. A Guilherme Picheth pour sa bonne humeur et les soirées footbalistisques que j’ai pu passer avec lui, à Mariane Lira pour son accueil, sa bienveillance et l’amitié que nous avons lié lors de mon arrivée au laboratoire. A Sarah Palacio, pour les bons moments lors des expériences réalisées ensemble et sa bonne humeur, à Henrique Rodrigues Marcelihno, pour ses « bonnes » blagues. Pensée également aux autres étudiants brésiliens que j’ai pu rencontrer içi : Andre Leandro, Junior Xavier, Luis Guerzoni, Cassiana Mendes, Elquio Eleamen Oliveira.

Merci à mes amis « extra-labo », plus particulièrement Guillaume, Vincent, Hadrien, Yoann avec qui j’ai pu décrocher de la science de temps en temps et qui ont réussi à comprendre la finalité de mes travaux de thèse.

Enfin, merci à ma famille, ma mère, mon père et mon frère pour leur soutien de tous les jours et pour m’avoir permis d’arriver jusqu’içi. Merci à mes cousins, oncles et tantes, grands-parents, pour leurs encouragements et pour qui ça n’a pas toujours été simple de comprendre si j’étais encore étudiant ou si, oui, je travaillais vraiment.

SOMMAIRE

LISTE DES ABREVIATIONS 6

INTRODUCTION GENERALE 9

LA NANOMEDECINE 10
SUCCES ET ECHECS 12
LES POINTS LIMITANTS 12
PROBLEMATIQUE ETUDIEE 15
CONTEXTE ET OBJECTIFS DE LA THESE 16
ORGANISATION GENERALE DU MANUSCRIT 17
BIBLIOGRAPHIE 18
SUMMARY OF THE GENERAL INTRODUCTION 22

PARTIE BIBLIOGRAPHIQUE 25

CHAPITRE I : LES ENJEUX DE LA CARACTERISATION DES NANOMEDECINES DANS LE PROCESSUS DE TRANSLATION CLINIQUE 27

AVANT-PROPOS 27

A THOUGHT ABOUT THE CHARACTERIZATION OF NANOMEDICINES: A FIELD UNDER CONSTRUCTION BETWEEN REGULATORY AND METHODOLOGICAL ASPECTS NEEDED TO ACCELERATE CLINICAL DEVELOPMENTS 29

ABSTRACT 30
I. INTRODUCTION 31
II. RELEVANT PHYSICOCHEMICAL CHARACTERISTICS OF NANOMEDICINES DETECTED BY BIOLOGICAL SYSTEMS WITH IMPLICATION ON THEIR *IN VIVO* FATE 32
II.1. THE MYSTERY OF NMS *IN VIVO* FATE IS DRIVEN BY THEIR INITIAL PROPERTIES 32
II.2. NMS CHARACTERISTICS CONTROLLING THEIR INTERACTIONS WITH BLOOD PROTEINS 33
II.3. NMS CHARACTERISTICS CONTROLLING THEIR INTERACTIONS WITH CELLS 34
II.4. CONCLUDING REMARKS IN THE LIGHT OF EXAMPLES TAKEN IN BIOLOGICAL SYSTEMS FOUND IN MOTHER NATURE 35
III. GENERAL STRATEGIES FOR NANOMEDICINE CHARACTERIZATION AND RECOMMENDATIONS OF HEALTH AUTHORITIES 37
III.1. THE CHARACTERIZATION REVOLUTION BROUGHT BY "NANO"-MEDICINES 37
III.2. TOWARDS NEW GUIDELINES ADAPTED TO NANOMEDICINES 38
III.3. HEALTH AGENCIES POSITIONS 40
IV. RECOMMENDED PHYSICOCHEMICAL PARAMETERS FOR NMS CHARACTERIZATION 42
V. ACUTE CHARACTERIZATION OF NANOMEDICINES FOR A WARRANTED *IN VIVO* REPRODUCIBILITY 49
V.1. CHALLENGES FOR FUTURE CHARACTERIZATION OF NMS 49
V.2. NEO-CHARACTERIZATION OF NMS INTRODUCING NEW METHODS OR NEW PARAMETERS TO INVESTIGATE 50
V.2.1. Assessing the synthetic identity of NMs 50
V.2.2. Assessing the biological identity of NMs 51
VI. CONCLUSION 55

VII. ABBREVIATIONS 56
VIII. BIBLIOGRAPHY 57

PARTIE EXPERIMENTALE 67

AVANT-PROPOS 69

CHAPITRE II : MULTI-IMMUNOELECTROPHORESE 2D MINIATURISEE EN SERIE : IMMUNOANALYSE DE L'ACTIVATION DE LA PROTEINE C3 CAUSEE PAR LES NANOPARTICULES 71

AVANT-PROPOS 71

SERIAL MULTIPLE CROSSED IMMUNOELECTROPHORESIS AT A MICRO SCALE: A STAMP-SIZE 2D IMMUNOANALYSIS OF PROTEIN C3 ACTIVATION CAUSED BY NANOPARTICLES 73

ABSTRACT 74
I. INTRODUCTION 75
II. MATERIALS AND METHODS 76
II.1. MATERIALS 76
II.2. NANOPARTICLE PREPARATION AND CHARACTERIZATION 77
II.2.1. Preparation of the NPs 77
II.2.2. Nanoparticle characterization 77
II.3. PREPARATION OF SAMPLES TO BE ANALYZED BY C-IE AND MULTICROSSED-IE 78
II.4. CROSSED IMMUNOELECTROPHORESIS 78
II.4.1. C-IE classical method 78
II.4.2. New serial multiple crossed IE at a micro scale (MultiCrossed-IE) 78
II.4.2.1. Evaluation of the heat resistance of the antibody 78
II.4.2.2. Preparation of the gel for MultiCrossed-IE 79
II.4.2.3. Electrophoresis runs 79
II.4.3. Scanning and quantification 79
II.5. ROBUSTNESS AND PRECISION OF THE METHOD 81
II.5.1. Sample preparation 81
II.5.2. Exploration of robustness and precision of the method 81
II.5.3. Statistical analysis of the MultiCrossed-IE 82
II.6. CHARACTERIZATION OF C3 ACTIVATION INDUCED BY NANOPARTICLES 83
III. RESULTS 84
III.1. NANOPARTICLE CHARACTERIZATION 84
III.2. HEAT RESISTANCE OF THE ANTIBODY 84
III.3. MULTICROSSED-IE (VERSUS ORGINAL METHOD) 85
III.4. STUDY OF THE ROBUSTNESS AND PRECISION OF THE METHOD 86
III.5. COMPLEMENT C3 ACTIVATION TRIGGERED BY NANOPARTICLES 86
IV. DISCUSSION 89
V. REFERENCES 91
SUPPORTING INFORMATION 93

CHAPITRE III : CONTROLE DE L'ACTIVATION DU COMPLEMENT ET DE LA VOIE EMPRUNTEE VIA L'ARCHITECTURE MOLECULAIRE DES CHAINES DE DEXTRANE GREFFEES A LA SURFACE DE LA NANOPARTICULE 101

AVANT-PROPOS 101

TUNING COMPLEMENT ACTIVATION AND PATHWAY THROUGH CONTROLLED MOLECULAR ARCHITECTURE OF DEXTRAN CHAINS IN NANOPARTICLE CORONA 103

ABSTRACT 104
I. INTRODUCTION 105
II. MATERIALS AND METHODS 108
II.1. MATERIALS 108
II.2. PREPARATION OF NANOPARTICLES BY REDOX RADICAL EMULSION POLYMERIZATION (RREP) 108
II.3. PREPARATION OF NANOPARTICLES BY ANIONIC EMULSION POLYMERIZATION (AEP) 109
II.4. PURIFICATION OF NANOPARTICLES 109
II.5. EVALUATION OF NANOPARTICLE CONCENTRATIONS IN DISPERSIONS 109
II.6. MEASUREMENT OF PARTICLE SIZE AND ZETA POTENTIAL 109
II.7. EVALUATION OF COMPLEMENT ACTIVATION BY TWO-DIMENSIONAL (2-D) IMMUNOELECTROPHORESIS OF C3110
III. RESULTS 112
III.1. NANOPARTICLES CHARACTERISTICS 112
III.2. *IN VITRO* COMPLEMENT ACTIVATION 112
IV. DISCUSSION 120
V. CONCLUSION 126
VI. BIBLIOGRAPHY 127
SUPPLEMENTARY MATERIAL 133

CHAPITRE IV : VERS UNE ANALYSE QUALITE DE L'ACTIVATION DU COMPLEMENT PAR LES NANOMEDECINES : DEVELOPPEMENT D'UNE METHODE SPR 137

AVANT PROPOS 137

ASSESSMENT OF COMPLEMENT ACTIVATION BY NANOPARTICLES AS A QUALITY REQUIREMENT: DEVELOPMENT OF A SPR BASED METHOD AND COMPARISON WITH CURRENT HIGH THROUGHPUT METHODS 139

ABSTRACT 140
I. INTRODUCTION 141
II. MATERIAL AND METHODS 141
II.1. MATERIALS 143
II.2. METHODS 143
II.2.1. NPs synthesis and characterization 144
II.2.2. Sample preparation 144
II.2.3. Surface Plasmon Resonance (SPR) 145
II.2.3.1. Antibody immobilization 145
II.2.3.2. Specificity assays and control serums 145
II.2.3.3. NP-serum studies 145

II.2.4. Multi-crossed 2D Immunoelectrophoresis (µC-IE) 145
II.2.5. ELISA 146
III. RESULTS 146
III.1. SETUP OF A REGENERABLE SPR CHIP FOR THE DIRECT ASSESSMENT OF COMPLEMENT ACTIVATION BY NANOPARTICLES 146
III.1.1. Antibody immobilization 146
III.1.2. Specificity assays and control serums 146
III.1.3. Chip longevity 148
III.2. SPR, µC-IE AND ELISA COMPARISON OF THE ASSESSMENT OF COMPLEMENT ACTIVATION PRODUCED BY NPS 149
III.3. INVESTIGATION OF POSSIBLE BIAS INVOLVED IN COMPLEMENT ACTIVATION EVALUATION METHODS 150
IV. DISCUSSION 152
V. CONCLUSION 156
VI. BIBLIOGRAPHY 157
SUPPLEMENTARY MATERIAL 160

CHAPITRE V : CARACTERISATION FINE DE LA SURFACE DES NANOMEDECINES AVEC DES SONDES MOLECULAIRES PAR ELECTROPHORESE CAPILLAIRE : VERS UNE EVALUATION DE LA COUVERTURE DE SURFACE 165

AVANT-PROPOS 165

SHARP CHARACTERIZATION OF NANOMEDICINES' SURFACE WITH MOLECULAR PROBES BY CAPILLARY ELECTROPHORESIS: TOWARDS UNDERSTANDING AND EVALUATION OF SURFACE COVERAGE 167

ABSTRACT 168
I. INTRODUCTION 169
II. MATERIALS AND METHODS 171
II.1. MATERIALS 171
II.2. METHODS 172
II.2.1. NPs synthesis and characterization 172
II.2.2. Sample preparation 172
II.2.3. Sample analysis 173
II.2.3.1. Capillary zone electrophoresis analysis 173
II.2.3.2. Gel immunoprecipitation 175
II.2.4. Data treatment and method precision 175
III. RESULTS 176
III.1. DEVELOPMENT OF THE METHOD 176
III.1.1. Methods' performance 176
III.1.2. Optimal NP/protein ratio seeking 178
III.2. APPLICATION OF THE METHOD TO EVALUATE SURFACE COVERAGE OF NMS THROUGH THE SHIELD-EFFECT TOWARDS PROTEIN ADSORPTION 180
IV. DISCUSSION 186
V. CONCLUSION 189
VI. BIBLIOGRAPHY 190

SUPPLEMENTARY MATERIAL **194**

DISCUSSION GENERALE **199**

INTERACTIONS DES NMS AVEC LE SYSTEME DU COMPLEMENT 202
LA PREPARATION DE L'ECHANTILLON DANS L'INTERACTION NM-PROTEINE 207
CARACTERISATION DE LA SURFACE REACTIVE DES NANOMEDECINES 209
DEMARCHE DES METHODES DEVELOPPEES 210
VISION PERSONNELLE ET PERSPECTIVES 212
RÉFÉRENCES BIBLIOGRAPHIQUES 215
SUMMARY OF THE GENERAL DISCUSSION **219**

CONCLUSION GENERALE **223**

ANNEXES METHODOLOGIQUES **227**

ANNEXE 1 : PRINCIPE DE L'IMMUNOELECTROPHORESE BIDIMENSIONNELLE **229**
ANNEXE 2 : PRINCIPE DE L'ELECTROPHORESE CAPILLAIRE **230**
ANNEXE 3 : PRINCIPE DE LA RESONANCE PLASMONIQUE DE SURFACE **232**
ANNEXE 4 : INTRODUCTION AU SYSTEME DU COMPLEMENT **233**

ANNEXE BIBLIOGRAPHIQUE **235**

CURRICULUM VITAE **255**
LISTE DES PUBLICATIONS **257**
LISTE DES COMMUNICATIONS **258**

Liste des abréviations

2D-IE: Two-dimensional immunoelectrophoresis
AFM: Atomic force microscopy
ANOVA: Analysis of variance
API: Active pharmaceutical ingredient
ASTM: American Society for Testing and Materials
BSAI: Biological Surface Adsorption Index
C-IE: Crossed immunoelectrophoresis
C_3A_{50}: Protein C3 activation at 50%
CARPA: Complement Activation Related Pseudo Allergy
CE: Capillary electrophoresis
CRO: Contract research organization
CS: Complement system
CVF: Cobra venom factor
CZE: Capillary zone electrophoresis
DCS: Differential centrifugal sedimentation
D_H: Hydrodynamic diameter
DLS: Dynamic light scattering
ELISA: Enzyme-linked immunosorbent assay
ELS: Electrophoresis light scattering
EM: Electron microscopy
EMA: European medicine agency
EOF: Electroosmotic flow
EP: Emulsion polymerization
EPR: Enhanced Permeation and Retention
EU-NCL: European Nanomedicine Characterization Laboratory
FDA: Food and drug administration
FFF: Field flow fractionation
GC-MS: Gas chromatography - mass spectrometry
GUM: Guide to the expression of uncertainty in measurement
HAGG: Heat-activated gamma globulin
IBCA: Isobutylcyanoacrylate
ICH: International Conference on Harmonisation of Technical Requirements for Registration of Pharmaceuticals for Human Use
ID: Immunodiffusion
IE: Immunoelectrophoresis
ISO: International Organization for Standardization
LC-MS: Liquid chromatography - mass spectrometry
MALS: Multi-angle light scattering
M_C: Mass concentration
MultiCrossed-IE: Serial multiple crossed immunoelectrophoresis at a micro scale
N. Meningitidis: *Neisseria Meningitidis*
NaMe: Nafamostat mesylate
NC: Nanocarrier
NCL: Nanotechnology Characterization Laboratory
NM: Nanomedicine
NMR: Nuclear magnetic resonance

NP: Nanoparticle
OECD: Organization for Economic Co-operation and Development
PD: Pharmacodynamics
PEG: Polyethylene glycol
PEO: Polyethylene oxide
pI: Isoelectric point
PIBCA: poly(isobutylcyanoacrylate)
PK: Pharmacokinetics
PTA: Particle tracking analysis
RC: Repellent capacity
RSD: Relative standard deviation
RU: Response unit
SAXS: Small angle X-ray scattering
S_C: Surface concentration
SEC: Size exclusion chromatography
SEM: Scanning electron microscopy
SIMS: Secondary ion mass spectrometry
SPE: Solid phase extraction
SPR: Surface plasmon resonance
SUSTU: SUrface proteo- mics, Safety, Targeting, Uptake
TEM: Transmission electron microscopy
TRPS: Tunable resistive pulse sensing
VBS: Veronal buffer saline
WAXS: Wide angle X-ray scattering
µC-IE: multi-crossed 2D immunoelectrophoresis

Introduction générale

(see english summary p.22)

La Nanomédecine

L'avancée des connaissances scientifiques alliée aux progrès techniques permet de développer de nouvelles technologies pour faire face à de nombreux challenges jusqu'içi hors d'atteinte. L'émergence des nanotechnologies en est un excellent exemple, dont les applications sont profitables dans de nombreux domaines tels que l'énergie, les matériaux, le digital, l'alimentation, l'industrie cosmétique ainsi que dans le domaine médical [1-4]. Nous assistons à un développement exponentiel de ces technologies pour la médecine, faisant même apparaître le terme « nanomédecine » (NM) au début des années 2000 [5,6]. On désigne par nanomédecine le domaine des entités supramoléculaires d'ordre nanométrique fabriquées à des fins thérapeutiques, diagnostiques ou combinant les deux (théranostique). Généralement, ce terme est limité pour des nanomatériaux présentant au moins une dimension comprise entre 1 et 100 nm [7-9]. Cependant, la limite des propriétés nanométriques n'étant pas figée à 100 nm [7,8], nous étendrons l'utilisation du préfixe « nano » pour désigner des objets compris entre 1 et plusieurs centaines de nm içi (jusqu'à 300 nm). Ces entités peuvent être de nature métallique (or, fer, zinc), inorganique (silice), lipidique ou encore polymère, et présenter une très grande diversité en termes de forme, greffage de polymère en surface, ligands [6,10] (cf. Fig. 1).

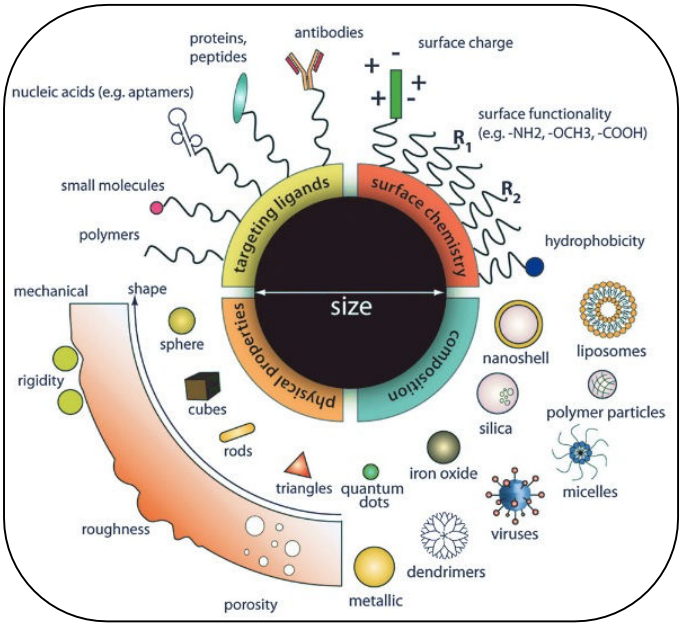

Figure 1 : Illustration de la diversité des nanosystèmes actuels, de par leur nature chimique, forme, propriétés physico-chimiques et fonctionnalisation (reproduit depuis [10] avec l'autorisation de The Royal Society of Chemistry).

Apparus bien avant la création du domaine des nanomédecines avec le concept de « magic bullet » de Paul Elrich au début du 20ème siècle, les nanomatériaux à visée médicinale ont déjà fait l'objet de nombreuses recherches, se développant années après années [11]. Alliant chimie, physique, physico-chimie, biologie, sciences pharmaceutiques et médicales, cette discipline requiert une étroite collaboration entre scientifiques de ces différents domaines. L'utilité finale des nanomatériaux pour la médecine est multiple. Du point de vue thérapeutique, le nanomédicament comporte plusieurs bénéfices potentiels [12]:

- Meilleur ciblage des tissus pour la libération du principe actif : efficacité du traitement accrue pour une dose injectée réduite, diminution de la toxicité et des effets indésirables
- Protection du principe actif d'une dégradation précoce dans le milieu biologique
- Dans certains cas, permettre une libération prolongée du principe actif pour une action continue dans le temps

Physiquement, les nanomédecines sont composées d'une enveloppe pouvant contenir une ou plusieurs molécules d'intérêt biologique. Cette enveloppe a été modifiée au fil du temps en lui apportant des caractéristiques de furtivité vis à vis du système immunitaire, puis en y greffant des agents de ciblage [13]. On peut aujourd'hui recenser trois générations de nanomédecines [14,15] (cf. Fig. 2) :

- La 1ère génération : constituée de nanoparticules de formulation relativement simple contenant le principe actif. En général, ces systèmes sont rapidement reconnus par le système immunitaire et pris en charge par ce dernier. Ils peuvent cibler de manière passive un agent actif vers des cellules ou organes du système immunitaire.
- La 2ème génération : constituée d'un cœur nanoparticulaire greffé d'une couronne de polymère hydrophile, ayant pour but de limiter l'adsorption de protéines, diminuer l'opsonisation et ainsi prolonger le temps de circulation dans l'organisme. Dans le cas du cancer, cela favorise l'accumulation dans les tumeurs via l'effet EPR (Enhanced Permeability and Retention) qui permet aux NMs de traverser l'endothélium et de s'accumuler au niveau des cellules tumorales où la vascularisation est hétérogène et perméable [13,16]. C'est le ciblage passif.
- La 3ème génération : elle consiste en des NMs de 2ème génération où sont attachés des agents de ciblages (protéines, peptides, aptamères, RNA) ayant pour fonction de cibler

des tissus et cellules spécifiques et ainsi améliorer encore la spécificité et l'efficacité du traitement. On parle de ciblage actif.

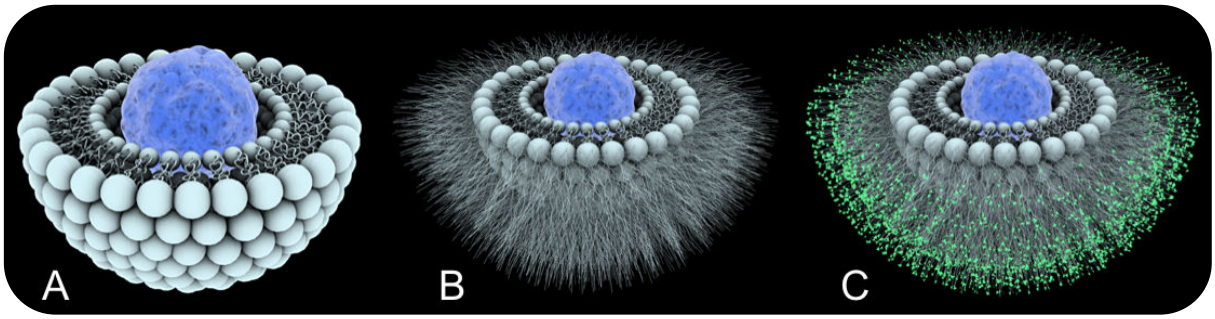

Figure 2 : représentation des 3 générations de nanomédecines dans le cas d'un liposome. A : Liposome de 1ère génération ; B : liposome de deuxième génération avec une couronne de polymère hydrophile ; C : liposome de 3ème génération avec des ligand de ciblage attachés au polymère hydrophile en surface (© François CAILLAUD/SAGASCIENCE/CNRS Photothèque).

Succès et échecs

Au niveau clinique, les premières nanoparticules à visée thérapeutique ont atteint le marché au milieu des années 1990s (Liposomes – Ambisome®, Doxil®). S'en est suivit un essor de la recherche et de l'investissement des entreprises biotechnologiques et des grands laboratoires pharmaceutiques. Aujourd'hui, on dénombre de nombreuses nanomédecines en essais cliniques et plusieurs sur le marché, ce qui témoigne du fort potentiel et des avancées réalisées [17-22]. Cependant, une fort taux d'attrition des nanomédecines en phase clinique reste à déplorer [23-25].

Les points limitants

Ce sont les caractéristiques inhérentes aux nanomatériaux qui rendent la translation entre recherche en laboratoire et clinique particulièrement difficile. La complexité apportée par ces nanovecteurs de par leur composition, leur ratio surface/volume important ainsi que leur taille les rendant actifs à l'échelle biologique rend la compréhension de leur devenir *in vivo* très compliquée [26,27]. A ce jour, il est encore impossible d'élaborer une nanomédecine de façon rationnelle en maitrisant tous ces aspects. La difficile transposition des effets rencontrés en laboratoire de recherche jusqu'en clinique, aussi appelée « vallée de la mort », rend le développement d'une NM très risqué pour les entreprises pharmaceutiques [28,29].

Une revue publiée par Chan et al. en 2016 faisait remarquer que seulement 0.7% de la dose de NM injectée atteignait les tissus de la tumeur ciblée, sur une moyenne de plus de 200

travaux publiés ces 10 dernières années [30]. Ce pourcentage d'efficacité de ciblage apparaît faible mais il ne prend pas en compte les nombreux autres avantages apportés par la forme nanomédecine au niveau du tissu cible. Notamment, de nombreuses molécules qui pénètrent mal dans les cellules sous forme libre atteignent plus efficacement les compartiments intracellulaires lorsqu'elles sont encapsulées dans ces nanovecteurs. Le principe actif reste également protégé d'une dégradation extracellulaire tant qu'il reste associé à la nanomédecine. Cette étude motive aussi la poursuite des efforts destinés à comprendre les mécanismes qui gouvernent le devenir de la NP *in vivo*. La difficulté réside notamment dans le fait que les propriétés initiales de la nanomédecine (taille, charge, chimie de surface), aussi appelée identité synthétique, sont totalement bouleversées une fois la NM dans un milieu biologique après administration. Elle acquiert alors une identité biologique (cf. Fig. 3) [31].

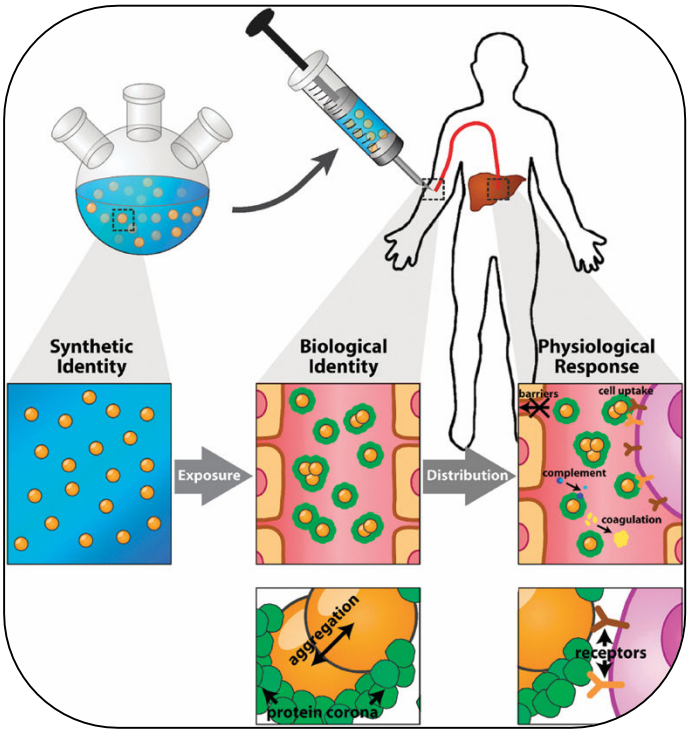

Figure 3 : Illustration des notions d'identités synthétiques et biologique acquise après administration (reproduit depuis [31] avec l'autorisation de The Royal Society of Chemistry).

Dans le cas de l'administration intraveineuse, cette identité biologique est conférée en grande partie par l'adsorption de protéines sériques à la surface de la NM, aussi appelée « protéine corona » [32,33]. Cette dernière va alors modifier la taille, la charge apparente, les propriétés chimiques de surface et les interactions de la NM avec les éléments biologiques, pour impacter finalement sa biodistribution [34-36]. La prochaine étape dans le développement de la nanomédecine consiste en la compréhension de la corrélation entre identité synthétique et

biologique [37]. L'idéal est de déterminer quels sont les paramètres initiaux de la NM qui influencent sa future identité biologique et donc son devenir physiologique. Des modèles de prédictions tendent à être mis au point afin de progresser dans ce sens et pouvoir prédire le devenir d'une nanomédecine à partir de ses propriétés intrinsèques (cf. Fig. 4) [38-41].

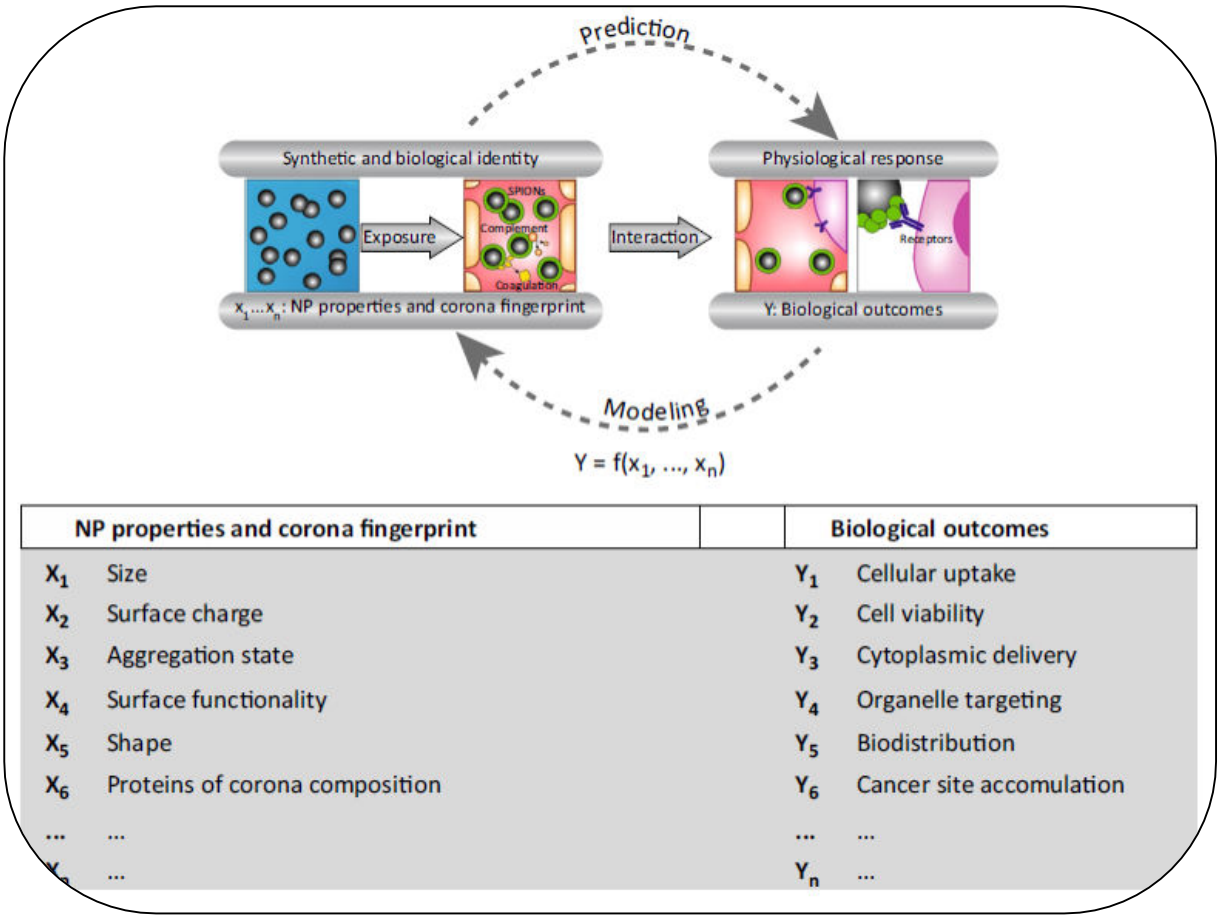

Figure 4 : Modèle de prédiction de la réponse physiologique à partir de l'identité synthétique d'une NM (reproduit depuis [38] avec la permission d'Elsevier).

Ces interactions ont également un impact sur la possible toxicité associée à l'administration de nanomédecines. Les composants de la réponse immunitaire innée présents dans le compartiment sanguin sous forme de protéines (système du complément) peuvent être source de réactions d'hypersensibilité menant à des conséquences plus ou moins graves [42]. Les méthodes de caractérisation actuelles ne permettent pas d'identifier assez finement les caractéristiques critiques qui jouent un rôle déterminant dans le devenir de NMs [38]. Il est donc également impossible d'identifier les paramètres pertinents qu'il serait nécessaire de vérifier pour le contrôle de la conformité d'un lot de NMs quant à la reproductibilité de son comportement *in vivo* et à sa toxicité.

Problématique étudiée

La caractérisation des NMs apparaît comme un des leviers qui permettrait de mieux rationaliser le design des NMs dans un premier temps et de réduire l'attrition de ces systèmes en phase de développement clinique, en garantissant une meilleure reproductibilité de leur comportement *in vivo* [43,44].

➔ **Vers une meilleure compréhension des nanomédecines**. Au vu de l'importance des interactions entre protéines et NMs, il apparaît très important de pouvoir comprendre et contrôler ces interactions se produisant après administration. En phase de recherche, l'étude directe de la protéine corona est utilisée pour comprendre le devenir de la NM *in vivo* et trouver une possible corrélation [38,45]. Il a été montré que la protéine corona avait des effets sur la furtivité de la NM [46,47], sa biodistribution ainsi que sa capture cellulaire [45,48,49]. Cependant, les méthodes d'étude de la protéine corona utilisées actuellement souffrent de nombreux désavantages principalement de par leur complexité ainsi que les nombreux biais pouvant être introduits lors de l'incubation (type de plasma, durée, conditions de flux, température) [33,50-53] et les étapes de traitement de l'échantillon (centrifugation, désorption, lavages) précédant l'analyse [38,51,54].

D'autres techniques telles que l'électrophorèse capillaire (EC), la résonance plasmonique de surface (SPR) ou encore la titration de calorimétrique isotherme (ITC) permettent de caractériser la surface des nanoparticules de manière plus systématique mais moins directes sont utilisées [55]. Ce type de caractérisation semble être plus facilement applicable dans un contexte de contrôle qualité en clinique.

➔ **Vers une meilleure maitrise des paramètres et du contrôle qualité des NMs.** Après les études précliniques et animales, de plus en plus de NMs sont testées en clinique. Cependant, les méthodes de caractérisation permettant de certifier une interaction reproductible entre NMs et éléments biologiques ne sont pas adaptées à une utilisation en contexte clinique [43]. Ces méthodes sont souvent fastidieuses, complexes et coûteuses. L'échec des études de phase clinique peut dans certains cas être dû à un mauvais contrôle des phénomènes se produisant autour de la NM *in vivo*, menant à des résultats inconsistants. Des méthodes permettant de contrôler une interaction reproductible entre des éléments biologiques et la NM sont indispensables pour améliorer le contrôle qualité de ces systèmes complexes. Des

méthodes de caractérisation physicochimique plus fines sont aussi nécessaires afin de garantir une reproductibilité face à la finesse des processus biologiques.

Contexte et Objectifs de la thèse

Cette thèse a été réalisée dans le cadre d'un consortium financé par BPI France (Projet NICE: Nano Innovation for CancEr) [56] réunissant deux acteurs industriels développant actuellement des nanomédecines en phase clinique (Onxeo - Livatag® Phase III; Nanobiotix - NBTXR3 Phase II/III) [57,58], deux partenaires académiques (CNRS et CEA-LETI – Lipidots, LipIMage Phase préclinique) [59,60] ainsi que le groupe Amatsi, spécialisé en développement pharmaceutique [61]. Le CNRS, représenté par l'Institut Galien Paris Sud a pour mission de développer des méthodes permettant une meilleure caractérisation des NMs, notamment avec les milieux biologiques. La première partie de cette thèse a été de comprendre les besoins de ces compagnies en réalisant une étude des différentes méthodes utilisées aujourd'hui et leur applicabilité en contexte clinique. Cela nous a permis d'identifier les problématiques et points limitants de ces méthodes pour une utilisation en clinique. L'objectif principal des travaux de cette thèse a été de proposer et développer des méthodes utilisables en routine pour une caractérisation des lots cliniques de nanomédecines. Ces méthodes doivent donc être accessibles, peu coûteuses, facilement utilisables, applicables à un grand nombre d'échantillons, automatisables et limiter les étapes de préparation d'échantillon. Les méthodes développées ont été dirigées vers l'évaluation des interactions de NMs avec les protéines plasmatiques et avec les protéines du système du complément.

Les méthodes développées au cours de ce travail pour une analyse en routine des caractéristiques des NMs peuvent être utilisées à des fins plus fondamentales qui ont permis, par exemple, d'étudier des phénomènes en vue d'améliorer la compréhension du comportement des systèmes nanoparticulaires en présence d'entités biologiques.

Organisation générale du manuscrit

Le présent manuscrit de thèse comprend une partie bibliographique sur les enjeux actuels posés par la caractérisation des nanomédecines destinées à un usage clinique. Elle ouvre la discussion sur les méthodes actuellement appliquées et à développer.

La partie expérimentale présentera ensuite les différentes méthodes développées au cours de ces travaux de thèse pour une caractérisation en routine des nanomédecines en phase clinique et leurs applications. Elle sera divisée en 4 chapitres présentant respectivement :

- le développement d'une méthode haut débit d'immunoélectrophorèse sur gel en deux dimensions pour mesurer l'activation du système du complément générée par des nanoparticules.

- l'application de cette méthode d'immunoélectrophorèse à haut débit pour l'investigation de la voie d'activation privilégiée par les nanoparticules.

- le développement d'une méthode utilisant la résonnance plasmonique de surface pour étudier l'activation du système du complément de façon automatisée.

- le développement d'une méthode d'électrophorèse capillaire permettant de doser des protéines utilisées comme sondes moléculaires à la surface de nanoparticules. Les propriétés de couverture de surface des nanoparticules sont ainsi évaluées.

Une discussion générale reprendra les différents aspects abordés sur l'ensemble du travail avant de conclure et tirer les perspectives sur lesquelles ouvrent ces travaux.

Bibliographie

1) Heiligtag, F. J. & Niederberger, M. The fascinating world of nanoparticle research. *Materials Today* **16,** 262–271 (2013).
2) Abhilash, M. Potential applications of nanoparticles, *International Journal of Pharma and Bio Sciences* **1**, (2010).
3) United States National Nanotechnology Initiative: Benefits and applications of nanotechnology. https://www.nano.gov/you/nanotechnology-benefits . *Consulted on August 2017*
4) Heath, J. R. Nanotechnologies for biomedical science and translational medicine. *Proceedings of the National Academy of Sciences* **112,** 14436–14443 (2015).
5) Krukemeyer, M.G., Krenn, V., Huebner, F., Wagner, W., & Resch, R. History and Possible Uses of Nanomedicine Based on Nanoparticles and Nanotechnological Progress. *Journal of Nanomedicine & Nanotechnology* **06,** (2015).
6) Ventola, C. L. The nanomedicine revolution: part 1: emerging concepts. *Pharmacy and Therapeutics* **37,** 512 (2012).
7) Potocnik, J. COMMISSION RECOMMENDATION of 18 October 2011 on the definition of nanomaterial (Text with EEA relevance) (2011/696/EU). *Official Journal of the European Union* L 275/38 http://eur-lex.europa.eu/LexUriServ/LexUriServ.do?uri=OJ:L:2011:275:0038:0040:EN:PDF (2011). *Consulted on August 2017*
8) Pérez de la Ossa D.H. Quality aspects of Nano-based medicines. *at SME Workshop: Focus on quality for medicines containing chemical entities. http://www.ema.europa.eu/docs/en_GB/document_library/Presentation/2014/04/WC500165444.pdf* (2014). *Consulted on August 2017*
9) Guidance for Industry Considering Whether an FDA-Regulated Product Involves the Application of Nanotechnology.https://www.fda.gov/regulatoryinformation/guidances/ucm257698.htm (2014). *Consulted on August 2017*
10) Chou, L. Y. T., Ming, K. & Chan, W. C. W. Strategies for the intracellular delivery of nanoparticles. *Chem. Soc. Rev.* **40,** 233–245 (2011).
11) Strebhardt, K. & Ullrich, A. Paul Ehrlich's magic bullet concept: 100 years of progress. *Nature Reviews Cancer* **8,** 473–480 (2008).
12) Wang, Y.-F., Liu, L., Xue, X., & Liang, X.-J. Nanoparticle-based drug delivery systems: What can they really do *in vivo*? *F1000Research* **6**, 681 (2017).
13) Huynh, N. T., Roger, E., Lautram, N., Benoît, J.-P. & Passirani, C. The rise and rise of stealth nanocarriers for cancer therapy: passive versus active targeting. *Nanomedicine* **5,** 1415–1433 (2010).
14) Couvreur, P. & Vauthier, C. Nanotechnology: Intelligent Design to Treat Complex Disease. *Pharmaceutical Research* **23,** 1417–1450 (2006).
15) Couvreur, P., Gref, R., Andrieux, K. & Malvy, C. Nanotechnologies for drug delivery: Application to cancer and autoimmune diseases. *Progress in Solid State Chemistry* **34,** 231–235 (2006).
16) Greish, K. in *Cancer Nanotechnology: Methods and Protocols* (eds. Grobmyer, S. R. & Moudgil, B. M.) 25–37 (Humana Press, 2010).
17) Anselmo, A. C. & Mitragotri, S. Nanoparticles in the clinic: Nanoparticles in the Clinic. *Bioengineering & Translational Medicine* **1,** 10–29 (2016).
18) Sainz, V., Conniot, J., Matos, A. I., Peres, C., Zupanŏiŏ, E., Moura, L., Silva, L. C., Florindo, H. F. & Gaspar, R. S. Regulatory aspects on nanomedicines. *Biochemical and Biophysical Research Communications* **468,** 504–510 (2015).
19) Tinkle, S., McNeil, S. E., Mühlebach, S., Bawa, R., Borchard, G., Barenholz, Y. C., Tamarkin, L. & Desai, N. Nanomedicines: addressing the scientific and regulatory gap: Nanomedicines. *Annals of the New York Academy of Sciences* **1313,** 35–56 (2014).
20) Weissig, V., Pettinger, T. & Murdock, N. Nanopharmaceuticals (part 1): products on the market. *International Journal of Nanomedicine* 4357 (2014).

21) Ragelle, H., Danhier, F., Préat, V., Langer, R. & Anderson, D. G. Nanoparticle-based drug delivery systems: a commercial and regulatory outlook as the field matures. *Expert Opinion on Drug Delivery* **14,** 851–864 (2017).
22) Attia, D.A. Nanocarriers Third Generation as Targeted Delivery Systems for Cancer Therapy. https://www.researchgate.net/publication/280934727_Review_article_of_Nanocarriers_Third_Generation_as_Targeted_Delivery_Systems_for_Cancer_Therapy (2015). *Consulted on August 2017*
23) Hare, J. I., Lammers, T., Ashford, M. B., Puri, S., Storm, G. & Barry, S. T. Challenges and strategies in anti-cancer nanomedicine development: An industry perspective. *Advanced Drug Delivery Reviews* **108,** 25–38 (2017).
24) Ashford, M., Cornier, J., Owen, A., Kwade, A. & Van de Voorde, M. in *Pharmaceutical Nanotechnology: Innovation and Production* 697–734 (Wiley-VCH Verlag GmbH & Co. KGaA, 2017).
25) Venditto, V. J. & Szoka, F. C. Cancer nanomedicines: So many papers and so few drugs! *Advanced Drug Delivery Reviews* **65,** 80–88 (2013).
26) Perkin, E. & Gubala, V. Nanomaterials–On the Brink of Revolution? Or the Endless Pursuit of Something Unattainable? *Chemistry International* **39,** 10–13 (2017).
27) Halappanavar, S., Vogel, U., Wallin, H. & Yauk, C. L. Promise and peril in nanomedicine: the challenges and needs for integrated systems biology approaches to define health risk: Systems biology for nanomedicine and nanotoxicology. *Wiley Interdisciplinary Reviews: Nanomedicine and Nanobiotechnology* e1465 (2017).
28) Landesman-Milo, D. & Peer, D. Transforming Nanomedicines From Lab Scale Production to Novel Clinical Modality. *Bioconjugate Chemistry* **27,** 855–862 (2016).
29) Ledford, H. Bankruptcy of nanomedicine firm worries drug developers. *Nature* **533,** 304–305 (2016).
30) Wilhelm, S., Tavares, A. J., Dai, Q., Ohta, S., Audet, J., Dvorak, H. F. & Chan, W. C. W. Analysis of nanoparticle delivery to tumours. *Nature Reviews Materials* **1,** 16014 (2016).
31) Walkey, C. D. & Chan, W. C. W. Understanding and controlling the interaction of nanomaterials with proteins in a physiological environment. *Chem. Soc. Rev.* **41,** 2780–2799 (2012).
32) Hadjidemetriou, M. & Kostarelos, K. Nanomedicine: Evolution of the nanoparticle corona. *Nature Nanotechnology* **12**, 288–290 (2017).
33) Rahman, M., Laurent, S., Tawil, N., Yahia, L. & Mahmoudi, M. in *Protein-Nanoparticle Interactions* **15,** 21–44 (Springer Berlin Heidelberg, 2013).
34) Chen, R. & Riviere, J. E. Biological and environmental surface interactions of nanomaterials: characterization, modeling, and prediction: Biological and environmental surface interactions of nanomaterials. *Wiley Interdisciplinary Reviews: Nanomedicine and Nanobiotechnology* **9,** e1440 (2017).
35) Aggarwal, P., Hall, J. B., McLeland, C. B., Dobrovolskaia, M. A. & McNeil, S. E. Nanoparticle interaction with plasma proteins as it relates to particle biodistribution, biocompatibility and therapeutic efficacy. *Advanced Drug Delivery Reviews* **61,** 428–437 (2009).
36) Monopoli, M. P., Aberg, C., Salvati, A. & Dawson, K. A. Biomolecular coronas provide the biological identity of nanosized materials. *Nat Nano* **7,** 779–786 (2012).
37) Fadeel, B., Feliu, N., Vogt, C., Abdelmonem, A. M. & Parak, W. J. Bridge over troubled waters: understanding the synthetic and biological identities of engineered nanomaterials: Bridging nanotoxicology and nanomedicine. *Wiley Interdisciplinary Reviews: Nanomedicine and Nanobiotechnology* **5,** 111–129 (2013).
38) Caracciolo, G., Farokhzad, O. C. & Mahmoudi, M. Biological Identity of Nanoparticles In Vivo: Clinical Implications of the Protein Corona. *Trends in Biotechnology* **35,** 257–264 (2017).
39) Lynch, I., Afantitis, A., Leonis, G., Melagraki, G. & Valsami-Jones, E. in *Advances in QSAR Modeling: Applications in Pharmaceutical, Chemical, Food, Agricultural and Environmental Sciences* (ed. Roy, K.) 385–424 (Springer International Publishing, 2017).

40) Walkey, C. D., Olsen, J. B., Song, F., Liu, R., Guo, H., Olsen, D. W. H., Cohen, Y., Emili, A. & Chan, W. C. W. Protein Corona Fingerprinting Predicts the Cellular Interaction of Gold and Silver Nanoparticles. *ACS Nano* **8,** 2439–2455 (2014).
41) Szebeni, J. Complement activation-related pseudoallergy: an innate response to nanomedicines acting as pseudo-viruses. *European Journal of Nanomedicine* **7,** (2015).
42) Winkler, D. A., Mombelli, E., Pietroiusti, A., Tran, L., Worth, A., Fadeel, B. & McCall, M. J. Applying quantitative structure–activity relationship approaches to nanotoxicology: Current status and future potential. *Toxicology* **313,** 15–23 (2013).
43) Salvador Morales, C., Khorasani, A. A. & Weaver, J. Closing the gap: accelerating the translational process in nanomedicine by proposing standardized characterization techniques. *International Journal of Nanomedicine* 5729 (2014).
44) Wei, A., Mehtala, J. G. & Patri, A. K. Challenges and opportunities in the advancement of nanomedicines. *Journal of Controlled Release* **164,** 236–246 (2012).
45) Miceli, E., Kar, M. & Calderon, M. Interactions of organic nanoparticles with proteins in physiological conditions. *J. Mater. Chem. B* **5,** 4393–4405 (2017).
46) Schöttler, S., Becker, G., Winzen, S., Steinbach, T., Mohr, K., Landfester, K., Mailänder, V. & Wurm, F. R. Protein adsorption is required for stealth effect of poly(ethylene glycol)- and poly(phosphoester)-coated nanocarriers. *Nature Nanotechnology* **11,** 372–377 (2016).
47) Aoyama, M., Hata, K., Higashisaka, K., Nagano, K., Yoshioka, Y. & Tsutsumi, Y. Clusterin in the protein corona plays a key role in the stealth effect of nanoparticles against phagocytes. *Biochemical and Biophysical Research Communications* **480,** 690–695 (2016).
48) Beck, M., Mandal, T., Buske, C. & Lindén, M. Serum protein adsorption enhances active leukemia stem cell targeting of mesoporous silica nanoparticles. *ACS Applied Materials & Interfaces* (2017).
49) Brun, E. & Sicard–Roselli, C. Could nanoparticle corona characterization help for biological consequence prediction? *Cancer nanotechnology* **5,** 7 (2014).
50) Dai, Q., Guo, J., Yan, Y., Ang, C.-S., Bertleff-Zieschang, N. & Caruso, F. Cell-Conditioned Protein Coronas on Engineered Particles Influence Immune Responses. *Biomacromolecules* **18,** 431–439 (2017).
51) Dell'Orco, D., Lundqvist, M., Oslakovic, C., Cedervall, T. & Linse, S. Modeling the Time Evolution of the Nanoparticle-Protein Corona in a Body Fluid. *PLoS ONE* **5,** e10949 (2010).
52) Palchetti, S., Pozzi, D., Capriotti, A. L., Barbera, G. L., Chiozzi, R. Z., Digiacomo, L., Peruzzi, G., Caracciolo, G. & Laganà, A. Influence of dynamic flow environment on nanoparticle-protein corona: From protein patterns to uptake in cancer cells. *Colloids and Surfaces B: Biointerfaces* **153,** 263–271 (2017).
53) Bonvin, D., Aschauer, U., Alexander, D. T. L., Chiappe, D., Moniatte, M., Hofmann, H. & Mionić Ebersold, M. Protein Corona: Impact of Lymph Versus Blood in a Complex In Vitro Environment. *Small* **13,** 1700409 (2017).
54) Pisani, C., Gaillard, J. C., Dorandeu, C., Charnay, C., Guari, Y., Chopineau, J., Devoisselle, J. M., Armengaud, J. & Prat, O. Experimental separation steps influence the protein content of corona around mesoporous silica nanoparticles. *Nanoscale* **9,** 5769–5772 (2017).
55) Carrillo-Carrion, C., Carril, M. & Parak, W. J. Techniques for the experimental investigation of the protein corona. *Current Opinion in Biotechnology* **46,** 106–113 (2017).
56) http://consortiapedia.fastercures.org/consortia/nice/ *Consulted on August 2017*
57) http://www.onxeo.com/en/nos-produits/portefeuilles-produits/orphelins-oncologie/ *Consulted on August 2017*
58) http://www.nanobiotix.com/_fr/nbtxr3/ *Consulted on August 2017*
59) Boisseau, P. Lipidots® Les gouttelettes qui diagnostiquent et qui soignent. http://extranet.insight-outside.fr/upload/compte179/Base/inscriptions_programme/document/12985-Lipidots_Midi%20Minatec.pdf *Consulted on August 2017*
60) Jacquart, A., Kéramidas, M., Vollaire, J., Boisgard, R., Pottier, G., Rustique, E., Mittler, F., Navarro, F. P., Boutet, J., Coll, J.-L. & others. LipImage™ 815: novel dye-loaded lipid nanoparticles for long-

term and sensitive in vivo near-infrared fluorescence imaging. *Journal of biomedical optics* **18,** 101311–101311 (2013).

61) http://www.amatsigroup.com/fr/ *Consulted on August 2017*

Summary of the general introduction

The burgeoning field of Nanomedicine is seen as a potential revolution in medicine, having possibilities of applications in therapeutic and diagnostic areas. Nanomaterials actors in this field are very small nano-objects (from 1 to several hundreds of nanometers) made of different chemical nature (metal, lipid, polymer, inorganic). The main improvements provided by such complex structures are a better targeting of damaged tissues, a protection of the active drug from precocious degradation or even a sustained release of the drug to ensure a prolonged effect over time.

The conception of nanomedicines (NMs) has evolved with the increasing comprehension of these systems since several decades. In this thesis, the case of NMs destined to be admnistered through the intravenous route has been studied. The first generation of nanomedicines was conceived as bare nanoparticles being rapidly cleared by the immune system. The second generation incorporated hydrophilic macromolecules on the surface of nanoparticles in order to reduce this rapid clearance and prolong the residence in bloodstream, hence increasing the chance to reach target tissues by passive targeting. The third generation is today under development and adds targeting moieties on the surface of nanomedicines in order to improve the efficacy of targeting towards well-defined tissue and cells (cf. Figure 2).

However, it is still scarce for NMs to reach the market. This difficult translation from bench to bedside has been partly explained by the lack of knowledge about NMs' becoming after administration. The initial synthetic identity is actually replaced by a biological identity acquired *in vivo* (cf. Figure 3). This newly acquired identity, mainly influenced by the adsorption of blood proteins, is responsible for the fate of NMs. The lack of characterization methods hampers the comprehension of phenomena mastering this identity modification. This incomplete NM's characterization also leads to unexplained inconsistencies in *in vivo* response observed during some clinical trials. The challenge for improving NMs development is to better understand them and be able to control them in details.

The purpose of this thesis was to develop methods applicable in routine for a better characterization of NMs and their interactions with blood proteins. This thesis was conducted

in the context of NICE consortium gathering companies currently carrying out clinical trials on nanomedicines (Onxeo, Nanobiotix).

This manuscript first presents a bibliographic part on current stakes of NMs characterization for a clinical use (chapter I).

Then, the experimental part presents methods developed during this thesis. First, a method of bidimensionnal immunoelectrophoresis for the assessment of complement activation by nanomedicines in a high throughput way was developed (chapter II) and applied to a mechanistic study of complement activation by nanoparticles (chapter III).

Then, a chip was developed for the automated assessment of complement activation by surface plasmon resonance (SPR) (chapter IV).

Finally, a method using capillary electrophoresis was proposed as a novel approach to characterize NMs' surface coverage properties (chapter V).

All the developped methods and results obtained through the different chapters were further discussed in a general discussion before drawing the conclusion and perspectives of this thesis work.

Partie bibliographique

Chapitre I : Les enjeux de la caractérisation des nanomédecines dans le processus de translation clinique

Avant-propos : La caractérisation des nanomédecines en phase clinique est très importante pour garantir une bonne conformité des lots et ainsi une activité biologique reproductible, indispensable pour la consistance des résultats et la sécurité d'utilisation en clinique. Dans cette partie, une revue de l'état de la caractérisation actuelle des nanomédecines en contexte clinique est proposée et mise en confrontation avec le degré d'exigence rencontré dans les processus biologiques. Des exemples de la finesse des systèmes biologiques sont étayés pour illustrer le degré de précision rencontré dans ces processus. Confrontés à cette réalité, les autorités de régulation recommandent la caractérisation de certains paramètres bien définis de la nanomédecine tels que la taille, la charge, la morphologie, et autres informations sur la cinétique de libération du principe actif par exemple. Un état de l'art des méthodes couramment utilisées actuellement est réalisé en tenant compte des avantages et faiblesses associés à ces méthodes. La précision et les informations obtenues par la caractérisation de routine telle qu'elle est effectuée actuellement ne semblent pas pouvoir garantir une totale reproductibilité des interactions de la nanomédecine avec les milieux biologiques. De nouveaux horizons sont proposés pour améliorer ces limites de la caractérisation actuelle. Plusieurs pistes sont envisageables pour le développement de nouvelles méthodes de caractérisation. Certaines pourraient permettre d'obtenir des informations plus précises sur la nanomédecine, d'autres pourraient directement faire intervenir des composés biologiques pour garantir une interaction précise et reproductible en mimant les conditions d'utilisation.

Projet d'article

A thought about the characterization of nanomedicines: a field under construction between regulatory and methodological aspects needed to accelerate clinical developments

Jean-Baptiste Coty, Christine Vauthier*

Institut Galien Paris-Sud, CNRS, Univ. Paris-Sud, Université Paris-Saclay, 5 rue Jean-Baptiste Clément, 92290 Châtenay-Malabry, France

***Corresponding author:** Dr. Christine Vauthier, CNRS UMR 8612, Institut Galien Paris Sud, Univ. Paris-Sud, Université Paris-Saclay, 5, rue Jean-Baptiste Clément, 92296 Châtenay-Malabry, France. Fax: +33 146835946. E-mail: christine.vauthier@u-psud.fr

Abstract

The nanotechnology revolution offers many expectations for the improvement of medicine treatments. At present, nanomedicine (NM) development is hampered by methodological barriers for a better characterization and a wider understanding of their *in vivo* behavior. While regulatory agencies setup guidelines to support NM translation from bench to bedside, the gap is still hardly overcome by main nanomedicines. One lever for filling this gap is a better characterization of NMs. Here, we review the current methodologies routinely used for clinical release of nanomedicine batches in compliance with official guidelines. We confront them to the extreme sharpness of biological systems and finally discuss future possible orientations for a better characterization of NMs, from physicochemical to biological fields.

Keywords: Characterization, nanomedicine, biological systems, architecture, quality control

I. Introduction

Since the early age of nanotechnologies, nanomedicines (NMs) are considered as the most revolutionary way to design medicines bringing high potential for the development of treatments for non-curable diseases and for diseases of severe prognostic (e.g. cancer, infections, cardiovascular diseases, neurodegenerative deseases). An increasing number of emerging small companies as well as big pharmas are exploring the Nanomedicine's field for its promises [1-3]. However, the number of 50 marketed NMs (among which the most known AmBisome® (1990), Doxil® (1995), Abraxane® (2005), Onivyde® (2015)) appears inconsistently low compared with the tremendous research activities in academics and clinics [4-7]. The gap for the translation of advances made in research laboratories to the patient is so huge that it earned the title of "death valley" [8]. Many challenges have been identified as bottlenecks for the clinical translation of NMs. One part concerns the complexity of the diseases to be treated. Designing efficient nanomedicines requires a better understanding of their mechanisms of action including the interactions occurring between NMs and biological systems. In turn, a better knowledge of NMs' characteristics is needed to complete this understanding. Another part concerns the production of nanomedicines including the scale-up of preparation methods and quality controls that are needed to achieve batch to batch consistency [8,9]. In both cases, the achievement of a relevant characterization of NMs is needed. At present, it is still a difficult task to fix. One reason is the need to further understand which parameters are governing their *in vivo* fate and activity. A second reason is found in the few number of methods that are operational to achieve a proper characterization of nanomedicines on a daily basis.

The purpose of the present review paper was to discuss the physicochemical characterization of NMs considering differences in characteristics that can be detected by biological systems with potential influence on their *in vivo* fate, hence interfering with their activity and safety. As the world of Nanomedicine includes many different types of nanotechnologies, this analysis considered nanoparticles (NPs) which size was larger than that of blood proteins. The analysis also focused on NMs intended to be administered by the intravenous route, as they represent most of systems considered in development of treatments for cancer, severe infections and neurodegenerative diseases among all nanotechnologies developed as nanomedicines [10,11]. The first part of the paper analyses the physicochemical parameters that are relevant from biological systems' side to discriminate NMs (I). The paper then reviews

the present recommended strategies for NMs characterization in the light of guidelines provided by health agencies (II). The next parts discuss properties and methods for NMs characterization. Those that are readily applicable for quality control analyses were presented first (III). Then, characteristics that may be interesting to evaluate due to their relevance regarding their influence on biological system responses were discussed. Other potentially interesting methods currently in development were also presented (IV).

II. Relevant physicochemical characteristics of nanomedicines detected by biological systems with implication on their *in vivo* fate

II.1. The mystery of NMs *in vivo* fate is driven by their initial properties

One concern in clinical development of nanomedicines is to be able to warrant their safety and the reproducibility of their activity from batch to batch. The same consideration applies in the development of generic nanomaterials (nanosimilars). Here, it is proposed to examine differences in physicochemical characteristics that biological systems can detect with implication on the *in vivo* fate of nanomedicines and potential impacts on their activity and safety.

Obviously, the *in vivo* fate of nanomedicines introduced in the general circulation is governed by interactions with components of the different biological environments and barriers found on their way to the site of action. Understanding these interactions and controlling nanoparticle characteristics that are influencing them are challenges for the development of safe and efficient nanomedicines [12]. So far, most works focused on the understanding of interactions occurring directly after NMs introduction in the bloodstream. This is consistent with the fact that events happening at this stage have a tremendous implication on NMs' biodistribution [13,14]. This has been understood in the early development of NMs and led to the definition of two types of NMs with distinct pharmacokinetics (PK). NMs showing a long half-life (hours) in the bloodstream were classified as "stealth" while "non-stealth" NMs are rapidly cleared from the bloodstream (within minutes) and accumulate in organs rich in macrophages (liver, spleen) [15-19]. Recently, efforts were intensified to identify more precisely NMs' characteristics controlling these interactions [20-23]. A summary of data analyzing the degree of sensitivity of phenomena implicated in protein adsorption and activation of the complement system with nanoparticles is given below. Other studies have

investigated parameters governing interactions between NMs and cells expected to occur at the target site. The end of this part points out two examples taken from Mother nature that further illustrates the high sensitivity of biological systems, able to detect subtle changes in structural characteristics of entities they are confronted with.

II.2. NMs characteristics controlling their interactions with blood proteins

Two distinct ways to study properties influencing NMs interactions with blood proteins are described.

(i) The identification of the "adsorbome" of proteins forming the so-called "protein corona" around the NM, providing a new biological identity supplanting the initial synthetic identity of the nanomaterial [24]. It consists in the identification of the proteins adsorbed onto the NM after contact with blood plasma. The throughput and accuracy of such a study has been greatly improved by the development of systems of liquid chromatography coupled to mass spectrometry (LC-MS) on this purpose. Among these studies, several parameters of NMs have been put under lights for their influence on this adsorbome [25-27]. More precisely, the size [28-32], the shape [33], but even more the surface chemistry and the charge of NMs were found to strongly impact the protein corona composition [29,31,34-38]. While polyethylene glycol (PEG) surfaces have been widely studied since the middle of the 1990's [19,39-41], other surface chemistries are being explored for their stealth properties too (polysaccharides, synthetic surfactants) [42-44]. Besides, these studies showed that for a given chemical nature, the length, the density as well as the conformation of the surface were determinant in regards to protein interactions [40,45-47], emphasizing the need for a precise characterization of NM's surface properties and control of the surface architecture too.

(ii) The assessment of interactions with proteins of biochemical cascades is another way to study interactions of NMs with blood proteins more directed towards safety [48,49]. Coagulation and complement systems consist in groups of proteins that regulate body's homeostasis towards foreign agents. Interactions of NMs with proteins and cells of the coagulation system are important because they can lead to reactions such as hemorrhage or conversely thrombosis [50]. A review described some known interactions between different kind of nanomaterials and the coagulation system [51]. It emphasized that NMs' size, charge, surface composition were also involved in interactions with the coagulation system. So far, most studies focused on the interactions between NMs and the complement cascade, thus

being more deeply described in this review. Complement proteins are part of the first barrier of innate immunity encountered by the nanomaterial in the blood. A premature detection of NMs by this system leads to their opsonization and capture by macrophages. NMs are then mainly retained in the liver hence biasing all their biodistribution. Several studies showed that above cited NMs properties influenced the triggering of this cascade [52-54]. Once again, the surface architecture has been proved to be very important concerning complement activation with different type of macromolecules composing the NP shell (PEG [55-59], polysaccharides [60-64]).

II.3. NMs characteristics controlling their interactions with cells

To promote interactions with target cells, ligands can be attached on the nanoparticle surface. In general, nanoparticles bearing such ligands are more likely to be taken up by cells exhibiting the corresponding receptors [65-67]. Little is known about the number of requested ligand per nanoparticle to improve internalization of the nanomedicine by the target cells. It can be reasonably assumed that the internalization pathway is defined by the type of targeted receptor in this case. Besides, nanoparticles can be internalized by cells even in the absence of targeting moiety by several mechanisms [68-71]. Some studies showed the importance of surface charge, geometry and even architecture on cellular uptake of NMs [70,72-75]. However, very little is known about nanoparticle characteristics that control cell internalization phenomenon. The situation is even more complex because the above mentioned protein corona has been identified to also influence the cellular uptake [45,72,73,76-78]. Today, only punctual observations are available without enough comparative studies allowing a better understanding of critical parameters intervening in interactions between cells and NMs. The correlation between synthetic parameters of the NM, biological acquired identity and cellular uptake is not understood although models are being established to connect them [29,79,80]. Once in the cell, the intracellular trafficking also depends on NMs characteristics. While nucleus is often the targeted organelle, the NMs properties must make them able to escape the endosome in order to produce the desired activity [68,69,71].

II.4. Concluding remarks in the light of examples taken in biological systems found in Mother nature

As pointed out above, modifications in the surface architecture of nanoparticles can dramatically affect the way these nano-objects developed as nanomedicines are seen by the organism after intravenous injection, with possible influence on their *in vivo* fate. This is due to the high sensitivity of biological systems that are capable to distinguish very small structural differences that may occur at a molecular level. The extremely high degree of precision shown by biological systems is illustrated below through two examples taken from Mother Nature.
At first, the bacterial capsules of *Neisseria meningitidis* (*N. Meningitidis*) embody the sensitivity of biological systems. Among them, the sialic acid capsular polysaccharides expressed by *N. Meningitidis* serogroups B and C are very similar [81,82]. The complexity of the finding of an efficient vaccine against *N. Meningitidis* serogroup B comparatively to the C type was explained by the non-immunogenicity of the B serogroup and its ability to escape the immune system [83]. This form, not detected by the immune system, is responsible for severe infections while serogroups A and C types are more easily cleared. This is due to the capsule conformation which has a very strong impact on the becoming of the bacteria in the host body. The difference lies in the substitution differing from one carbon on the polysaccharide capsule: while *N. Meningitidis serogroup* C has a poly(alpha 2-9 acid acetyl neuraminic) capsule composition, the B type capsule is made of poly(alpha 2-8 acid N-acetyl neuraminic) [82,84] (see Fig. 1A). This small chemical change implies a conformation modification of the final sialic acid, which modifies negative charges exposure and steric hindrance effects [85,86]. It has also been proofed that *N. Meningitidis* serogroup B capsule composition was similar to those found in an endogen neuronal protein, playing a great role in its non-immunogenicity [87]. This is an example showing the extreme sensitivity of biological systems, that can be recognized or not depending on the displacement of substitution of one carbon in the chain, inducing conformational changes in the final structure. This example easily translates to the NMs field with the importance of the surface architecture on their *in vivo* fate.

Then, the antigen-antibody interaction is another proof of the sensitivity of biological systems. Modification of few amino acids (a.a) in a chain of more than 1300 a.a allows a dramatic change in antigen-antibody interaction. Indeed, a sequence of five a.a is responsible for the

specific interaction between an antigen and an antibody that form an antigen-antibody complex with an extremely high specificity. Modification of one or several amino acids on the paratope and/or epitope can reduce the strength of the interaction by three orders of magnitude, thus hampering the formation of the complex [88]. These interactions are a combination of electrostatic interactions added to a favorable conformation of the epitope's chain [89]. While Immunoglobulins G are proteins around 10 nm in size, their action is driven by a couple of a.a. A study was performed to identify key residues involved in interactions between platelet receptor glycoprotein Iba (GPIba) and a monoclonal antibody 6B4, that could be used as an inhibitor of overexpressed interaction of GPIba with Von Willebrand Factor that can lead to thrombosis [88]. We can see in the paratope-epitope simulation of H-bond interaction mapping for protein and monoclonal antibody 6B4 that four amino acids from the antibody paratope and 2 a.a from the protein epitope are strongly implied in the affinity between the two entities (red colors in Fig. 1B). Translating this example to the NM field, this is typically the complex issue observed in the grafting of targeting moieties on NMs. Most of these moieties are antibodies, RNA, aptamers or again proteins, grafted in a targeting purpose to be recognized by receptors on specific cells. However, current coupling methods used with these complex molecules are not precise enough to choose the exact location of grafting. Moreover, characterization methods are not sensitive enough to determine in which conformation the grafted moiety stands on the nanoparticle surface. This is a huge issue encountered today in NMs design and characterization [20,23]. Thus, it is difficult to assess the efficacy of such targeting strategy and the way to improve it since it is not possible to achieve a precise characterization yet.

These examples, combined to all the data gathered on the influence of NMs characteristics on their interactions *in vivo* after an intravenous administration, highlight the great importance of the required keenness for NMs characterization. As seen, a modification of NM surface architecture can be at the root of major changes in terms of biodistribution. Hence, the NM design is a very subtle process which impacts the becoming of the NM from its entry into the bloodstream to its fate inside the cell. The sharpness of the elements and processes encountered *in vivo* requires a very fine control, characterization and understanding of these initial parameters.

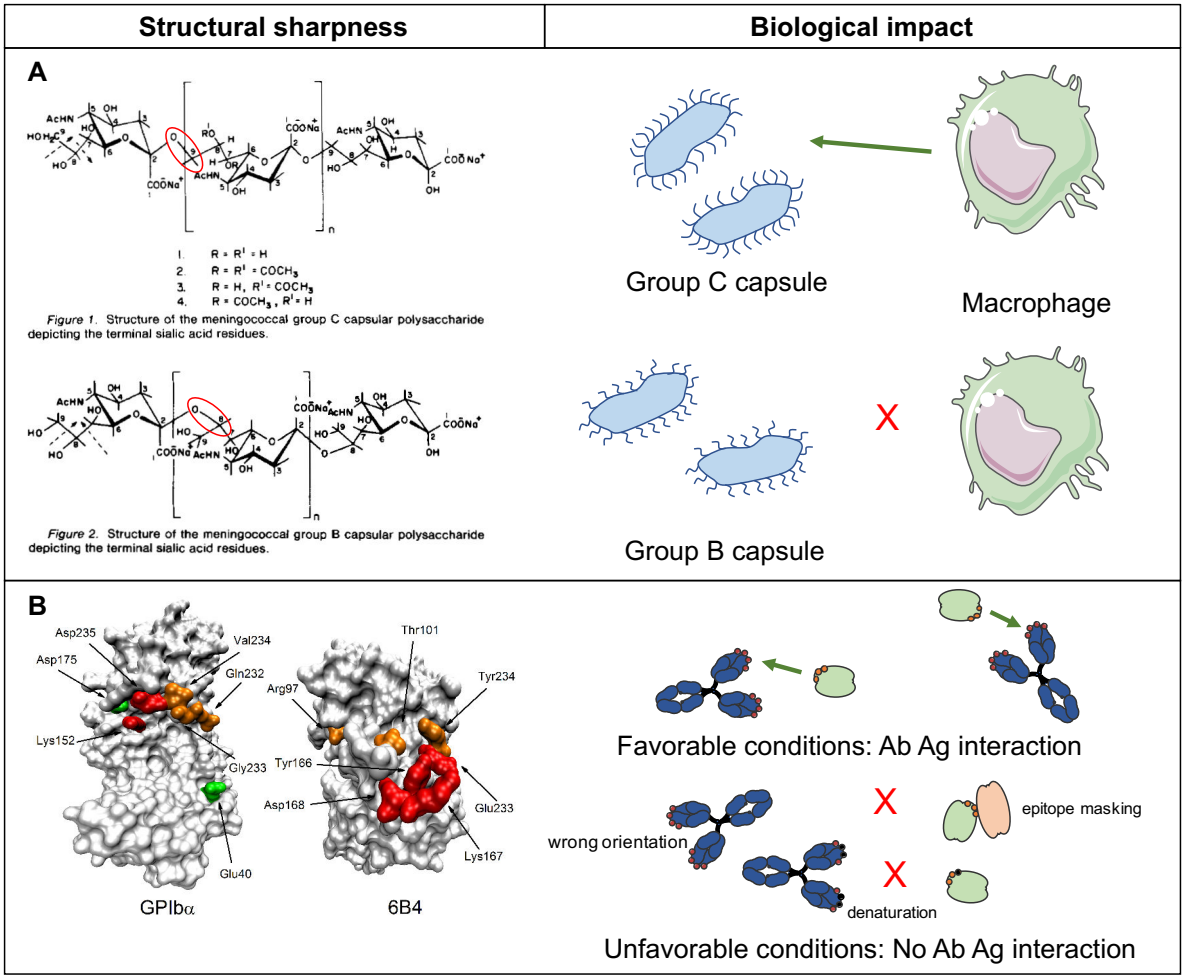

Figure 1: Examples of structural sharpness found in Mother nature and their biological impact. A: polysaccharide structure of *N. Meningitidis* capsules of B and C serogroups. Left part reproduced from [84] with permission from The American Association of Immunologists, Inc. Copyright 1981.
B: Identification of amino acids implied in antibody antigen recognition. Left part reproduced from [88].

III. General strategies for nanomedicine characterization and recommendations of health authorities

III.1. The characterization revolution brought by “nano”-medicines

It is now well established that a lack of proper and rational characterization is one of the main blocking step of NMs translation from bench to bedside [22,90,91]. Firstly, the lack of established characterization at a preclinical stage is one of the bottleneck for nanomaterials access to the market [92]. Then, an incomplete characterization of batches during clinical testing reduces the strength of the NM assessment in clinics. This is acknowledged by the fact

that many formulations are being stopped because of unknown causes, which could have been detected with a proper characterization.

Due to the disrupting complexity of nanoformulations, traditional approaches for medicine regulation cannot be applied without a significant adaptation to the nature of the pharmaceutical object [92,93]. The emergence of the field of nanomedicine brings a huge deal for a renewed regulatory process. Indeed, added to the nano- scale, the overexpressed surface area, the multi-component composition of such technologies makes even more difficult their characterization and the understanding of their *in vivo* behavior. To illustrate this difficulty, table 1 gives a brief comparison of the major differences between conventional medicines and nanomedicines including implications on their respective characterization.

	Conventional medicine	**Nanomedicine**
Composition	Active Pharmaceutical ingredient (API) + excipients	API within the nanocarrier (NC) (complex assembly)
Transport of the API	Single molecule solubilized	Within the NC (biodistribution and release profile modified)
Biological activity	API dependent	Nanocarrier + API dependent
Characterization	API identity (chemical signature by NMR, UV, IR) Solubility – Dissolution rate Purity, contaminants free	API identity NM properties: Size, charge, morphology, drug loading and release Purity, contaminants free
	Biological activity and safety warranted	**Not enough to ensure full biological activity and safety**

Table 1: Major differences encountered between conventional drug medicine and nanomedicines when bridging the translation gap.

III.2. Towards new guidelines adapted to nanomedicines

A panel of parameters to be assessed and methods have been implemented by the Nanotechnology Characterization Laboratory (NCL), created in 2004 to reach these issues related to NM clinical translation. Assay cascades for assessing physicochemical properties as well as *in vitro* and *in vivo* testing procedures were setup to guide companies dealing with such entities [94]. Two main categories can be distinguished, namely the non-biological and biological assays:

- The first category of methods aims to characterize intrinsic properties of the nanomedicine through its physicochemical characteristics (size, charge, composition, morphology, concentration, API loading, free of contaminants).
- The second category includes techniques investigating interactions of the nanomedicine with biological entities encountered *in vivo*. This involves hematocompatibility tests (hemolysis, cytokine proliferation), investigation of interferences with biochemical cascades (complement, coagulation), *in vitro* cellular or tissue assays and *in vivo* studies [95]. This part is notably pointed out in the development of nanosimilars that can have different interactions with blood components [5,96-98].

NCL has now extended to Europe since 2015 with the creation of EU-NCL (European Nanomedicine Characterization Laboratory) [99]. They give an encouraging way to fix guidelines and unavoidable parameters to be assessed for every NM before being sent to clinical studies. This process led to the assessment of new properties related to the nano-character of the new drug. Some recent reviews discussed about these evolving aspects of NMs regulation and approvals [4,7,95,100,101].

The point that seems to be less regulated and controlled is the characterization needed for the release of a NM batch prior to clinical use. Indeed, added to conventional tests for batch release of medicines, additional tests must be performed over the entire final nano-object. The complexity is greatly augmented in these systems and batch release cannot be treated the same as for “simple” drugs. As the research and potentiality offered by these new forms of medicines brings a lot of researchers and companies working on it, a strong effort of regulatory aspect had to follow this wave for a faster and safer translation to the clinics. The NCL assay cascade is valuable in a context of evaluation of the nanomedicine before its launching in clinical trials. However, once the study launched or when the product is on the market, every single batch cannot be screened for conformity taking into account all the considered parameters, due to the extreme tediousness of the task, associated to a considerable cost. Some critical parameters are chosen as markers ensuring the reproducibility of the NM effect once administered. Methods on this purpose may naturally be picked from the previously mentioned assay cascades. The most important is to identify a set of key parameters that will be relevant to detect a possible modification in NM characteristic influencing the *in vivo* behavior [102,103]. So far, it is assumed that a case by

case selection of this set of parameters has to be made due to the huge diversity of systems encountered in the world of nanomedicines (polymer based, inorganic, lipid, nanocrystal) [92,104].

III.3. Health agencies positions

Aware of current characterization limitations, European and American regulatory agencies (European Medicine agency (EMA) and Food and Drug Administration (FDA) respectively) opened reflections about future development needed.

EMA points out the matter of batch to batch consistency in its reflection papers about different kinds of nanomaterials. Notably, reflection papers related to block copolymer medicinal products [105], liposomes for intravenous delivery [106] and iron based nanocolloids [107] recommended to identify critical quality attributes that will have an impact on the behavior of the NM *in vivo* (PK, PD, safety, efficacy). Most of the parameters cited there are not directly focused on the "nano" character of the NM. Namely, control of the raw material (lipids, copolymers, carbohydrates) for purity, composition, stability before their use in a complex system, manufacturing process (reconstitution procedure, sterility), stability over time, or again parameters related to the mode of administration (eg. osmolality, degradation rate and location, drug release rate and location) are mentioned to be controlled. When directly dealing with the full nanomaterial characterization by itself, quality parameters proposed are all linked to its physicochemical properties. These parameters are typically size, size distribution, surface charge, morphology, drug loading and release profile, and *in vitro* stability. EMA warn about the necessity to develop methods that guarantee a better reproducibility for batch release. In a communication about quality in 2014, EMA still stressed the need for more specific guidance on the quality of nanomedicines, the identification of critical parameters and the implementation of new characterization methods [108].

On the FDA side, the nanotechnology task force published in 2007 raised a scientific issue about the understanding of nanomedicine interactions with biological systems [104,109]. It has also been claimed that a need for new methods is urgent. Common parameters for quality were cited as size (surface area and size distribution), chemical composition (such as purity and crystallinity), surface properties (surface reactivity, surface groups, inorganic/organic coatings), solubility, shape and aggregation state. It was also mentioned that the NCL would be a major actor of the development of screening tools for nanomedicine characterization.

Since 2007, a final guidance was published by FDA, mainly concerning nanotechnologies in food and cosmetics [110]. To our knowledge, no major update has been released directly concerning nanomedicines.

International Standard Organization (ISO) and Organization for Economic Co-operation and Development (OECD) have planted the properties of interest for nanotoxicology. These properties are similar to those mentioned by medicine agencies, i.e. particle size and size distribution, aggregation/agglomeration, shape, surface area/porosity, composition, surface chemistry, surface charge, solubility [111-113]. Meanwhile, Contract Research Organizations (CROs) in charge of quality control of NMs are focused on physicochemical properties as well, in compliance with current guidelines. Nevertheless, some biological tests are proposed as optional for NMs bearing targeting moieties [114].

To sum up, in practice, properties checked for a batch release are fixed by the company developing the NM in accordance with regulatory experts. A consensus is taken on a case by case basis in regard with current feasibility of such controls in routine. Apart from contaminants and basic parameters needed for intravenous administration of any drug (impurities dosage, API degradation, residual solvents, metal traces) and characteristics of the route of administration (pH, osmolality, pyrogen-free, endotoxin free, sterility)), only few parameters specific to the nanomaterial are requested. They are linked to the drug loading/release properties[18] and to the characterization of several physicochemical properties consistently with available methods allowing their determination. For example, some mentioned parameters (e.g. surface properties in FDA task force [104]) cannot be properly characterized with today's accessible methods. It is noteworthy that efficiency of current criteria defined to ensure the reproducibility of NMs' *in vivo* fate and methodology used for determining safety and quality of NMs are under debate [20,115]. It appears clear for actors in the field of pharmaceutical development that the biological studies are non-applicable on a quality control routine basis [101]. For instance, *in vivo* animal studies are generally considered unethical to be used in systematic controls above the fact that they are time consuming, requires specific facilities, highly trained lab-workers and expensive. Tests performed in cell cultures can be envisaged although they are generally complex and demanding. In the following parts of this review paper, the determination of physicochemical parameters characterizing NMs was examined in terms of methodologies and discussed

regarding the degree of precision of biological systems as highlighted earlier. Physicochemical parameters presently recommended for quality control evaluation of NM were considered first. The final part discusses other parameters that may be of interest to characterize pointing out the methodological outcomes.

IV. Recommended physicochemical parameters for NMs characterization

The list of physicochemical characteristics recommended for testing the conformity of a NM, includes size, size distribution, morphology, surface charge, surface chemistry, drug loading and releasing profile, concentration, stability. The **concentration and stability** are related to the population of nanomaterials included in the nanomedicine. The stability includes two aspects in the case of NMs. As for all medicines, they need to show chemical stability over time but also the stability against aggregation or agglomeration because NMs act as a population of individual nano-objects. This is generally done evaluating the size, the size distribution, the morphology and the surface charge to verify that these characteristics are preserved over time. The other parameters of the list define what is called the "synthetic identity" of the nanomaterial and are expected to influence its *in vivo* fate [24,116].

For a clinical use, all batches of produced NMs must be submitted to a characterization cascade that aims to prove batch to batch consistency, assuming that the performed characterization is relevant enough to warrant biological activity and safety of the medicine. Methods used to achieve these characterizations must be robust, straightforward, easy to carry out on a systematic basis, affordable and, if possible, automatable. Recently, an ISO document providing the different measurement techniques validated for nanomaterial characterization was published [117]. Table 2 gives an overview of methods recommended for the characterization of physicochemical parameters. This table also highlights ISO standards when existing for the considered methods and notices the availability of marketed instruments for a routine evaluation of the corresponding parameter.

Property	Method	Measurand	Advantages	Drawbacks
Size [92,94,95,99,116,117,119,121]	Dynamic Light Scattering (DLS) * ‡	Hydrodynamic diameter	Easy handling, low cost, rapid	Not appropriate for multimodal dispersions, low resolution, not adapted to non-spherical NPs
	Particle tracking analysis (PTA) * ‡	Hydrodynamic diameter	Easy handling, low cost, rapid, particle by particle	More optimization than DLS, resolution limited for very small particles, not adapted to non-spherical NPs
	Tunable Resistive Pulse sensing (TRPS) * †	Raw diameter	Easy Handling, low cost, rapid, particle by particle	Not adapted to small particles (<40nm), not adapted to non-spherical NPs
	Differential centrifugal sedimentation (DCS) * ‡	Hydrodynamic diameter	Easy handling, separative, high resolution	Long for low density particles, not adapted to non-spherical NPs
	Field Flow Fractionation (FFF) coupled to detector (Multi-angle LS, DLS)**	Hydrodynamic diameter	Separative, high resolution, automatable, shape discriminant	Conditions optimization, calibration required, biased by large particles, expertise needed
	Electron microscopy (EM: SEM, TEM, Cryo-TEM) ** ‡	Core diameter	Direct visualization, shape information, high resolution	Labour intensive, low throughput, dried sample, low density atoms less sensitive, possible artifacts
Size distribution [92,94,95,99,116,117,119,121]	DLS * ‡	Polydispersity index	Gives a brief idea of the polydispersity	Small particles hidden by larger ones, not adapted for multimodal dispersions
	PTA * ‡	Size of populations	Particle by particle	Size resolution limited
	TRPS * †	Size of populations	Particle by particle	Not adapted to small particles

	DCS * ‡	Size of populations	Separative	Difficult rotation velocity optimal for multimodal samples
	FFF coupled to detector (DLS, MALS) **	Size of populations	Separative, high resolution	Biased by large particles, expertise needed
	Electron microscopy ** ‡	Size of populations	High resolution, particle by particle, visualization	Low throughput
Morphology [92,94,95,99,116,117]	Electron microscopy ** ‡	Morphology	Direct visualization, general shape (sphere, rod, complex shape), plain or core-shell	Expertise needed, low throughput, low density atoms less sensitive, possible artifacts
	X-ray diffraction (SAXS, WAXS) ** ‡	Structural information	Very sensible, supramolecular organization	High expertise needed, not direct access to shape
	Atomic Force Microscopy (AFM) **	Topography	High resolution	Expertise needed, lateral resolution limited, not direct access to shape
Surface charge [92,94,99,116,117]	Electrophoretic light Scattering (ELS) * ‡	Zeta potential	Easy handling, low cost, rapid	Not appropriate for multimodal dispersions, highly dependent on conditions (conductivity, pH, solvent), apparent value
	Zeta Particle tracking analysis *	Zeta Potential	Easy handling, low cost, rapid, particle by particle	Resolution limited for very small particles, apparent value
	TRPS * †	Zeta Potential	Easy handling, low cost, rapid, particle by particle	Not adapted to small particles (<40 nm), apparent value
	Electroacoustic spectroscopy * ‡	Zeta Potential	Adapted to concentrated samples	Complex model, non-trivial sample information required, apparent value

Surface chemistry [92-94,99,101,116,117,143-146]	X-ray Photoelectron Spectroscopy (XPS) ** ‡	Surface composition	Semi quantitative, chemical analysis	Dried sample, artifacts, outer layer information (10 nm depth), expertise needed
	Secondary Ion Mass Spectroscopy (SIMS) ** ‡	Surface composition	3D resolution, surface and inner component analysis, high sensitivity	Expertise, dried sample, harsh conditions may modify NPs
	NMR *	Amount of grafted macromolecule	High sensitivity, automatable	Deuterated medium needed, no information about the conformation
	Chromatography-Mass spectrometry *	Amount of grafted macromolecule	Available, quantitative	No information about disposition, conformation, homogeneity
	UV-vis/ FLuo Spectroscopy *	Targeting ligand attachment	Low cost, straightforward, quantification	No information about ligand orientation, ligand dependent
	Surface Plasmon Resonance **	Targeting ligand attachment	High sensitivity	Indirect, lack of robust methods
Drug Loading/Release [92,94,95,99,116,147,148]	Liquid chromatography *	Drug loading	Quantitative, easily automatable, high sensitivity	Sample preparation optimization required, NP must be solubilized, possible interferences
	Chromatography (SEC, SPE) *	Drug release	Robust, low elution volumes, complex system applicable (plasma)	Low throughput, dilution, induced drug release
	Dialysis *	Drug release	Equilibrium conditions, soft method, medium continuity	Long equilibration time, difficult with complex media, dilution, adsorption to the membrane
	Ultrafiltration *	Drug release	Small volumes, rapid, no dilution	Membrane clogging by particles, adsorption to the membrane, harsh method

Table 2: Main methods used for current NMs physicochemical characterization. Advantages and drawbacks

*Methods for which affordable instruments and batch measurements are available; ** Methods mostly applied in research laboratories; ‡ ISO Standard note available; † ISO standard note in preparation.

First and foremost, size is a critical parameter of a nanomaterial for its *in vivo* fate, notably playing a role in the EPR (Enhanced Permeability and Retention) effect and modulating interactions with biological entities (e.g. protein adsorption depends on surface curvature) [30]. In practice, for **size and size distribution** measurement, DLS is the batch method by excellence due to its accessibility, low cost, easy handling and having been described in an ISO standard [118]. All mentioned methods accessible via marketed instruments are accurate to determine size of monomodal dispersions. However, caution should be taken for an application to the characterization of dispersions with a multimodal size distribution [119-121]. A better resolution is accessible with methods such as TRPS, PTA or including a separative coupling (differential centrifugal sedimentation, FFF-MALS-DLS), that are now available for routine analysis and should be more systematically used to demonstrate the homogeneity of size distribution prior to deal with DLS. It is now recommended to cross a batch size measurement such as DLS with another technique based on particle by particle measurement [105-107,121]. Application of these methods is expending since the recent market introduction of these instruments [122-126] and ISO standards published yet [127,128].

Electron microscopy is suggested to be used to reinforce the value of size obtained by other methods and to obtain additional information on the sample, such as **morphology**, which is hardly obtained by other methods today. This method is not used in routine yet, being labor-intensive and rather unsuitable at a high-throughput. However, efforts for its automation are ongoing as acknowledged by the development of systems for high throughput EM analysis either by automated sampling [129] or high throughput image analysis [130]. Such improvements for a better efficiency of EM have already been seen in the field of virus detection [131-133]. The development of a facilitated access and use of EM is even eagerly awaited since the arrival of diversified nanosystems for which EM is the only way to evaluate a core size and define the morphology (stars, cubes, hexagons, rods) [134-136]. Shape and morphology of a nanomaterial influence its blood circulation (margination effect [137]) and interactions with cells [138,139] compared with spherical counterparts. Although electron microscopy is the only method that can provide a direct evaluation of the size of nanomedicines, it is performed on dried samples. This is in contrast with other methods which offer size measurement in aqueous conditions that are closer systems compared with

biological environments. So far, size measurements were qualified for a measure in a very simple matrix (purified aqueous samples), which gives information on the pristine nanomaterial. Methods for a pertinent evaluation of NMs size in biological medium (plasma, interstitial fluids) are under development, they are mentioned in the last part of this review.

Then, **the surface charge** determines interactions with proteins and cells [140]. This is commonly evaluated through the measurement of an apparent zeta potential with the same apparatus as used for size measurement. The duality of commercialized apparatus allows either a simultaneous measurement of size and charge (TRPS), or a possibility to assess both using different working modes included in the same instrument (ELS). Zeta potential is highly dependent on the analysis conditions (dispersion medium, system parameters), that is why only an apparent zeta potential can be determined. It is noteworthy that efforts about standardization of such methods are being made to ensure a qualified measure with robust protocols [104,141,142].

Surface chemistry and architecture have been shown to be very important to control protein adsorption *in vivo*, influencing interactions with cell and even biocompatibility of the nanocarrier [105,106]. The control of a reproducible density of grafting is very challenging. As size measurement cannot ensure this parameter, it is acknowledged that more characterization methods are needed on this purpose [22,92,95,101,143]. So far, chromatographic methods are used in destructive conditions to do so [116,144,145]. A method investigating the 3D structure of NMs surface providing information on its chemical nature is the Secondary Ion Mass Spectrometry (SIMS) [145,146]. The accessibility of such an instrument is nevertheless limited and it does not provide with information about the architecture of the NM surface. When targeting moieties are attached to the surface, a quantitation of these moieties is required but only indirect methods to check their orientation are available today [18] and does not allow a clear characterization of their spatial arrangement.

Drug loading and release are commonly assessed whereas bias still can hamper the true value of encapsulated and released drug amount. As excess amount of API could become toxic upon release, side effects could be observed. The phenomenon of burst release can also influence patient tolerability as well as efficacy. These parameters can be evaluated by quantitative dosage of the API. The problematic step is to achieve a proper separation between free and

entrapped drug in physiological media. This is mainly done via chromatography techniques (SEC, SPE) as well as equilibrium methods (dialysis, ultrafiltration). Drug release can also be monitored by membrane diffusion method such as dialysis [147,148].

Data included in table 2 highlights a lack of “ready to use” methodologies for several parameters (morphology, surface chemistry: grafting density, ligand attachment), thus pointing out a methodological bottleneck for the achievement of a straightforward full quality control evaluation of nanomedicines. Tremendous efforts are ongoing to fill out this gap [22]. Reference and standard materials needed for the validation of methods of characterization are also under development. It must be mentioned that the NCL has considerably contributed to the development of characterization assays for nanomedicines, developing numerous protocols and becoming a reference laboratory for the characterization of nanomedicines entering clinical development [94].

Besides, the series of physicochemical parameters that are used to define the synthetic identity of nanomaterials composing NM are probably not enough to ensure reproducible and expected results in biological media [20,102]. They depict nanomaterial properties at a relative “macroscopic level” in comparison with the sensitivity of biological systems. This notion is illustrated in figure 2 through examples of additional details perceived by biological systems. It is thus highly probable that “quiet changes” which may appear between batches are not detected during NM control and certification whereas having a non-negligible impact for the *in vivo* behavior, including biodistribution and safety of the NM. The challenge is to develop routine methods that reach biological system sensitivity and are able to detect the very small changes on NMs that are relevant for biological systems.

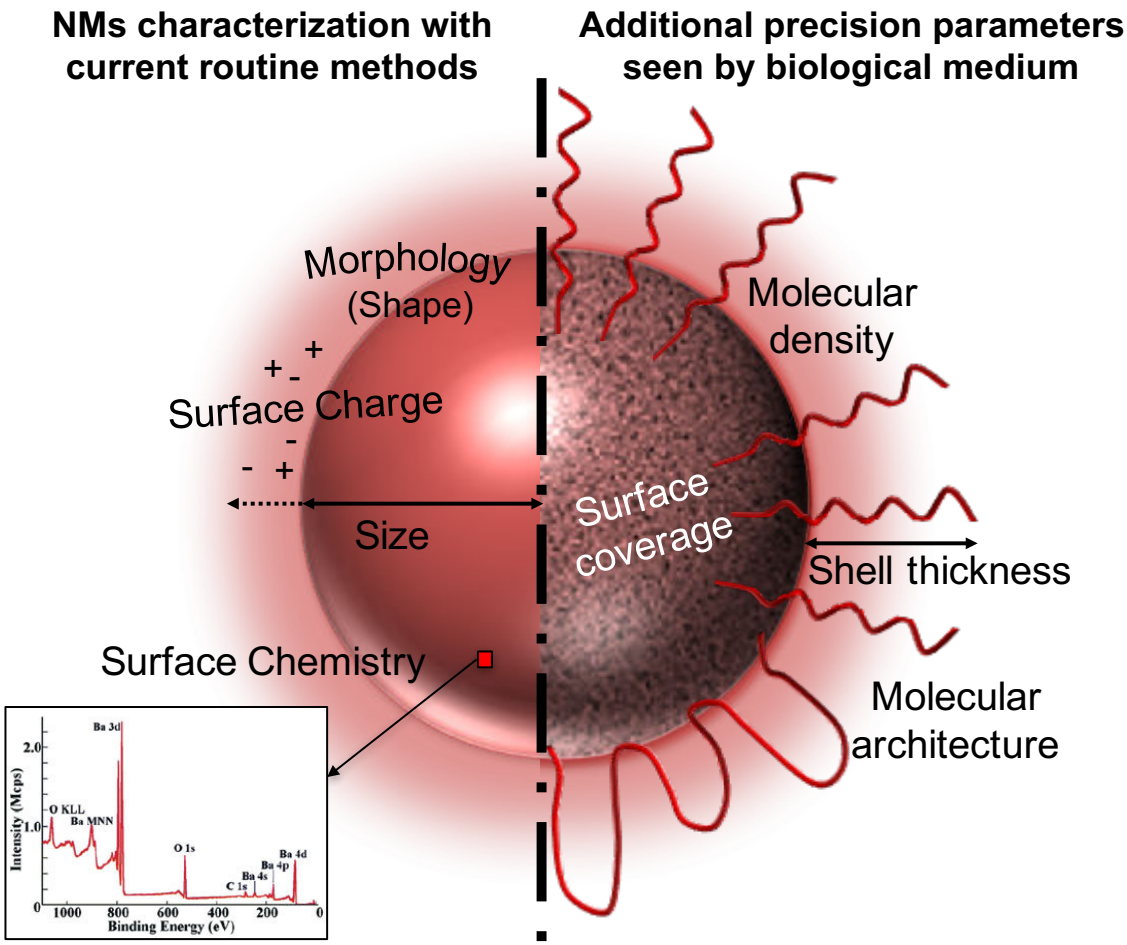

Figure 2: Illustration of the precision gap between current NMs' parameters determined in routine characterization versus details perceived by biological systems.

V. Acute characterization of nanomedicines for a warranted *in vivo* reproducibility

V.1. Challenges for future characterization of NMs

As pointed out earlier, biological systems are highly sensitive to small modifications of the synthetic identity of nanomaterials composing a nanomedicine. Modifications of size, morphology and surface charge of the synthetic identity can be assessed through well-established methods. However, as mentioned in the first part of the review, biological systems are also sensitive to subtle modifications such as the molecular architecture of hydrophilic molecules grafted on nanoparticle surface.

A joint effect of all synthetic parameters of the NM coupled to physiological conditions define the biological identity which is determinant for the *in vivo* fate of the NM [21]. Some computational studies tend to predict the behavior of a NM from its synthetic identity. This is

the road to a more rational design and characterization of NMs for a reproducible action *in vivo* [149]. However, these correlations are not clearly established and it appears risky to only control the currently evaluated physicochemical parameters to ensure a full *in vivo* reproducibility of a NM batch [150]. Recently, Lynch et al. stressed that current models used to predict biological outcomes from pristine parameters are not sufficient and need to be developed [79]. Furthermore, methods determining physicochemical properties by themselves are not enough robust to produce a high valuable characterization, except for size measurements that are the most documented today [79,119]. This pitfall can further be explained by the fact that the level of precision of current characterization methods applied in routine for NMs are much lower compared to biological systems sensitivity to detect changes in the synthetic identity of nanomaterials. So, there is an urgent need for methods assessing new parameters characterizing the synthetic identity of nanomedicines on a routine basis and at a much higher level of precision than already used methods [22,92,143]. These new parameters would appear as extensive information about NMs added to current commonly characterized properties.

V.2. Neo-characterization of NMs introducing new methods or new parameters to investigate

V.2.1. Assessing the synthetic identity of NMs

As seen in the previous part, the interaction for antibody-antigen recognition might be dependent on a series a five amino-acid in a certain conformation. Compared to the current control of the grafting of targeting antibodies, it is impossible to tell if the orientation is optimal for a possible interaction. Some methods are developed on this purpose and try to map the accessible conjugates on the NMs. Among them, one uses 2D fluorescence difference spectroscopy to directly detect the attachment of ligand molecules to a nanoparticle surface [151]. In the same idea, an epitope mapping has been established by Dawson and coworkers using immunogold labelling (Fig. 3D) [152,153]. This method can be used for assessing targeting attachment success as well as orientation of grafted antibodies.

As highlighted earlier, methods for evaluating macromolecular grafting on NPs surface are lacking. Recently, Green Fluorescent Protein was used as a probe to measure PEG grafting efficacy on silica NPs. This was proofed to be efficient in elucidating a proper PEG grafting at a molecular level [154].

V.2.2. Assessing the biological identity of NMs

Finally, another way to test the nanomaterial directly for certain interactions is to directly deal with *in vitro* tests applicable routinely. The strong impact of protein adsorption on the nanocarrier after intravenous injection is remarkably overlooked during routine characterization of nanomaterials although deeply studied in research laboratories [155]. There is a lack of applicable methods at a high throughput allowing a rapid testing of produced batch that hamper the control of their interactions with biological medias. One on the main drawback is the demanding preparation required when working with biological elements, added to the high cost associated to bio-reagents (antibodies, plasma, proteins). An effort can also be made in order to design *in vitro* methods that would reduce these drawbacks allowing them to be part of the common battery of tests performed on a batch of nanomedicine.

At first, the determination of the protein corona formed around NPs after contact with plasma proteins constitute one of the most important test performed in research to study the biological identity of NMs that is highly sensitive to the physicochemical identity of the NMs. This study is commonly made by LC-MS-MS and allows an identification of the protein adsorbed on NMs [28,29,37,38]. As performed in a relevant biological media, it is one of the most pertinent assay today for mimicking the biological identity of NMs. For a routine use, this method suffers from a lack of standardization especially because of the numerous variables of incubation conditions (temperature, dynamic/static, plasma source) and sample preparation steps (protein desorption, separation) which currently limit a universal evaluation of the protein corona [156,157]. This method also requires a specific equipment and a heavy data treatment. Moreover, the interpretation of the mass of data generated by this study is still not complete as the role of the different proteins found in the corona are not clearly established yet. The way to interpret the data has also been questioned due to the high averaging of proteins adsorbed obtained from millions of nanoparticles, rather than a particle by particle corona analysis [158].

Another approach is developed for a rapid screening of NMs interactions with biological systems. Namely, Kuruvila et al. developed a method called SUSTU (SUrface proteo- mics, Safety, Targeting, Uptake) [159]. This method allows the study of the protein corona external surface that could be used to assess the *in vivo* behavior reproducibility of the NM. This method, while being still demanding experimentally, is proposed as a tool for NM prototyping

in an integrated platform (Fig. 3A). Another group develops a screening method to study interactions of proteins with different NPs using fluorophore molecules affine to hydrophobic regions. They monitored the fluorescence in presence of different NP-Protein couples and could make assumption on adsorption behaviors thanks to the changes in fluorescence intensity (cf Fig. 3C). Developed in a 96-well format, this method can be considered as a possible candidate for NP-protein interactions routine screening [160].

To study more precisely the interaction on NMs with proteins and small molecules, Riviere's group developed a Biological Surface Adsorption Index (BSAI) in 2010. This model uses small molecules to probe the NM surface (Fig. 3B) [161]. By modelling the adsorption behavior of these probes, they could predict the adsorption of small molecules onto different nanomaterials [162]**.** The amount of adsorbed probes onto NMs was determined by gas chromatography coupled to mass spectrometry (GC-MS), allowing a high throughput analysis. The authors have thus defined an index that could be used to characterize NMs surfaces and predict their adsorption behavior, giving possible correlations of biodistribution and membrane interactions. Along with the current difficulties encountered by predictive models from physicochemical parameters, such methods introducing bio-elements like proteins might be a solution for an access to new information. They are sensitive to the steric hindrance found at the nanoparticle surface created by the molecular architecture of the macromolecules grafted on the nanoparticle surface.

A less sensible but more straightforward way to study the reproducibility of interactions between plasma proteins and NMs would be the measurement of size change occurring once both are in contact. EU-NCL proposed a FFF-MALS-DLS method for the batch to batch testing of plasma protein adsorption onto NMs [99]. Indeed, a reproducible elution profile could be the proof of a controlled interaction. With this method, the modification of size provided by proteins adsorption is measured. However, no indication about the composition of the protein corona is provided. Along the same lines, a recent method using Single Particle Extinction and Scattering (SPES) was developed to follow the NM size upon incubation in serum [163]. This optical method uses light scattering on a particle by particle analysis to study NMs distribution in presence of biological fluids. This prototype considers two parameters for size measurements, namely the polarizability and the optical thickness of the NM. This study about *in situ* size measurement has also been done using TRPS [125,164]. These methods could

complement current batch size measurements by DLS, all providing a biological relevance added to the pristine NM diameter measured so far.

Finally, complement system activation assays give indications on possible risks of complement activation related pseudo allergy (CARPA) [165-166]. An *in vitro* assessment of complement activation could be required by health authorities prior to batch release. We proposed the establishment of an indicator of complement C3 activation ($C3A_{50}$) for the characterization of NMs' tendency to activate the complement system [167]. The value of this indicator differs depending on the nanoparticle's surface characteristics and is sensitive to the architecture of macromolecules grafted on the nanoparticle surface. The method using 2D-electrophoresis was optimized for a high-throughput sample analysis.

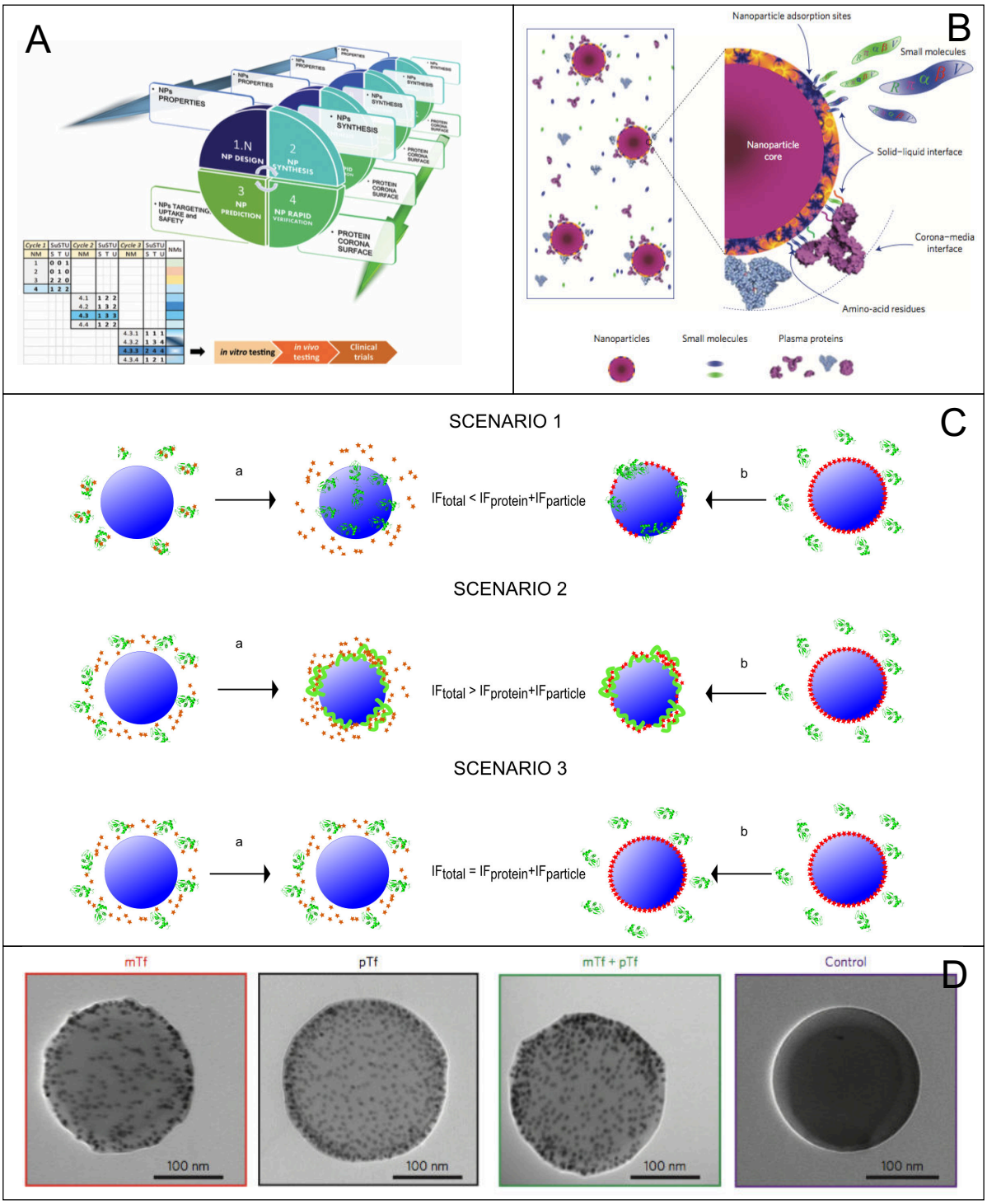

Figure 3: Candidate methods for a new routine characterization of NMs. A: Principle of the SUSTU integrated platform. B: Illustration of the BSAI index determination. C: Fluorescence scenarios for NPs adsorption characterization. D: Epitope mapping for ligand attachment characterization ((A) was reproduced from [159] with permission of the Royal Society of chemistry, (B) was reprinted from [161] and (D) from [152] with permission from Macmillan Publishers Ltd, copyright (2010), (C) was reproduced from [160]).

VI. Conclusion

Facing the current hurdles of translation of NMs, a smarter characterization of nanomaterials is urgently needed. Regulatory agencies have worked on the gap between conventional drug and nanomedicines establishing new guidelines, defining properties specific to nanomaterials. These guidelines for NM batch release focus on the description of intrinsic properties of nanomaterials composing nanomedicines, whereas it is pointed out that the biological identity formed *in vivo* is the one driving the fate of the NM. Even for these key physicochemical parameters that seems to be the best controlled until now, many improvements are needed to achieve a more precise and robust investigation. However, the sensitivity found in biological system does not allow for such a “macro-characterization” of nanomaterials as it is the case now. An effort on methods development, accessibility, automation, relevance and sensitivity is upcoming. This passes by the improvement of certain current methods, the establishment of new ones, and the introduction of biological components in routine tests. A better control of NM batches is expected to come from these new methods and some with biological components may be relevant to detect critical points for *in vivo* reproducibility.

Acknowledgments

BPI-France, project NICE

VII. Abbreviations

AFM: Atomic force microscopy
API: Active pharmaceutical ingredient
BSAI: Biological Surface Adsorption Index
CARPA: Complement activation related pseudo allergy
CRO: Contract research organization
DCS: Differential centrifugal sedimentation
DLS: Dynamic light scattering
ELS: Electrophoresis light scattering
EM: Electron microscopy
EMA: European medicine agency
EPR: Enhanced permeation and retention
EUNCL: European Nanomedicine Characterization Laboratory
FDA: Food and drug administration
FFF: Field flow fractionation
GC-MS: Gas chromatography - mass spectrometry
ISO: International Standard Organization
LC-MS: Liquid chromatography-mass spectrometry
MALS: Multi-angle light scattering
NC: Nanocarrier
NCL: Nanotechnology Characterization Laboratory
N. Meningitidis: *Neisseria Meningitidis*
NM: Nanomedicine
NMR: Nuclear magnetic resonance
NP: Nanoparticle
OECD: Organization for Economic Co-operation and Development
PD: Pharmacodynamics
PEG: Polyethylene glycol
PK: Pharmacokinetics
PTA: Particle tracking analysis
SAXS: Small angle X-ray scattering
SEC: Size exclusion chromatography
SEM: Scanning electron microscopy
SIMS: Secondary ion mass spectrometry
SPE: Solid phase extraction
SUSTU: SUrface proteo- mics, Safety, Targeting, Uptake
TEM: Transmission electron microscopy
TRPS: Tunable resistive pulse sensing
WAXS: Wide angle X-ray scattering

VIII. Bibliography

1) Leem Comité Biotech – Applications des nanotechnologies à la médecine. https://www.etp-nanomedicine.eu/public/press-documents/publications/public-documents/bionest-partners-2014-nanomedicine-study-leem/Rapport final version definitive.pdf (2013). *Consulted on August 2017*
2) Ventola, C. L. The nanomedicine revolution: part 1: emerging concepts. *Pharmacy and Therapeutics* **37,** 512 (2012).
3) Wang, Y.-F., Liu, L., Xue, X., & Liang, X.-J. Nanoparticle-based drug delivery systems: What can they really do *in vivo*? *F1000Research* **6**, 681 (2017).
4) Sainz, V., Conniot, J., Matos, A. I., Peres, C., Zupanŏiŏ, E., Moura, L., Silva, L. C., Florindo, H. F. & Gaspar, R. S. Regulatory aspects on nanomedicines. *Biochemical and Biophysical Research Communications* **468,** 504–510 (2015).
5) Tinkle, S., McNeil, S. E., Mühlebach, S., Bawa, R., Borchard, G., Barenholz, Y. C., Tamarkin, L. & Desai, N. Nanomedicines: addressing the scientific and regulatory gap: Nanomedicines. *Annals of the New York Academy of Sciences* **1313,** 35–56 (2014).
6) Weissig, V., Pettinger, T. & Murdock, N. Nanopharmaceuticals (part 1): products on the market. *International Journal of Nanomedicine* 4357 (2014).
7) Ragelle, H., Danhier, F., Préat, V., Langer, R. & Anderson, D. G. Nanoparticle-based drug delivery systems: a commercial and regulatory outlook as the field matures. *Expert Opinion on Drug Delivery* **14,** 851–864 (2017).
8) Landesman-Milo, D. & Peer, D. Transforming Nanomedicines From Lab Scale Production to Novel Clinical Modality. *Bioconjugate Chemistry* **27,** 855–862 (2016).
9) Peer, D., Cornier, J., Van de Voorde, M., Cornier, J., Owen, A., Kwade, A. & Van de Voorde, M. in *Pharmaceutical Nanotechnology: Innovation and Production* 735–742 (Wiley-VCH Verlag GmbH & Co. KGaA, 2017).
10) P, B. Nanomedicines can Offer Improved Therapeutic Efficacy through Various Parenteral Routes of Administration. *Journal of Nanomedicine & Nanotechnology* **07,** (2016).
11) Mansour, H. & Park, C.-W. in *The Clinical Nanomedicine Handbook* 321–338 (CRC Press, 2013).
12) Neagu, M., Piperigkou, Z., Karamanou, K., Engin, A. B., Docea, A. O., Constantin, C., Negrei, C., Nikitovic, D. & Tsatsakis, A. Protein bio-corona: critical issue in immune nanotoxicology. *Archives of Toxicology* **91,** 1031–1048 (2017).
13) Gunawan, C., Lim, M., Marquis, C. P. & Amal, R. Nanoparticle-protein corona complexes govern the biological fates and functions of nanoparticles. *J. Mater. Chem. B* **2,** 2060–2083 (2014).
14) Alexis, F., Pridgen, E., Molnar, L. K. & Farokhzad, O. C. Factors Affecting the Clearance and Biodistribution of Polymeric Nanoparticles. *Molecular Pharmaceutics* **5,** 505–515 (2008).
15) Peracchia, M. T., Desmaële, D., Vauthier, C., Labarre, D., Fattal, E., d'Angelo, J. & Couvreur, P. in *Targeting of Drugs 6: Strategies for Stealth Therapeutic Systems* (eds. Gregoriadis, G. & McCormack, B.) 225–239 (Springer US, 1998).
16) Verrecchia, T., Spenlehauer, G., Bazile, D. V., Murry-Brelier, A., Archimbaud, Y. & Veillard, M. Non-stealth (poly (lactic acid/albumin)) and stealth (poly (lactic acid-polyethylene glycol)) nanoparticles as injectable drug carriers. *Journal of Controlled Release* **36,** 49–61 (1995).
17) Bazile, D., Prud'homme, C., Bassoullet, M.-T., Marlard, M., Spenlehauer, G. & Veillard, M. Stealth Me. PEG-PLA nanoparticles avoid uptake by the mononuclear phagocytes system. *Journal of pharmaceutical sciences* **84,** 493–498 (1995).
18) Gref, R., Domb, A., Quellec, P., Blunk, T., Müller, R. H., Verbavatz, J. M. & Langer, R. The controlled intravenous delivery of drugs using PEG-coated sterically stabilized nanospheres. *Advanced Drug Delivery Reviews* **16,** 215–233 (1995).
19) Passirani, C., Barratt, G., Devissaguet, J.-P. & Labarre, D. Interactions of nanoparticles bearing heparin or dextran covalently bound to poly (methyl methacrylate) with the complement system. *Life sciences* **62,** 775–785 (1998).

20) Polo, E., Castagnola, V., Dawson, K. A., Cornier, J., Owen, A., Kwade, A. & Van de Voorde, M. in *Pharmaceutical Nanotechnology: Innovation and Production* 63–80 (Wiley-VCH Verlag GmbH & Co. KGaA, 2017).
21) Fadeel, B., Feliu, N., Vogt, C., Abdelmonem, A. M. & Parak, W. J. Bridge over troubled waters: understanding the synthetic and biological identities of engineered nanomaterials: Bridging nanotoxicology and nanomedicine. *Wiley Interdisciplinary Reviews: Nanomedicine and Nanobiotechnology* **5,** 111–129 (2013).
22) Salvador Morales, C., Khorasani, A. A. & Weaver, J. Closing the gap: accelerating the translational process in nanomedicine by proposing standardized characterization techniques. *International Journal of Nanomedicine* 5729 (2014).
23) Wilhelm, S., Tavares, A. J., Dai, Q., Ohta, S., Audet, J., Dvorak, H. F. & Chan, W. C. W. Analysis of nanoparticle delivery to tumours. *Nature Reviews Materials* **1,** 16014 (2016).
24) Walkey, C. D. & Chan, W. C. W. Understanding and controlling the interaction of nanomaterials with proteins in a physiological environment. *Chem. Soc. Rev.* **41,** 2780–2799 (2012).
25) Foroozandeh, P. & Aziz, A. A. Merging Worlds of Nanomaterials and Biological Environment: Factors Governing Protein Corona Formation on Nanoparticles and Its Biological Consequences. *Nanoscale Research Letters* **10,** (2015).
26) Nguyen, V. H. & Lee, B.-J. Protein corona: a new approach for nanomedicine design. *International Journal of Nanomedicine* **Volume 12,** 3137–3151 (2017).
27) Kharazian, B., Hadipour, N. L. & Ejtehadi, M. R. Understanding the nanoparticle–protein corona complexes using computational and experimental methods. *The International Journal of Biochemistry & Cell Biology* **75,** 162–174 (2016).
28) Schäffler, M., Semmler-Behnke, M., Sarioglu, H., Takenaka, S., Wenk, A., Schleh, C., Hauck, S. M., Johnston, B. D. & Kreyling, W. G. Serum protein identification and quantification of the corona of 5, 15 and 80 nm gold nanoparticles. *Nanotechnology* **24,** 265103 (2013).
29) Walkey, C. D., Olsen, J. B., Song, F., Liu, R., Guo, H., Olsen, D. W. H., Cohen, Y., Emili, A. & Chan, W. C. W. Protein Corona Fingerprinting Predicts the Cellular Interaction of Gold and Silver Nanoparticles. *ACS Nano* **8,** 2439–2455 (2014).
30) Tenzer, S., Docter, D., Rosfa, S., Wlodarski, A., Kuharev, J., Rekik, A., Knauer, S. K., Bantz, C., Nawroth, T., Bier, C., Sirirattanapan, J., Mann, W., Treuel, L., Zellner, R., Maskos, M., Schild, H. & Stauber, R. H. Nanoparticle Size Is a Critical Physicochemical Determinant of the Human Blood Plasma Corona: A Comprehensive Quantitative Proteomic Analysis. *ACS Nano* **5,** 7155–7167 (2011).
31) Lundqvist, M., Stigler, J., Elia, G., Lynch, I., Cedervall, T. & Dawson, K. A. Nanoparticle size and surface properties determine the protein corona with possible implications for biological impacts. *Proceedings of the National Academy of Sciences* **105,** 14265–14270 (2008).
32) Clemments, A. M., Botella, P. & Landry, C. C. Protein Adsorption From Biofluids on Silica Nanoparticles: Corona Analysis as a Function of Particle Diameter and Porosity. *ACS Applied Materials & Interfaces* **7,** 21682–21689 (2015).
33) Gagner, J. E., Lopez, M. D., Dordick, J. S. & Siegel, R. W. Effect of gold nanoparticle morphology on adsorbed protein structure and function. *Biomaterials* **32,** 7241–7252 (2011).
34) Saha, K., Rahimi, M., Yazdani, M., Kim, S. T., Moyano, D. F., Hou, S., Das, R., Mout, R., Rezaee, F., Mahmoudi, M. & Rotello, V. M. Regulation of Macrophage Recognition through the Interplay of Nanoparticle Surface Functionality and Protein Corona. *ACS Nano* **10,** 4421–4430 (2016).
35) Lai, W., Wang, Q., Li, L., Hu, Z., Chen, J. & Fang, Q. Interaction of gold and silver nanoparticles with human plasma: Analysis of protein corona reveals specific binding patterns. *Colloids and Surfaces B: Biointerfaces* **152,** 317–325 (2017).
36) Kurtz-Chalot, A., Villiers, C., Pourchez, J., Boudard, D., Martini, M., Marche, P. N., Cottier, M. & Forest, V. Impact of silica nanoparticle surface chemistry on protein corona formation and consequential interactions with biological cells. *Materials Science and Engineering: C* **75,** 16–24 (2017).

37) Sakulkhu, U., Mahmoudi, M., Maurizi, L., Coullerez, G., Hofmann-Amtenbrink, M., Vries, M., Motazacker, M., Rezaee, F. & Hofmann, H. Significance of surface charge and shell material of superparamagnetic iron oxide nanoparticle (SPION) based core/shell nanoparticles on the composition of the protein corona. *Biomater. Sci.* **3,** 265–278 (2015).
38) Vogt, C., Pernemalm, M., Kohonen, P., Laurent, S., Hultenby, K., Vahter, M., Lehtiö, J., Toprak, M. S. & Fadeel, B. Proteomics Analysis Reveals Distinct Corona Composition on Magnetic Nanoparticles with Different Surface Coatings: Implications for Interactions with Primary Human Macrophages. *PLOS ONE* **10,** e0129008 (2015).
39) Leroux, J.-C., Gravel, P., Balant, L., Volet, B., Anner, B. M., Allémann, E., Doelker, E. & Gurny, R. Internalization of poly(D,L-1actic acid) nanoparticles by isolated human leukocytes and analysis of plasma proteins adsorbed onto the particles. *Journal of Biomedical Materials Research* **28,** 471–481 (1994).
40) Gref, R., Lück, M., Quellec, P., Marchand, M., Dellacherie, E., Harnisch, S., Blunk, T. & Müller, R. . 'Stealth' corona-core nanoparticles surface modified by polyethylene glycol (PEG): influences of the corona (PEG chain length and surface density) and of the core composition on phagocytic uptake and plasma protein adsorption. *Colloids and Surfaces B: Biointerfaces* **18,** 301–313 (2000).
41) Peracchia, M. T., Harnisch, S., Pinto-Alphandary, H., Gulik, A., Dedieu, J. C., Desmaele, D., d'Angelo, J., Müller, R. H. & Couvreur, P. Visualization of in vitro protein-rejecting properties of PEGylated stealth® polycyanoacrylate nanoparticles. *Biomaterials* **20,** 1269–1275 (1999).
42) Lemarchand, C., Gref, R. & Couvreur, P. Polysaccharide-decorated nanoparticles. *European Journal of Pharmaceutics and Biopharmaceutics* **58,** 327–341 (2004).
43) Labarre, D., Vauthier, C., Chauvierre, C., Petri, B., Muller, R. & Chehimi, M. Interactions of blood proteins with poly(isobutylcyanoacrylate) nanoparticles decorated with a polysaccharidic brush. *Biomaterials* **26,** 5075–5084 (2005).
44) Müller, J., Bauer, K. N., Prozeller, D., Simon, J., Mailänder, V., Wurm, F. R., Winzen, S. & Landfester, K. Coating nanoparticles with tunable surfactants facilitates control over the protein corona. *Biomaterials* **115,** 1–8 (2017).
45) Walkey, C. D., Olsen, J. B., Guo, H., Emili, A. & Chan, W. C. W. Nanoparticle Size and Surface Chemistry Determine Serum Protein Adsorption and Macrophage Uptake. *Journal of the American Chemical Society* **134,** 2139–2147 (2012).
46) Pozzi, D., Colapicchioni, V., Caracciolo, G., Piovesana, S., Capriotti, A. L., Palchetti, S., De Grossi, S., Riccioli, A., Amenitsch, H. & Laganà, A. Effect of polyethyleneglycol (PEG) chain length on the bio–nano-interactions between PEGylated lipid nanoparticles and biological fluids: from nanostructure to uptake in cancer cells. *Nanoscale* **6,** 2782 (2014).
47) Pozzi, D., Caracciolo, G., Capriotti, A. L., Cavaliere, C., La Barbera, G., Anchordoquy, T. J. & Laganà, A. Surface chemistry and serum type both determine the nanoparticle–protein corona. *Journal of Proteomics* **119,** 209–217 (2015).
48) Aggarwal, P., Hall, J. B., McLeland, C. B., Dobrovolskaia, M. A. & McNeil, S. E. Nanoparticle interaction with plasma proteins as it relates to particle biodistribution, biocompatibility and therapeutic efficacy. *Advanced Drug Delivery Reviews* **61,** 428–437 (2009).
49) Dobrovolskaia, M. A., Neun, B. W., Man, S., Ye, X., Hansen, M., Patri, A. K., Crist, R. M. & McNeil, S. E. Protein corona composition does not accurately predict hematocompatibility of colloidal gold nanoparticles. *Nanomedicine: Nanotechnology, Biology and Medicine* **10,** 1453–1463 (2014).
50) Ilinskaya, A. N. & Dobrovolskaia, M. A. Nanoparticles and the blood coagulation system. Part I: benefits of nanotechnology. *Nanomedicine* **8,** 773–784 (2013).
51) Ilinskaya, A. N. & Dobrovolskaia, M. A. Nanoparticles and the blood coagulation system. Part II: safety concerns. *Nanomedicine* **8,** 969–981 (2013).
52) Thomas, S. N., van der Vlies, A. J., O'Neil, C. P., Reddy, S. T., Yu, S. S., Giorgio, T. D., Swartz, M. A. & Hubbell, J. A. Engineering complement activation on polypropylene sulfide vaccine nanoparticles. *Biomaterials* **32,** 2194–2203 (2011).

53) Salvador-Morales, C., Zhang, L., Langer, R. & Farokhzad, O. C. Immunocompatibility properties of lipid–polymer hybrid nanoparticles with heterogeneous surface functional groups. *Biomaterials* **30,** 2231–2240 (2009).
54) Vonarbourg, A., Passirani, C., Saulnier, P. & Benoit, J.-P. Parameters influencing the stealthiness of colloidal drug delivery systems. *Biomaterials* **27,** 4356–4373 (2006).
55) Peracchia, M. T., Vauthier, C., Passirani, C., Couvreur, P. & Labarre, D. Complement consumption by poly(ethylene glycol) in different conformations chemically coupled to poly(isobutyl 2-cyanoacrylate) nanoparticles. *Life Sciences* **61,** 749–761 (1997).
56) Vittaz, M., Bazile, D., Spenlehauer, G., Verrecchia, T., Veillard, M., Puisieux, F. & Labarre, D. Effect of PEO surface density on long-circulating PLA-PEO nanoparticles which are very low complement activators. *Biomaterials* **17,** 1575–1581 (1996).
57) Hamad, I., Al-Hanbali, O., Hunter, A. C., Rutt, K. J., Andresen, T. L. & Moghimi, S. M. Distinct Polymer Architecture Mediates Switching of Complement Activation Pathways at the Nanosphere−Serum Interface: Implications for Stealth Nanoparticle Engineering. *ACS Nano* **4,** 6629–6638 (2010).
58) D'Addio, S. M., Saad, W., Ansell, S. M., Squiers, J. J., Adamson, D. H., Herrera-Alonso, M., Wohl, A. R., Hoye, T. R., Macosko, C. W., Mayer, L. D., Vauthier, C. & Prud'homme, R. K. Effects of block copolymer properties on nanocarrier protection from in vivo clearance. *Journal of Controlled Release* **162,** 208–217 (2012).
59) Chen, C. C. & Borden, M. A. The role of poly(ethylene glycol) brush architecture in complement activation on targeted microbubble surfaces. *Biomaterials* **32,** 6579–6587 (2011).
60) Bertholon, I., Vauthier, C. & Labarre, D. Complement Activation by Core–Shell Poly(isobutylcyanoacrylate)–Polysaccharide Nanoparticles: Influences of Surface Morphology, Length, and Type of Polysaccharide. *Pharmaceutical Research* **23,** 1313–1323 (2006).
61) Zandanel, C. & Vauthier, C. Poly(isobutylcyanoacrylate) Nanoparticles Decorated with Chitosan: Effect of Conformation of Chitosan Chains at the Surface on Complement Activation Properties. *Journal of Colloid Science and Biotechnology* **1,** 68–81 (2012).
62) Labarre, D. The Interactions between Blood and Polymeric Nanoparticles Depend on the Nature and Structure of the Hydrogel Covering the Surface. *Polymers* **4,** 986–996 (2012).
63) Coty, J.-B., Eleamen Oliveira, E. & Vauthier, C. Tuning complement activation and pathway through controlled molecular architecture of dextran chains in nanoparticle corona. *International Journal of Pharmaceutics* **532**, 769-778 (2017).
64) Yu, K., Lai, B. F. L., Foley, J. H., Krisinger, M. J., Conway, E. M. & Kizhakkedathu, J. N. Modulation of Complement Activation and Amplification on Nanoparticle Surfaces by Glycopolymer Conformation and Chemistry. *ACS Nano* **8,** 7687–7703 (2014).
65) Kumar Khanna, V. Targeted Delivery of Nanomedicines. *ISRN Pharmacology* **2012,** 1–9 (2012).
66) Gao, H., Yang, Z., Zhang, S., Cao, S., Shen, S., Pang, Z. & Jiang, X. Ligand modified nanoparticles increases cell uptake, alters endocytosis and elevates glioma distribution and internalization. *Scientific Reports* **3,** (2013).
67) Yao, V. J., D'Angelo, S., Butler, K. S., Theron, C., Smith, T. L., Marchiò, S., Gelovani, J. G., Sidman, R. L., Dobroff, A. S., Brinker, C. J., Bradbury, A. R. M., Arap, W. & Pasqualini, R. Ligand-targeted theranostic nanomedicines against cancer. *Journal of Controlled Release* **240,** 267–286 (2016).
68) Yameen, B., Choi, W. I., Vilos, C., Swami, A., Shi, J. & Farokhzad, O. C. Insight into nanoparticle cellular uptake and intracellular targeting. *Journal of Controlled Release* **190,** 485–499 (2014).
69) Behzadi, S., Serpooshan, V., Tao, W., Hamaly, M. A., Alkawareek, M. Y., Dreaden, E. C., Brown, D., Alkilany, A. M., Farokhzad, O. C. & Mahmoudi, M. Cellular uptake of nanoparticles: journey inside the cell. *Chem. Soc. Rev.* **46,** 4218–4244 (2017).
70) Hillaireau, H. in *Polymer Nanoparticles for Nanomedicines: A Guide for their Design, Preparation and Development* (eds. Vauthier, C. & Ponchel, G.) 291–323 (Springer International Publishing, 2016).
71) Hillaireau, H. & Couvreur, P. Nanocarriers' entry into the cell: relevance to drug delivery. *Cellular and Molecular Life Sciences* **66,** 2873–2896 (2009).

72) Seo, S.-J., Chen, M., Wang, H., Kang, M. S., Leong, K. W. & Kim, H.-W. Extra- and intra-cellular fate of nanocarriers under dynamic interactions with biology. *Nano Today* **14,** 84–99 (2017).
73) Carnovale, C., Bryant, G., Shukla, R. & Bansal, V. Size, shape and surface chemistry of nano-gold dictate its cellular interactions, uptake and toxicity. *Progress in Materials Science* **83,** 152–190 (2016).
74) Kang, J. H., Jang, W. Y. & Ko, Y. T. The Effect of Surface Charges on the Cellular Uptake of Liposomes Investigated by Live Cell Imaging. *Pharmaceutical Research* **34,** 704–717 (2017).
75) Lira, M. C. B., Santos-Magalhães, N. S., Nicolas, V., Marsaud, V., Silva, M. P. C., Ponchel, G. & Vauthier, C. Cytotoxicity and cellular uptake of newly synthesized fucoidan-coated nanoparticles. *European Journal of Pharmaceutics and Biopharmaceutics* **79,** 162–170 (2011).
76) Beck, M., Mandal, T., Buske, C. & Lindén, M. Serum protein adsorption enhances active leukemia stem cell targeting of mesoporous silica nanoparticles. *ACS Applied Materials & Interfaces* (2017).
77) Barrán-Berdón, A. L., Pozzi, D., Caracciolo, G., Capriotti, A. L., Caruso, G., Cavaliere, C., Riccioli, A., Palchetti, S. & Laganà, A. Time Evolution of Nanoparticle–Protein Corona in Human Plasma: Relevance for Targeted Drug Delivery. *Langmuir* **29,** 6485–6494 (2013).
78) Bigdeli, A., Palchetti, S., Pozzi, D., Hormozi-Nezhad, M. R., Baldelli Bombelli, F., Caracciolo, G. & Mahmoudi, M. Exploring Cellular Interactions of Liposomes Using Protein Corona Fingerprints and Physicochemical Properties. *ACS Nano* **10,** 3723–3737 (2016).
79) Lynch, I., Afantitis, A., Leonis, G., Melagraki, G. & Valsami-Jones, E. in *Advances in QSAR Modeling: Applications in Pharmaceutical, Chemical, Food, Agricultural and Environmental Sciences* (ed. Roy, K.) 385–424 (Springer International Publishing, 2017).
80) Caracciolo, G., Farokhzad, O. C. & Mahmoudi, M. Biological Identity of Nanoparticles In Vivo: Clinical Implications of the Protein Corona. *Trends in Biotechnology* **35,** 257–264 (2017).
81) Spinosa, M. R., Progida, C., Talà, A., Cogli, L., Alifano, P. & Bucci, C. The Neisseria meningitidis Capsule Is Important for Intracellular Survival in Human Cells. *Infection and Immunity* **75,** 3594–3603 (2007).
82) Swartley, J. S., Marfin, A. A., Edupuganti, S., Liu, L.-J., Cieslak, P., Perkins, B., Wenger, J. D. & Stephens, D. S. Capsule switching of Neisseria meningitidis. *Proceedings of the National Academy of Sciences* **94,** 271–276 (1997).
83) Huve, P. Comprendre et éviter la capture des nanoparticules de poly(acide-lactique) par le système des phagocytes mononucléaires – Thèse de doctorat (1994).
84) Jennings, H. J. & Lugowski, C. Immunochemistry of groups A, B, and C meningococcal polysaccharide-tetanus toxoid conjugates. *J. Immunol.* **127,** 1011 (1981).
85) Kahler, C. M., Martin, L. E., Shih, G. C., Rahman, M. M., Carlson, R. W. & Stephens, D. S. The (α2→8)-linked polysialic acid capsule and lipooligosaccharide structure both contribute to the ability of serogroup B Neisseria meningitidis to resist the bactericidal activity of normal human serum. *Infection and immunity* **66,** 5939–5947 (1998).
86) Tzeng, Y.-L. & Stephens, D. S. Epidemiology and pathogenesis of Neisseria meningitidis. *Microbes and infection* **2,** 687–700 (2000).
87) Finne, J., Bitter-Suermann, D., Goridis, C. & Finne, U. An IgG monoclonal antibody to group B meningococci cross-reacts with developmentally regulated polysialic acid units of glycoproteins in neural and extraneural tissues. *J. Immunol.* **138,** 4402 (1987).
88) Fang, X., Fang, Y., Liu, L., Liu, G. & Wu, J. Mapping Paratope on Antithrombotic Antibody 6B4 to Epitope on Platelet Glycoprotein Ibalpha via Molecular Dynamic Simulations. *PLoS ONE* **7,** e42263 (2012).
89) Frank, S. A. *Immunology and evolution of infectious disease*. *Chapter 4, Specificity and Cross-Reactivity* (Princeton University Press, 2002).
90) Kaur, I. P., Kakkar, V., Deol, P. K., Yadav, M., Singh, M. & Sharma, I. Issues and concerns in nanotech product development and its commercialization. *Journal of Controlled Release* **193,** 51–62 (2014).
91) Wei, A., Mehtala, J. G. & Patri, A. K. Challenges and opportunities in the advancement of nanomedicines. *Journal of Controlled Release* **164,** 236–246 (2012).

92) Borgos, S. E. F., Cornier, J., Owen, A., Kwade, A. & Van de Voorde, M. in *Pharmaceutical Nanotechnology: Innovation and Production* 135–156 (Wiley-VCH Verlag GmbH & Co. KGaA, 2017).
93) Stern, S., McNeil, S., Patri, A. & Dobrovolskaia, M. in *Nanotechnology for Cancer Therapy* 105–137 (CRC Press, 2006).
94) NCL assay cascade protocols. https://ncl.cancer.gov/resources/assay-cascade-protocols *Consulted on August 2017*
95) Ashford, M., Cornier, J., Owen, A., Kwade, A. & Van de Voorde, M. in *Pharmaceutical Nanotechnology: Innovation and Production* 697–734 (Wiley-VCH Verlag GmbH & Co. KGaA, 2017).
96) Szebeni, J. & Storm, G. Complement activation as a bioequivalence issue relevant to the development of generic liposomes and other nanoparticulate drugs. *Biochemical and Biophysical Research Communications* **468,** 490–497 (2015).
97) Moghimi, S.M. & Farhangrazi, Z.S. Defining and characterizing nonbiological complex drugs (NBCDs) — is size enough? The case for liposomal doxorubicin generics ('liposomal nanosimilars') for injection. *Generics and Biosimilars Initiative Journal* **3**, 56–57 (2014).
98) Wibroe, P. P., Ahmadvand, D., Oghabian, M. A., Yaghmur, A. & Moghimi, S. M. An integrated assessment of morphology, size, and complement activation of the PEGylated liposomal doxorubicin products Doxil®, Caelyx®, DOXOrubicin, and SinaDoxosome. *Journal of Controlled Release* **221,** 1–8 (2016).
99) EU-NCL assay cascade protocols. http://www.euncl.eu/about-us/assay-cascade/ *Consulted on August 2017*
100) Papaluca, M., Ehmann, F., Pita, R., Hernan, D., Cornier, J., Owen, A., Kwade, A. & Van de Voorde, M. in *Pharmaceutical Nanotechnology: Innovation and Production* 497–520 (Wiley-VCH Verlag GmbH & Co. KGaA, 2017).
101) Xu, X. & Khan, M. A. in *Polymer Nanoparticles for Nanomedicines: A Guide for their Design, Preparation and Development* (eds. Vauthier, C. & Ponchel, G.) 615–633 (Springer International Publishing, 2016).
102) Desai, N. Challenges in Development of Nanoparticle-Based Therapeutics. *The AAPS Journal* **14,** 282–295 (2012).
103) Chen, R. & Riviere, J. E. Biological and environmental surface interactions of nanomaterials: characterization, modeling, and prediction: Biological and environmental surface interactions of nanomaterials. *Wiley Interdisciplinary Reviews: Nanomedicine and Nanobiotechnology* **9,** e1440 (2017).
104) FDA Nanotechnology Task Force Report 2007 https://www.fda.gov/ScienceResearch/SpecialTopics/Nanotechnology/ucm2006659.htm (2007). *Consulted on August 2017*
105) EMA Reflection paper on surface coatings: general issues for consideration regarding parenteral administration of coated nanomedicine products. http://www.ema.europa.eu/docs/en_GB/document_library/Scientific_guideline/2013/08/WC500147874.pdf (2013). *Consulted on August 2017*
106) EMA Reflection paper on the data requirements for intravenous liposomal products developed with reference to an innovator liposomal product. http://www.ema.europa.eu/docs/en_GB/document_library/Scientific_guideline/2013/03/WC500140351.pdf (2013). *Consulted on August 2017*
107) EMA Reflection paper on the data requirements for intravenous iron-based nano-colloidal products developed with reference to an innovator medicinal product. http://www.ema.europa.eu/docs/en_GB/document_library/Scientific_guideline/2013/03/WC500140351.pdf (2015). *Consulted on August 2017*
108) Pérez de la Ossa D.H. Quality aspects of Nano-based medicines. *at SME Workshop: Focus on quality for medicines containing chemical entities. http://www.ema.europa.eu/docs/en_GB/document_library/Presentation/2014/04/WC500165444.pdf* (2014). *Consulted on August 2017*

109) Pena, C. A FDA Perspective on Nanomedicine - Current Initiatives in the US. http://www.ema.europa.eu/docs/en_GB/document_library/Presentation/2010/09/WC500096201.pdf (2010). *Consulted on August 2017*
110) FDA guidance for industry : Safety of nanomaterials in cosmetic products. https://www.fda.gov/cosmetics/guidanceregulation/guidancedocuments/ucm300886.htm (2014). *Consulted on August 2017*
111) Tantra, R., Jarman, J. C. & Robinson, K. N. in *Nanomaterial Characterization* 1–24 (John Wiley & Sons, Inc, 2016).
112) ISO/TR 13014:2012: Nanotechnologies – Guidance on Physico-Chemical Characterization of Engineered Nanoscale Materials for Toxicologic Assessment. ISO; 2012.
113) OECD, Guidance on sample preparation and dosimetry for the safety testing of manufactured nanomaterials, in Working Party on Manufactured Nanomaterials. OECD; 2012.
114) http://www.quality-assistance.com/analytical-services/nanomedicine-products *Consulted on August 2017*
115) Ventola, C. L. The Nanomedicine Revolution: Part 3: Regulatory and Safety Challenges. *Pharmacy and Therapeutics* **37,** 631–639 (2012).
116) Clogston, J. D., Crist, R. M. & McNeil, S. E. in *Polymer Nanoparticles for Nanomedicines: A Guide for their Design, Preparation and Development* (eds. Vauthier, C. & Ponchel, G.) 187–203 (Springer International Publishing, 2016).
117) ISO/TR 18196:2016(en): Nanotechnologies — Measurement technique matrix for the characterization of nano-objects. ISO; 2016.
118) ISO 22412:2017 : Particle size analysis — Dynamic light scattering (DLS). ISO; 2017.
119) Linsinger, T.P.J., Roebben, G., Gilliland, D., Calzolai, L., Rossi, F., Gibson, N. & Klein, C. Requirements on measurements for the implementation of the European Commission definition of the term 'nanomaterial'. *JRC Reference Report* (2012).
120) Bartczak, D. & Goenaga-Infante, H. in *Nanomaterial Characterization* 63–80 (John Wiley & Sons, Inc, 2016).
121) Varenne, F., Makky, A., Gaucher-Delmas, M., Violleau, F. & Vauthier, C. Multimodal Dispersion of Nanoparticles: A Comprehensive Evaluation of Size Distribution with 9 Size Measurement Methods. *Pharmaceutical Research* **33,** 1220–1234 (2016).
122) Tian, X., Nejadnik, M. R., Baunsgaard, D., Henriksen, A., Rischel, C. & Jiskoot, W. A Comprehensive Evaluation of Nanoparticle Tracking Analysis (NanoSight) for Characterization of Proteinaceous Submicron Particles. *Journal of Pharmaceutical Sciences* **105,** 3366–3375 (2016).
123) Vogel, R., Willmott, G., Kozak, D., Roberts, G. S., Anderson, W., Groenewegen, L., Glossop, B., Barnett, A., Turner, A. & Trau, M. Quantitative Sizing of Nano/Microparticles with a Tunable Elastomeric Pore Sensor. *Anal. Chem.* **83,** 3499–3506 (2011).
124) Mat Azmi, I. D., Wu, L., Wibroe, P. P., Nilsson, C., Østergaard, J., Stürup, S., Gammelgaard, B., Urtti, A., Moghimi, S. M. & Yaghmur, A. Modulatory Effect of Human Plasma on the Internal Nanostructure and Size Characteristics of Liquid-Crystalline Nanocarriers. *Langmuir* **31,** 5042–5049 (2015).
125) Blundell, E. L. C. J., Healey, M. J., Holton, E., Sivakumaran, M., Manstana, S. & Platt, M. Characterisation of the protein corona using tunable resistive pulse sensing: determining the change and distribution of a particle's surface charge. *Analytical and Bioanalytical Chemistry* **408,** 5757–5768 (2016).
126) Arancon, R. A. D., Lin, S. H. T., Chen, G., Lin, C. S. K., Lai, J., Xu, G. & Luque, R. Nanoparticle tracking analysis of gold nanomaterials stabilized by various capping agents. *RSC Adv.* **4,** 17114–17119 (2014).
127) ISO 19430:2016(en): Particle size analysis — Particle tracking analysis (PTA) method. ISO; 2016.
128) ISO 13318-1:2001(en) Determination of particle size distribution by centrifugal liquid sedimentation methods — Part 1: General principles and guidelines. ISO; 2001.

129) Hu, M., Vink, M., Kim, C., Derr, K., Koss, J., D'Amico, K., Cheng, A., Pulokas, J., Ubarretxena-Belandia, I. & Stokes, D. Automated Electron Microscopy for Evaluating Two-dimensional Crystallization of Membrane Proteins. *Journal of Structural Biology* **171,** 102–110 (2010).
130) Laramy, C. R., Brown, K. A., O'Brien, M. N. & Mirkin, C. A. High-Throughput, Algorithmic Determination of Nanoparticle Structure from Electron Microscopy Images. *ACS Nano* **9,** 12488–12495 (2015).
131) Zhang, Y., Hung, T., Song, J. & He, J. Electron microscopy: essentials for viral structure, morphogenesis and rapid diagnosis. *Science China Life Sciences* **56,** 421–430 (2013).
132) Vale, F. F., Correia, A. C., Matos, B., Moura Nunes, J. F. & Alves de Matos, A. P. Applications of transmission electron microscopy to virus detection and identification. *Microscopy: science, technology, applications and education* **1,** (2010).
133) Goldsmith, C. S. & Miller, S. E. Modern Uses of Electron Microscopy for Detection of Viruses. *Clinical Microbiology Reviews* **22,** 552–563 (2009).
134) Plascencia-Villa, G., Bahena, D., Rodríguez, A. R., Ponce, A. & José-Yacamán, M. Advanced microscopy of star-shaped gold nanoparticles and their adsorption-uptake by macrophages. *Metallomics* **5,** 242 (2013).
135) Zhao, Y., Wang, Y., Ran, F., Cui, Y., Liu, C., Zhao, Q., Gao, Y., Wang, D. & Wang, S. A comparison between sphere and rod nanoparticles regarding their in vivo biological behavior and pharmacokinetics. *Scientific Reports* **7,** (2017).
136) Khodashenas, B. & Ghorbani, H. R. Synthesis of silver nanoparticles with different shapes. *Arabian Journal of Chemistry* (2015).
137) Toy, R., Peiris, P.M., Ghaghada, K.B. & Karathanasis E. Shaping cancer nanomedicine: the effect of particle shape on the in vivo journey of nanoparticles. *Nanomedicine* **9,** 121–134 (2013).
138) Zhao, J., Lu, H., Wong, S., Lu, M., Xiao, P. & Stenzel, M. H. Influence of nanoparticle shapes on cellular uptake of paclitaxel loaded nanoparticles in 2D and 3D cancer models. *Polym. Chem.* **8,** 3317–3326 (2017).
139) Xie, X., Liao, J., Shao, X., Li, Q. & Lin, Y. The Effect of shape on Cellular Uptake of Gold Nanoparticles in the forms of Stars, Rods, and Triangles. *Scientific Reports* **7,** (2017).
140) Allen, C., Qiu, T. A., Pramanik, S., Buchman, J. T., Krause, M. O. P. & Murphy, C. J. Research highlights: investigating the role of nanoparticle surface charge in nano–bio interactions. *Environ. Sci.: Nano* **4,** 741–746 (2017).
141) Varenne, F., Botton, J., Merlet, C., Beck-Broichsitter, M., Legrand, F.-X. & Vauthier, C. Standardization and validation of a protocol of size measurements by dynamic light scattering for monodispersed stable nanomaterial characterization. *Colloids and Surfaces A: Physicochemical and Engineering Aspects* **486,** 124–138 (2015).
142) Varenne, F., Botton, J., Merlet, C., Vachon, J.-J., Geiger, S., Infante, I. C., Chehimi, M. M. & Vauthier, C. Standardization and validation of a protocol of zeta potential measurements by electrophoretic light scattering for nanomaterial characterization. *Colloids and Surfaces A: Physicochemical and Engineering Aspects* **486,** 218–231 (2015).
143) Belsey, N. A., Shard, A. G. & Minelli, C. in *Nanomaterial Characterization* 153–178 (John Wiley & Sons, Inc, 2016).
144) Rabanel, J.-M., Hildgen, P. & Banquy, X. Assessment of PEG on polymeric particles surface, a key step in drug carrier translation. *Journal of Controlled Release* **185,** 71–87 (2014).
145) Baer, D. R., Engelhard, M. H., Johnson, G. E., Laskin, J., Lai, J., Mueller, K., Munusamy, P., Thevuthasan, S., Wang, H., Washton, N., Elder, A., Baisch, B. L., Karakoti, A., Kuchibhatla, S. V. N. T. & Moon, D. Surface characterization of nanomaterials and nanoparticles: Important needs and challenging opportunities. *Journal of Vacuum Science & Technology A: Vacuum, Surfaces, and Films* **31,** 050820 (2013).
146) Kim, Y.-P., Shon, H. K., Shin, S. K. & Lee, T. G. Probing nanoparticles and nanoparticle-conjugated biomolecules using time-of-flight secondary ion mass spectrometry. *Mass Spectrometry Reviews* **34,** 237–247 (2015).

147) Ambardekar, V. V. & Stern, S. T. in *Non-Biological Complex Drugs* (eds. Crommelin, D. J. A. & de Vlieger, J. S. B.) **20,** 261–287 (Springer International Publishing, 2015).
148) Charrueau, C. & Zandanel, C. in *Polymer Nanoparticles for Nanomedicines: A Guide for their Design, Preparation and Development* (eds. Vauthier, C. & Ponchel, G.) 439–503 (Springer International Publishing, 2016).
149) Bai, X., Liu, F., Liu, Y., Li, C., Wang, S., Zhou, H., Wang, W., Zhu, H., Winkler, D. A. & Yan, B. Toward a systematic exploration of nano-bio interactions. *Toxicology and Applied Pharmacology* **323,** 66–73 (2017).
150) Paliwal, R., Babu, R. J. & Palakurthi, S. Nanomedicine Scale-up Technologies: Feasibilities and Challenges. *AAPS PharmSciTech* **15,** 1527–1534 (2014).
151) DeLong, R. & Husrt, M. Two-dimensional fluorescence difference spectroscopy characterization of nanoparticles and their interactions. Patent US 20170131272 A1. (2017).
152) Kelly, P. M., Åberg, C., Polo, E., O'Connell, A., Cookman, J., Fallon, J., Krpetić, Ž. & Dawson, K. A. Mapping protein binding sites on the biomolecular corona of nanoparticles. *Nature Nanotechnology* **10,** 472–479 (2015).
153) Kelly, P. & Dawson, K. A method of labelling a target molecule forming part of a corona of molecules on a surfaces of a nanosized object. Patent US 20170146527. (2017).
154) Zhang, W., Ma, M., Zhang, X., Zhang, Z., Saleh, S. M. & Wang, X. Fluorescent proteins as efficient tools for evaluating the surface PEGylation of silica nanoparticles. *Methods and Applications in Fluorescence* **5,** 024003 (2017).
155) Lin, S., Mortimer, M., Chen, R., Kakinen, A., Riviere, J. E., Davis, T. P., Ding, F. & Ke, P. C. NanoEHS beyond toxicity – focusing on biocorona. *Environ. Sci.: Nano* **4,** 1433–1454 (2017).
156) Pisani, C., Gaillard, J. C., Dorandeu, C., Charnay, C., Guari, Y., Chopineau, J., Devoisselle, J. M., Armengaud, J. & Prat, O. Experimental separation steps influence the protein content of corona around mesoporous silica nanoparticles. *Nanoscale* **9,** 5769–5772 (2017).
157) Lundqvist, M., Augustsson, C., Lilja, M., Lundkvist, K., Dahlbäck, B., Linse, S. & Cedervall, T. The nanoparticle protein corona formed in human blood or human blood fractions. *PLOS ONE* **12,** e0175871 (2017).
158) Forest, V. & Pourchez, J. The nanoparticle protein corona: The myth of average. *Nano Today* **11,** 700–703 (2016).
159) Kuruvilla, J., Farinha, A. P., Bayat, N. & Cristobal, S. Surface proteomics on nanoparticles: a step to simplify the rapid prototyping of nanoparticles. *Nanoscale Horiz.* **2,** 55–64 (2017).
160) Nasir, I., Fatih, W., Svensson, A., Radu, D., Linse, S., Cabaleiro Lago, C. & Lundqvist, M. High Throughput Screening Method to Explore Protein Interactions with Nanoparticles. *PLOS ONE* **10,** e0136687 (2015).
161) Xia, X.-R., Monteiro-Riviere, N. A. & Riviere, J. E. An index for characterization of nanomaterials in biological systems. *Nature Nanotechnology* **5,** 671–675 (2010).
162) Chen, R. & Riviere, J. E. in *Modelling the Toxicity of Nanoparticles* (eds. Tran, L., Bañares, M. A. & Rallo, R.) **947,** 207–253 (Springer International Publishing, 2017).
163) Sanvito, T., Bigini, P., Cavanna, M. V., Fiordaliso, F., Violatto, M. B., Talamini, L., Salmona, M., Milani, P. & Potenza, M. A. C. Single particle extinction and scattering optical method unveils in real time the influence of the blood components on polymeric nanoparticles. *Nanomedicine: Nanotechnology, Biology and Medicine* (2017).
164) Sikora, A., Shard, A. G. & Minelli, C. Size and ζ-Potential Measurement of Silica Nanoparticles in Serum Using Tunable Resistive Pulse Sensing. *Langmuir* **32,** 2216–2224 (2016).
165) Szebeni, J. Complement activation-related pseudoallergy: A new class of drug-induced acute immune toxicity. *Toxicology* **216,** 106–121 (2005).
166) Szebeni, J. Hemocompatibility testing for nanomedicines and biologicals: predictive assays for complement mediated infusion reactions. *European Journal of Nanomedicine* **4,** (2012).
167) Coty, J.-B., Varenne, F., Vachon, J.-J. & Vauthier, C. Serial multiple crossed immunoelectrophoresis at a microscale: A stamp-sized 2D immunoanalysis of protein C3

activation caused by nanoparticles: Proteomics and 2-DE. *ELECTROPHORESIS* **37,** 2401–2409 (2016).

Partie expérimentale

Avant-propos : Une fois administrées par voie intraveineuse, les nanomédecines vont interagir avec des éléments biologiques retrouvés dans le compartiment sanguin, notamment les protéines plasmatiques. Les méthodes permettant une caractérisation des interactions entre nanomédecines et protéines plasmatiques de façon journalière pour un contrôle de ces interactions sont rares. En effet, les méthodes existantes pour étudier ce genre d'interaction souffrent soit d'un coût excessivement élevé (ex : Tests Elisa), soit d'un savoir-faire où d'une manipulation excessivement complexe limitant leur utilisation (ex : identification et quantification de la protéine corona par LC-MSMS). Dans cette partie, nous présenterons les méthodes développées au cours de ces travaux de thèse qui viennent en réponse aux problématiques evoquées ci-dessus.

Le chapitre II présente une méthode d'immunoélectrophorèse en deux dimensions revisitée et adaptée à une utilisation à haut débit en routine. Cette méthode permet de tester le pouvoir d'activation du complément de nanoparticules en mesurant la quantité de protéine C3 clivée. Il est possible d'analyser 35 échantillons sur une seule plaque d'électrophorèse.

Dans le chapitre III, cette méthode est appliquée à l'étude plus précise de la voie d'activation du complément empruntée par des nanoparticules modèles. Des modifications de composition du tampon d'incubation ont permis de privilégier et/ou bloquer le déclenchement de certaines voies de la cascade du complément afin d'identifier le mécanisme d'activation du complément prépondérant.

Le chapitre IV décrit une méthode d'étude de l'activation du complément par résonnance plasmonique de surface (SPR). Cette technique permet de mesurer de façon automatisée le degré d'activation du complément en détectant des fragments spécifiques libérés après activation.

Dans le chapitre V, une méthode de caractérisation de la surface des nanoparticules via des sondes protéiques est présentée. L'utilisation de l'électrophorèse capillaire permet une étude, sans étape de prétraitement et automatisable, de la capacité d'adsorption d'une protéine donnée sur la nanoparticule à étudier. On peut en déduire des informations sur l'accessibilité des protéines à la surface de la nanoparticule, caractérisant ainsi les propriétés de couverture des nanoparticules par les chaines de polymères hydrophiles qui y sont généralement greffées.

Chapitre II : Multi-Immunoélectrophorèse 2D miniaturisée en série : immunoanalyse de l'activation de la protéine C3 causée par les nanoparticules

Avant-propos : Le système du complément est le principal acteur de la réponse humorale du système immunitaire. Il est composé d'un ensemble de protéines dont l'activation fonctionne en une cascade de réactions biochimiques. L'activation de cette cascade conduit, dans le cas des nanomédecines (NMs), à l'opsonisation de ces dernières lorsqu'elles sont détectées par le système immunitaire, menant à leur capture par les macrophages et une accumulation dans le foie. Une description plus précise de la cascade du système du complément est donnée en *annexe méthodologique n°4*. En général, la conception des NMs est faite de telle sorte à éviter ce phénomène d'activation du complément et améliorer le profil de la biodistribution. Ceci est généralement réalisé par le greffage de macromolécules hydrophiles (PEG, polysacharides) (cf. NMs de 2ème génération) qui réduisent l'adsorption de protéines et notamment des protéines du système du complément. De plus, l'activation du système du complément est suspectée dans des réactions hyperallergiques pouvant intervenir lors de l'injection de nanomédecines (CARPA : Complement Acitvation Related Pseudo Allergy) et pouvant conduire jusqu'à la mort du patient. L'interaction des NMs avec le système du complément, bien que pouvant être à l'origine de phénomènes majeurs lors d'une utilisation en clinique, n'est pas systématiquement testée lors de la libération d'un lot clinique de NMs. Les méthodes trop complexes ou coûteuses peuvent empêcher l'établissement de tels tests en routine. Dans ce chapitre, nous proposons une méthode de test à haut débit de l'activation de la protéine C3 par immunoélectrophorèse 2D sur gel. Le principe de l'immunoélectrophorèse bidimensionnelle est rappelé en *annexe méthodologique n°1*. La méthode développée au cours de ce travail permet une analyse à haut débit du clivage de la protéine C3. Une application de cette méthode consiste à déterminer un nouvel indicateur caractérisant la capacité des NMs à activer le système du complément ($C3A_{50}$).

Publié dans : *Electrophoresis* (2016), ***37***, 2401–2409

Serial multiple crossed immunoelectrophoresis at a micro scale: a stamp-size 2D immunoanalysis of protein C3 activation caused by nanoparticles

Jean-Baptiste Coty, Fanny Varenne, Jean-Jacques Vachon, Christine Vauthier*

Institut Galien Paris-Sud, CNRS, Univ. Paris-Sud, Université Paris-Saclay, 5 rue Jean-Baptiste Clément, 92290 Châtenay-Malabry, France

***Correspondence:** Dr. Christine Vauthier, CNRS UMR 8612, Institut Galien Paris Sud, Univ. Paris-Sud, Université Paris-Saclay, 5, rue Jean-Baptiste Clément, 92296 Châtenay-Malabry, France. Fax: +33 146835946. E-mail: christine.vauthier@u-psud.fr

Abstract

Crossed immunoelectrophoresis (C-IE) is used to detect and quantify specific proteins. An application allowed the evaluation of complement system activation by nanomaterials. The work aimed to improve the C-IE toward a higher throughput and less tedious method. A new concept was implemented to prepare and run agarose gels. The 1st and the 2nd dimension of electrophoresis were performed on a single gel plate, prepared before the beginning of the analysis. Several samples were migrated simultaneously on the same migration line. Up to 35 analyses were run at once, providing stamp-sized electrophoregrams (2.8x3 cm) maintaining the performance of the original method performed on 5x7 cm gel slabs. Robustness and precision of the method were demonstrated through a validation approach using ANOVA. Handling, experimental duration, amount of reagents and overall cost of one analysis were considerably reduced compared to the original method. With the same equipment, 7 times more analyses can be performed in one run. C-IE can be used to analyze many types of proteins. The new experimental modalities were suitable for the application developed in the present work that was to evaluate activation of protein C3 of the complement system triggered by nanomaterials.

Abbreviations: 2D-IE: Two-dimensional immunoelectrophoresis, ANOVA: Analysis of Variance, C_3A_{50}: Protein C3 activation at 50%, CARPA: Complement Activation Related PseudoAllergy, C-IE: Crossed immunoelectrophoresis, D_H: Hydrodynamic diameter, DLS: Dynamic light scattering, ELS: Electrophoresis light scattering, EP: Emulsion polymerization, GUM: guide to the expression of uncertainty in measurement, IBCA: Isobutylcyanoacrylate, ICH: International Conference on Harmonisation of Technical Requirements for Registration of Pharmaceuticals for Human Use, ISO: International Organization for Standardization, NaMe: Nafamostat Mesylate, NP(s): Nanoparticle(s), M_C: Mass concentration, S_C: Surface concentration, VBS: Veronal Buffer Saline, MultiCrossed-IE: Serial multiple crossed immunoelectrophoresis at a micro scale

Keywords: Complement system, crossed immunoelectrophoresis, protein C3, robustness

I. Introduction

It is now quite well established that nanomaterials circulating in the blood, either intentionally when used as nanomedicines, or accidentally after exposition to pollutants, are subjected to recognition by the immune system [1-3]. Although still not fully established, it seems that the activation of the complement system may be one of the first event responsible for the clearance of nanomaterials from the blood, associated with uptake by macrophages of the immune system [4]. The complement system is also at the root of hypersensitivity and allergic reactions. Among them, the development of Complement Activation Related PseudoAllergy (CARPA) that is still not entirely understood, and can have a dramatic issue for patients [5, 6]. Thus, there is an interest to evaluate the propensity of a nanomaterial to activate the complement system, as it is one of the possible ways to assess its nanotoxicity.

In vitro tests on this purpose are well established including western blot, CH50 assay (Total Hemolytic Complement assay), ELISA, C-IE or immunoprecipitation tests [7-11]. Among them, the C-IE (or 2D-IE) of the complement C3 protein was not so much applied due to the tedious operating conditions, although it allows to reveal the cleavage of the protein C3 of the cascade in a non-debated manner [12-14]. Complement protein C3 is a protein that intervenes in the final pathway of the complement cascade, being common to all known pathways that trigger activation of the cascade [15, 16]**.** Measurement of protein C3 cleavage allows the assessment of complement activation, independently of the pathway triggering the activation. In the obtained electrophoregram, a first peak corresponds to native C3, which may partially or totally disappear after activation, to be replaced by a second and sometimes a third peak, corresponding to cleaved components of C3 [17]. The method can be applied on samples directly obtained from the incubation with the serum without the need to remove the tested nanomaterial, as it is the case with other methods such as CH50 assay [8] and Western Blot.

Today, there is a need for methods to the study of complement activation by a large number of nanomaterials. The demanding protocol of the C-IE hampers its development at the expense of the direct information provided from the reading and analysis of gels.

The purpose of the present work was to develop a high throughput analytical method based on C-IE, by achieving serial multiple crossed immunoelectrophoresis at a micro scale (MultiCrossed-IE) on a single agarose gel plate. Although several migrations of samples can be

achieved in parallel on a gel plate, the novelty of the work was to incorporate samples to be analyzed on the same line of migration. The new approach was applied to the investigation of the activation of component C3 of the complement system triggered by three types of known nanoparticles, tested at different levels of activation. The robustness of the method was assessed by testing the influence of sample's position on the gel plate, the electrophoresis apparatus, the analyst and the sample preparation. The precision of the method was evaluated via the intra- and inter-day variation.

The method was then applied to the evaluation of the amount of NP's surface that induces a cleavage of 50% of the native C3 into fragments (C_3A_{50}). This value could be proposed as a new parameter characterizing nanomaterials in terms of their capacity to trigger activation of the complement system, thus breaking the limit of previous methods that only allowed comparison of few nanomaterials tested for a same concentration expressed as the exposed surface.

II. Materials and Methods

II.1. Materials

Isobutylcyanoacrylate (IBCA) was purchased from Orapi (Saint-Vulbas, France). Dextran 17.7 kDa and cerium (IV) ammonium nitrate were provided by Fluka (Saint-Quentin-Fallavier, France). Dextran 66.7 kDa, Tricine, Tris base (Sigma 7-9®), Sodium chloride, EDTA sodium salt and Bromophenol blue were purchased from Sigma (Saint-Quentin-Fallavier, France). Nitric acid was supplied by Prolabo (Paris, France). Human serum was prepared from plasma provided by Etablissement Français du Sang (EFS) (Rungis, France). Polyclonal anti-human C3 antibody raised in goat was purchased from Fitzgerald antibodies (Acton, USA). Coomassie brilliant blue R-250, calcium lactate and glacial acetic acid were supplied by Thermo Fisher Scientific (Villebon-sur-Yvette, France). Gel-Fix™ for agarose (265x150 mm) was purchased from Serva Electrophoresis (Heidelberg, Germany). Nafamostat mesylate (NaMe) was obtained from Abcam (Cambridge, UK).

II.2. Nanoparticle preparation and characterization

II.2.1. Preparation of the NPs

NPs were prepared by emulsion polymerization (EP) adapting protocols proposed by Chauvierre et al. [18], according to Bertholon et al. [14]. The NPs R17 and R66 were obtained by redox radical EP using dextran 17.7 kDa and 66.7 kDa respectively. Cerium IV ammonium nitrate (2 mL, 8.10^{-2} M in HNO_3 0.2 N) and IBCA (0.5 mL) were successively added in a solution of dextran (0.136 g in 8 mL HNO_3 0.2 N, 40°C), purged with argon. The polymerization was pursued for 1h at 40°C. NP A66 was prepared by anionic EP with dextran 66.7 kDa. IBCA (0.5 mL) was added to a solution of dextran (0.136 g in 10 mL HNO_3 0.2 N, 40°C). The polymerization was pursued for 24h at 40°C. At the end the polymerization, dispersions were cooled in an ice bath and purified by dialysis against Milli-Q® water using Spectra/Por membrane (MWCO 100,000 Da, Spectrum Laboratories, Irving, USA). Purified NP dispersions were stored at 4°C until use.

II.2.2. Nanoparticle characterization

Evaluation of the size and surface charge: Hydrodynamic diameter (D_H) of nanoparticles was measured at 20°C by dynamic light scattering (DLS). Surface charge was assessed evaluating the zeta potential from measurements of the electrophoretic mobility by electrophoresis light scattering (ELS), using Smoluchowski's model. Measurements were carried out using a ZetaSizer Nano ZS90 (Malvern Instruments, Orsay, France).

Determination of the mass concentration: Mass concentration of NP in dispersions (M_C in $mg.mL^{-1}$) was determined by a gravimetric method. Known volume of the dispersion (300 µL) was freeze-dried with a Christ Alpha 1-2 LDplus (Bioblock Scientific, Illkirch, France) for 24h. The dried weight was used to determine the M_C.

Calculation of the NP surface area concentration: The surface concentration (S_C in $cm^2.mL^{-1}$) developed by the NP per mL of dispersion was calculated from Eq. 1 [19], using the mass concentration (M_C in $mg.mL^{-1}$), the D_H (in cm), and the density of tested nanoparticles (d in $mg.cm^{-3}$), which was previously reported by Vauthier et al. [20]. S_C

$$S_C = \frac{6*MC}{d*DH} \quad (1)$$

II.3. Preparation of samples to be analyzed by C-IE and MultiCrossed-IE

Human serum (25 µL) was incubated with a given surface of nanoparticles (50 µL) dispersed in Veronal Buffer Saline (VBS) (25 µL). The VBS contained 0.15 mM Ca^{2+} and 0.5 mM Mg^{2+} ions and was prepared as described by Kazatchkine et al. [21]. Samples were incubated for 1h at 37°C. Then, they were immediately cooled to 4°C in an ice bath. For the robustness and precision study, EDTA and NaMe were added in order to stop proteolytic reactions occurring in the process of complement system activation [22] (4.13 µL of EDTA disodium salt 0.5 M and 2.16 µL of NaMe at 10 $mg.mL^{-1}$). Samples were then either immediately analyzed by C-IE or stored at -20°C until use within the few next days. The surface of NP exposed in the sample (s_{sample} in $cm^2.mL^{-1}$), can be calculated using Equation 2, with the volume of NP dispersion (v in mL) in the total volume of incubation (Vtot in mL).

$$Ssample = \frac{SC*v}{Vtot} \quad (2)$$

II.4. Crossed Immunoelectrophoresis

II.4.1. C-IE classical method

The C-IE method was detailed by Walker [23], then applied to C3 protein by Passirani et al. [11]. Samples were prepared as described in 2.3. Then, 5µL of each sample were filled into wells formed on a 1% agarose gel plate (13x10 cm) for the first dimension of electrophoresis. After 1h15min of separation, bands corresponding to each sample were cut and disposed on Gel-Fix™ films (5x7 cm each). Agarose gel 1% containing the antibody was then casted on the remaining free area of the film for the second dimension electrophoresis that lasted for 18h using a Multiphor II electrophoresis system (GE Healthcare, Velizy-Villacoublay, France). Five samples were run at the same time on five different gel slabs (5x7cm).

II.4.2. New serial multiple crossed IE at a micro scale (MultiCrossed-IE)

II.4.2.1. Evaluation of the heat resistance of the antibody

The heat resistance of the antibody was assessed by radial immunodiffusion [24]. A gel plate was prepared on a Gel-Fix™ film with a solution of agarose 0.7% containing human serum (0.17 $\mu L/cm^2$ of gel), in Tricine buffer (Calcium Lactate 1 mM, TRIS 63 mM, Tricine 27 mM, in milliQ® water, pH 8.6). Wells were formed in the agarose gel to receive 4 µL of pre-heated (20, 50, 55, 60, 65, 70, 75, 80 and 90°C) antibody solutions (1.4 $mg.mL^{-1}$ in PBS) for 4 minutes. The

gels were placed in a humid chamber for 24h prior drying and staining with Coomassie blue [25]. The diameter of the precipitated rings was measured to calculate the areas of circles. The latter were plotted against the corresponding temperature at which the antibody was heated.

II.4.2.2. Preparation of the gel for MultiCrossed-IE

Agarose gel 1% (40 mL) was prepared in Tricine buffer. When the temperature of the gel reached 60°C, 1.17 mL of anti-C3 antibody at 1 $mg.mL^{-1}$ in PBS was added. After rapid homogenization, the solution was spread on a 15x20 cm Gel-Fix™ film (Fig. 1A). After solidification, five 8 mm bands were removed as illustrated in Figure 1B, C,D. Each gap was then filled with 1.8 mL of a 1% agarose gel prepared in Tricine buffer (Fig. 1E). Wells were formed at the same time using a homemade comb (Fig. 1F). A distance of 2.5 cm was left between wells, allowing seven samples to be run in series in a band of 20 cm long (i.e. 35 samples to be run in a 15x20 cm gel, Fig. 1G). A second well on the left side of each band was made under the sample well, in order to run Bromophenol blue as an indicator of migration for the first dimension of the electrophoresis.

II.4.2.3. Electrophoresis runs

The tricine buffer was used as electrophoresis buffer. The gel was placed in Multiphor II electrophoresis system (GE Healthcare, Velizy-Villacoublay, France) and wells were filled with 2.5 µL of samples for the serial migration. Bromophenol blue (1.3 $mg.mL^{-1}$, 2.5 µL) was placed in the secondary wells on the left (Fig. 1H). Samples were then subjected to the first dimension electrophoresis (600 V, 16 mA, 100 W), freely migrating in the agarose gel band according to their molecular weight and charge. Electrophoresis was stopped when the blue indicators have crossed 6 cm. Then, the gel was turned by 90° to achieve the second dimension corresponding to the rocket immunoelectrophoresis (500 V, 12 mA, 100 W), that lasted for 3h30min. Gels were dried and stained as described previously [25].

II.4.3. Scanning and quantification

The gels were scanned at a resolution of 800 dpi (Scanner Epson Perfection V100 Photo) (Fig. 1I). Area under peaks was integrated using ImageJ software (Fig. 1J). The first peak on the left side was recognized as native C3, whereas the second peak from the left was attributed to

protein fragments derived from C3 cleavage. The % of activation was expressed as the ratio of peak area of cleaved protein regarding the total peak area of C3 native and fragments.

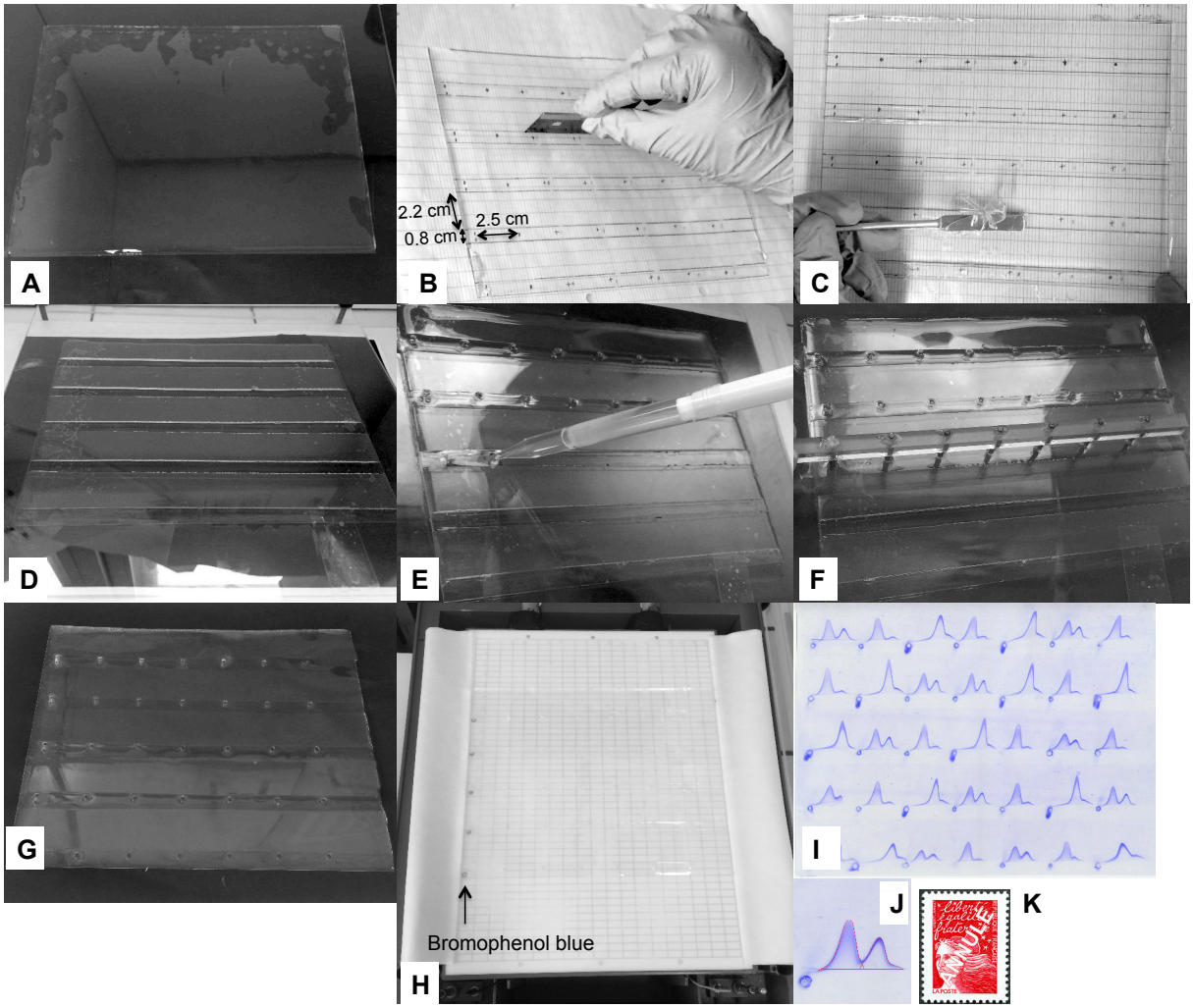

Figure 1: Preparation of the gel plates for MultiCrossed-IE. A) Agarose gel slab containing anti-C3 antibody. B) Cutting of gel bands following a template. C) Removing pre-cut bands with a spatula. D) Gel with cut bands. E) Agarose gel filling of the bands. F) Application of the comb for wells formation. G) Final gel ready for sample loading. H) Gel loaded with samples and indicator for first dimension migration. I) Numerized gel after 2D migration, staining and drying. J) Example of integration of electrophoregram peaks. K) Comparison with a stamp at the same size scale (©La Poste, 2001, Eve Luquet).

II.5. Robustness and precision of the method

II.5.1. Sample preparation

Three samples with different degrees of activation of the C3 protein were prepared from dispersions R66, R17 and A66 used at a surface concentration of 1934, 1874 and 3934 $cm^2.mL^{-1}$ respectively. These samples appropriately corresponded to low (A0), partial (A50) and full activation (A100) of the protein C3 and were prepared as mentioned in section 2.3.

II.5.2. Exploration of robustness and precision of the method

Several factors were tested in order to investigate the robustness and precision of the method, as described by ICH [26] and ISO standard [27]. The robustness of a method reflects its capacity to give unaffected results under small variation of the measurement conditions and thus give indications about its reliability for a normal usage [26, 27].

Factors considered in the robustness study were:

- The position of the sample on the slab gel. Two different gels containing the same samples disposed at different positions were run on the same day on the same electrophoresis tank.

- The electrophoresis system. Two different gels with samples at the same position in both gels were simultaneously run on two distinct electrophoresis systems.

- The influence of the analyst. Two different experimenters did the same experiment, using the same samples on the same system. Each experimenter prepared its own gel, ran the electrophoresis independently and analyzed the obtained gel after coloration.

- The sample preparation. A total of five preparations of each sample (A0, A50 or A100) were realized the same day. Each sample was analyzed on one gel slab.

The precision of a method expresses the closeness between a series of measurements under defined conditions [26, 27]. The precision was investigated through intra-day variation (repeatability) and inter-day variation (intermediate precision).

Three models of NP samples [14, 28] were repeated and analyzed for their ability to give the same activation under variations of the above mentioned experimental factors as summarized in Table 1. It is noteworthy that the gel preparation was independent for each experiment.

II.5.3. Statistical analysis of the MultiCrossed-IE

The investigation of the robustness and precision of the method was performed by means of ANOVA tests, as described in the GUM [29] and the standard ISO [30]. The General Linear Model of ANOVA test in Minitab 16.0 was used on this purpose. Briefly, ANOVA test allows determining whether one or several factors have a significant influence on the response of the measured variable, here the % activation of the protein C3. ANOVA was applied after verification of the hypotheses allowing its applicability, namely the normal distribution of residuals (Ryan-Joiner's test) and variances homoscedasticity (Levene's model).

The robustness was assessed through the factors position, system, analyst and sample preparation by means of the p-value. The p-value corresponds to the probability to find the observed, or more extreme, results when the null hypothesis is true i.e. the studied factor has no significant effect on the variable response. If the p-value is higher than the significance level fixed at 0.05 in this work, it suggests that the data are consistent with the assumption that the null hypothesis is true and the null hypothesis has to be accepted. So, the tested factor did not introduce significant difference on the response variable when p-value resulting from its associated ANOVA was higher than 0.05. The threshold for the p-value was chosen consistently with those generally found in the literature. To study the precision of the method, we assessed the intermediate precision and the repeatability via the calculation of the RSD of % C3 activation values determined for A0, A50 and A100.

A

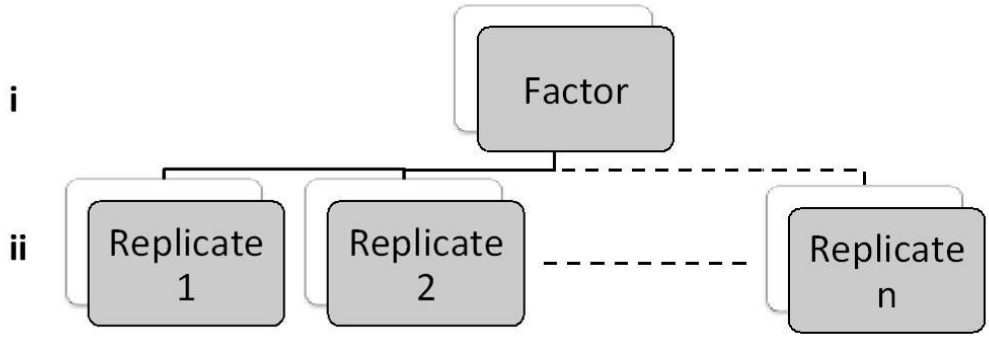

B

		A0		A50		A100	
Robustness	**i**	**ii**	**p-value**	**ii**	**p-value**	**ii**	**p-value**
Position	2	8	0.461	10	0.772	11	0.926
System	2	9	0.296	9	0.461	11	0.711
Analyst	2	9	0.135	9	0.312	7	0.146
Sample prep	5	6	0.433	6	0.786	5	0.325
Precision	**i 3**	**ii 7**	**RSD**	**ii 8**	**RSD**	**ii 8**	**RSD**
Intra-day			*19.3*		*6.5*		*2.2*
Inter-day			*3.4*		*3.2*		*0.9*

Table 1: Evaluation of robustness and precision of the MultiCrossed-IE monitoring the activation of the protein C3 by three samples of nanoparticles showing low activation (A0), medium activation (A50) and high activation (A100) of the protein C3. A: General design of ANOVA tests used for factors influence of the position of the sample (Position), electrophoresis system (System), analyst (Analyst), sample preparation (Sample prep) and day (Intra-day and Inter-day). i and ii represent the number of levels of the tested factor and the number of replicates made for a given sample in each gel respectively. B: Results of the statistical analysis by ANOVA tests. Robustness was evaluated by p-values (The factor did not introduce a significant difference for a p-value > 0.05, see paragraph 2.5.3.). Precision was assessed by RSD values.

II.6. Characterization of C3 activation induced by nanoparticles

Samples of the three types of NP were prepared with different amounts of surface area (ranging from 500 to 4950 $cm^2.mL^{-1}$) and analyzed by MultiCrossed-IE. The % of activation of protein C3 was determined and plotted against the concentration of NPs expressed in surface

area ($cm^2.mL^{-1}$). The concentration in NPs producing 50% of the cleavage of the protein C3 was defined as the C_3A_{50}.

III. Results

III.1. Nanoparticle characterization

Hydrodynamic diameter, Polydispersity index (PDI), zeta potential, mass and surface concentration of NP in dispersions are summarized in Table 2 and were consistent with those found in previous works [14, 28, 31].

NP	D_H (nm)*	PDI*	Zeta potential ** (mV)	M_C*** ($mg.mL^{-1}$)	S_C ($cm^2.mL^{-1}$)	C_3A_{50}**** ($cm^2.mL^{-1}$)
R17	193	0,03	-11.7	49.1	$13.4 \cdot 10^3$	1625
A66	88	0,1	-5,6	36.9	$22.1 \cdot 10^3$	1500
R66	281	0,04	-5.2	52.8	$9.9 \cdot 10^3$	> 4900

Measured by *DLS, **ELS, ***gravimetric method, ****MultiCrossed-IE

Table 2: Characteristics of the three dispersions of model NPs used in the study and values of C_3A_{50} determined by MultiCrossed-IE.

III.2. Heat resistance of the antibody

To prepare agarose gel plates for the MultiCrossed-IE, the agarose gel must be spread on a 15x20 cm Gel-Fix™ film. During this operation, the antibody is added to a hot agarose solution and must resist to the high temperature required to cast a homogeneous gel plate. A preliminary experiment aimed to determine the maximum temperature at which full activity of the antibody was preserved. This was assessed by a radial immunodiffusion method designed on this purpose. As shown in Figure S1, decrease of the immunodiffusion circle areas was clearly observed for anti-C3 antibody samples heated above 60°C that can be explained by the denaturation of the antibody. The full activity of the antibody was preserved after heating at 60°C which was the maximum temperature that can be used to prepare gel plates. Gels for the MultiCrossed-IE were then casted at 60°C.

III.3. MultiCrossed-IE (versus orginal method)

The gel plate was conceived to achieve the migration of 7 samples on the same horizontal line. 5 bands were built in the gel for a parallel migration of samples. Compared with the original method [11] allowing 5 samples to be analyzed at once on individual 5x7 cm gel plates, the designed serial electrophoresis provided 35 stamp-sized electrophoregrams (2.8x3 cm). It was checked that performances of the original method were preserved in the stamp-size electrophoregrams obtained from the MultiCrossed-IE (Table 3 and Fig. S2).

	Original method	**MultiCrossed-IE**
Electrophoresis Duration	19 h 15 min	4 h 45 min
Number of analyzes	5	35
Quantity of Ab/analysis	130 µg	34 µg
Volume of Gel/analysis	6.6 mL	1.4 mL
Gel-Fix™ surface/analysis	35 cm^2	8.4 cm^2
Sample consumption/ analysis	5 µL	2.5 µL
Gel plate cost/analysis	0.57 €	0.14 €
Electrophoregrams of A50 at a same size scale* - Comparison with a the size of a stamp (©La Poste, 2001, Eve Luquet)	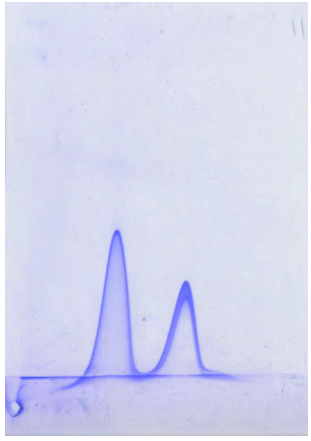	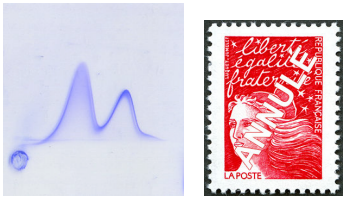

*See more in Fig. S2

Table 3: Comparison of the main features between the original method and MultiCrossed-IE.

III.4. Study of the robustness and precision of the method

For the evaluation of robustness and precision, samples A0, A50 and A100 were prepared with inhibitors of complement cascade added at the end of the incubation. Same samples could be analyzed several times to investigate the robustness and precision of the MultiCrossed-IE using statistical analysis by ANOVA. Different factors were independently assessed. Hypotheses verifications for the ANOVA analysis are shown in S3. The obtained p-values and RSDs for the different tested factors are depicted in Table 1. Results showed that there was no significant bias introduced by the position of a sample on the gel plate, the electrophoresis system, the analyst doing the experiment and the preparation of the sample. It is noteworthy that no significant difference was found even when two different analysts applied the experiment. This means that the results were not significantly different analyzing the 3 different samples (A0, A50 and A100) while the method was performed on gels made by the two independent analysts and the analyses of the electrophoregrams were carried out independently by the two analysts. Robustness was verified for a confidence level of 95% performing MultiCrossed-IE on identical samples. For the precision, RSDs of intra-day variation reflecting the repeatability and RSDs of inter-day variation corresponding to intermediate precision were summarized in the lower part of Table 1B. The RSD values found for the inter-day were below 4% for all samples (A0, A50 and A100). This indicated that there was no variation added by the day of the experiment. The repeatability remains constant from one day to another. The p-value associated to inter-day variation was also determined giving p-values of 0.814, 0.169 and 0.300 for A0, A50 and A100 respectively. As all these values were superior to 0.05 showing that no significant variation was introduced by the factor day (see paragraph 2.5.3).

III.5. Complement C3 activation triggered by nanoparticles

The interaction of nanomaterials with blood proteins is a matter of contact between these two entities and is thus driven by the amount of surface engaged in this process. Hence, the surface of NP exposed to serum proteins impacts on the strength of interaction triggered and this phenomenon can be exploited to define a characteristic of a given nanomaterial toward its ability to activate the complement cascade. Protein C3 activation patterns were studied for the three nanoparticles used as reference samples providing with different levels of activation. Investigating the % of cleaved C3 fragments produced by different amounts of NP's incubated

in serum, the surface of NP that activates 50% of protein C3 present in the sample was determined (C_3A_{50}). NPs R17 and A66 have reached full activation with the highest tested concentrations. The curve giving the % activation as a function of the concentration showed a sigmoidal shape (Fig. 2). The C_3A_{50} that could be determined were 1625 $cm^2.mL^{-1}$ (6.0 $mg.mL^{-1}$) for R17 and 1500 $cm^2.mL^{-1}$ (2.5 $mg.mL^{-1}$) for A66 (Table 2). The results were consistent with data of the literature reporting a high % of activation of these two types of NP at a tested surface of 2000 $cm^2.mL^{-1}$ [14, 28]. Nanoparticle R66 does not activate the complement above 20% up to a surface concentration of 4950 $cm^2.mL^{-1}$ (26.4 $mg.mL^{-1}$) (Fig. 4C). The activation observed was just above the level of the spontaneous activation of C3 observed in the experimental conditions used in this study (9% of activation). These results were also consistent with previous data provided at a surface of 2000 $cm^2.mL^{-1}$ [28]. The very low capacity of these NP to activate the complement system revealed here is consistent with their stealth properties reported in vivo [32] and the property of their dextran corona to hamper interactions of the NP core with protein C3 [33].

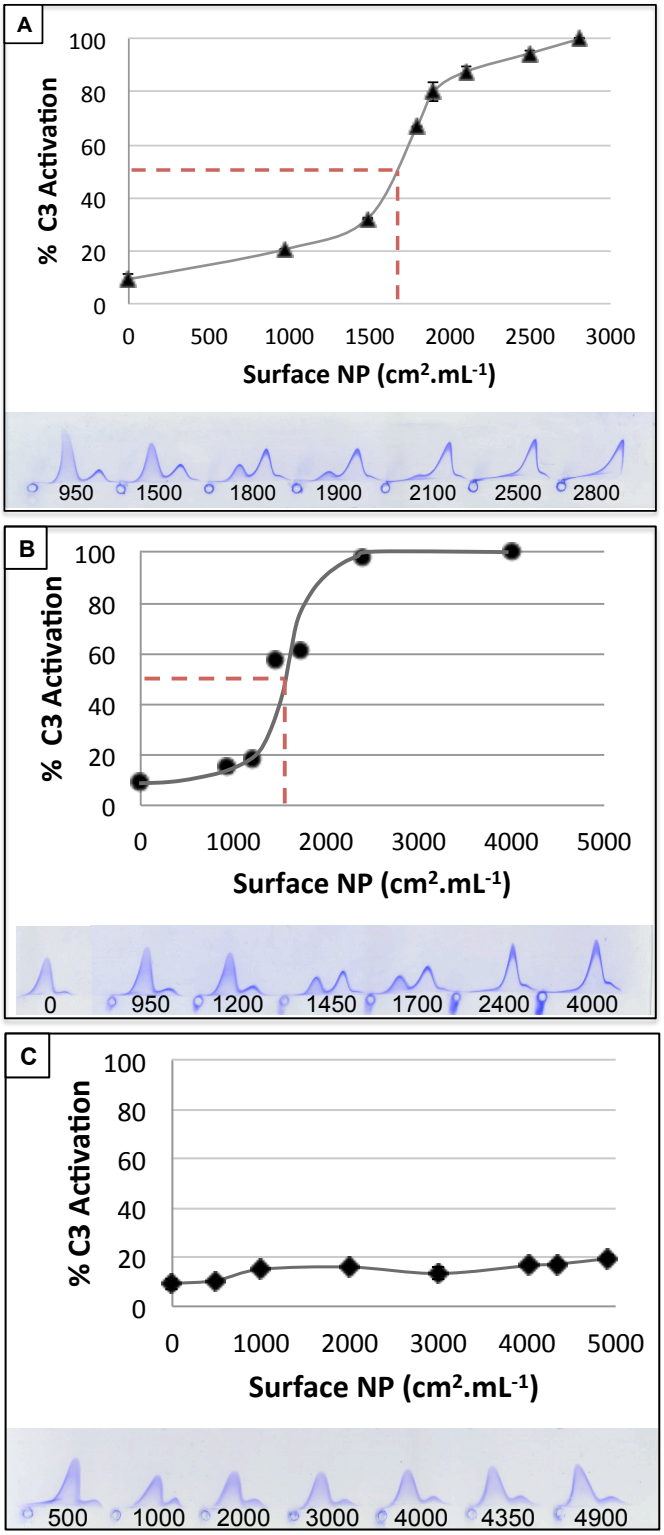

Figure 2: Determination of C_3A_{50} for the three model NPs R17 (A), A66 (B) and R66 (C). Top - Graph representing the values of C3 % activation obtained in function of NP concentration for R17, A66 and R66 respectively. Bottom – Electrophoregrams obtained by MultiCrossed-IE with increasing concentration in NP added in the sample test. Values correspond to tested surface of NP in $cm^2.mL^{-1}$

IV. Discussion

C-IE is a quite old method [34], which was used in several immunological applications [35]. The originality of the proposed method includes the possibility to migrate samples in series during the first and second dimensions. Traditional methods used to make several migrations in parallel during the first dimension, before cutting bands of the 1st dimension gel to transpose on the second dimension gel containing the antibody for the IE [11, 35]. The method proposed in this work greatly simplifies the complex handling found in previous methods while it did not affect the performance. With the new method, one single gel is prepared and the only manipulation between the first and the second electrophoresis is to turn the gel by 90°. The overall time required to perform the 2D electrophoresis runs was also considerably reduced (4h45min against 19h15min with the previous method). Simultaneously, the number of analysis performed in one run was multiplied by 7. Because the size of gel for one sample was reduced to the size of a stamp (from 5x7 cm to 2.8x3 cm), a significant reduction of the amount of reagents was also achieved (Gel-Fix™, gel, antibody, sample), hence reducing the cost for one analysis. The different improvements are summarized in Table 3.

ANOVA is commonly used in validation of chromatographic methods [36, 37]. In the present study, it was applied to validate an electrophoretic method. To carry on this validation, we have performed experiments with a large number of gels. The results have demonstrated that the method is remarkably robust varying different factors. Indeed, the robustness study of the developed MultiCrossed-IE showed that position, electrophoresis system, analyst and preparation of the sample did not have a significant influence on the results of C3 activation. RSDs for intra and inter-day variations conformed with values found in the literature. Level of complement C3 activation is a complex process that is not fixed and evolves with time. For this study, standards did not exist, it was thus necessary to halt the evolution of C3 activation after the time of incubation, in order to use a sample several times for the validation purpose. Further activation was blocked by addition of EDTA and NaMe. We could then store and re-use the same sample for validation of the tested factor.

The proposed method of the MultiCrossed-IE was applied to determine the pattern of activation of C3 triggered by the three model NPs used in the present work. NP concentration was expressed by means of the exposed surface. Indeed, NPs have different size while protein adsorption depends on the available area on nanoparticle surface. Contact of proteins with

NP surface are responsible for the activation of the complement cascade and it appeared logical to express the quantity of nanoparticles by the surface exposed reported to the volume of sample.

Thanks to the high throughput capacity given by the new MultiCrossed-IE method, it was applied to screen the influence of the amount of surface of NP tested on the level of complement C3 activation. A new parameter was defined as the surface concentration that induces 50% of protein C3 cleavage after 1h of incubation with serum at 37°C (C_3A_{50}). The values determined for the three types of NP may be of interest to class them and could eventually help to anticipate their accumulation in the immune system after intravenous administration or their capacity to induce a CARPA reaction. The new MultiCrossed-IE now provides with the opportunity to determine this characteristic from a validated method of evaluation of complement C3 protein activation. This is in contrast with many other methods that only allow comparisons at a single tested concentration and are eventually based on an indirect evaluation of C3 activation such as the CH50.

New modalities of the application of C-IE were established allowing high throughput and making easier the handling by performing MultiCrossed-IE on a single gel plate. Demonstration of the robustness of the proposed protocol towards different factors and improvements of the method should renew the interest of C-IE methods for the analysis of specific proteins. A straightforward application is the evaluation of the activation of protein C3 of the complement system triggered by nanomaterials. It allows the evaluation of nanomaterial interactions with the immune system, which are important to anticipate their safety and biodistribution.

This work was financially supported by BPI France – Project NICE.

The authors declare no conflict of interest.

V. References

1) Zolnik, B. S., González-Fernández, Á., Sadrieh, N., Dobrovolskaia, M. A., *Endocrinology* 2010, *151*, 458–465.
2) Boraschi, D., Duschl, A., *Nanoparticles and the immune system: safety and effects*, Academic Press, Oxford 2013.
3) Dobrovolskaia, M. A., Aggarwal, P., Hall, J. B., McNeil, S. E., *Mol. Pharm.* 2008, *5*, 487–495.
4) Moghimi, S. M., Andersen, A. J., Ahmadvand, D., Wibroe, P. P., Andresen, T. L., Hunter, A. C., *Adv. Drug Deliv. Rev.* 2011, *63*, 1000–1007.
5) Szebeni, J., *Toxicology* 2005, *216*, 106–121.
6) Szebeni, J., *Mol. Immunol.* 2014, *61*, 163–173.
7) Harboe, M., Thorgersen, E. B., Mollnes, T. E., *Adv. Drug Deliv. Rev.* 2011, *63*, 976–987.
8) Salvador-Morales, C., Sim, R. B., in: Dobrovolskaia, M. A., McNeil, S.E. (Eds), *Handbook of immunological properties of engineered nanomaterials, World Scientific,* Singapore 2013, pp. 357–384.
9) Mollnes, T. E., Jokiranta, T. S., Truedsson, L., Nilsson, B., Rodriguez de Cordoba, S., Kirschfink, M., *Mol. Immunol.* 2007, *44*, 3838–3849.
10) Neun, B. W., Ilinskaya, A., Dobrovolskaia, M. A., *Analysis of Complement Activation by EIA,* NCL Method ITA-5.2 Version 1.2, 2015. http://ncl.cancer.gov/NCL_Method_ITA-5.2.pdf (consulted on October 2015).
11) Passirani, C., Barratt, G., Devissaguet, J.-P., Labarre, D., *Life Sci.* 1998, *62*, 775–785.
12) Mosqueira, V. C. F., Legrand, P., Gulik, A., Bourdon, O., Gref, R., Labarre, D., Barratt, G., *Biomaterials* 2001, *22*, 2967–2979.
13) Vonarbourg, A., Passirani, C., Saulnier, P., Simard, P., Leroux, J. C., Benoit, J. P., *J Biomed Mater Res A* 2006, *78A*, 620–628.
14) Bertholon, I., Vauthier, C., Labarre, D., *Pharm. Res.* 2006, *23*, 1313–1323.
15) Nilsson, B., Ekdahl, K. N., Mollnes, T. E., Lambris, J. D., *Mol. Immunol.* 2007, *44*, 82–94.
16) Leslie, M., *Science* 2012, *337*, 1034–1037.
17) Gros, P., Milder, F. J., Janssen, B. J. C., *Nat. Rev. Immunol.* 2008, *8*, 48–58.
18) Chauvierre, C., Labarre, D., Couvreur, P., Vauthier, C., *Macromolecules* 2003, *36*, 6018–6027.
19) Vittaz, M., Bazile, D., Spenlehauer, G., Verrecchia, T., Veillard, M., Puisieux, F., Labarre, D., *Biomaterials* 1996, *17,* 1575–1581.
20) Vauthier, C., Schmidt, C., Couvreur, P., *J Nanopart Res* 1999, *1*, 411–418.
21) Kazatchkine, M., Nydegger, U., Hauptmann, G., *Techniques du complément*, Éd. INSERM, 1985.
22) Bergseth, G., Ludviksen, J. K., Kirschfink, M., Giclas, P. C., Nilsson, B., Mollnes, T. E., *Mol. Immunol.* 2013, *56*, 232–239.
23) Walker, J. M., in: Walker, J. M. (Ed.), *The Protein Protocols Handbook*, Springer, 1996, pp. 763–768.
24) Mancini, G., Carbonara, A.0., Heremans J.F., *Immunochemistry* 1965, 2, 235–254.
25) Walker, J. M., in: Walker, J. M. (Ed.), *The Protein Protocols Handbook*, Springer, 1996, pp. 757-762.
26) ICH Harmonized Tripartite Guideline, Validation of analytical procedures: Text and Methodology Q2(R1), Current Step 4 version, Parent Guideline dated 27 October 1994, (Complementary Guideline on Methodology dated 6 November 1996 incorporated in November 2005). http://www.ich.org/fileadmin/Public_Web_Site/ICH_Products/Guidelines/Quality/Q2_R1/Step4/Q2_R1__Guideline.pdf (consulted on May 2016).
27) ISO 5725-1:1994: Accuracy (trueness and precision) of measurement methods and results - Part 1: General principles and definitions.
28) Labarre, D., Vauthier, C., Chauvierre, C., Petri, B., Muller, R., Chehimi, M., *Biomaterials* 2005, *26*, 5075–5084.
29) Guide to the expression of uncertainty in measurement, JCGM 100:2008 GUM 1995 with minor corrections. http://www.bipm.org/utils/common/documents/jcgm/JCGM_100_2008_E.pdf (consulted on May 2016).

30) ISO 5725-3:1994: Accuracy (trueness and precision) of measurements methods and results - Part 3: Intermediate measures of the precision of a standard measurement method.
31) Bertholon, I., Hommel, H., Labarre, D., Vauthier, C., *Langmuir* 2006, *22*, 5485–5490.
32) Alhareth, K., Vauthier, C., Bourasset, F., Gueutin, C., Ponchel, G., Moussa, F., *Eur J Pharm Biopharm* 2012, *81*, 453–457.
33) Vauthier, C., Persson, B., Lindner, P., Cabane, B., *Biomaterials* 2011, *32*, 1646–1656.
34) Laurell, C. B., *Anal. Biochem.* 1965, *10*, 358–361.
35) Grubb, A. O., *Scand. J. Immunol.* 1983, *17*, 113–124.
36) Vander Heyden, Y., De Braekeleer, K., Zhu, Y.,Roets, E., Hoogmartens, J., De Beer, J., Massart, D. L., *J. Pharmaceut. and Biomed.* 1999, *20*, 875-887.
37) Careri, M., Elviri, L., Mangia, A., *J. AOAC Int.* 2001, *84*, 1383-1392.

Supporting information

Serial multiple crossed immunoelectrophoresis at a micro scale: a stamp-size 2D immunoanalysis of protein C3 activation caused by nanoparticles

Jean-Baptiste Coty, Fanny Varenne, Jean-Jacques Vachon, Christine Vauthier*

Institut Galien Paris-Sud, CNRS, Univ. Paris-Sud, Université Paris-Saclay, 5 rue Jean-Baptiste Clément, 92290 Châtenay-Malabry, France

***Correspondence:** Dr. Christine Vauthier, CNRS UMR 8612, Institut Galien Paris Sud, Univ. Paris-Sud, Université Paris-Saclay, 5, rue Jean-Baptiste Clément, 92296 Châtenay-Malabry, France. Fax: +33 146835946. E-mail: christine.vauthier@u-psud.fr

S1: Heat resistance of the antibody

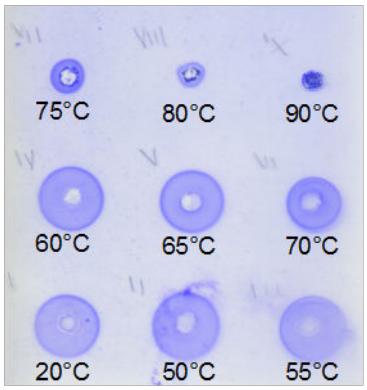

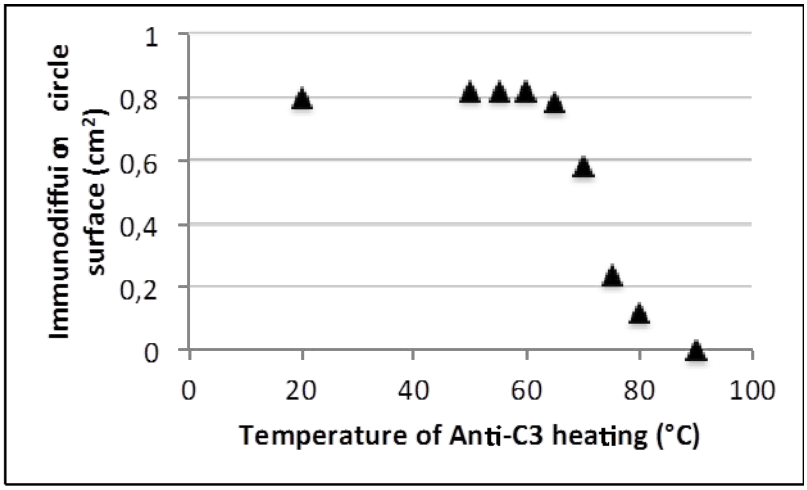

Figure S1: (A) Immunoprecipitated rings obtained after 24h of radial immunodiffusion for indicated heating of antibodies. (B) Plot of immunoprecipitated circles areas against temperature of antibody heating.

S2: Comparison between classical IE and MuliCrossed-IE

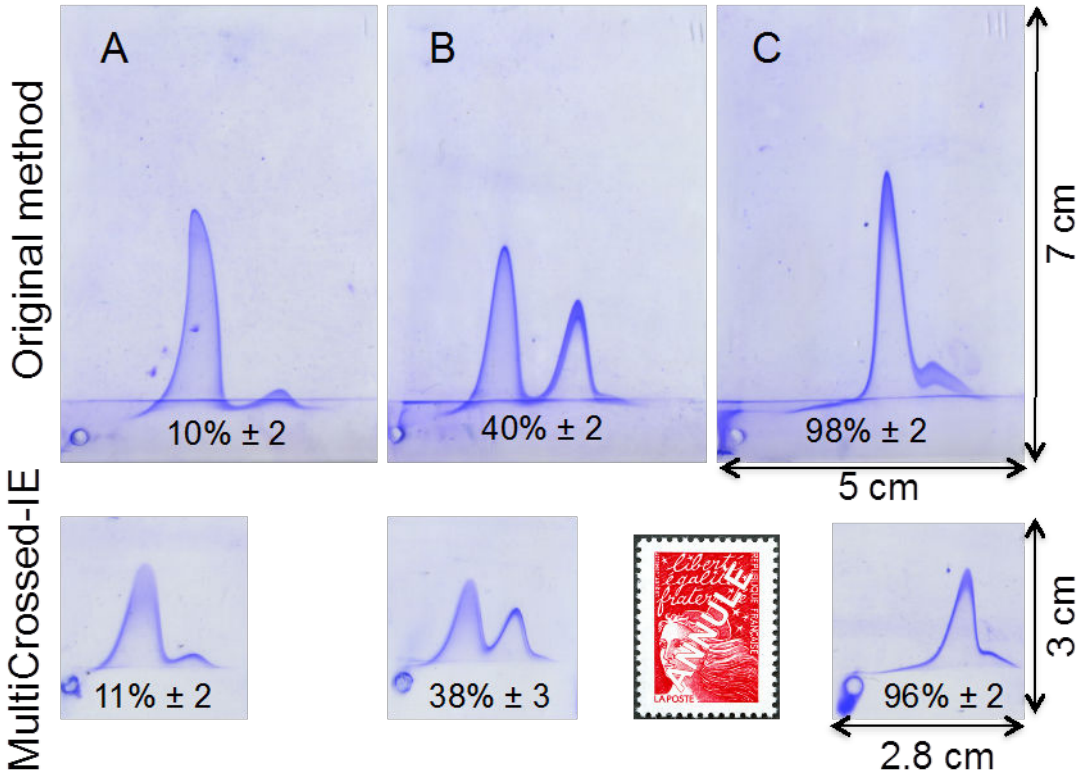

Figure S2: Comparison of the original size immunoelectrophoregrams (raw on the top) with the stamp-size obtained from the MultiCrossed-IE (raw on the bottom). A stamp (©La Poste, 2001, Eve Luquet) is shown for size comparison with stamp-size electrophoregram. – A, B and C correspond to A0, A50 and A100 respectively. Percentages correspond to the % of C3 activation.

S3: Verification of ANOVA's hypotheses: Normal distribution of residues (Ryan-Joiner's test) and Variance's homoscedasticity (Levene's test)

S3-A: Distribution of residues and Ryan-Joiner's Test results for robustness study of tested factors: Position (a), System (b), Analyst (c), Sample preparation (d) and Day (e).

(a) Position factor

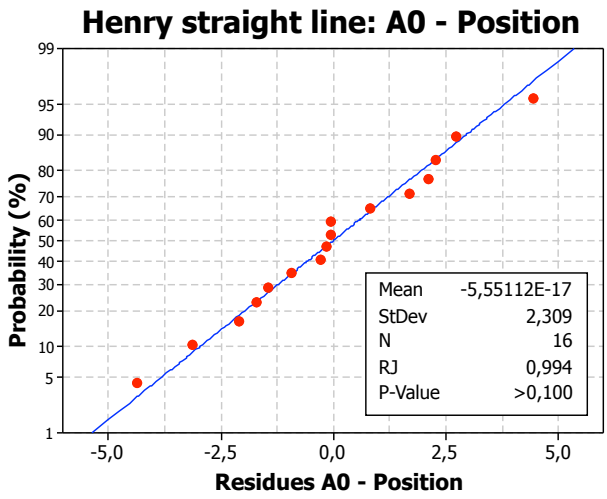

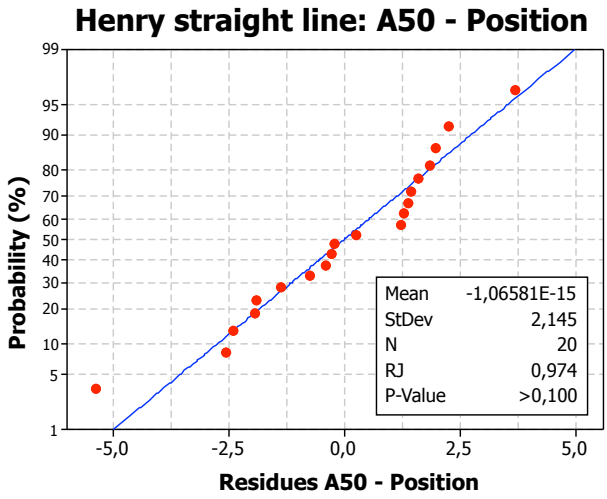

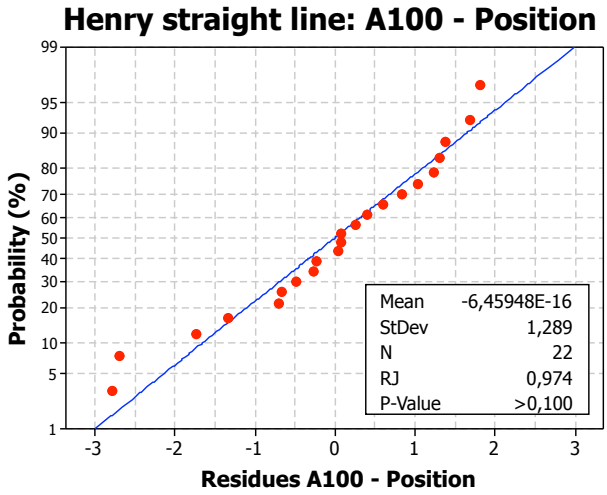

(b) System factor

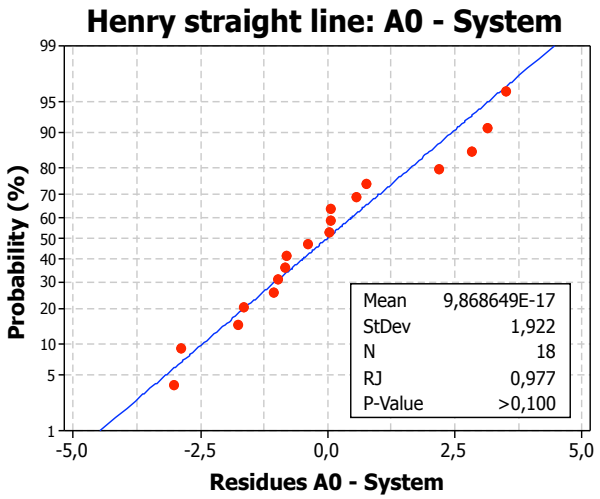

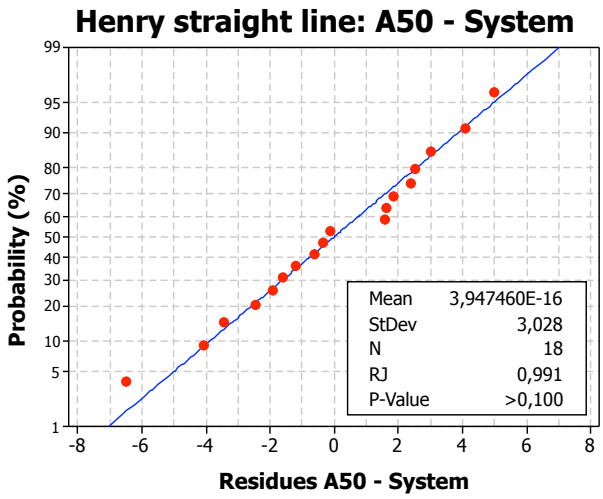

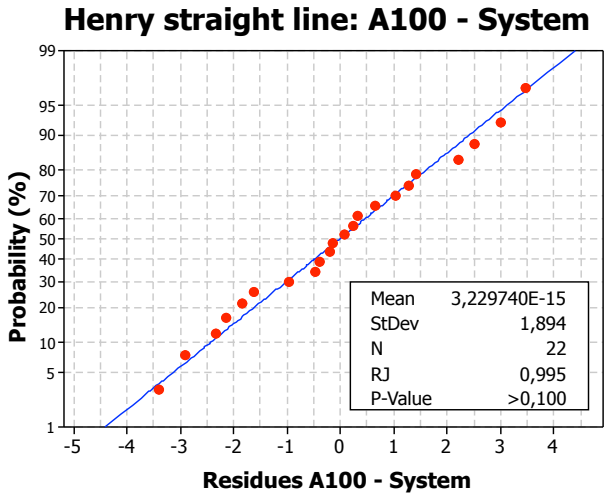

(c) Analyst factor

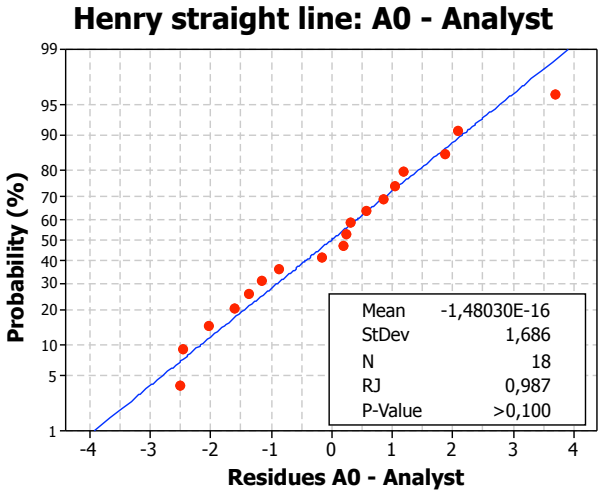

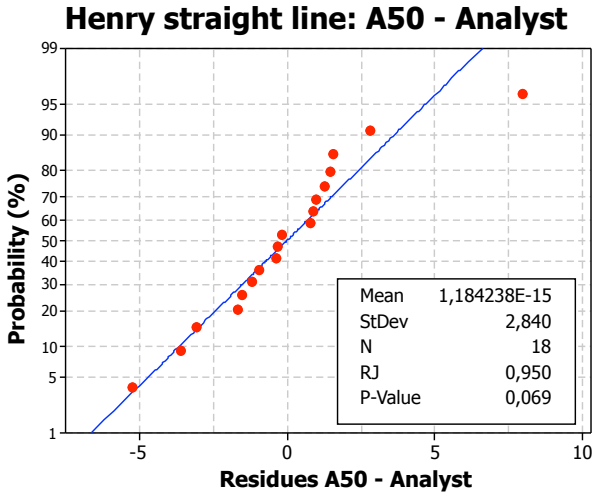

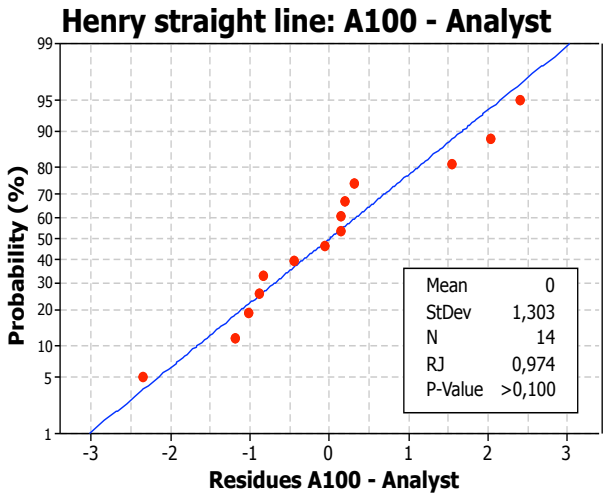

(d) Sample preparation factor

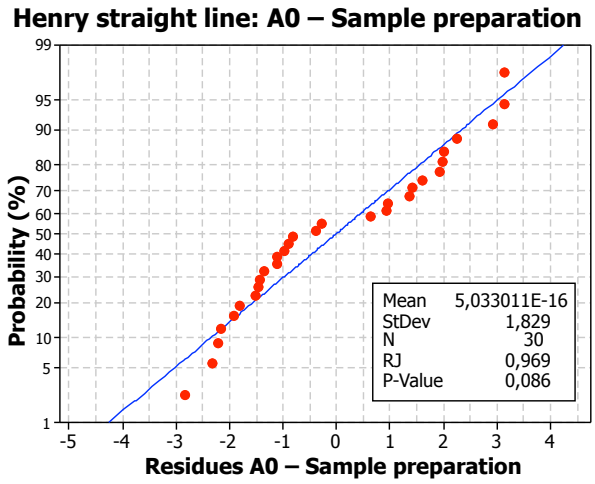

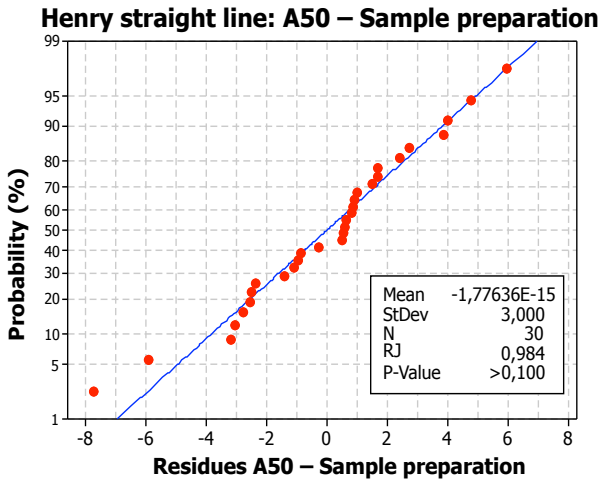

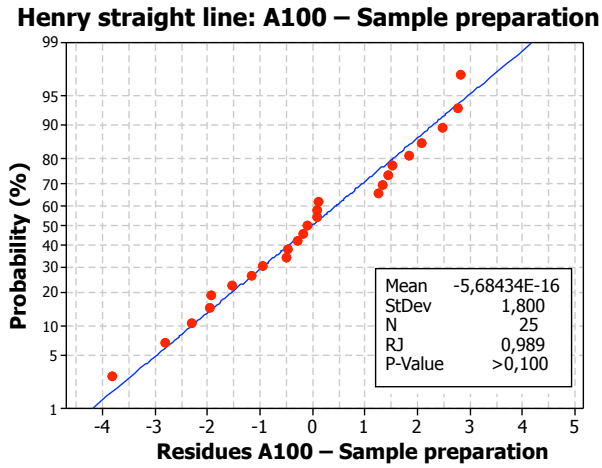

(e) Day factor

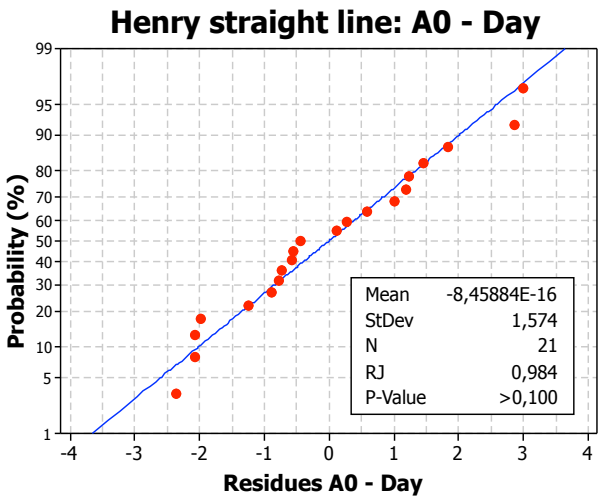

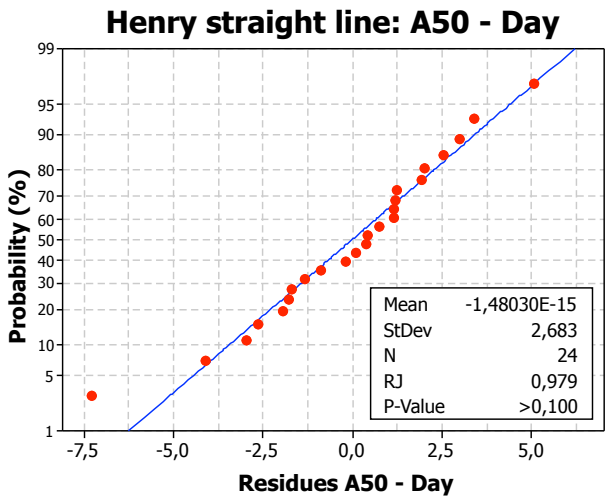

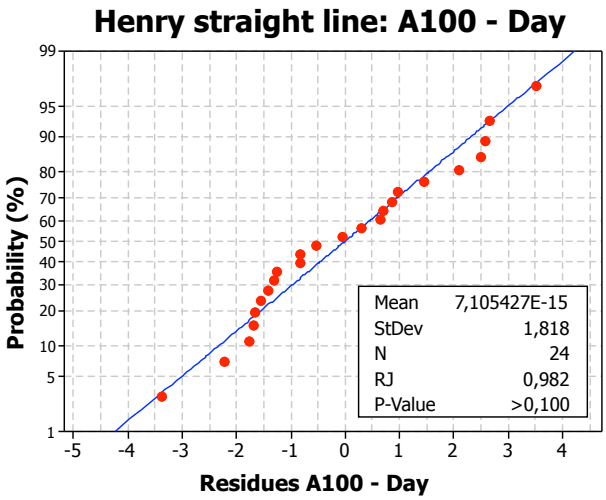

S3-B: Robustness study – Results for Levene's test

Factor	Levene's test p-value		
	A0	A50	A100
Position	0.461	0.772	0.926
System	0.296	0.461	0.711
Analyst	0.135	0.312	0.146
Sample preparation	0.156	0.449	0.384
Day	0.814	0.169	0.300

Chapitre III : Contrôle de l'activation du complément et de la voie empruntée via l'architecture moléculaire des chaînes de dextrane gréffées à la surface de la nanoparticule

Avant-propos : L'étude de l'activation du complément par les nanomédecines (NMs) est une étape préliminaire pour assurer leur biocompatibilité. L'activation de cette cascade fait suite au contact de certaine protéines, appelées osponines, avec les nanomédecines injectées. Les protéines du complément constituent la majeure partie de ces opsonines. Il existe aujourd'hui trois voies connues menant à l'activation de cette cascade, faisant intervenir différentes opsonines et acteurs de la cascade. Ces voies sont rappelées plus précisément en *annexe méthodologique n°4*. Cependant, les propriétés de la NM qui régissent ces interactions ne sont pas encore clairement élucidées. Il est connu que le greffage de polymères formant la couronne en surface de la NM joue un rôle majeur dans ces interactions. Dans ce chapitre, nous étudions la réponse du système du complément à des nanoparticules modèles présentant diverses architectures des chaînes de dextrane en surface. La conformation ainsi que la densité des chaînes greffées s'est montrée être très importante, donnant des résultats d'activation du complément très différents entre ces nanoparticules. Les voies d'activation empruntées ont été étudiées en modifiant la composition du tampon d'incubation. Une compréhension rationnelle du comportement des NMs vis à vis du système du complément pourrait aider à privilégier une stratégie de greffage du polymère en surface lors de la conception de la NM. La méthode d'immunoélectrophorèse en série présentée dans le chapitre I a permis cette étude nécessitant l'analyse de nombreux échantillons, liés au nombre important de conditions expérimentales à appliquer. L'amélioration du débit d'anlayse de cette méthode permet ainsi de nouvelles études, elle a également permis d'étudier d'autres systèmes nanoparticulaires lors de collaborations (cf. *annexe bibliographique*).

Publié dans: *International Journal of Pharmaceutics* (2017), **532** (2), 769-778

Tuning complement activation and pathway through controlled molecular architecture of dextran chains in nanoparticle corona

Jean-Baptiste Coty[a], Elquio Eleamen Oliveira[a,b], Christine Vauthier[a]*

[a] Institut Galien Paris-Sud, CNRS, Univ. Paris-Sud, Châtenay-Malabry, France.
[b] Centro de Ciências Biológicas e Sociais Aplicadas, Universidade Estadual da Paraíba, João Pessoa, PB 58070450, Brazil

*Corresponding Author:
Christine Vauthier
Institut Galien Paris-Sud, CNRS UMR 8612, Univ. Paris-Sud, Faculté de Pharmacie, 5 Rue J.B. Clément, 92296 Châtenay-Malabry, France.
Fax : +33 1 46 83 59 46 / Phone : + 33 1 46 83

Abstract

The understanding of complement activation by nanomaterials is a key to a rational design of safe and efficient nanomedicines. This work proposed a systematic study investigating how molecular design of nanoparticle coronas made of dextran impacts on mechanisms that trigger complement activation. The nanoparticles used for this work consisted of dextran-coated poly(isobutylcyanoacrylate) (PIBCA) nanoparticles have already been thoroughly characterized. Their different capacity to trigger complement activation established on the cleavage of the protein C3 was also already described making these nanoparticles good models to investigate the relation between the molecular feature of their corona and the mechanism by which they triggered complement activation. Results of this new study shows that complement activation pathways can be selected by distinct architectures formed by dextran chains composing the nanoparticle corona. Assumptions that explain the relation between complement activation mechanisms triggered by the nanoparticles and the nanoparticle corona molecular feature were proposed. These results are of interest to better understand how the design of dextran-coated nanomaterials will impact on interactions with the complement system. It can open perspectives with regard to the selection of a preferential complement activation pathway or prevent the nanoparticles to activate the complement system, based on a rational choice of the corona configuration.

Keywords: Nanoparticles, complement activation pathway, corona, molecular feature, molecular architecture

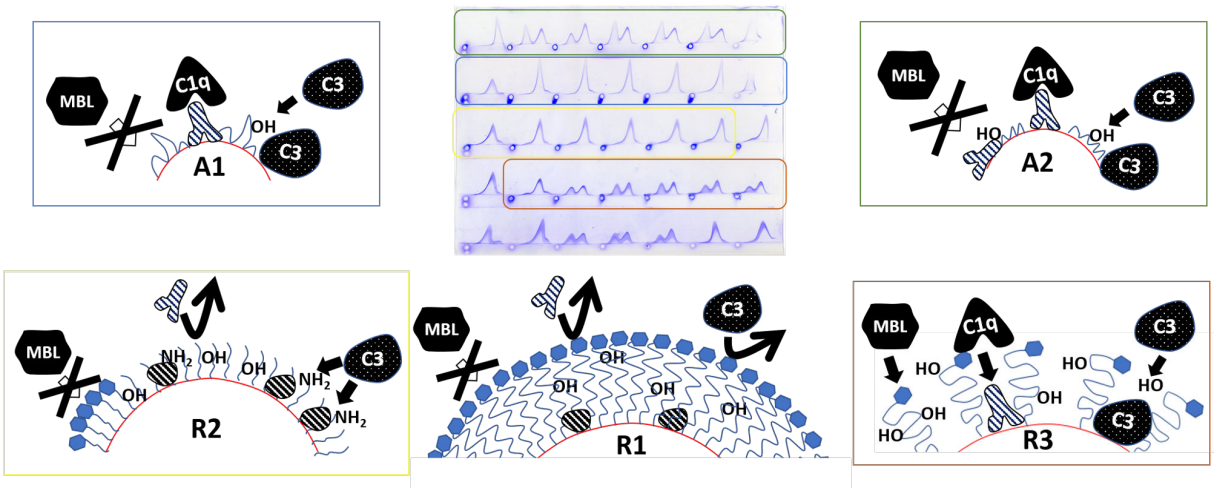

I. Introduction

Nanoparticles have been extensively studied as drug delivery systems for therapeutic purposes (Couvreur and Vauthier 2006, Crucho and Barros, 2015, Li et al., 2015, Shi et al., 2017). Success to improve therapeutic index of molecules carried by such systems depends on the fate of the nanoparticles in the body. The rational design of new carriers is pending to a better understanding of the relationship between nanoparticles' properties and their interactions with the biological medium surrounding the nanoparticles once they are in the body (Clogston et al., 2016, Ilinskaya and Dobrovolskaia, 2016a, 2016b, Orfi and Szebeni, 2016, Szeto and Lavik, 2016, Truel and Nienboss, 2013, Xiang et al., 2013). In general, nanoparticles are designed to be administered intravenously. Once in the blood, they are immediately confronted with components of the innate immune system (Anchordoquy et al., 2017, Dobrovolskaia and McNeil, 2013, Moghimi and Farhangrazi, 2013, Szebeni, 2014). Without specific engineering, nanoparticles are generally recognized by the innate immune system and rapidly cleared from the bloodstream due to the uptake by the mononuclear phagocyte system (MPS) (Bazile et al., 1995, D'Addio et al., 2012, Gref et al., 1995, 1994, Peracchia et al. 1999, Suk et al. 2016). Several works have demonstrated that the grafting of a hydrophilic corona at the surface of the nanoparticles can reduce the uptake by MPS. Hydrophilic polymers, such as poly-ethylene glycol (PEG), polysaccharides (e.g. dextran, heparin, and chitosan) and polyphosphoesters were the most used materials on this purpose (Alhareth et al., 2012, Bazile et al., 1995, Bertholon et al., 2006a, D'Addio et al., 2012, Gref et al., 1995, 1994, Moghimi and Szebeni, 2003, Muller et al., 2017, Lemarchand et al., 2006, Peracchia et al., 1999, Suk et al., 2016). However, a review of the literature shows that even with a hydrophilic corona, some nanocarriers undergo a rapid clearance that is accompanied by the activation of the complement system (Alhareth et al., 2012, Gref et al., 2000, Moghimi et al., 2003, Szebeni, 2014). The effectiveness of the hydrophilic shell to reduce uptake by MPS is associated with its capability to reduce interactions of blood proteins with the nanoparticle surface. All parameters that define the molecular feature of the hydrophilic corona formed around the nanoparticles, i.e. chain length, grafting density, composition and structural arrangement of the chains, were found important factors influencing the *in vivo* fate of nanoparticles (Chen and Borden, 2011, D'Addio et al., 2012, Du et al., 2015, Hamad et al.,

2010, Muller et al., 2017, Peracchia et al., 1997, Toda et al., 2010, Szebeni et al., 2015, Szeto and Lavik, 2016, Vonarbourg et al., 2006).

The complement system (CS) has an important role in innate immunity to recognize and eliminate pathogens, defective cells and foreign biomaterial devices, including nanoparticles circulating in the blood (Carroll and Sim, 2011). The CS consists of more than 30 plasma and cell-membrane proteins. It is the most important biochemical cascade that defines the type of “danger” signals sent to the rest of the immune system after it has detected an intruder, hence defining the type of response. Its activation can be triggered essentially by three distinct routes, the classical, lectin and alternative pathways (Gasque, 2004, Harboe et al., 2011, Merle et al., 2015). The classical pathway is activated primordially by the interaction of C1q with immunoglobulins. Non-immune molecules such as the C reactive protein (CRP) can also trigger the classical pathway. The lectin pathway is triggered by the recognition of carbohydrate patterns exhibited on the surface of foreign particles. Proteins involved in the recognition are the mannose-binding lectin (MBL), the H-, L- or M-ficolins or the collectin 11. Activation of the alternative pathway depends on spontaneous hydrolysis of the internal thioester bond found in protein C3 that can be triggered by nucleophilic groups found on the intruder surfaces. The three pathways converge to generate the C3 convertase and the terminal membrane attack complex (MAC) C5b-9. Activation of the CS also leads to the release of many types of anaphylatoxins which contribute to the inflammatory process (Carrol and Sim, 2011).

Interactions of proteins of the CS with colloidal particles can trigger the complement cascade (Bertholon et al., 2006a, Dobrovolskaia and McNeil, 2013, Ilinskaya and Dobrovolskaia, 2016a, 2016b, Lorenze-Abalde et al. 2016, Moghimi and Farhangrazi, 2013, Szebeni, 2014, Szebeni et al., 2012, Vorup-Jensen and Boesen, 2011). Then, the production of opsonins such as C3b lead to a rapid capture of nanocarriers by the MPS resulting in a short circulation time in the blood. While this effect can compromise the efficacy of delivery systems, another consequence of the activation of the complement system concerns its safety when it gives rise to hypersensitivity reactions called complement activation-related pseudoallergy (CARPA) (Andersen et al., 2012, Szebeni, 2014, 2012, Szebeni et al., 2012).

Nanoparticles based on biodegradable poly(alkylcyanoacrylate) polymers were widely investigated as drug delivery systems (Couvreur and Vauthier, 2006, Nicolas and Couvreur,

2009, Nicolas et al., 2013, Nicolas and Vauthier, 2011, Vauthier et al., 2007). These colloidal carriers have shown many advantages in terms of drug protection, long stability, biocompatibility, biodegradability and drug delivery potential. Different preparation methods can be used to generate poly(isobutylcyanoacrylate) PIBCA nanoparticles having hydrophilic coronas of various compositions and molecular architectures modulating their capacity to activate the complement system and their biodistribution (Vauthier, 2015). A series of PIBCA nanoparticles with different hydrophilic coronas made of dextran was thoroughly characterized in previous works (Bertholon et al., 2006b, 2006c, Chauvierre et al., 2004, Labarre et al., 2005, Vauthier et al., 2011, 2009). These nanoparticles could serve as models to improve our understanding of the influence of the molecular feature of the hydrophilic polymers of the nanoparticle corona on biological mechanisms involved in efficacy and safety of nanoparticles. Such a work would be consistent with the need to develop systematic studies providing results required to improve our capacity to design efficient and safe nanoparticulate drug delivery systems on more rational basis (Clogston et al., 2016, Szeto and Lavik, 2016, Truel and Nienhaus, 2013, Xiang et al., 2013).

The goal of the present work was to evaluate how molecular characteristics of the corona of dextran-coated PIBCA nanoparticles could interfere in the activation of the complement system, including the resolution of the involved pathway(s). Activation of the complement cascade was acknowledged in a systematic way by evidencing protein C3 cleavage using a high-throughput serial 2D immuno-electrophoresis method (Coty et al., 2016). Pathways were differentiated incubating nanoparticles and serum with calcium and magnesium to highlight complement activation triggered through all pathways and with magnesium only to evidence the contribution to activation of the alternative pathway that is a calcium independent pathway (Des Prez et al., 1975, Hamad et al., 2010, Labarre et al., 1993). Results were discussed in the light of our knowledge on the molecular characteristics of the nanoparticle corona.

II. Materials and Methods

II.1. Materials

Isobutylcyanoacrylate (IBCA) was synthesized and provided by Orapi (Saint-Vulbas, France). Chemicals purchased from Sigma (Saint-Quentin-Fallavier, France) were tricine, Tris base (Sigma 7-9®), sodium chloride, EDTA sodium salt, dextran 66.7 kDa, and bromophenol blue. Dextran 17.7, cerium (IV) ammonium nitrate, nitric acid, and chloride acid were supplied by Fluka (Saint-Quentin-Fallavier, France). Nitric acid was purchased from Prolabo (Paris, France). Calcium lactate, glacial acetic acid, coomassie brilliant blue R-250 were supplied by Thermo Fisher Scientific (Villebon-sur-Yvette, France). Gel-Fix™ for agarose (265x150 mm) was obtained from Serva Electrophoresis (Heidelberg, Germany). Nafamostat mesylate (NM) was obtained from Abcam (Cambridge, UK). All chemicals were of reagent grade and used as purchased.

Polyclonal anti-human C3 antibody raised in goat was purchased from Fitzgerald antibodies (Acton, USA). Serum was prepared from human plasma obtained from healthy donors from Etablissement Français du Sang (EFS) (Rungis, France). Heat-activated gamma globulin (HAGG) and Cobra Venom Factor (CVF) were purchased from TECO Medical (Rambouillet, France) to be used as positive control for the activation of the complement system.

II.2. Preparation of nanoparticles by redox radical emulsion polymerization (RREP)

Three types of RREP nanoparticles were prepared according to the method described by Bertholon et al. (2006c). R1 and R2 were prepared as follow using dextran 66.7 kDa and dextran 17.7 kDa respectively at a concentration of 1.3%. Dextran (0.1356 g) was dissolved in 8 mL of 0.2 N nitric acid. After 10 min bubbling with argon at 40°C, the polymerization was initiated adding successively and under vigorous stirring 2 mL of a solution of cerium (IV) ammonium nitrate (8×10^{-2} M) in 0.2 N nitric acid and 0.5 mL of IBCA. The reaction was allowed to continue for 1 h at 40°C. At the end, the dispersion was cooled down in an ice bath.

R3 was prepared following the same method using a concentration of dextran 66.7 kDa of 0.5%. Dextran 66.7 kDa (0.0502 g) was dissolved in 9.3 mL of 0.2 N nitric acid following the above described protocol. The polymerization was started by adding successively 0.7 mL of a solution of cerium (IV) ammonium nitrate (8×10^{-2} M) in 0.2 N nitric acid and 0.5 mL of IBCA. At the end of the polymerization the dispersion was cooled down at 4°C.

II.3. Preparation of nanoparticles by anionic emulsion polymerization (AEP)

Nanoparticles A1 were prepared according to the method described in Bertholon et al. (2006c). Dextran 66.7 kDa (0.1375g) was dissolved in 10 mL of 0.2 N nitric acid (pH 1). IBCA (0.5 mL) was added to the solution and stirred for 24h at 40°C. At the end of the polymerization, the dispersion was cooled down in an ice bath.

Nanoparticles A2 were prepared according to the method of Couvreur et al. (1979) Dextran 66.7 kDa (0.05 g) was dissolved in 10mL of a solution of 3 mM HCl (pH 2.5). Then, 100 µL of IBCA was added while the system was placed under vigorously stirring. The polymerization was lasted for 3 h at room temperature.

II.4. Purification of nanoparticles

All nanoparticle dispersions were purified by dialysis against water after polymerization Spectra/Por membrane with molecular weight cutoff 100 KDa). After purification, they were stored at 4°C until use.

II.5. Evaluation of nanoparticle concentrations in dispersions

To estimate nanoparticles' concentration in dispersions, aliquots of 100 µL each were freeze-dried and weighed. The determination was done in triplicated. Results were given as the mean of the three determinations in $mg.mL^{-1}$. This concentration was converted into a concentration expressed in surface area per volume unit to be used in tests designed to evaluate complement activation triggered by the nanoparticles. The conversion was obtained using the equation given in Vittaz et al. (1996) taking the hydrodynamic diameter of the nanoparticles measured by dynamic light scattering (see paragraph 2.6) and the volume mass of the nanoparticles at 1.14 (Vauthier et al. 1999).

II.6. Measurement of particle size and zeta potential

The mean hydrodynamic diameter of the nanoparticles was evaluated by dynamic light scattering using a Zetasizer Nano ZS90 (Malvern Instruments, Orsay, France) operating at 90°. The samples (5-20µL) were diluted in MilliQ® water (1mL).

The zeta potential of the nanoparticles was evaluated from the measurements of the electrophoretic mobility of the nanoparticles using a Zetasizer Nano ZS90 (Malvern

Instruments, Orsay, France). Dilutions of the samples were performed in an aqueous solution of 1 mM NaCl.

II.7. Evaluation of complement activation by two-dimensional (2-D) immunoelectrophoresis of C3

Complement activation triggered by the nanoparticles was assessed by evaluating conversion of C3 into activated fragments of lower molar mass by serial multiple crossed immunoelectrophoresis at a microscale using polyclonal antibody to human C3 (Coty et al. 2016). Pathway by which complement activation was triggered was identified incubating nanoparticles and serum with buffers containing different concentrations in calcium and magnesium in order to highlight the part of the activation due to calcium dependent/independent mechanisms (Banda et al., 2014, Des Pres et al., 1975, Hamad et al., 2010, 2008, Labarre et al., 1993).

Veronal buffered saline named VBS^{2+} containing 5 mM diethylmalonylurea, 0.15 mM calcium chloride, 0.5 mM magnesium chloride, 150 mM sodium chloride, pH 7.4 was used to investigate complement activation triggered by all pathways. Veronal buffer saline named $VBSMg^{2+}$X/EGTA containing 5 mM diethylmalonylurea, 0.5 to 10 (X) mM magnesium chloride, 150 mM sodium chloride, 10 mM EGTA pH 7.4 were used for incubations of the nanoparticles with human serum to investigate complement activation triggered by calcium independent pathways including the alternative pathway. It is noteworthy that the composition of VBS^{2+} and of VBSMg0.5mM/EGTA corresponded to those generally found in the literature and in commercial assays to assess in vitro evaluation of complement activation (Des Prez et al., 1975, Hamad et al., 2010, Labarre et al., 1993, Neun et al., 2015).

Nanoparticle dispersions (50 µL) were incubated under gentle agitation for 1 h at 37°C with 25 µL human serum and 25 µL VBS^{2+} or $VBSMg^{2+}$X/EGTA to evaluate the activation of the complement system triggered by the nanoparticles produced in the different conditions of incubations. Concentrations in nanoparticles involved in the test were expressed as the surface area per volume unit ($cm^2.mL^{-1}$) to ensure a relevant comparison between the different nanoparticles that were characterized by different sizes.

In one series of experiments, nanoparticles were tested using VBS^{2+} at a concentration in nanoparticles of 2000 $cm^2.mL^{-1}$. A second series of experiments were performed using $VBSMg^{2+}$X/EGTA at concentrations in magnesium (X) ranging from 0.5 to 10 mM at the same

concentration in nanoparticles (2000 $cm^2.mL^{-1}$). In a second series of experiments, the nanoparticles were tested for their capacity to activate CS in VBS^{2+} at a higher concentration (4000 $cm^2.mL^{-1}$ for nanoparticles R1, R2 and A1, 2500 and 2800 $cm^2.mL^{-1}$ for nanoparticles A2 and R3 respectively). Nanoparticles activating CS in these conditions were then tested in calcium free media using $VBSMg^{2+}X$/EGTA buffers at concentrations in magnesium (X) ranging from 0.5 to 10 mM. A series of control experiments were added as follow. A sample of serum in which the nanoparticles were replaced by Milli-Q® water was tested to evaluate the rate of spontaneous activation of CS triggered in all different conditions of incubations used in this study. Cobra venom factor (CVF) and heat agglomerated gamma-globulins (HAGG) were used as positive control of the activation of CS. With CVF, activation of CS was expected to occur in all the tested conditions because CVF is a strong complement activator through the alternative pathway. CVF structure being very similar to C3b, it allows the spontaneous formation of C3 and C5 convertases spontaneously (Vogel ad Fritzinger, 2010). In contrast, with the heat-aggregated gamma globulins (HAGG), activation that is expected to occur through the classical pathway should not induce the cleavage of the protein C3 while incubations were performed in the absence of calcium ions ($VBSMg^{2+}X$/EGTA). These positive control samples were selected consistently with those used in protocol evaluating the activation of the complement system proposed by the Nanomedicine Characterization Laboratory in the USA (Neun et al., 2015)

After incubation, the cleavage of the C3 protein was evaluated analyzing 2.5 µL of the incubation medium by 2D immunoelectrophoresis performed in agarose gels containing a polyclonal anti-human C3 antibody that recognizes both native and activated C3. The 2D immuoelectrophoresis was performed as described in Coty et al. (2016). Briefly, an agarose gel (1% in agarose) containing the antibody was casted on a gel bond slab (15 x 20 cm) at 60°C. 5 bands of 1cm each were cut and removed to be replaced by neutral agarose gel at 1%. Seven wells were formed in lines in the bands of neutral agarose gel where 2.5µL of samples were deposited for analysis. The gel slab was charged with 35 samples and the first dimension of the electrophoresis (16mA, 600V, 100W) was run in the presence of bromophenol blue as migration marker. When the migration marker has run for 6 cm from the well (approximatively 1h15min), the electrophoresis was stopped, the gel slab was turned from 90° and the second electrophoresis was started (12mA, 500V, 100W) for 3h30min. At the end of the

electrophoresis, the gel slab was dried using papers and then stained with coomassie blue. The obtained gel slab was scanned at a high resolution and the electrophoregrams were analyzed to evaluate the area of the peak corresponding to the native C3 protein and that of the activated fragments using image J. The final results were expressed as the percentage of the area of the peaks corresponding to the activated fragments (ACAF) per the sum of the areas measured for peaks corresponding to the native (AC3) and activated fragments (ACAF):

R = ACAF/(AC3 + ACAF)

All determinations were made in triplicates.

III. Results

III.1. Nanoparticles Characteristics

Characteristics of nanoparticle dispersions are given in table 1. Results agreed well with those found in previous studies emphasizing the reproducibility of the preparation of this series of nanoparticles regarding their principal physicochemical characteristics (Alhareth et al., 2012, Bertholon et al., 2006a, 2006b, Vauthier et al., 2011, 2009).

Nº	Polymerization method	Dextran Mw, percentage added in the polymerization medium	d_H (nm)	PDI	Zeta Potential (mV)
R1	RREP at pH 1	66.7 kDa, 1.3%	291± 0.6	0.069	-4.45
R2	RREP at pH 1	17.7 kDa, 1.3%	234 ± 1.7	0.077	-12.6
R3	RREP at pH 1	66.7 kDa, 0.5%	291± 1.0	0.040	-5.31
A1	AEP at pH1	66.7 kDa, 1.3%	85 ± 0.7	0.056	-4.33
A2	AEP at pH2.5	66.7 kDa, 0.5%	113 ± 1.1	0.147	-6.37

Table 1: Hydrodynamic diameter, polydispersity index and zeta potential of the nanoparticles prepared by the different methods and used in the current work.
RREP: redox radical emulsion polymerization, AEP: anionic emulsion polymerization, Mw: Molecular Weight.

III.2. *In vitro* complement activation

Activation of the complement system was investigated highlighting the cleavage of the protein C3 after incubation of nanoparticles with serum using a recently developed high-throughput 2D immunoelectrophoresis method (Coty et al. 2016). An example of a gel plate resulting from

present study was presented in supplementary material S1. The protein C3 is the first protein of the complement cascade that is activated regardless of the activation pathway triggered. Activation of the complement system requires divalent cations including magnesium and calcium. The classical and lectin pathways need calcium and magnesium being calcium dependent while the alternative pathway that is calcium independent only requires magnesium. Based in these specificities, it is possible to investigate pathways by which nanotechnologies trigger the complement system by varying the concentration in calcium in testing conditions (Banda et al., 2014, Des Pres et al., 1975, Hamad et al., 2010, Labarre et al., 1993).

Figures 1, 2 and 3 show the cleavage of the protein C3 observed after incubation of serum with nanoparticles in the different conditions. Figure 1 demonstrated the relevancy of the test reporting the analysis performed with different control samples.

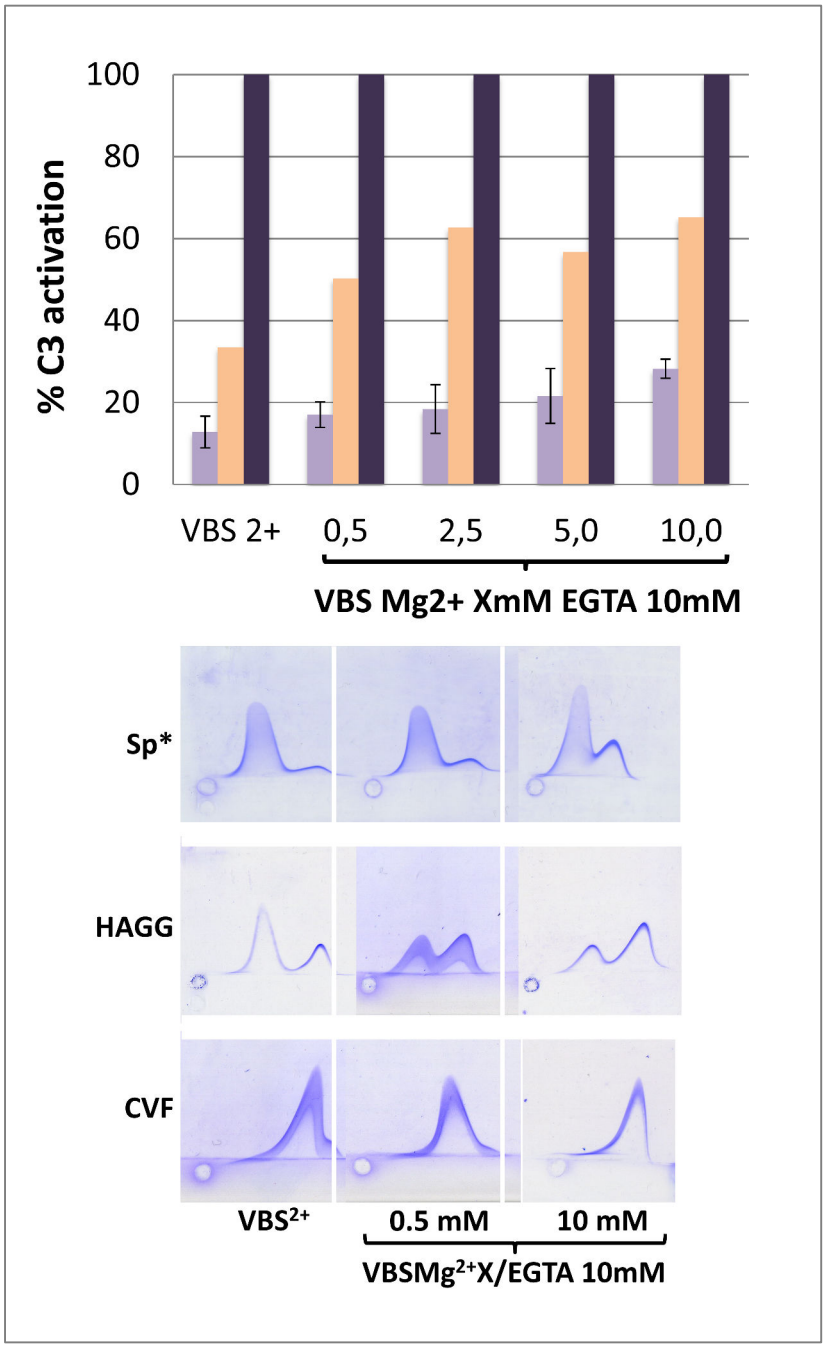

Figure 1: Protein C3 cleavage produced in controlled experiments. The upper part shows percentage of protein C3 cleavage in samples used to test spontaneous activation (Sp*) (purple columns) and used as positive controls of complement activation using Heat Agglutinated Gamma Globulins (HAGG) (orange columns) and cobra venom (CVF) (Black columns). The lower part shows examples of the immunoelectrophoregrams obtained from the analysis of protein C3 in the different incubated serum.

Spontaneous activation produced in negative control samples incubated in VBS^{2+} remained low at a level generally found in the conditions in which the test was performed (Bertholon et al., 2006a, Vauthier et al., 2011). Spontaneous activation evaluated in the absence of calcium

ions (tests performed in VBSMg^{2+}X/EGTA) also showed a low level of cleavage of the protein C3 but it tended to increase with the concentration of magnesium ions. This increase remained at a low level including at the highest concentration in magnesium (10 mM). Assays performed with the positive control including CVF revealed a total conversion of the protein C3 in all conditions used to perform the test. The results were consistent with the use of this compound as a positive control of the activation cascade by calcium independent pathways (Vogel and Fritzinger, 2010). Positive control including HAGG produced a partial conversion of C3 in VBS^{2+} that was increased in VBSMg^{2+}X/EGTA to reach a plateau value around 60% conversion at 2.5 mM magnesium. This positive control was expected to trigger the complement cascade through calcium dependent pathways. Unexpectedly, our method of monitoring of the complement system revealed that the protein C3 was even more cleaved when incubations were performed in media depleted in calcium ions. Consistently with results evaluating spontaneous activation, more C3 was cleaved in the presence of increasing concentrations in magnesium ions until it reached a plateau value at 60% conversion that was much higher than the spontaneous activation measured at corresponding concentrations in magnesium.

Figure 2 reports the activation determined after incubation of nanoparticles (2000 cm²/mL) in serum with VBS^{2+}. The different nanoparticles produced different level of complement activation at the tested concentration that were acknowledged by the different percentage of activated C3 found on the 2D immunoelectrophoresis gels. These results were consistent with those of previous studies (Bertholon et al., 2006a, Chauvierre et al., 2003, Coty et al., 2016, Labarre et al., 2005, Vauthier et al., 2011) (See figure S2 in supporting information showing a comparison with previous measurements). Consistencies of the results over time emphasized the robustness of the preparation methods used to synthesize this series of nanoparticles that shows different capacities to trigger the activation of the complement system in a reproducible manner.

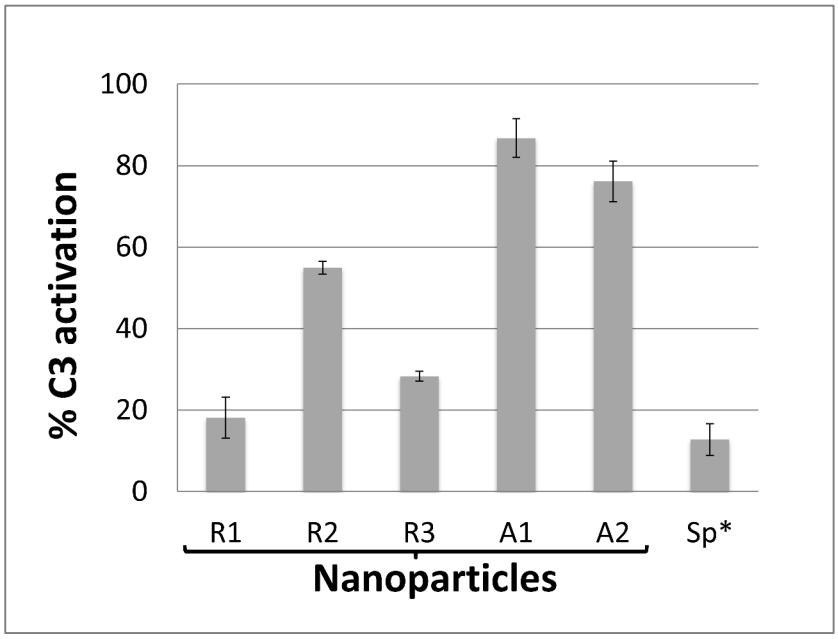

Figure 2: Percentage of protein C3 cleaved after incubation of the different nanoparticles in serum in VBS^{2+}. Sp*: spontaneous activation found in a test performed in same experimental conditions but without nanoparticles.

Figure 3 shows results of experiments investigating complement activation produced by each type of nanoparticles in media that contained different concentrations in calcium and magnesium. These experiments were used to elucidate the preferred pathway by which the different nanoparticles triggered activation of CS. Capacity of nanoparticles to trigger complement activation through calcium dependent pathways could be highlighted by a reduction of activation between incubation in VBS^{2+} containing both calcium and magnesium and in $VBSMg^{2+}X/EGTA$ that contained only magnesium.

All nanoparticles did not show full activation in VBS^{2+} at the concentration of 2000 $cm^2.mL^{-1}$ that was the concentration tested in VBS^{2+} in our previous works. Thus, it was decided to also include a concentration that produced 100% of C3 conversion in VBS^{2+} in the series of tests considered in the present work. This could be achieved by increasing the concentration of the majority of the nanoparticles up to 4000 $cm^2.mL^{-1}$ except for nanoparticle R1. Several situations can be described from the obtained results as summarized in table 2.

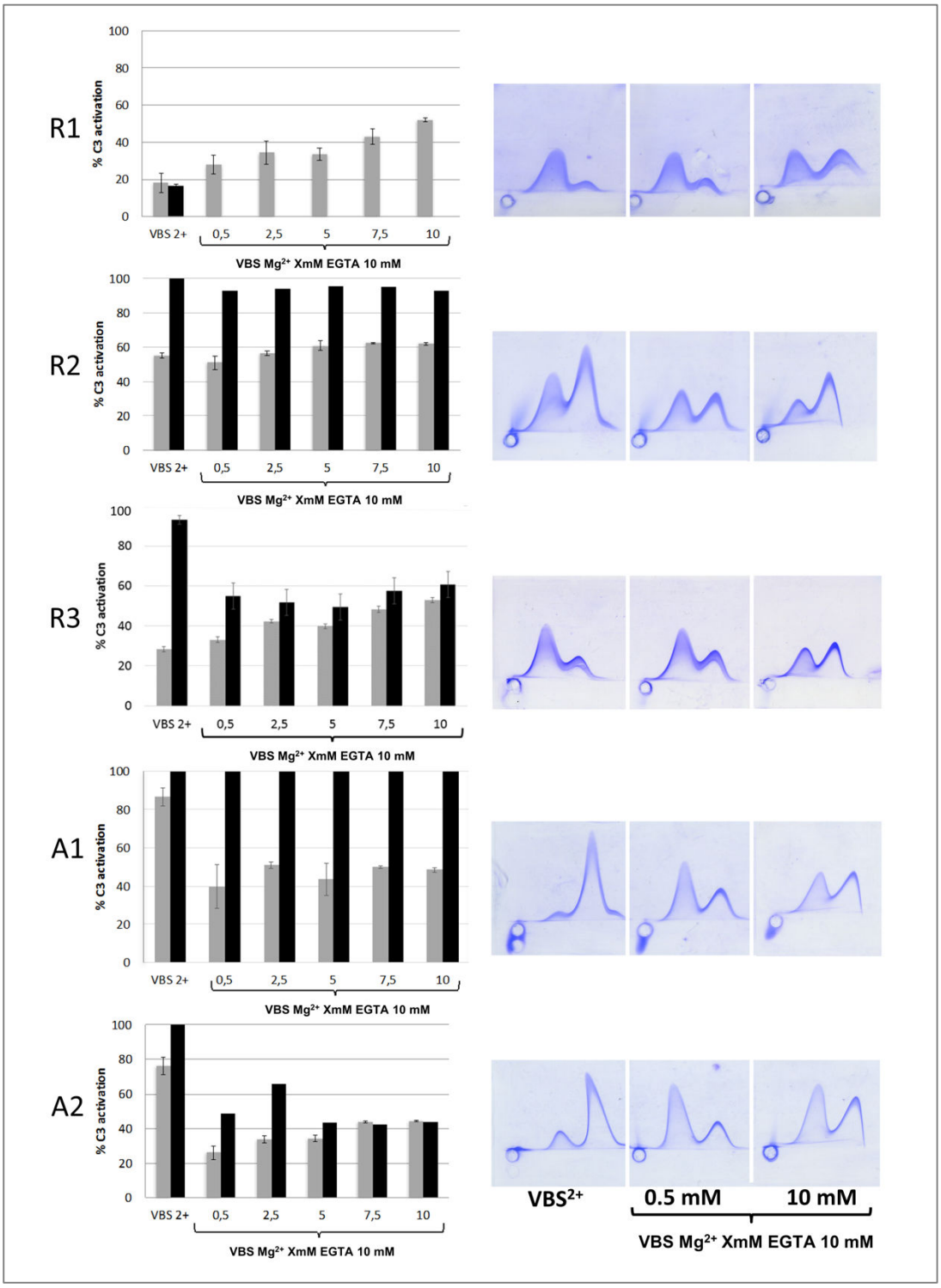

Figure 3: Activation of protein C3 produced by the different nanoparticles incubated in various conditions. Left side: percentages of cleavage of protein C3 produced in the different incubation media by 2 distinct concentrations in nanoparticles. Grey columns: 2000 cm²/mL, dark columns: concentrations in nanoparticles required to produce 100% cleavage in VBS^{2+}. 2500 cm² mL^{-1} for nanoparticle A2, 2800 cm² mL^{-1} for nanoparticle R3, 4000 cm² mL^{-1} for nanoparticles A1 and R2. Right side: examples of immunoelectrophoregrams analysis protein C3 after incubation of samples containing 2000 cm² mL^{-1} nanoparticles in different conditions.

Table 2: Summary of the activation of the complement cascade triggered by the different nanoparticles in the different conditions of incubations

	R1	R2	R3	A1	A2
Model of the molecular feature of the dextran corona *	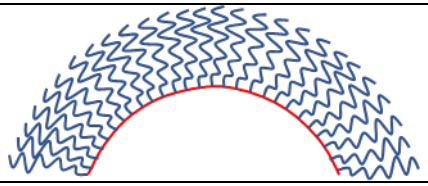	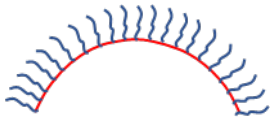	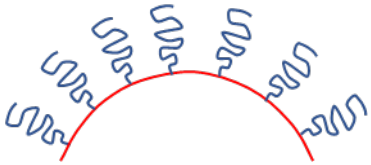		
2000 cm²/mL VBS^{2+}	No activation (spontaneous) 18%	Partial activation 55%	Weak activation 28%	Strong activation 87%	Strong activation 76%
2000 cm²/mL $VBSMg^{2+}X/EGTA$	Activation increased with [Mg] up to 52% conversion	No effect of calcium depletion No effect of the increase of [Mg]	Activation increased with [Mg] up to 50% conversion	Marked effect of calcium depletion No effect of the increase of [Mg]	Marked effect of calcium depletion Activation increased with [Mg]
Maximum surface VBS^{2+}	4000 cm²/mL No activation (spontaneous) 17%	4000 cm²/mL Full activation 100%	2800 cm²/mL Strong activation 93%	4000 cm²/mL Full activation 100%	2500 cm²/mL Full activation 100%
Maximum surface $VBSMg^{2+}X/EGTA$	Not determined	Almost no effect of calcium depletion No effect of the increase of [Mg]	Marked effect of calcium depletion No effect of the increase of [Mg]	No effect of calcium depletion	Marked effect of calcium depletion No effect of the increase of [Mg]
Summary	No activation in VBS^{2+}, increase of the activation with increasing [Mg] in calcium free media	Activation by alternative pathway	Activation by classical and alternative pathways At a low concentration in nanoparticles activation increased with [Mg] in calcium free media	Low concentration in nanoparticles: Activation by classical and alternative pathways High concentration in nanoparticles: activation by the alternative pathway.	Activation by classical and alternative pathways. At a low concentration in nanoparticles activation increased with [Mg] in calcium free media

*: Models proposed for the molecular architecture of dextran chains at the surface of nanoparticles R1, R3 and A2 were fully demonstrated (Vauthier et al., 2011, 2009). Those illustrated for nanoparticles R2 and A1 were suggested based on the molecular architecture of the polymer composing the nanoparticles and the molecular architecture shown for the other nanoparticles produced by the same methods of polymerization. The size scale shown by surface curvatures on the proposed models are consistent with sizes of the nanoparticles.

Considering tests performed at the lowest concentration in nanoparticles (2000 $cm^2.mL^{-1}$), three different cases could be distinguished. (i) Activation was markedly reduced while calcium was removed from incubation media. This situation was observed with nanoparticles A1 and A2. (ii) Activation was significant and remained at the same level in all incubation media. This situation was found studying nanoparticles R2. (iii) In the third situation, the level of activation showed in VBS^{2+} was close to that found for the spontaneous activation. This situation was observed with nanoparticles R1 and R3 consistently with previous works and suggesting that at this concentration and in the conditions of the test these nanoparticles were inert towards the complement system (Coty et al., 2016). However, in calcium free media containing increasing concentrations of magnesium, activation frankly increased above spontaneous activation to pass above 50% conversion of C3 at the highest concentration in magnesium (10 mM).

Nanoparticles tested at concentrations producing 100% activation in VBS^{2+} showed two types of behaviors. Nanoparticles A1 and R2 showed a full activation whatever the composition of the buffers. In contrast, a clear decrease of activation could be highlighted when evaluations were performed in calcium free media considering nanoparticles A2 and R3. No effect of the magnesium concentration was highlighted in this case. Consistent results were obtained comparing the low and high concentrations in nanoparticles considering nanoparticles A2 and R2. Conversely, at the highest concentration in nanoparticles A1 no differences in the activation level was observed while a marked difference could be highlighted in tests performed with a lower concentration in nanoparticles. Again, in contrast to tests performed at the lowest concentration, nanoparticles R3 produced almost a full C3 activation (93%) at the concentration of 2800 $cm^2.mL^{-1}$. Pathways of complement activation produced by these nanoparticles could be elucidated using this concentration in nanoparticles. For nanoparticles R1, it was not surprising that the activation produced remained at the level of the spontaneous activation since we have never reached the concentration threshold testing their capacity to activate the complement system at even higher concentrations than those used in the current work (Coty et al., 2016).

IV. Discussion

The complement system is the first line host response of the innate immune system involved when the body is confronted to pathogens and any type of foreign materials circulating in the blood. Its role in detection of nanoparticles is crucial. It determines their biological functionalities, defining efficacy and safety that are linked to their immunogenic, immunosuppressive and stealth properties (Szeto and Lavik, 2016). Response of the complement system to nanoparticles can be manipulated varying characteristics of nanomaterials. For instance, size, surface composition and charge of nanomaterials influence the response of the complement system. These characteristics are generally well controlled during particle synthesis and easy to evaluate using physicochemical characterization techniques used in routine (Clogston et al., 2016, Varenne et al., 2015a, 2015b,). Activation pathways can be controlled by the molecular architecture of the polymer composing the nanoparticle corona (Hamad et al., 2010). Although it is technically possible to engineer nanoparticles with a desired structure, the lack of clear and precise guidelines to direct this design are still hampering this achievement (Szeto and Lavik, 2016). Systematic studies investigating the influence of molecular feature of nanoparticle corona on their interactions with the complement system are awaited to clarify and complete guidelines. Such studies require series of nanoparticles for which the corona structure has been resolved (Hamad et al., 2010, Hristov et al., 2015, Thomas et al., 2011). We have developed a series of polysaccharide-coated poly(isobutylcyanoacrylate) (PIBCA) nanoparticles and models of the molecular architecture of their corona were established from evidences obtained from different experimental works using different techniques (Bertholon et al. 2006b, 2006c, Chauvierre et al., 2004, Vauthier, 2015, Vauthier et al. 2011, 2009). The 5 dextran-coated nanoparticles selected for the present work showed different capacities to activate the complement system in in vitro conditions that were non-selective to discriminate pathways and based on the evaluation of the cleavage of the protein C3. Being all coated with dextran, these 5 nanoparticles exhibited the same surface composition and almost the same surface charges that was slightly negative. Nanoparticles A1 and A2 showed almost same hydrodynamic diameter (d_H = 100 nm) and nanoparticles R1 (d_H =291 ± 1 nm), R2 (d_H = 234 ± 2 nm) and R3 (d_H =291 ± 1 nm) were of larger diameters (Table 1). Models proposed from previous work to account for the architecture of dextran chains in the nanoparticle corona are

shown in table 2 (Vauthier, 2015, Vauthier et al., 2011, 2009). General characteristics including the size and zeta potential of the nanoparticles synthesized for this work were consistent with those of previous studies as well as their capacity to activate CS evaluated in VBS^{2+} (see figure S2). Reproducibility obtained across different works acknowledged the robustness of the methods of synthesis of the nanoparticles and of our testing method of complement activation based on the highlight of the cleavage of protein C3 (Coty et al., 2016). This has motivated the achievement of a new work that investigated the influence of the architecture of the nanoparticle corona on their interactions with CS discriminating pathways that triggered complement activation.

Consistently with observations made by other authors investigating poly(ethyleneglycol)-coated nanoparticles, the dextran-coated nanoparticles considered here also showed a switch of complement activation pathway depending on the architecture of dextran chains in the corona (Hamad et al., 2010) (Table 2). Besides, they appealed several remarks. At first, exhibiting hydroxyl groups on their surfaces, these nanoparticles were expected to activate strongly the complement system (Szeto and Lavik, 2016, Thomas et al., 2011). Although true for nanoparticles A1, A2, R2 and R3, the nanoparticles R1 did not produced any complement activation in VBS^{2+} up to the highest tested concentration. Due to the presence of hydroxyl groups in the corona, it was also expected that the nanoparticles would trigger complement activation by the alternative pathway, i.e. a calcium independent mechanism, according to a mechanism that induces the cleavage of the unstable strained thioester bond of protein C3 when it meets nucleophiles (Thomas et al., 2011). A work by Banda et al. highlighted that dextran-coated superparamagnetic iron oxide nanoworms triggered complement activation by both the alternative and lectine pathways (Banda et al., 2014). Nanoparticles R2 appeared very selective as they triggered complement activation only through the alternative pathway. The nanoparticles A1, A2 and R3 were far less selective as they triggered complement activation by both calcium dependent and independent pathways. Consistently with the work of Banda et al. it can be suggested that they triggered complement activation through the lectin and alternative pathways respectively (Banda et al., 2014). Factors such as the composition and charge of the nanoparticle surface could not be incriminated to explain the differences that were highlighted because they were mostly identical between nanoparticles. All nanoparticles were not of the same size and this factor has been identified to influence the

way nanoparticles interact with the innate immune system including CS (Alexis et al., 2008, Clogston et al., 2016, Lorenzo-Abalde et al., 2016). Here the largest nanoparticles R1 (d_H = 291 ± 1 nm) escaped complement activation although it was expected from the literature that such a property was reserved to nanoparticles having a much smaller size, preferentially bellow 200 nm (Alexis et al., 2008, Lorenzo-Abalde et al., 2016). For the other nanoparticles, the factor size finally reveals not being a critical factor towards complement activation. Indeed, we could observe a similar behavior of activation between R3 (291 nm) and A2 (113 nm).

Thus, it became relevant to us that the architecture of dextran chains in nanoparticles' corona greatly influenced activation of CS. Differences between the nanoparticles occurs at the molecular size scale. They are generally not detected by routinely applied physicochemical characterization methods but can appear huge at the size scale of proteins producing dramatic effects on the functionality and safety of the nanomaterial (Clogston et al., 2016, Hamad et al., 2010, Hristov et al., 2015,). In relation with model architectures of their corona, the nanoparticles R2 showing a thin corona made of a dense brush of dextran promoted activation through calcium independent mechanism only (alternative pathway). The 3 other types of nanoparticles A1, A2 and R3 were having a corona that allowed a higher accessibility of their surface to protein adsorption triggered activation by both calcium dependent (classical and/or lectin pathways) and independent (alternative pathway) mechanisms (Labarre et al., 2005, Vauthier et al., 2009). Results can be explained taking into account the accessibility of the nanoparticle surface to proteins. Nanoparticles which surfaces were accessible to large proteins (nanoparticles A1, A2 and R3) that includes immunoglobulins and protein C3 triggered activation through different pathways. Activation by the classical pathway can be triggered by immunoglobulins adsorbed on the nanoparticle surface while activation through the alternative pathway can be triggered by nucleophiles exposed on dextran chains or by the adsorbed proteins (Figure 4) (Anderson et al., 2005, Chen et al., 2016, Labarre et al., 2005, Vauthier et al., 2011, 2009). Activation triggered by the lectin pathway can occur if the polysaccharide chain shows an accessible free end chain, assuming that the configuration allowing interactions with the mannose binding lectin should be similar to that of oligosaccharides found on cell/bacteria/virus surfaces. The low density of the brush formed by dextran chains at the surface of nanoparticles R3 may be able to react with the mannose binding protein hence activating CS through the lectin pathway as well (Banda et al., 2014). In

contrast, it can be assumed that the accessibility to the chain ends of dextran anchored at the surface of nanoparticles A1 and A2 is greatly hindered due to the loop and train configurations. Therefore, it was believed that the activation of CS due to a calcium dependent pathway triggered by these nanoparticles mainly occurred through the classical pathway. Due to the formation of a dense brush of dextran chains, coronas of nanoparticles R1 and R2 hamper adsorption of large proteins but small proteins can manage to adsorb on the nanoparticle core surface (Vauthier et al., 2011). The brush of nanoparticles R2 was formed with dextran of a low molecular weight. The brush thickness could be thin enough to let adsorbed proteins to protrude out of the brush. Nucleophiles from these proteins could react with the thioester bond of C3 protein explaining the selectively of the activation of the complement cascade through the alternative pathway (Figure 4). In the case of nanoparticle R1, results from previous work informed that the C3 protein cannot penetrate in the brush formed by dextran chains. Hence, C3 cannot be exposed to the hydroxyl groups of dextran that may trigger its activation through the alternative pathway or to glucose units that may be recognized by the lectin pathway. Due to the brush thickness formed by dextran of a high molecular weight (49 nm as evaluated in a previous work (Vauthier et al., 2011), it was assumed that proteins of small size adsorbed on the nanoparticle core surface were totally engulfed in the brush being not accessible to react with the protein C3 (Vauthier et al., 2011). Also the glucose units of the dextran chains were not accessible to trigger complement activation by the lectin pathway explaining their low capacity to activate the complement system. Regulation of the activation caused by the different types of dextran coronas' architectures depends on the accessibility of the protein C3 to hydroxyl groups of dextran chains and on the capacity of the corona to allow proteins adsorption on the nanoparticle surface. Results suggest that accessibility of protein C3 to nucleophiles determined activation triggered by the alternative pathway (calcium independent route). It is assumed that nanoparticles can trigger the classical pathway (calcium dependent route) when large proteins such as immunoglobulins can adsorb on their surface and by the lectin pathway in the case glucose units that may be recognized by the mannose binding lectin protein were accessible.

Secondly, comparisons of the behaviors found between nanoparticles A1, A2 and nanoparticles R2 point out a methodological issue. At the lower concentration in nanoparticles, they all showed a partial activation in VBS^{2+} and, as expected, raising the

concentration in nanoparticles produced 100% activation. Results of tests performed in calcium depleted buffers (VBSMg^{2+} XmM/EGTA) were consistent at both concentrations with nanoparticles A2 and R2. At the lower concentration, nanoparticles A1 did not show preferential complement activation pathway but at the highest concentration they appeared selective as activation was triggered only through calcium independent pathways. The competition between different activation pathways highlighted at the lower concentration in nanoparticles A1 was hidden when tests were performed with a highest concentration in nanoparticles. Thus, it may be recommended to explore these mechanisms at different concentrations in nanoparticles including total and partial activations.

Finally, during these evaluations some intriguing results were observed with samples that gave low level of complement activation in VBS^{2+} and/or at low concentration in Magnesium in calcium free buffers (VBSMg^{2+} 0.5mM/EGTA). An increase of activation was monitored while increasing the concentration in magnesium in the sample frankly above that of the spontaneous activation evaluated in same media. This effect, that was not yet described, concerns us. We were unable to find an explanation and further work would be necessary to explain it.

Figure 4: Assumptions on mechanisms behind interactions with proteins of the complement system that may interfere with the pathway that triggered complement activation as the function of the molecular architectures of dextran chains in the corona of the 5 types of PIBCA nanoparticle. Architecture found on nanoparticle R1 surface hampers activation of the complement system because it can hinder adsorption of large proteins and interactions with more specific proteins of the complement system (mannose binding lectin (MBL) (MBL) and protein C3 (C3)). Architecture shown by nanoparticles R2 only let access of protein C3 to nucleophiles found on small proteins ( ) that can adsorb on this surface and protrude out of the brush formed by dextran chains of a low molecular weight. Architectures of the surfaces of nanoparticles R3, A1 and A2 allow large proteins to reach the nanoparticle surfaces. Immunoglobulins ( ) can adsorb on these surfaces. Complement activation can be triggered through the classical pathway that involves recognition of adsorbed immunoglobulins by protein C1q (C1q). Protein C3 can also adsorb on these surfaces leading to a possible direct activation through the cleavage of the unstable thioester group hidden in the protein structure. Activation of the protein C3 can also be triggered by nucleophilic groups of dextran chains that might be accessible for a reaction with the thioester bond considering these architectures. Reactions that involved protein C3 straightforward trigger complement

activation through the alternative pathway. Finally, activation through the mannose binding lectin pathway can also be envisaged with the architecture of dextran chains proposed for the nanoparticles R3 that assumes a quite free access of the MBL to terminal glucose units of dextran chains. This pathway is probably not functioning with nanoparticles A1 and A2 because dextran chains of their corona form loops and trains in which access of the MBL to terminal glucose units of the dextran chains might be difficult due to steric hindrance effects.

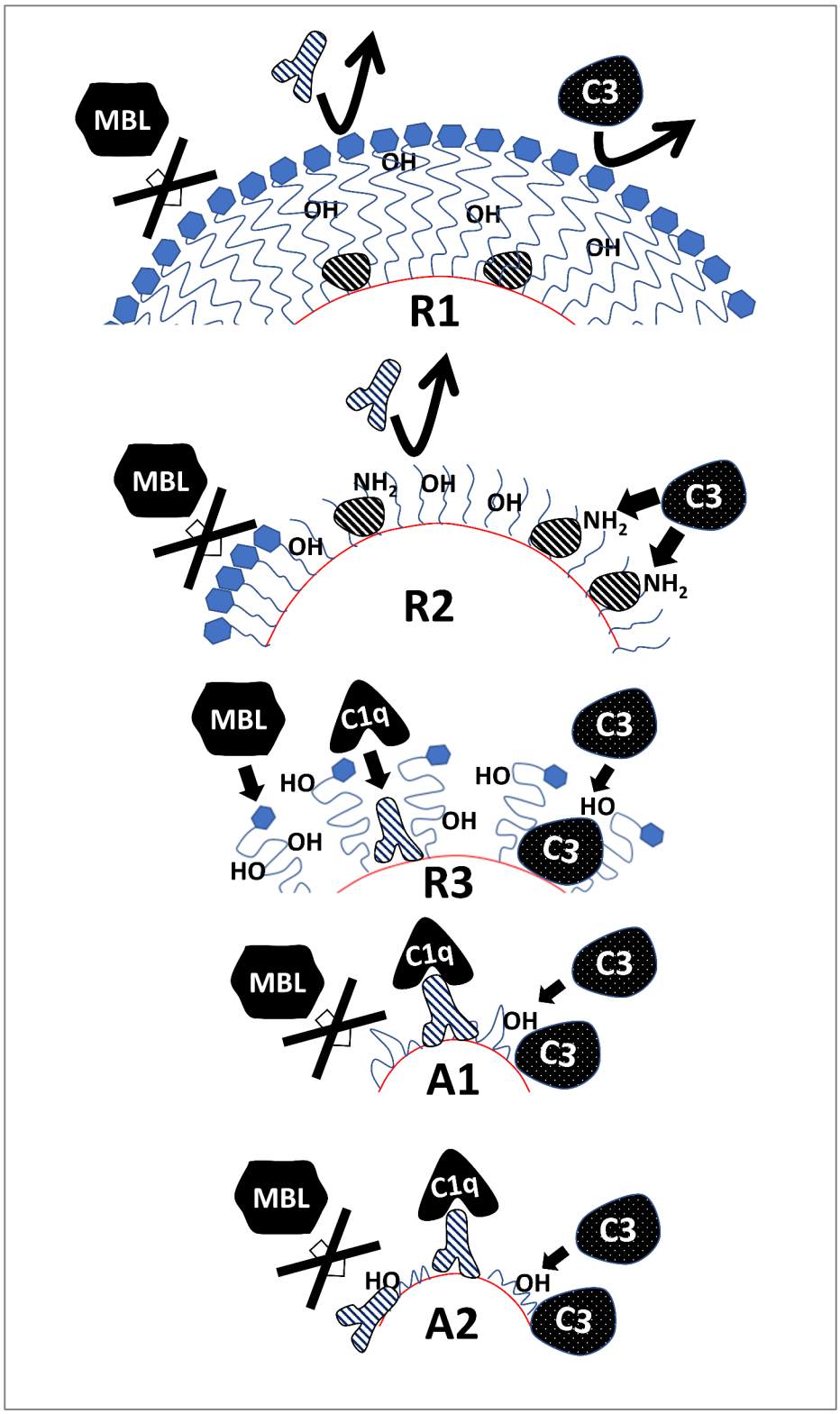

V. Conclusion

This work was a systematic study investigating how molecular design of nanoparticle coronas made of dextran matters on mechanisms that trigger complement activation. Dextran-coated PIBCA nanoparticles used for this work were already thoroughly characterized and known to display different capacities to triggered complement activation based on the highlight of the cleavage of protein C3. The new set of results shows that complement activation pathways can be selected by distinct architectures formed by dextran chains composing the nanoparticle corona. It also suggests assumptions that explain the relation between these mechanisms and the nanoparticle corona molecular feature. The results are of interest to rationalize the design of dextran-coated nanomaterials having defined biological perspectives that can be tuned from their interactions with the complement system. It provides with indications on how to design dextran coatings that will select complement activation pathways or prevent the nanoparticles to activate the complement system on a rational basis Although this work has resolved how molecular design of nanoparticle corona made of dextran can control mechanisms that trigger complement activation, additional works are now needed to fully understand the consequences of the activation of protein C3 produced by these nanoparticles on the full response of the innate immune system. Further work will also be needed to elucidate the occurrence of an unexplained activation of the complement system reported for the first time with low activating nanoparticles while tested in calcium free media containing increasing concentrations of magnesium.

Acknowledgements

The authors acknowledge the financial support from CNPq - PDE grant number 245564/2012-8 (Brazil) and from BPI-France, Project NICE.

VI. Bibliography

Alexis, F., Pridgen, E., Molnar, L.K., Farokhzad, O.C., 2008. Factors affecting the clearance and biodistribution of polymeric nanoparticles. Mol. Pharm. 5,505-515.

Alhareth, K., Vauthier, C., Bourasset, F., Gueutin, C., Ponchel, G., Moussa, F., 2012. Conformation of surface-decorating dextran chains affects the pharmacokinetics and biodistribution of doxorubicin-loaded nanoparticles. Eur. J. Pharm. Biopharm. 81, 453-457.

Andersen, A.J., Wibroe, P.P., Moghimi, S.M., 2012 Perspectives on carbon nanotube-mediated adverse immune effects. Adv. Drug Deliv. Rev. 64,1700-1705.

Anderson, J., Ekdahl, K.N., Lambris, J.D., Nilsson, B., 2005. Binding of C3 fragments on top of adsorbed plasma proteins during complement activation on a model biomaterial surface. Biomaterials. 26, 1477-1485.

Anchordoquy, T.J., Barenholz, Y., Boraschi, D., Chorny, M., Decuzzi, P., Dobrovolskaia, M.A., Farhangrazi, Z.S., Farrell, D., Gabizon, A., Ghandehari, H., Godin, B., La-Beck, N.M., Ljubimova, J., Moghimi, S.M., Pagliaro, L., Park, J.H., Peer, D., Ruoslahti, E., Serkova, N.J., Simberg, D., 2017. Mechanisms and Barriers in Cancer Nanomedicine: Addressing Challenges, Looking for Solutions. ACS Nano. 11,12-18.

Banda, N.K., Mehta, G., Chao, Y., Wang, G., Inturi, S., Fossati-Jimack, L., Botto, M., Wu, L., Moghimi, S.M., Simberg D., 2014. Mechanisms of complement activation by dextran-coated superparamagnetic iron oxide (SPIO) nanoworms in mouse versus human serum. Part. Fibre Toxicol. 11,64. doi: 10.1186/s12989-014-0064-2.

Bazile, D., Prud'homme, C., Bassoullet, M.T., Marlard, M., Spenlehauer, G., Veillard, M., 1995. Stealth Me.PEG-PLA nanoparticles avoid uptake by the mononuclear phagocytes system. J. Pharm. Sci. 84, 493-498.

Bertholon, I., Vauthier, C., Labarre D., 2006a. Complement activation by core-shell poly(isobutylcyanoacrylate)-polysaccharide nanoparticles : Influences of surface morphology, length, and type of polysaccharide. Pharm. Res. 23, 1313-1323.

Bertholon, I., Hommel H, Labarre D, Vauthier C., 2006b. Properties of polysaccharides grafted on nanoparticles investigated by EPR. Langmuir. 2006 Jun 6;22(12):5485-90.

Bertholon, I., Lesieur, S., Labarre, D., Besnard, M., Vauthier, C., 2006c. Characterization of dextran-poly(isobutylcyanoacrylate) copolymers obtained by redox radical and anionic emulsion polymerization. Macromolecules. 39, 3559-3567.

Carroll, M.V., Sim, R.B., 2011. Complement in health and disease. Adv. Drug Deliv. Rev. 63,965-975.

Chauvierre, C., Labarre, D., Couvreur, P., Vauthier, C. 2003. Novel polysaccharide-decorated poly(isobutyl cyanoacrylate) nanoparticles. Pharm. Res. 20,1786-1793.

Chauvierre, C., Vauthier, C., Labarre, D., Hommel, H., 2004. Evaluation of the surface properties of dextran-coated poly(isobutylcyanoacrylate) nanoparticles by spin-labelling coupled with electron resonance spectroscopy. Colloid Polym. Sci. 282:1016–1025.

Chen, C.C., Borden, M.A., 2011. The role of poly(ethylene glycol) brush architecture in complement activation on targeted microbubble surfaces. Biomaterials. 32, 6579-6587.

Chen, F., Wang, G., Griffin, J.I., Brenneman, B., Banda, N.K., Holers, V.M., Backos, D.S., Wu, L., Moghimi, S.M., Simberg D. (2016). Complement proteins bind to nanoparticle protein corona and undergo dynamic exchange in vivo. Nat. Nanotechnol. http://dx.doi.org/10.1038/nnano.2016.269.

Clogston, J.D., Crist, R.M., McNeil, S.E., 2016. Physico-chemical characterization of polymer nanoparticles: challenge and present limitations. In: Vauthier, C., Ponchel, G. (Eds.), Polymer nanoparticles for nanomedicines. Springer International Publishing, Cham, Switzerland, chap 7, pp. 187-204.

Coty, J.B., Varenne, F., Vachon, J.J., Vauthier, C., 2016 Serial multiple crossed immunoelectrophoresis at a microscale: A stamp-sized 2D immunoanalysis of protein C3 activation caused by nanoparticles. Electrophoresis. 37,2401-2409.

Couvreur, P., Kante, B., Roland, M., Guiot, P., Bauduin, P., Speiser, P. 1979. Polycyanoacrylate nanocapsules as potential lysosomotropic carriers: preparation, morphological and sorptive properties. J. Pharm. Pharmacol. 31,331-332.

Couvreur, P., Vauthier, C., 2006. Nanotechnology: intelligent design to treat complex disease. Pharm. Res. 23, 1417-1450.

Crucho, C.I.C., Barros, M.T., 2015. Formulation of functionalized PLGA polymeric nanoparticles for targeted drug delivery. Polymer. 68:41-46.

D'Addio, S.M., Saad, W., Ansell, S.M., Squiers, J.J., Adamson, D.H., Herrera-Alonso, M., Wohl, A.R., Hoye, T.R., Macosko, C.W., Mayer, L.D., Vauthier, C., Prud'homme, R.K., 2012. Effects of block copolymer properties on nanocarrier protection from in vivo clearance. J. Control. Release. 162, 208-217.

Des Prez, R.M., Bryan, C.S., Hawiger, J., Colley, D.G., 1975. Function of the classical and alternate pathways of human complement in serum treated with ethylene glycol tetraacetic acid and MgCl2-ethylene glycol tetraacetic acid. Infect. Immun. 11, 1235-1243.

Dobrovolskaia, M.A., McNeil, S.E., 2013. Handbook of immunological properties of engineered nanomaterials. Vol 1.: Frontiers in nanobiomaterial research. World Scientific Publishing Co. Pte. Ltd., Singapore.

Du, X.J., Wang, J.L., Liu, W.W., Yang, J.X., Sun, C.Y., Sun, R., Li, H.J., Shen, S., Luo, Y.L., Ye, X.D., Zhu, Y.H., Yang, X.Z., Wang, J., 2015. Regulating the surface poly(ethylene glycol) density of polymeric nanoparticles and evaluating its role in drug delivery in vivo. Biomaterials. 69:1-11.

Gasque, P., 2004. Complement: a unique innate immune sensor for danger signals. Mol. Immunol. 41, 1089-1098.

Gref R., Domb, A., Quellec, P., Blunk, T., Müller, R.H., Verbavatz, J.M., Langer, R., 1995. The controlled intravenous delivery of drugs using PEG-coated sterically stabilized nanospheres. Adv. Drug Deliv. Rev. 16, 215-233.

Gref, R., Lück, M., Quellec, P., Marchand, M., Dellacherie, E., Harnisch, S., Blunk, T., Muller, R.H., 2000. 'Stealth' corona-core nanoparticles surface modified by polyethylene glycol (PEG): influences of the corona (PEG chain length and surface density) and of the core composition on phagocytic uptake and plasma protein adsorption. Colloids Surf B Biointerfaces. 18, 301-313.

Gref, R, Minamitake Y, Peracchia MT, Trubetskoy V, Torchilin V, Langer R. Biodegradable long-circulating polymeric nanospheres. Science. 1994 Mar 18;263(5153):1600-3.

Hamad, I., Al-Hanbali, O., Hunter, A.C., Rutt, K.J., Andresen, T.L., Moghimi, S.M., 2010. Distinct polymer architecture mediates switching of complement activation pathways at the nanosphere-serum interface: implications for stealth nanoparticle engineering. ACS Nano. 4, 6629-6638.

Hamad, I., Hunter, A.C., Szebeni ,J., Moghimi, S.M., 2008. Poly(ethylene glycol)s generate complement activation products in human serum through increased alternative pathway turnover and a MASP-2-dependent process. Mol. Immunol. 46, 225-232.

Harboe, M., Thorgersen, E.B., Mollnes, T.E., 2011. Advances in assay of complement function and activation. Adv. Drug Deliv. Rev. 63, 976-987.

Hristov, D.R., Rocks, L., Kelly, P.M., Thomas, S.S., Pitek, A.S., Verderio, P., Mahon, E., Dawson, K.A., 2015. Tuning of nanoparticle biological functionality through controlled surface chemistry and characterisation at the bioconjugated nanoparticle surface. Sci Rep. 5, 17040. http://dx.doi.org/10.1038/srep17040.

Ilinskaya, A.N., Dobrovolskaia, M.A., 2016a. Understanding the correlation between in vitro and in vivo immunotoxicity test for nanomedicines. J. Control. Release. 172, 456-466.

Ilinskaya, A.N., Dobrovolskaia, M.A., 2016b. Interaction between nanoparticles and plasma proteins : effects on nanoparticle biodistribution and toxicity. In: Vauthier, C., Ponchel, G. (Eds.), Polymer nanoparticles for nanomedicines. Springer International Publishing, Cham, Switzerland, chap 15, pp. 505-520.

Labarre, D., Montdargent, B., Carreno, M.P., Maillet, F., 1993. Strategy for in vitro evaluation of the Interactions between biomaterials and complement system. J. App. Biomaterials. 4, 231-240.

Labarre, D., Vauthier, C., Chauvierre, C., Petri, B., Muller, R.H., Chehimi, M.M., 2005. Interactions of blood proteins with poly (isobutylcyanoacrylate) nanoparticles decorated with a polysaccharidic brush. Biomaterials. 26, 5075-5084.

Lemarchand, C., Gref, R., Passirani, C., Garcion, E., Petri, B., Müller, R., Costantini, D., Couvreur, P., 2006. Influence of polysaccharide coating on the interactions of nanoparticles with biological systems. Biomaterials. 27, 108-118.

Li, J., Wang, Y., Liang, R., An, X., Wang, K., Shen, G., Tu, Y., Zhu, J., Tao, J., 2015. Recent advances in targeted nanoparticles drug delivery to melanoma. Nanomedicine. 11, 769-794.

Lorenzo-Abalde, S., Simon-Vazquez, R., Peleteiro Olmedo, M., Lozano-Fernandez, T., Estevez-Martinez, O., Fernandez-Carrera, A., Gonzalez-Fernandez, A., 2016. Evaluating the interactions between proteins and components of the immune system with polymer nanoparticles. In: Vauthier, C., Ponchel, G. (Eds.), Polymer nanoparticles for nanomedicines. Springer International Publishing, Cham, Switzerland, chap 9, pp. 221-290.

Merle, N.S., Church, S.E., Fremeaux-Bacchi, V., Roumenina, L.T., 2015. Complement System Part I – Molecular Mechanisms of Activation and Regulation. Front. Immunol. 6, 262. http://dx.doi.org/10.3389/fimmu.2015.00262

Moghimi, S.M., Szebeni, J., 2003. Stealth liposomes and long circulating nanoparticles: critical issues in pharmacokinetics, opsonization and protein-binding properties. Prog. Lipid Res. 42, 463-478.

Moghimi, S.M., Farhangrazi, Z.S., 2013. Nanomedicine and the complement paradigm. Nanomedicine: Nanotechnol. Biol. Med. 9, 458-460.

Müller, J., Bauer, K.N., Prozeller, D., Simon, J., Mailänder, V., Wurm, F.R., Winzen, S., Landfester, K., 2017. Coating nanoparticles with tunable surfactants facilitates control over the protein corona. Biomaterials. 2017 115, 1-8.

Neun, B. W., Ilinskaya, A., Dobrovolskaia, M. A., Analysis of Complement Activation by EIA, NCL Method ITA-5.2 Version 1.2, 2015. Available from http://ncl.cancer. gov/NCL_Method_ITA-5.2.pdf (consulted on February 2017).

Nicolas, J., Couvreur, P., 2009. Synthesis of poly(alkyl cyanoacrylate)-based colloidal nanomedicines. Wiley Interdiscip Rev Nanomed Nanobiotechnol. 1, 111-127.

Nicolas, J., Mura, S., Brambilla, D., Mackiewicz, N., Couvreur, P., 2013. Design, functionalization strategies and biomedical applications of targeted biodegradable/biocompatible polymer-based nanocarriers for drug delivery. Chem. Soc. Rev. 42, 1147-1235.

Nicolas, J., Vauthier, C., 2011. Poly(alkylcyanoacrylate) nanosystems. In: Prokop A. (Ed.). Intracellular delivery. Fundamental and applications. Springer, New York. pp. 225-250.

Őrfi, E., Szebeni, J., 2016. The immune system of the gut and potential adverse effects of oral nanocarriers on its function. Adv. Drug. Deliv. Rev. 106, 402-409.

Peracchia, M.T., Fattal, E., Desmaële, D., Besnard, M., Noël, J.P., Gomis, J.M., Appel, M., d'Angelo, J., Couvreur, P., 1999. Stealth® PEGylated polycyanoacrylate nanoparticles for intravenous administration and splenic targeting. J. Control. Release. 60, 121-128.

Peracchia, M.T., Vauthier, C., Passirani, C., Couvreur, P., Labarre, D., 1997. Complement consumption by poly(ethylene glycol) in different conformations chemically coupled to poly(isobutyl 2-cyanoacrylate) nanoparticles. Life Sci. 61, 749-761.

Shi, J., Kantoff, P.W., Wooster, R., Farokhzad, O.C., 2017. Cancer nanomedicine: progress, challenges and opportunities. Nat. Rev. Cancer. 17, 20-37.

Suk, J.S., Xu, Q., Kim, N., Hanes, J., Ensign, L.M., 2016. PEGylation as a strategy for improving nanoparticle-based drug and gene delivery. Adv. Drug Deliv. Rev. 99, 28-51.

Szebeni, J., 2012. Hemocompatibility testing for nanomedicines and biologicals: predictive assays for complement mediated infusion reactions. Eur. J. Nanomed. 1, 33–53.

Szebeni, J., 2014. Complement activation-related pseudoallergy: a stress reaction in blood triggered by nanomedicines and biologicals. Mol. Immunol. 61, 163-173.

Szebeni, J., Bedőcs, P., Rozsnyay, Z., Weiszhár, Z., Urbanics, R., Rosivall, L., Cohen, R., Garbuzenko, O., Báthori, G., Tóth, M., Bünger, R., Barenholz, Y., 2012. Liposome-induced complement activation and related cardiopulmonary distress in pigs: factors promoting reactogenicity of Doxil and AmBisome. Nanomedicine. 8, 176-184.

Szebeni, J, Storm, G., 2015. Complement activation as a bioequivalence issue relevant to the development of generic liposomes and other nanoparticulate drugs. Biochem. Biophys. Res. Commun. 468, 490-497.

Szeto, G.L., Lavik, E.B., 2016. Materials design at the interface of nanoparticles and innate immunity. J. Mater. Chem. B Mater. Biol. Med. 4, 1610-1618.

Thomas, S.N., van der Vlies, A.J., O'Neil, C.P., Reddy, S.T., Yu, S.S., Giorgio, T.D., Swartz, M.A., Hubbell, J.A., 2011. Engineering complement activation on polypropylene sulfide vaccine nanoparticles. Biomaterials. 32, 2194-2203.

Toda, M., Arima, Y., Iwata, H., 2010. Complement activation on degraded polyethylene glycol-covered surface. Acta Biomaterialia. 6, 2642-2649.

Truel, L., Nienhaus, G.U., 2013. Nanoparticle interactions with plasma proteins as it relates to biodistribution. In: Dobrovolskaia, M.A., McNeil, S.E. (Eds.). Handbook of immunological properties of engineered nanomaterials. Vol 1.: Frontiers in nanobiomaterial research. World Scientific Publishing Co. Pte. Ltd., Singapore. Chap. 6, pp. 151-172.

Varenne, F., Botton, J., Merlet, C., Beck-Broichsitter, M., Legrand F.X., Vauthier, C., 2015a. Standardization and validation of a protocol of size measurements by dynamic light scattering for monodispersed stable nanomaterial characterization. Coll and Surf A., 486:124-138.

Varenne, F., Botton, J., Merlet, C., Vachon, J.J., Geiger, S., Infante, I.C., Chehimi, M.M., Vauthier, C., 2015b. Standardization and validation of a protocol of zeta potential measurements by electrophoretic light scattering for nanomaterial characterization. Coll. and Surf. A. 486, 218-231., Erratum: Coll. and Surf A., 2016, 498, 283-284.

Vauthier, C. 2015. Interactions of polysaccharide-coated nanoparticles with proteins. In: Sutariya, V.B., Pathak, Y. (Eds.). Biointeractions of nanomaterials. CRC Press Taylor & Francis group, Boca Raton. Chap. 18, pp. 365-382.

Vauthier, C., Labarre, D., Ponchel, G., 2007. Design aspects of poly(alkylcyanoacrylate) nanoparticles for drug delivery. J. Drug Target. 15, 641-663.

Vauthier, C., Lindner, P., Cabane, B., 2009. Configuration of bovine serum albumin adsorbed on polymer particles with grafted dextran corona. Coll. and Surf. B. 69, 207-215.

Vauthier, C., Persson, B., Lindner, P., Cabane, B., 2011. Protein adsorption and complement activation for di-block copolymer nanoparticles. Biomaterials. 32, 1646-1656.

Vauthier, C., Schmidt, C., Couvreur, P., 1999. Measurement of the Density of Polymeric Nanoparticulate Drug Carriers by Isopycnic Centrifugation. J. Nanoparticle Res. 1, 411-418.

Vittaz, M., Bazile, D., Spenlehauer, G., Verrecchia, T., Veillard, M., Puisieux, F., Labarre, D., 1996. Effect of PEO surface density on long-circulating PLA-PEO nanoparticles which are very low complement activators. Biomaterials. 17, 1575-1581.

Vogel, C.W., Fritzinger, D.C., 2010. Cobra venom factor: Structure, function, and humanization for therapeutic complement depletion. Toxicon. 56, 1198-1222.

Vonarbourg, A., Passirani, C., Saulnier, P., Benoit, J.P., 2006. Parameters influencing the stealthiness of colloidal drug delivery systems. Biomaterials. 27, 4356-4373.

Vorup-Jensen, T., Boesen, T., 2011. Protein ultrastructure and the nanoscience of complement activation. Adv. Drug Deliv. Rev. 63, 1008-1019.

Xiang, S.D., Fuschberger, M., Karlson, T.D.L., Hardy, C.L., Selonmulya, C., Plebanski, M., 2013. Nanoparticles, immunomodulation and vaccine delivery. In: Dobrovolskaia, M.A., McNeil, S.E. (Eds.). Handbook of immunological properties of engineered nanomaterials. Vol 1.: Frontiers in nanobiomaterial research. World Scientific Publishing Co. Pte. Ltd., Singapore. Chap 15, pp. 449-477.

Supplementary material

Tuning complement activation and pathway through controlled molecular architecture of dextran chains in nanoparticle corona

Jean Baptiste Coty[a], Elquio Eleamen Oliveira[a,b], Christine Vauthier[a]*

[a] Institut Galien Paris-Sud, CNRS, Univ. Paris-Sud, Châtenay-Malabry, France.

[b] Centro de Ciências Biológicas e Sociais Aplicadas, Universidade Estadual da Paraíba, João Pessoa, PB 58070450, Brazil

*Corresponding Author:

Christine Vauthier

Institut Galien Paris-Sud, CNRS UMR 8612, Univ. Paris-Sud, Faculté de Pharmacie, 5 Rue J.B. Clément, 92296 Châtenay-Malabry, France.

E-mail : christine.vauthier@u-psud.fr

Supplementary material 1

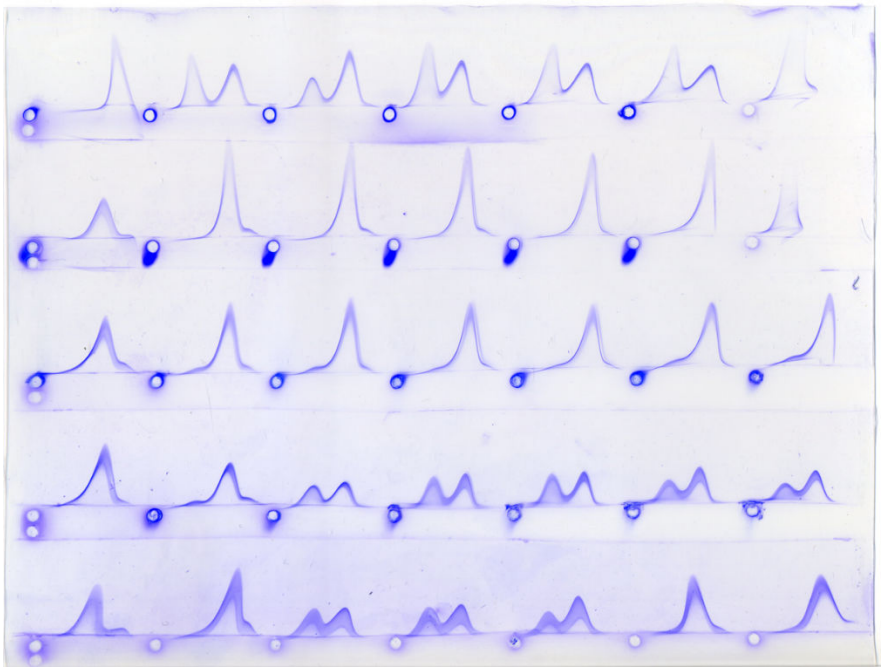

A2						
VBS 2+	VBS Mg2+ 0.5mM, EGTA	VBS Mg2+ 2.5mM, EGTA	VBS Mg2+ 5mM, EGTA	VBS Mg2+ 7.5mM, EGTA	VBS Mg2+ 10mM, EGTA	VBS 2+ sp*
A1						
VBS 2+	VBS Mg2+ 0.5mM, EGTA	VBS Mg2+ 2.5mM, EGTA	VBS Mg2+ 5mM, EGTA	VBS Mg2+ 7.5mM, EGTA	VBS Mg2+ 10mM, EGTA	VBS 2+ sp*
R2						**R3**
VBS 2+	VBS Mg2+ 0.5mM, EGTA	VBS Mg2+ 2.5mM, EGTA	VBS Mg2+ 5mM, EGTA	VBS Mg2+ 7.5mM, EGTA	VBS Mg2+ 10mM, EGTA	**VBS 2+**
CVF	**R3**					
VBS Mg2+ 2.5mM, EGTA	VBS 2+	VBS Mg2+ 0.5mM, EGTA	VBS Mg2+ 2.5mM, EGTA	VBS Mg2+ 5mM, EGTA	VBS Mg2+ 7.5mM, EGTA	VBS Mg2+ 10mM, EGTA
	CVF	**HAGG**	**HAGG**	**HAGG**	**CVF**	**CVF**
VBS 2+ sp*	VBS 2+	VBS Mg2+ 0.5mM, EGTA	VBS Mg2+ 0.5mM, EGTA	VBS Mg2+ 2.5mM, EGTA	VBS Mg2+ 0.5mM, EGTA	VBS Mg2+ 2.5mM, EGTA

Figure S1: Example of electrophoresis plate obtained from the Serial multiple crossed immunoelectrophoresis method* applied to evaluate cleavage of protein C3 in serum incubated in different conditions with nanoparticles.

*Coty JB, Varenne F, Vachon JJ, Vauthier C. Serial multiple crossed immunoelectrophoresis at a microscale: A stamp-sized 2D immunoanalysis of protein C3 activation caused by nanoparticles. Electrophoresis. 2016 Sep;37(17-18):2401-9. doi: 10.1002/elps.201500572.

Supplementary material 2

Activation of the protein C3 evaluated in different works. Results that were reproduced across the different studies while performed by different lab workers suggest a high reproducibility of the methods that were used to prepare the nanoparticles and of the method applied to evaluate complement activation.

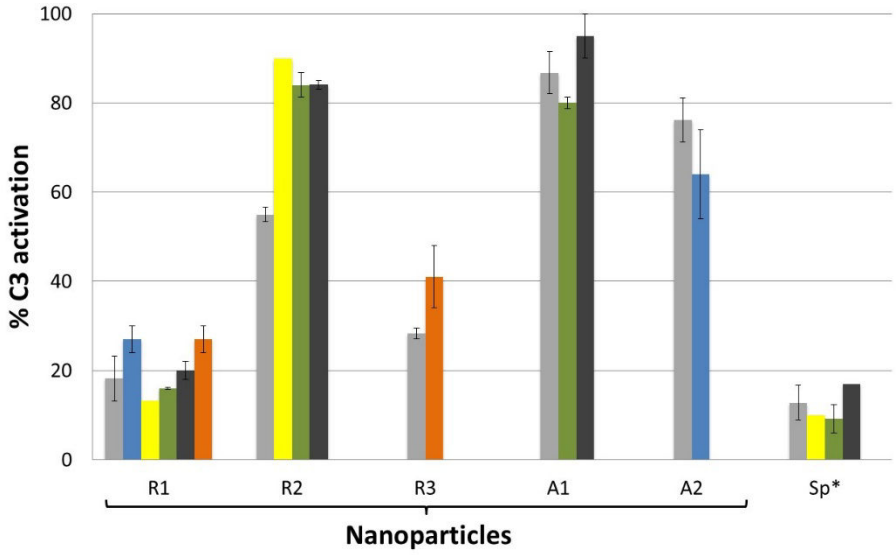

Figure S2: Complement activation given by a series of five dextran-coated nanoparticles as evaluated from the cleavage of protein C3 in different works. Tests were performed by incubating the nanoparticles at a concentration of 2000 $cm^2.mL^{-1}$ with serum in VBS^{2+}. Gray [1], blue [2], yellow [3], green [4], orange [5], black [6].

1. Current study.
2. Bertholon I, Vauthier C, Labarre D. Complement activation by core-shell poly(isobutylcyanoacrylate)-polysaccharide nanoparticles: Influences of surface morphology, length, and type of polysaccharide. Pharmaceutical Research. 2006;23(6):1313-23.
3. Chauvierre C., Labarre D., Couvreur P., Vauthier C. Novel polysaccharide-decorated poly(isobutyl cyanoacrylate) nanoparticles. Pharmaceutical Research 20,1786-1793, 2003.
4. Coty JB, Varenne F, Vachon JJ, Vauthier C. Serial multiple crossed immunoelectrophoresis at a microscale: A stamp-sized 2D immunoanalysis of protein C3 activation caused by nanoparticles. Electrophoresis. 2016 Sep;37(17-18):2401-9. doi: 10.1002/elps.201500572.
5. Vauthier C., Persson B., Lindner P., Cabane B. Protein adsorption and complement activation for di-block copolymer nanoparticles. Biomaterials, 32: 1646-1656 (2011), Available online 18 November 2010, doi:10.1016/j.biomaterials.2010.10.026.
6. Labarre D., Vauthier C., Chauvierre C., Petri B., Muller R.H., Chehimi M.M. Interactions of blood proteins with poly (isobutylcyanoacrylate) nanoparticles decorated with a polysaccharidic brush Biomaterials, 26: 5075-5084 (2005)

Chapitre IV : Vers une analyse qualité de l'activation du complément par les nanomédecines : developpement d'une méthode SPR

Avant propos : Le test d'activation du système du complément par des nanomédecines (NMs) est de premier intérêt pour un système destiné à être administré par voie intraveineuse. Aujourd'hui, ce test n'est pas réalisé de façon systématique pour un contrôle des lots de NMs produits. Etant donné des effets indésirables parvenus suite à l'activation du complément de certaines NMs, il apparaît nécessaire de contrôler la tendance de ces matériaux à déclencher la cascade du système du complément. Le coût ou la complexité des méthodes le permettant sont aujourd'hui un frein à la réalisation de cet essai en routine. Içi, nous proposons un test de l'activation du complément automatisé en utilisant la résonnance plasmonique de surface (SPR). Cette technique utilise la variation de l'angle de résonnance d'un rayon lumineux en fonction de la quantité d'interactions entre un récepteur et un ligand. Son principe est introduit plus en détail dans *l'annexe méthodologique n°3*. Dans notre cas, nous immobilisons des anticorps spécifiques de fragments de protéines du complément sur une puce en or, qui reconnaissent les fragments d'intérêt lors du passage d'un sérum incubé avec des nanoparticules. La réponse obtenue avec chaque anticorps permet d'évaluer le niveau d'activation du complément. Cette méthode permet d'utiliser de très faibles quantités d'anticorps et de sérum, et d'effectuer la détection de différents fragments du complément sur plusieurs canaux en même temps. Les résultats obtenus par cette méthode se sont montrés cohérents avec ceux obtenus par la µC-IE. De plus, une étude de l'impact de la préparation des échantillons a pu dévoiler un possible biais lors de l'étude de l'activation du complément par les NMs, notamment lorsque l'analyse est réalisée après le retrait des NMs de l'échantillon.

Projet d'article

Assessment of complement activation by nanoparticles as a quality requirement: development of a SPR based method and comparison with current high throughput methods

Jean-Baptiste Coty, Magali Noiray, Christine Vauthier*

Institut Galien Paris-Sud, CNRS, Univ. Paris-Sud, Université Paris-Saclay, 5 rue Jean-Baptiste Clément, 92290 Châtenay-Malabry, France

***Correspondence:** Dr. Christine Vauthier, CNRS UMR 8612, Institut Galien Paris Sud, Univ. Paris-Sud, Université Paris-Saclay, 5, rue Jean-Baptiste Clément, 92296 Châtenay-Malabry, France. Fax: +33 146835946. E-mail: christine.vauthier@u-psud.fr

Abstract

Assessment of nanomaterial safety is a major concern today, even more in the field of Nanomedicine. For those destined to an intravenous administration, the study of interactions with the complement system is a key step when assessing their safety. While ELISA is the common test used for *in vitro* studies thanks to its availability and simplicity of use, it has some drawbacks such as its high cost and its fragment dependency. Then, the recently renovated multi-crossed 2D immunoelectrophoresis method allows a costless and direct visualization of C3 fragmentation, but still being time consuming. In this article, we developed a method that combines the advantages of both methods, using Surface Plasmon Resonance (SPR). It provides a fast, automated technique for the detection of complement fragments in serum. The four channels chip permits a multiplexed assessment of complement fragments release at the same time. The mild regeneration of these channels allows for a very low consumption of specific antibodies. This method was compared with the two others mentioned above concerning their results in complement activation by a series of nanoparticles with known complement activation status. The method was then used to evaluate a bias that may occur while evaluating complement activation produced by nanoparticles with a detection based on specific complement fragments.

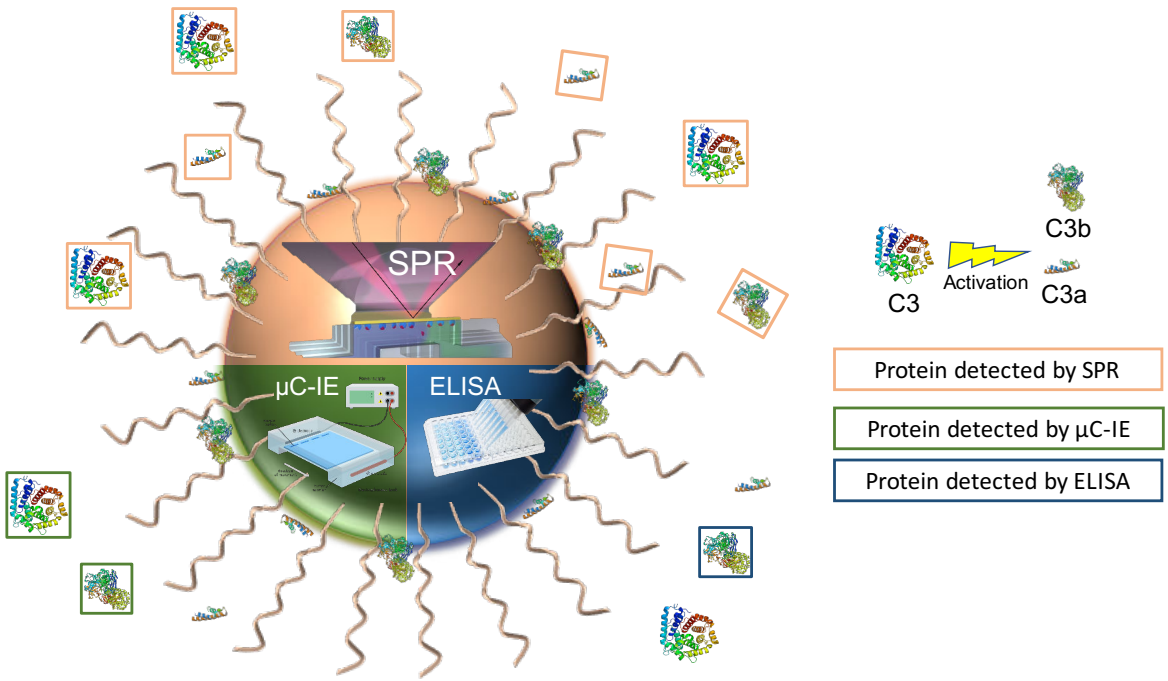

I. Introduction

The complement system is a major effector of the human innate and adaptive immunity. Consisting of 35 soluble blood proteins, this system can be activated through proteolytic cleavages that are arranged in a cascade when a foreign body is detected (bacteria, virus, nanomaterial). The triggering of this cascade leads to inflammation reactions by the release of anaphylatoxins (C3a, C5a) as well as enhancement of phagocytic activity and formation of lysis complex [1,2]. In the case of nanomedicines (NMs) used upon intravenous administration, complement proteins are the first barrier of immunity encountered by the nanomaterial in human blood. The biodistribution, circulation time, or the possible induced toxicity of these nanomaterials can be influenced by their interaction with the complement system [3,4]. Indeed, the interaction of NMs with complement proteins triggers this cascade that can lead to severe adverse reactions referenced in the CARPA (Complement Activation Related Pseudo Allergy) [5-7] and has even been linked to an enhancement of cancer tumor growth [8,9].

Despite these facts, complement activation has not been positioned as a priority assessment in NMs design and in their clinical batch release. While assays are recommended for complement activation of material devices by ISO (International Organization for Standardization) [10] and ASTM (American Society for Testing and Materials) [11], only few recommendations for the complement activation evaluation of intravenous drug are existing [12,13]. The development of a direct and automatable method on this purpose could favor its assessment hence improving the safety and knowledge about NMs links with the complement system. Today, the reference method used for *in vitro* complement activation assessment is ELISA (Enzyme-linked immunosorbent assay) [6,14-17]. This method was standardized and marketed available kits allow the detection of different specific fragments of the complement cascade (iC3b, Bb, C4d, SC5b9). However, this method suffers from its high cost. A method such as two-dimensional immunoelectrophoresis (2D-IE) allows a cheaper assessment of complement activation assessment with a global vision of C3 and its fragments [15,18]. This method was recently improved to be applicable on a higher throughput (multi-crossed 2D immunoelectrophoresis: µC-IE), but still remains time consuming. The use of a fully automatable technique such as surface plasmon resonance (SPR) to detect complement fragments in serum is another way to deal with complement assessment. SPR is widely used

for affinity and kinetics studies between a ligand and a given substrate. NM-protein interaction has already been studied by SPR by grafting the NMs onto the gold chip before flowing the biological medium and looking for interactions and kinetics of association-dissociation [19-21].

However, a major hurdle when working with complement system is the matrix complexity such as encountered in human serum where the non-specific protein binding is a real problem faced in SPR. Development of strategies to overcome this major drawback are emerging but require the engineering of complex chips [22-24]. This typically prevents many applications from being studied by SPR. Nevertheless, some groups already worked on complement detection by SPR with different approaches where the tested biomaterial is generally coated on the chip [25-27], that limits the possibilities of high throughput analysis of several distinct biomaterials.

Added to these aspects, antibody regeneration is another critical issue when working with SPR. In previously mentioned studies, specific antibodies were flowed on the surface and their binding on complement proteins interacting with the biomaterial surface increased the signal. This procedure supposes a high consumption of antibodies, hence a high cost. The other way is to coat specific antibodies on the chip and then flow activated serum for binding of specific fragments. The difficulty of this procedure is to regenerate coated antibodies to keep their functionality for other samples [28-30]. This was a challenge taken into account in our method development.

Finally, the way to detect complement activation by looking for a specific fragment is prone to possible artefacts such as adsorption of this specific component on the nanoparticle (NP) thus preventing its detection. A fragment of protein C3 that is quickly released is the C3a fragment (9000 Da), which acts as an anaphylatoxin, triggering inflammatory reactions. Several works reported a possible adsorption of this fragment on polymer surfaces, thus biasing their quantification when assessed in the serum supernatant [31]. The phenomenon was first evidenced on polymers forming dialysis membrane such as polyacrylonitrile or cellulose acetate [32,33]. Then, their adsorption onto different types of grafted polymers were studied by Montdargent *et al*. [34]. They showed that adsorption on polymer surface was occurring with anaphylatoxins C3a and C5a for neutral, anionic and cationic polymer surfaces. The adsorption greatly depended on the chemical nature of the polymer substituent group. In

the present work, we tested different NPs with the same chemical composition but different surface conformations and showed that this parameter was of importance too regarding C3a adsorption. These results were further put in relation with possible bias occurring with current established protocols for complement activation assessment.

The developed SPR method was confronted to standardized methods already used for complement activation assessment. Thus, the approach of this paper allowed a comparison between three methods (ELISA, SPR and µC-IE). Such a comparison has never been reported in the literature. Indeed, complement activation is generally evaluated only with commercially available assays, mostly ELISA.

The purpose of this work was to develop a SPR-based method for a simplified and cost-effective assessment of complement activation by NMs. Results obtained with this method were challenged with standardized and robust methods, namely ELISA and µC-IE. Finally, a complementary study aimed to evaluate the possible bias introduced by the presence of NPs in the medium and thus adapt the optimal conditions for reliable assays. To support this study, a series of five model NPs of the same chemical composition but bearing distinct surface density and conformation chains were used.

II. Material and methods

II.1. Materials

Chemicals: Isobutylcyanoacrylate (IBCA) was provided by Orapi (Saint-Vulbas, France). Tricine, Tris base (Sigma 7-9®), sodium chloride, EDTA sodium salt, dextran 66.7 kDa, and bromophenol blue were purchased from Sigma (Saint-Quentin-Fallavier, France). Dextran 17.7, cerium (IV) ammonium nitrate, and hydrochloric acid were supplied by Fluka (Saint-Quentin-Fallavier, France). Nitric acid was provided by Prolabo (Paris, France). Calcium lactate, glacial acetic acid, coomassie brilliant blue R-250 were supplied by Thermo Fisher Scientific (Villebon-sur-Yvette, France). Gel-Fix™ for agarose (265 x 150 mm) was obtained from Serva Electrophoresis (Heidelberg, Germany). Amine coupling kit, Series S Sensor Chip CM5, HBS-EP+ buffer 10X, NSB reducer and HCl-Glycine pH 2.5 were obtained from GE Healthcare (Velizy-Villacoublay, France). All chemicals were of reagent grade and used as purchased.

Biologicals: Goat IgG (purity > 80%) was obtained from Sigma (Saint-Quentin-Fallavier, France). Polyclonal anti-human C3 antibody raised in goat was purchased from Fitzgerald

antibodies (Acton, USA). Monoclonal anti-human C3a neoepitope produced in mouse came from antibodies-online GmbH (Aachen, Germany). Serum was prepared from human plasma obtained from healthy donors from Etablissement Français du Sang (EFS, agreement # 14/EFS/041) (Rungis, France). Heat-activated gamma globulin (HAGG) and Cobra Venom Factor (CVF) were purchased from TECO Medical (Rambouillet, France) to be used as positive controls for the activation of the complement system. Proteins C3b (purity > 90%) and C3c (purity > 80%) were provided by Acris Antibodies GmbH (Herford, Germany). Human complement C3a (purity > 98%) was purchased from Merck Calbiochem® (Fontenay-sous-Bois, France). Human complement C3 protein (purity > 85%) and Microvue™ complement iC3b EIA kit were purchased from Teco Medical (Rambouillet, France).

II.2. Methods

II.2.1. NPs synthesis and characterization

Five types of nanoparticles were prepared from well described emulsion polymerization methods of IBCA with dextran. The method and characteristics of the nanoparticles were thoroughly described in our previous works [35-37]. In this work, three NPs were obtained from radical redox emulsion polymerization (R1, R2 and R3), two others were prepared by anionic emulsion polymerization (A1 and A2). They differ by the density and conformation of dextran chains grafted on their surface as illustrated later in this article. They display different capacities to activate the complement system [37]. A table depicting the different properties of nanoparticles used in this work is available in supplementary information (S1).

II.2.2. Sample preparation

The five types of NPs were assessed at two different concentration (1000 and 3000 cm^2/mL) for complement activation. The incubation was prepared as described previously [20] by diluting human serum (1:4) in VBS^{2+} buffer (1:4) and NPs aqueous dispersion at the desired concentration (1:2) or water for controls. The final incubation volume was 100 µL. For the negative control, VBS^{2+} was replaced by VBS EDTA, that inhibits complement activation. The positive control was obtained by introducing CVF (5 µL), a strong activator of the complement cascade, in the incubation medium filled with water (45 µL) to reach the final volume of 100 µL. Medium activation was obtained by introducing HAGG (5 µL) in the incubation medium described above.

The incubation mixture was left at 37°C for an hour. After incubation, samples were kept in ice few minutes until analysis. Each sample was analyzed in triplicate by SPR and µC-IE and in duplicate by ELISA.

II.2.3. Surface Plasmon Resonance (SPR)

II.2.3.1. Antibody immobilization

SPR measurements were performed on a Biacore T100 instrument with a Series S sensor chip CM5 equipped with 4 channels (GE healthcare Life Sciences, Vélizy, France). Antibodies were immobilized onto the chip via a standard amine coupling consisting in a successive injection of 1-ethyl-3-(3-dimethylaminopropyl)carbodiimide hydrochloride (EDC) (75 mg/mL, 420 sec, 5 µL/min), N-hydroxysuccinimide (NHS) (11.5 mg/mL, 420 sec, 5 µL/min) and antibody (20 µg/mL) in 10 mM acetate buffer pH 4.5 (420 sec, 10 µL/min) to reach an immobilization level of 10,000 RU (Resonance Unit). The remaining blank were filled with ethanolamine-HCl pH 8.5 (1 M) to prevent for residual non-specific binding (NSB). NSB was assessed on a channel bearing a non-relevant antibody and another channel with a blank surface.

II.2.3.2. Specificity assays and control serums

Pure C3 (185 kDa), C3b (176 kDa) and C3c (140 kDa) proteins were tested at 140 µg/mL in HBS-EP+ buffer. Pure C3a (9,1 kDa) was analyzed at 70 µg/mL in HBS-EP+ buffer. Control serum samples incubated as described above were then diluted by 12.5 in the buffer (HBS-EP+/NSB reducer 9:1) to reach a final dilution factor of 50 for human serum (4 x 12.5). All samples were analyzed sequentially on the different channels at 25°C in the following conditions: flow rate: 40µL/min; contact time: 60 sec; dissociation time: 120 sec. Channels were then regenerated with a two steps procedure: (i) Glycine/HCl pH 2.5: contact time: 30 sec at 40 µL/min, (ii) NaOH 1 mM (30 sec at 40 µL/min). The SPR signal obtained is proportional to the mass of analyte interacting with the surface. The quantification of analyte binding on the channel was expressed in RU (1 RU = 1 pg/mm^2) and the report point was taken 10 seconds after the beginning of the dissociation. An example of SPR sensorgram is available in supplementary information S2.

II.2.3.3. NP-serum studies

All serums were prepared and analyzed as described in the previous paragraph. Analyzes were performed on the samples directly after incubation without additional step to remove the

nanoparticles. In few experiments, nanoparticles were removed from the samples prior to analysis to study the bias possibilities caused by the removal of the NPs. In this part, the incubated serums were centrifuged at 4°C for 45 min at 16.1 rcf (relative centrifugal force) with an Eppendorf centrifuge 5415R (Eppendorf, Montesson, France) prior to the dilution. Then, the supernatant was recovered for dilution preparation and analysis. Analyzed sera corresponding to these samples were identified as "samples without nanoparticles" in the results and discussion section.

II.2.4. Multi-crossed 2D Immunoelectrophoresis (µC-IE)

Multi-crossed 2D immunoelectrophoresis was performed as described previously [20,38]. In summary, a 1% agarose gel plate was prepared on Gel-Fix™ alternating plain agarose gel bands (0.8 cm wide) and agarose gel bands containing polyclonal anti-C3 antibody (2.2 cm wide) as explained in a previous work (20). Incubated samples were deposited on wells formed in the agarose gel bands to run the first dimension allowing the separation of proteins according to their molecular weight (600 V,16 mA). Then, the plate was turned by 90° to allow the second dimension electrophoresis leading to the immunoprecipitation of C3 protein and its fragments in the gel bands containing the polyclonal anti-C3 antibody (500 V, 12 mA). Gel was then dried and stained with Coomassie blue prior to analysis of %C3 activation.

II.2.5. ELISA

Elisa was performed following the instructor procedure. Briefly, the sample was diluted by 100 in the specimen diluent provided by the supplier. Then, the sample was deposited and incubated at room temperature for 30 min. Then, the plate was thoroughly washed with the wash solution. iC3b reagent was then added and left for 30 min before being washed. Substrate was added for 30min before adding the stop solution. The ELISA plate was read at 405 nm using LT-5000MS Elisa plate reader (Labtech France, Palaiseau).

III. Results

III.1. Setup of a Regenerable SPR chip for the direct assessment of complement activation by nanoparticles

III.1.1. Antibody immobilization

The SPR chip was grafted with a goat IgG with no affinity for complement fragments on channel 1 to give a non-specific reference channel. Antibody directed against human C3a neo-

epitope was coated on channel 2 at around 10,000 RU. Anti-human C3 polyclonal antibody was coated on the third channel at the same level of immobilization. Channel 4 exposed the raw surface of the chip for another reference with no affinity. In this chip, channels 1 and 4 could highlight possible non-specific adsorption while channels 2 and 3 could evaluate specific fragments of the complement system. It was assumed that the non-specific adsorption behavior monitored on channel 1 grafted with the non-specific goat IgG was consistent to that of channels 2 and 3, grafted with antibodies specific to complement fragments.

III.1.2. Specificity assays and control serums

At first, the specificity of the different channels towards different protein C3 fragments was assessed to ensure their relevance for the intended use. Results are depicted in figure 1A. The channel 1 showed no affinity for any of the tested proteins. Channel 2 was specific to C3a released fragment, confirming the ability of the antibody to detect the neo epitope of C3a only. Channel 3 could detect both C3 protein, C3b and C3c fragments, but not C3a.

Then, these channels were tested for their ability to detect these specific fragments in sera with different levels of C3 activation obtained from control samples made with known activators (HAGG, CVF) and inhibitors (EDTA) of complement activation. Flow conditions, buffer and sample dilution were optimized in order to give a relevant signal on the response for all channels. Results are presented in figure 1B. CVF is a positive control that produces complement C3 full fragmentation releasing C3a and C3b fragments. The results indicated that non-specific binding was quite important with serum, showing an important background level on channel 1. Nevertheless, channel 2 showed an ability to distinguish activated C3 samples from negative controls. Non-specific binding found on negative control was around 100 RU while the fully activated serum gave a response above 300 RU. We also found that non-specific signal was dependent on each channel. On channel 3, we observed a decrease of the signal for C3 activated samples meaning a decrease of the mass of protein binding to the immobilized antibody. The decrease is substantial but the amplitude is less important than for channel 2 between negative and positive full activated controls.

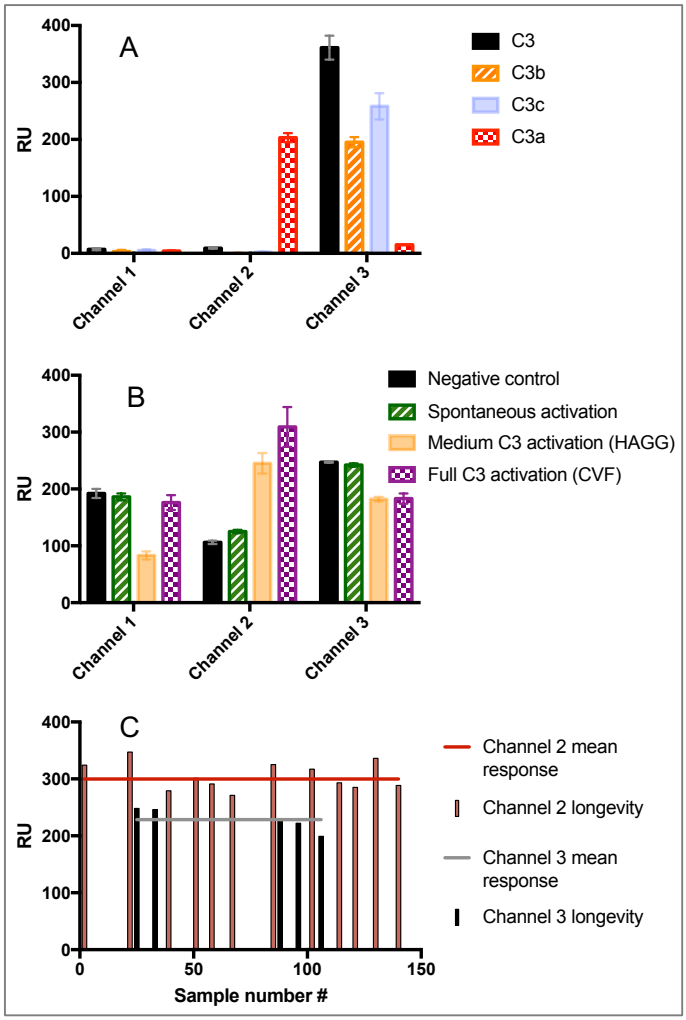

Figure 1: Evaluation of the SPR chip performance. A: Evaluation of antibodies specificities on SPR chip channels. B: channel response to control sera with different level of complement activation. C: Study of the longevity of specific antibodies to C3 fragments grafted on channels 2 and 3. *Channel 1: Goat IgG; Channel 2: Anti-C3a monoclonal antibody; Channel 3: Anti-C3 polyclonal antibody.*

III.1.3. Chip longevity

The regeneration was optimized to permit a sustained use of coated antibodies. The longevity of channel 2 was assessed with the fully activated sample (CVF) containing a maximum amount of C3a. The channel 3 longevity was monitored with the negative control (VBS EDTA) containing maximum of C3 native protein (Fig. 1C). A quite constant value for C3a detection in a fully activated control serum was obtained on Channel 2 along the analysis of almost 150 samples. A slight variation was observed between the different runs, but the relative standard deviation (RSD) for the positive control on channel 2 over the 150 analyses was < 10%. The behavior of channel 3 was similar to channel 2 showing good performance after regeneration.

The signal started to decrease slightly after nearly 100 analyses. A similar RSD value below 10% was also obtained on channel 3 for the longevity study.

III.2. SPR, µC-IE and ELISA comparison of the assessment of complement activation produced by NPs

The activation profile of five poly-IBCA NPs already well described were compared using three methods for complement activation assessment: SPR developed in this paper, µC-IE [20] and ELISA. The results of activation at two given surface concentrations of NPs (1000 and 3000 cm^2/mL) are presented in figure 2.

The activation of the complement cascade was respectively assessed by the detection of C3a fragment by SPR (channel 2), iC3b fragment by ELISA and the balance between native C3 and released fragment (C3b, C3c) by µC-IE. All these determinations are linked to the cleavage of the C3 protein of the complement system.

µC-IE was used as our reference method, giving reproducible results of complement activation based on the monitoring of the cleavage of the C3 protein as demonstrated in previous works [20,38]. At 1000 cm^2/mL, the level of activation expressed in µC-IE was quite low (below 30%) for all tested NPs. The same level was obtained for C3a fragment detected by SPR when comparing with values of negative and positive controls shown in figure 1. At 3000 cm^2/mL where A1, A2, R2 and R3 NPs are known to strongly activate the complement system [38], SPR measurements of C3a fragments released gave consistent results with C3 cleavage observed by µC-IE. The activation reached the same level as fully activated CVF control for NPs A1, A2, R2, R3 while R1 was non-activating. The ELISA detection of iC3b fragment gave high values of absorbance in all cases. Tendencies that might emerge from this method were counterbalanced by standard deviations that prevent from a possible distinction in terms of

iC3b released.

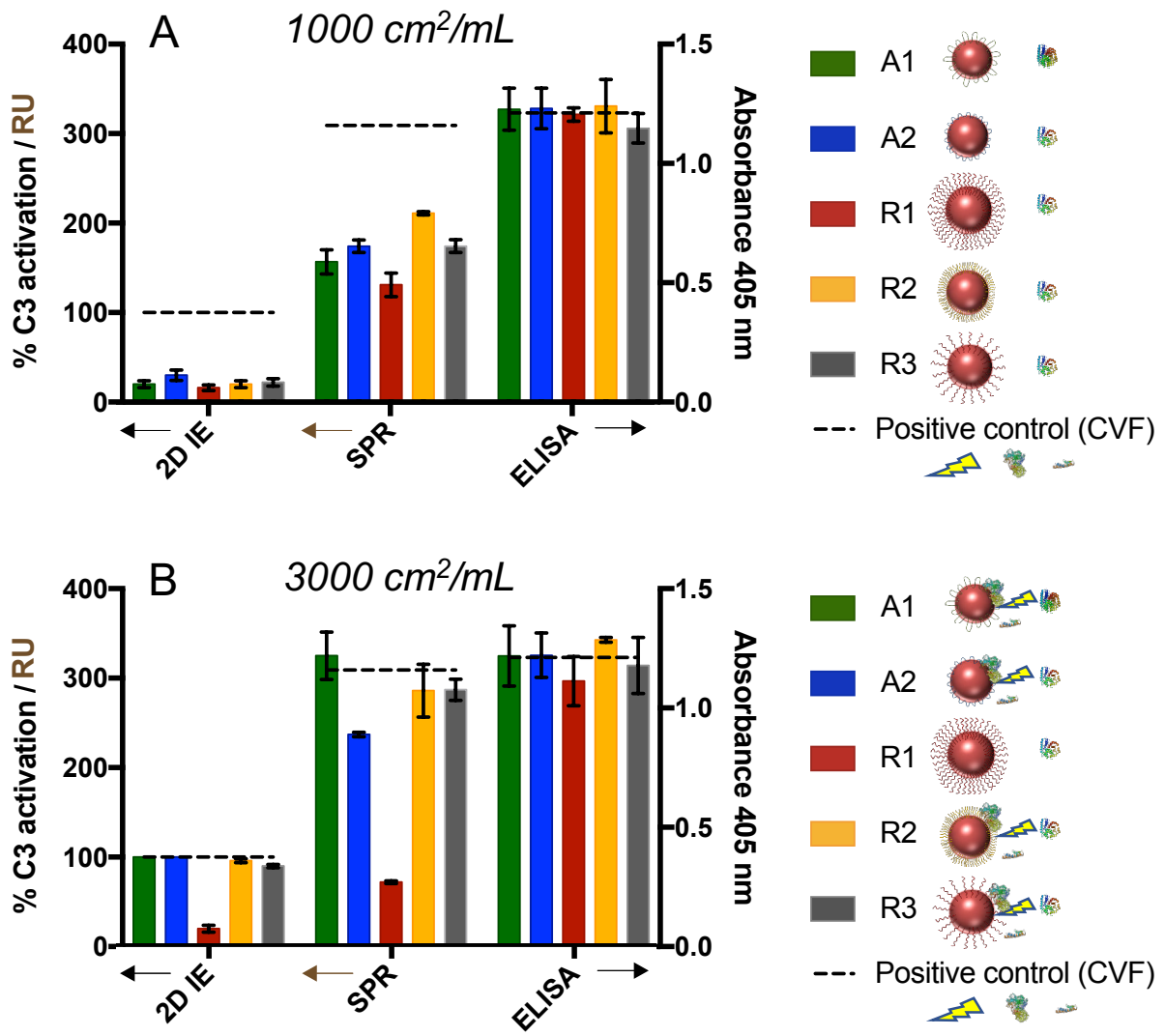

Figure 2: Complement activation by five types of NPs assessed by µC-IE, SPR (channel 2) and ELISA. Serum was exposed to 1000 cm2/mL (A) and 3000 cm2/mL (B) of nanoparticles. indicates the activation of C3 protein ( ), leading to the release of protein fragments C3b ( ) and C3a ( ).

III.3. Investigation of possible bias involved in complement activation evaluation methods

A study about sample preparation's influence was done with the SPR technique to evaluate possible bias involved in complement activation evaluation. To perform this investigation, nanoparticles were removed from the incubation medium by centrifugation prior to SPR analysis and the results were compared with those obtained analyzing the incubation medium

still containing the NPs. The SPR allows the sample to be flowed onto the channels for protein specific recognition. Released proteins are thus captured. In this part, we compared the effect of removal of NPs prior to SPR analysis. Results were depicted in figure 3A.

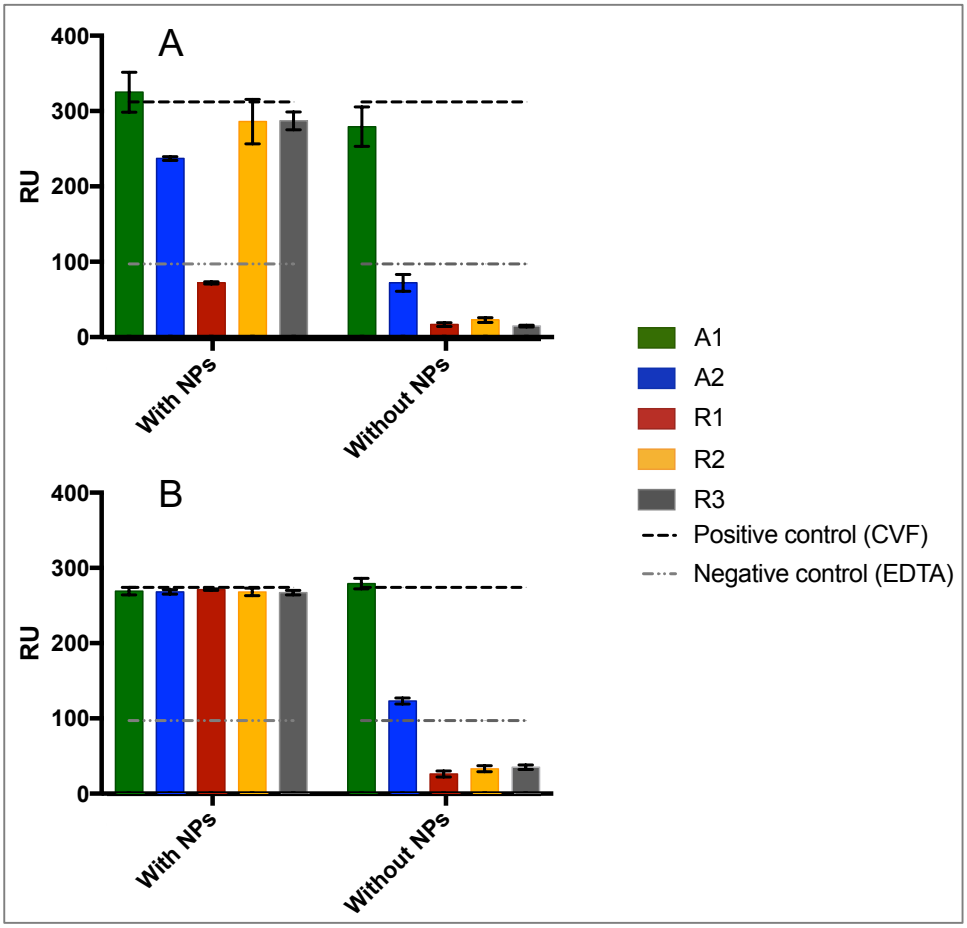

Figure 3: Comparison of C3a level detection by SPR before and after removal of NPs by centrifugation. A: on samples incubated with NPs for one hour. B: On samples fully activated by CVF and then incubated with NPs for one hour.

An important decrease of C3a signal was observed after removal of most NPs excepted for A1, which seemed to not disturb the determination of the C3a level. The observed effect was particularly pronounced for A2, R2 and R3 NPs where C3a signal dramatically felt after removal of NPs. NP R1, while producing only a little amount of C3a fragment also seemed to impact on its detection when removed prior to analysis.

Another assay was carried out with serum that was first fully activated with CVF, leading to a full conversion into C3a, and then incubated for one hour with nanoparticles (Fig. 3B). The purpose of this experiment was to investigate whether results from analysis of this fully activated serum could be disturbed by incubation and removal of nanoparticles due to

possible adsorption of the C3a protein. The signal on Channel 2 for C3a response was monitored before and after removal of the NPs (Fig. 3B). Observations made from the first study depicted in figure 3A were confirmed with this experiment. A strong decrease of C3a level was observed upon removal of NPs for A2, R1, R2, and R3, whereas A1 removal from the incubation medium did not significantly influence the level of detected C3a. A strong adsorption of the C3a fragment onto NPs was thus evidenced for A2, R1, R2 and R3. It is worth noting that A2 does not reduce the signal at the same level as R1, R2 and R3 NPs. Conversely, the response on channel 1, reference for non-specific binding, and channel 3, bearing anti-C3 polyclonal antibody, were almost unchanged between these two types of samples (see Supplementary Information S3). This meant that a strong adsorption of random serum proteins onto NPs was not at the root of the signal decrease observed on channel 2, but rather a very specific adsorption of C3a onto NPs.

IV. Discussion

A SPR chip bearing C3 specific antibodies for the assessment of complement activation by nanoparticles was optimized in this work. The detection of complement activation focused on C3 protein that is at the heart of the complement cascade. Monitoring the activation of this protein allows the assessment of global complement activation. In the developed chip, an antibody against C3a neo-epitope and a polyclonal anti-C3 antibody were used. The first allowed a specific detection of a released fragment resulting from C3 activation. The second permitted assessment of native C3 variation. We could observe a decrease of the signal on channel 3 grafted with polyclonal anti-C3 antibody upon complement activation (Fig. 1B), meaning a decrease of the mass of protein captured on the surface. This was consistent with the fragmentation of the native C3 (185 kDa) into smaller fragments recognized by this channel (C3b: 176 kDa and C3c: 139 kDa). Then, the C3a fragment was used as a finest revelator of C3 cleavage and thus complement cascade activation.

The aim was to develop an automatable method for a high throughput analysis of samples. The requirements for such an application were firstly to check the antibody specificity with pure proteins before testing their response to different level of activated serums. Specificity of antibodies grafted on channels 2 and 3 could be established using purified C3 proteins and various corresponding fragments produced during activation. Another requirement was the

wish to limit costs associated with the analysis. Usually, SPR analysis require the grafting of an antibody on the chip for each sample measurement. The regeneration steps destroy all proteins and then the primary antibody grafted on the chip is removed as well. The regeneration of the chip for removing all specific or non-specific bound proteins was optimized to ensure the antibody functionality and allow a longevity of the chip without the need to recoat the chip prior to each analysis. We showed that the grafted antibody was able to resist for at least 100 analytical cycles including sample analysis and chip regeneration. This can be considered as a good level of longevity. Moreover, no sandwich detection was used in this case. The amount of antibody used was thus extremely low, limiting the costs associated to their use. From that, we estimated the cost of consumables for one analysis by the three methods studied here, in regards with their respective characteristics of throughput, handling complexity and time consumption (cf. Table I). The estimated price per sample was calculated excluding the instruments prices, it comprised reagents, antibodies, buffers and supports (chip for SPR, gel support for µC-IE, ELISA plate). The price of a SPR analysis was found to be significantly lower than ELISA's, for an automated method allowing the detection of several fragments. The throughput of SPR is lower than other methods but presents the advantage to be easy-to-use and fully automated. The recently renovated µC-IE [18] offering a high throughput use (35 samples per plate) allows a direct visualization of the native C3 and its fragments, providing a global vision of C3 status, in contrast with the ELISA method. Among other advantages, the µC-IE method is much less expensive than the ELISA test. The inherent drawback of this method is its higher time consumption. However, it still can be applied for a deeper understanding of complement activation behavior and concentration studies [18,37,38].

	SPR	µC-IE	ELISA
Cost/sample	1.75 €	0.14 € [20]	6 €
Throughput	7 samples/hour	35 samples/6 hours	96 samples/3 hours
Handling	Easy	Technical for gel preparation (45 min)	Not complex. Pipetting can be automated
Time consumption	Fully automated	Gel preparation - No manipulation during electrophoresis (5h) - Gel staining	Full 3 hours
Information obtained	Multiplex fragment quantitation (C3a, C3)	Balance C3/fragments	Single fragment quantitation (iC3b)

Table 1: Comparison of SPR, µC-IE and ELISA methodological aspects towards a routine assessment of complement activation by nanomedicines. Advantages and drawbacks.

The analysis of complement activation of our five well known NPs already characterized for complement activation in previous works showed consistent results between µC-IE and SPR measurements. In contrast, the ELISA methods showed a very high background for all serum samples incubated with nanoparticles independently of the concentration and type of nanosystem. This unexplained result hampered the evaluation of complement activation produced by the different type of nanoparticles considered in this work. The ELISA test measured the protein iC3b which is a different fragment from those detected by the two other methods. Evaluating this fragment that results from the cleavage of the C3 protein into an inactivated C3b fragment could provide a very different insight of complement activation. However, the results obtained with the ELISA method could not be compared those obtained with SPR and µC-IE.

For a control quality analysis of complement activation, SPR could be the candidate of choice due to its simplicity and its possible automation. Nevertheless, while working with specific fragments, it should be verified that no bias or artefacts were interfering with the detection of the analyte. Indeed, in the present study we evaluated the influence of the preparation of a sample prior to its analysis by SPR. Indeed, in the literature, assessment of complement activation produced by nanoparticles is described on both serum samples still containing the nanoparticles [17] and on serum samples obtained after removal of the nanoparticles [39]. It

is generally not explained why analysis is performed on either serum although it has been described that several C3 fragments has the tendency to adsorb on polymer surfaces [34]. Our study including the removal of NPs showed that the procedure when dealing with assessment of NP-protein interaction and protein detection is very important. C3a was found to adsorb strongly on R1, R2 and R3 NPs, all bearing a brush conformation of dextran. On the contrary A1 did not adsorb C3a while A2 was adsorbing in a less extent than nanoparticles of the R series. The adsorption of C3a onto certain polymer surfaces has already been mentioned [32-34] and was confirmed in our study. It is noteworthy that it seems hard to predict this specific adsorption from generally known characteristics of the nanoparticles (i.e. composition, size and zeta potential). Indeed, in our study, all nanoparticles were coated with dextran and only a slight modification on dextran chain architecture between A1 and A2 leads to different behaviors of C3a adsorption. This highlights the fact that careful and critical study of results must be done when dealing with detection of a specific marker for detection of complement but also in other cases when dealing with nanoparticles. As suggested by the results, the removal of NPs prior to analysis may generate bias leading to false negative results that may have dramatic consequence when evaluating the safety of a nanomaterial. When NPs were still in the medium, C3a could be recognized by antibodies grafted on the SPR chip, supposing that this fragment might be at the external surface of NPs in the soft corona, and could be readily intercepted by antibodies grafted on the chip surface. The test in presence of CVF confirmed the fact that a specific adsorption of C3a occurred on NPs. Surprisingly, A1 did not adsorb C3a at all, while these NPs are known to adsorb protein of much larger size (data not published). Here, the C3a fragment mostly adsorbed on nanoparticles showing a lower surface curvature. In the context of characterization of interactions between nanomedicine and proteins, this is an insight into the specific adsorption of a small protein of the complement system. Among the known parameters affecting the adsorption, NPs' surface curvature and architecture are known to be of importance [40-42]. Here, these two parameters have a strong influence on C3a deposition onto nanoparticle surface. Results obtained from this part of the work brought new evidences that confirm the high complexity of phenomena governing protein adsorption onto NPs and the need for a better understanding of these interactions influencing the in vivo fate of nanoparticles.

V. Conclusion

A SPR based method for the evaluation of complement activation by nanoparticles through C3 protein fragmentation has been developed in this work. The optimized conditions allowed for a prolonged use of the chip after a single antibody immobilization. Results provided by this method were consistent with those of the multi-crossed 2D immunoelectrophoresis method, previously validated for complement activation evaluation. In contrast, no comparison with ELISA could be established due to a high non-specific background found with this method. The evidence of an artefact based on possible fragment adsorption onto NPs was shown by SPR considering analysis of samples containing or not the nanoparticles. This warn about caution required when performing complement activation analysis evaluating nanoparticles. Finally, the SPR method is a rapid and automatable which gave consistent results in terms of complement activation upon direct sample analysis without need of nanoparticle removal. This method could be the method of choice for a daily assessment of complement activation by nanomedicines and nanomaterials in general.

Acknowledgements

The authors acknowledge:

The financial support from BPI-France, Project NICE.

IPSIT Platform, Intermol (Chatenay-Malabry, France).

Abbreviations

ASTM: American Society for Testing and Materials
CARPA: Complement Activation Related Pseudo Allergy
CVF: Cobra venom factor
ELISA: Enzyme-linked immunosorbent assay
HAGG: Heat-activated gamma globulin
IBCA: Isobutylcyanoacrylate
ISO: International Organization for Standardization
NM: Nanomedicine
NP: Nanoparticle
RSD: Relative standard deviation
RU: Response unit
SPR: Surface plasmon resonance
2D-IE: Two-dimensional immunoelectrophoresis
µC-IE: Multi-crossed 2D immunoelectrophoresis

VI. Bibliography

1) Merle, N. S., Church, S. E., Fremeaux-Bacchi, V. & Roumenina, L. T. Complement System Part I: Molecular Mechanisms of Activation and Regulation. *Frontiers in Immunology* **6,** (2015).
2) Merle, N. S., Noe, R., Halbwachs-Mecarelli, L., Fremeaux-Bacchi, V. & Roumenina, L. T. Complement System Part II: Role in Immunity. *Frontiers in Immunology* **6,** (2015).
3) Dobrovolskaia, M. A., Aggarwal, P., Hall, J. B. & McNeil, S. E. Preclinical Studies To Understand Nanoparticle Interaction with the Immune System and Its Potential Effects on Nanoparticle Biodistribution. *Mol. Pharmaceutics* **5,** 487–495 (2008).
4) Nilsson, B., Ekdahl, K. N., Mollnes, T. E. & Lambris, J. D. The role of complement in biomaterial-induced inflammation. *Molecular Immunology* **44,** 82–94 (2007).
5) Szebeni, J. Complement activation-related pseudoallergy: A new class of drug-induced acute immune toxicity. *Toxicology* **216,** 106–121 (2005).
6) Szebeni, J. Hemocompatibility testing for nanomedicines and biologicals: predictive assays for complement mediated infusion reactions. *European Journal of Nanomedicine* **4,** (2012).
7) Szeto, G. L. & Lavik, E. B. Materials design at the interface of nanoparticles and innate immunity. *Journal of materials chemistry. B, Materials for biology and medicine* **4,** 1610–1618 (2016).
8) Markiewski, M. M., DeAngelis, R. A., Benencia, F., Ricklin-Lichtsteiner, S. K., Koutoulaki, A., Gerard, C., Coukos, G. & Lambris, J. D. Modulation of the anti-tumor immune response by complement. *Nature immunology* **9,** 1225–1235 (2008).
9) Moghimi, S. M. Cancer nanomedicine and the complement system activation paradigm: Anaphylaxis and tumour growth. *Journal of Controlled Release* **190,** 556–562 (2014).
10) ISO 10993-4:2017: Biological evaluation of medical devices – Part 4: Selection of tests for interactions with blood. ISO; 2017.
11) ASTMF1984: Standard Practice for testing for whole complement activation in serum by solid materials (2013).
12) FDA Guidance for Industry: Immunotoxicology Evaluation of Investigational New Drugs. https://www.fda.gov/downloads/drugs/guidancecomplianceregulatoryinformation/guidances/ucm079239.pdf (2002). *Consulted on August 2017*
13) EMA Reflection paper on the data requirements for intravenous liposomal products developed with reference to an innovator liposomal product. http://www.ema.europa.eu/docs/en_GB/document_library/Scientific_guideline/2013/03/WC500140351.pdf (2013). *Consulted on August 2017*
14) Harboe, M., Thorgersen, E. B. & Mollnes, T. E. Advances in assay of complement function and activation. *Advanced drug delivery reviews* **63,** 976–987 (2011).
15) Salvador-Morales, C. & Sim, R. B. Complement activation. *Handbook of immunological properties of engineered nanomaterials* 357–384 (2013).
16) Mollnes, T. E., Jokiranta, T. S., Truedsson, L., Nilsson, B., Rodriguez de Cordoba, S. & Kirschfink, M. Complement analysis in the 21st century. *Molecular Immunology* **44,** 3838–3849 (2007).
17) Neun, B.W, Ilinskaya, A., & Dobrovolskaia, M.A. NCL Method ITA-5.2: Analysis of Complement Activation by EIA. https://ncl.cancer.gov/sites/default/files/protocols/NCL_Method_ITA-5.2.pdf (2015). *Consulted on August 2017*
18) Coty, J.-B., Varenne, F., Vachon, J.-J. & Vauthier, C. Serial multiple crossed immunoelectrophoresis at a microscale: A stamp-sized 2D immunoanalysis of protein C3 activation caused by nanoparticles: Proteomics and 2-DE. *ELECTROPHORESIS* **37,** 2401–2409 (2016).
19) Schneider, C. S., Bhargav, A. G., Perez, J. G., Wadajkar, A. S., Winkles, J. A., Woodworth, G. F. & Kim, A. J. Surface plasmon resonance as a high throughput method to evaluate specific and non-specific binding of nanotherapeutics. *Journal of Controlled Release* **219,** 331–344 (2015).
20) Patra, A., Ding, T., Engudar, G., Wang, Y., Dykas, M. M., Liedberg, B., Kah, J. C. Y., Venkatesan, T. & Drum, C. L. Component-Specific Analysis of Plasma Protein Corona Formation on Gold Nanoparticles Using Multiplexed Surface Plasmon Resonance. *Small* **12,** 1174–1182 (2016).

21) Cedervall, T., Lynch, I., Lindman, S., Berggård, T., Thulin, E., Nilsson, H., Dawson, K. A. & Linse, S. Understanding the nanoparticle–protein corona using methods to quantify exchange rates and affinities of proteins for nanoparticles. *Proceedings of the National Academy of Sciences* **104,** 2050–2055 (2007).
22) Masson, J.-F., Battaglia, T. M., Cramer, J., Beaudoin, S., Sierks, M. & Booksh, K. S. Reduction of nonspecific protein binding on surface plasmon resonance biosensors. *Analytical and Bioanalytical Chemistry* **386,** 1951–1959 (2006).
23) Seokheun Choi and Junseok Chae. Methods of reducing non-specific adsorption in microfluidic biosensors. *Journal of Micromechanics and Microengineering* **20,** 075015 (2010).
24) Breault-Turcot, J. Développement d'outils analytiques pour la détection de biomolécules directement dans des fluides sanguins – Thèse de doctorat (2015).
25) Arima, Y., Toda, M. & Iwata, H. Surface plasmon resonance in monitoring of complement activation on biomaterials. *Advanced Drug Delivery Reviews* **63,** 988–999 (2011).
26) Hirata, I., Morimoto, Y., Murakami, Y., Iwata, H., Kitano, E., Kitamura, H. & Ikada, Y. Study of complement activation on well-defined surfaces using surface plasmon resonance. *Colloids and Surfaces B: Biointerfaces* **18,** 285–292 (2000).
27) Ricklin, D. & Lambris, J. D. in *Current Topics in Innate Immunity* (ed. Lambris, J. D.) 260–278 (Springer New York, 2007).
28) Drake, A. W. & Klakamp, S. L. A strategic and systematic approach for the determination of biosensor regeneration conditions. *Journal of Immunological Methods* **371,** 165–169 (2011).
29) Andersson, K., Areskoug, D. & Hardenborg, E. Exploring buffer space for molecular interactions. *Journal of Molecular Recognition* **12,** 310–315 (1999).
30) Makaraviciute, A., Ramanavicius, A. & Ramanaviciene, A. Development of a reusable protein G based SPR immunosensor for direct human growth hormone detection in real samples. *Anal. Methods* **7,** 9875–9884 (2015).
31) Szebeni, J. & Haima, P. Hemocompatibility of medical devices, blood products, nanomedicines and biologicals. *TECOmedical clinical and technical review* (2016).
32) Mares, J., Thongboonkerd, V., Tuma, Z., Moravec, J. & Matejovic, M. Specific adsorption of some complement activation proteins to polysulfone dialysis membranes during hemodialysis. *Kidney International* **76,** 404–413 (2009).
33) Kandus, A., Ponikvar, R., Drinovec, J., Kladnik, S. & Ivanovich, P. Anaphylatoxins C3a and C5a adsorption on acrylonitrile membrane of hollow-fiber and plate dialyzer--an in vivo study. *Int J Artif Organs* **13,** 176–180 (1990).
34) Montdargent, B., Toufik, J., Carreno, M.-P., Labarre, D. & Jozefowicz, M. Complement activation and adsorption of protein fragments by functionalized polymer surfaces in human serum. *Biomaterials* **13,** 571–576 (1992).
35) Bertholon, I., Lesieur, S., Labarre, D., Besnard, M. & Vauthier, C. Characterization of Dextran−Poly(isobutylcyanoacrylate) Copolymers Obtained by Redox Radical and Anionic Emulsion Polymerization. *Macromolecules* **39,** 3559–3567 (2006).
36) Couvreur, P., Kante, B., Roland, M., Guiot, P., BAuduin, P. & Speiser, P. Polycyanoacrylate nanocapsules as potential lysosomotropic carriers: preparation, morphological and sorptive properties. *Journal of Pharmacy and Pharmacology* **31,** 331–332 (1979).
37) Coty, J.-B., Eleamen Oliveira, E. & Vauthier, C. Tuning complement activation and pathway through controlled molecular architecture of dextran chains in nanoparticle corona. *International Journal of Pharmaceutics* **532**, 769-778 (2017).
38) Nguyễn, C. H., Putaux, J.-L., Santoni, G., Tfaili, S., Fourmentin, S., Coty, J.-B., Choisnard, L., Gèze, A., Wouessidjewe, D., Barratt, G., Lesieur, S. & Legrand, F.-X. New nanoparticles obtained by co-assembly of amphiphilic cyclodextrins and nonlamellar single-chain lipids: Preparation and characterization. *International Journal of Pharmaceutics* **531**, 444-456 (2017).
39) Wibroe PP, Moghimi SM. Complement Sensing of Nanoparticles and Nanomedicines. In: Hepel M, Zhong C-J, editors. Functional Nanoparticles for Bioanalysis, Nanomedicine, and Bioelectronic Devices Volume 2. Washington, DC: American Chemical Society; 2012. p. 365–82.

40) Walkey, C. D., Olsen, J. B., Guo, H., Emili, A. & Chan, W. C. W. Nanoparticle Size and Surface Chemistry Determine Serum Protein Adsorption and Macrophage Uptake. Journal of the American Chemical Society **134**, 2139–2147 (2012).
41) Gref, R., Lück, M., Quellec, P., Marchand, M., Dellacherie, E., Harnisch, S., Blunk, T. & Müller, R. . 'Stealth' corona-core nanoparticles surface modified by polyethylene glycol (PEG): influences of the corona (PEG chain length and surface density) and of the core composition on phagocytic uptake and plasma protein adsorption. *Colloids and Surfaces B: Biointerfaces* **18,** 301–313 (2000).
42) Pozzi, D., Colapicchioni, V., Caracciolo, G., Piovesana, S., Capriotti, A. L., Palchetti, S., De Grossi, S., Riccioli, A., Amenitsch, H. & Laganà, A. Effect of polyethyleneglycol (PEG) chain length on the bio–nano-interactions between PEGylated lipid nanoparticles and biological fluids: from nanostructure to uptake in cancer cells. *Nanoscale* **6,** 2782 (2014).

Supplementary material

Assessment of complement activation by nanoparticles as a quality requirement: development of a SPR based method and comparison with current high throughput methods

J-B. Coty, M. Noiray, C. Vauthier*

Institut Galien Paris-Sud, CNRS, Univ. Paris-Sud, University Paris-Saclay, Châtenay-Malabry, France.

***Correspondence:** Dr. Christine Vauthier, CNRS UMR 8612, Institut Galien Paris Sud, Univ. Paris-Sud, Université Paris-Saclay, 5, rue Jean-Baptiste Clément, 92296 Châtenay-Malabry, France. Fax: +33 146835946. E-mail: christine.vauthier@u-psud.fr

S1: Properties of model nanoparticles

NPs	Hydrodynamic diameter * (nm)	Zeta potential ** (mV)	Concentration *** (mg/mL)	Schematic representation
R1	286 ±14	-4 ±2	38 ±2	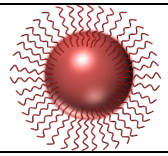
R2	208 ±4	-10 ±1	44 ±2	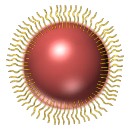
R3	281 ±6	-5 ±2	47 ±4	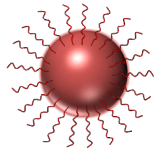
A1	88 ±2	-5 ±1	37 ±2	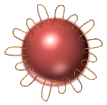
A2	159 ±10	-4 ±2	13 ±3	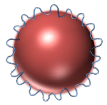
***by dynamic light scattering (DLS) ; **by electrophoretic light scattering (ELS) ; ***by gravimetry.**				

Table S1: **Physicochemical properties of model nanoparticles used for complement activation**. Hydrodynamic diameter, zeta potential, concentration and schematic representation of the NPs.

S2: Example of a sensorgram obtained by SPR

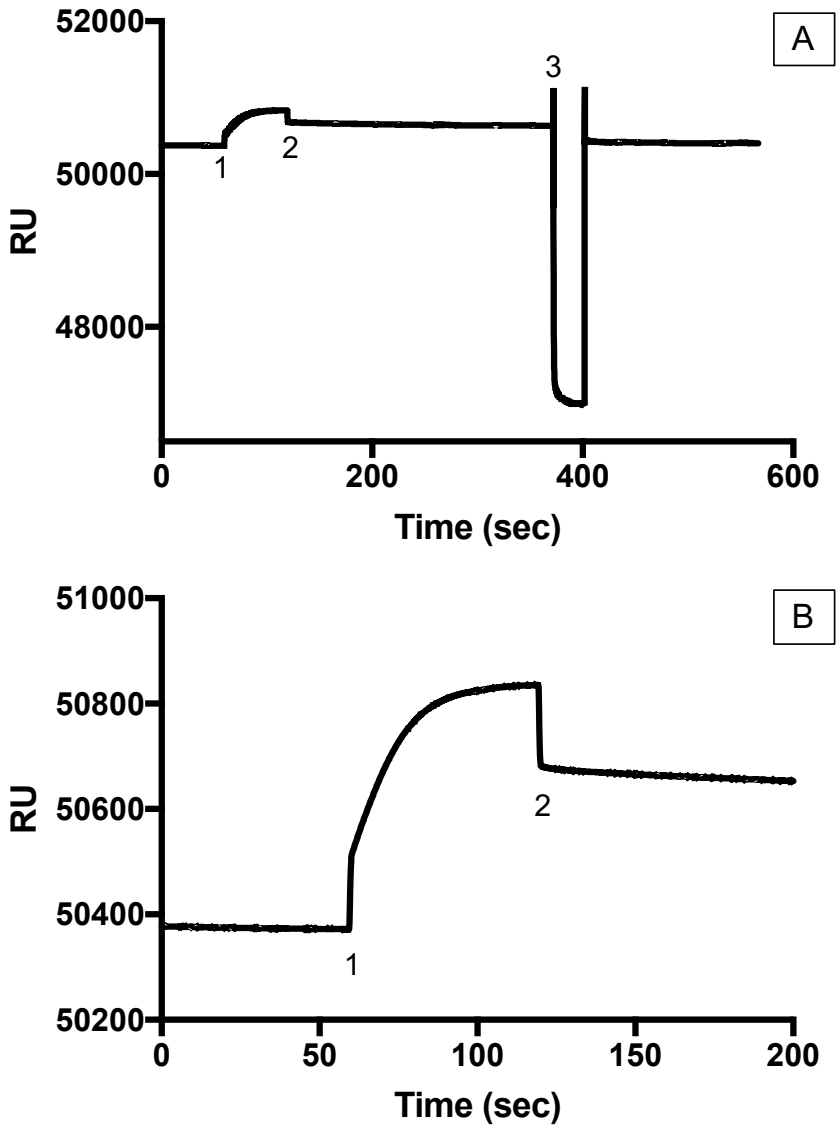

Figure S2: Sensorgram obtained on channel 2 (C3a) for the CVF sample.
(A) Full sensorgram. (B) Zoom of the binding/dissociation part.
1 represents the beginning of the association (injection of the sample)
2 represents the beginning of the dissociation (end of injection, buffer flow)
3 represents the beginning of the regeneration

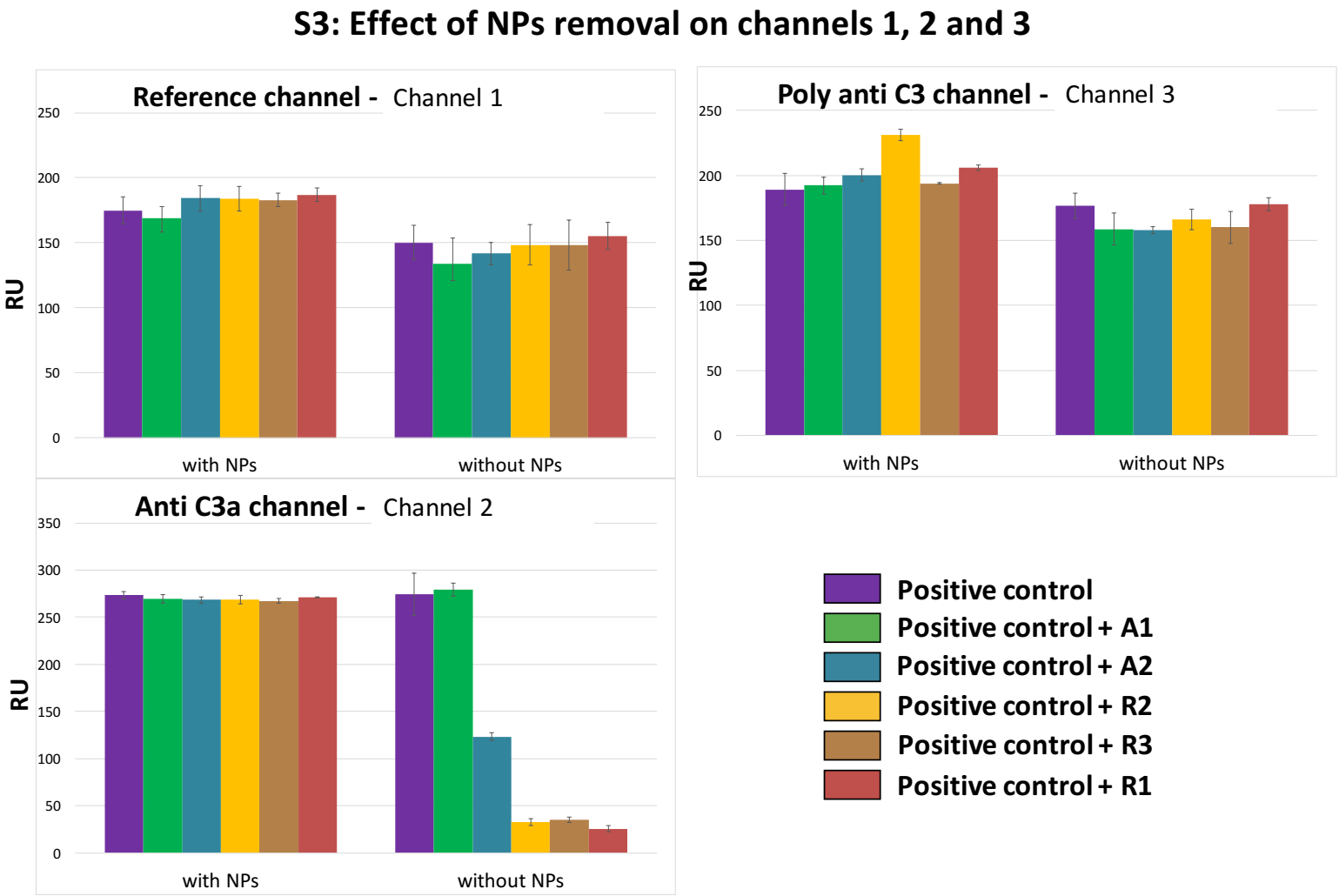

Figure S3: Responses obtained on channels 1, 2 and 3 for the study on NPS removal with positive controls.

Chapitre V : Caractérisation fine de la surface des nanomédecines avec des sondes moléculaires par électrophorèse capillaire : vers une évaluation de la couverture de surface

Avant-propos : La surface des nanomatériaux est le facteur déterminant des interactions entre nanoparticules et éléments biologiques, ce qui conditionne le devenir des NMs au sein de l'organisme. Actuellement, les méthodes permettant une caractérisation de ce paramètre sont très rares et souvent complexes à mettre en œuvre. Dans ce chapitre, nous proposons une méthode utilisant une approche originale pour caractériser la couverture de surface des nanomédecines avec l'utilisation de protéines en tant que sondes moléculaires. L'étude du comportement d'adsorption de protéines de différentes tailles est analysée par électrophorèse capillaire, dont le principe est rappelé en *annexe méthodologique n°2*. Le comportement de répulsion des nanoparticules testées envers une série de protéines sélectionnées ont permis de distinguer les différences de greffages existantes entre ces nanoparticules. Des nanoparticules présentant un greffage en surface peu dense ou en conformation boucle permettaient une plus forte adsorption de protéines de haute masse molaire comparées aux nanoparticules greffées avec des brosses denses. Ce type de caractérisation a pu être relié aux résultats d'activation du complément de ces différentes nanoparticules. L'électrophorèse capillaire permet d'utiliser un outil accessible et simple d'utilisation. L'analyse peut être réalisée dans des conditions standardisées et de façon directe sans étape de pré-traitement de l'échantillon après incubation.

Projet d'article

Sharp characterization of nanomedicines' surface with molecular probes by capillary electrophoresis: towards understanding and evaluation of surface coverage

J-B. Coty, F. Varenne, O. Garsaa, I. Le Potier, C. Smadja, M. Taverna, C. Vauthier*

Institut Galien Paris-Sud, CNRS, Univ. Paris-Sud, University Paris-Saclay, Châtenay-Malabry, France.

***Correspondence:** Dr. Christine Vauthier, CNRS UMR 8612, Institut Galien Paris Sud, Univ. Paris-Sud, Université Paris-Saclay, 5, rue Jean-Baptiste Clément, 92296 Châtenay-Malabry, France. Fax: +33 146835946. E-mail: christine.vauthier@u-psud.fr

Abstract

In the field of nanomedicines (NMs), a faithful characterization is needed for a better understanding of the *in vivo* outcomes of such nanomaterials. While size and surface charge measurements of nanomaterials have been widely developed and now well studied, other parameters that are still relevant for the understanding of NM behavior *in vivo* are not so well characterized. For instance, the reactive surface of nanomedicines, that are often grafted with macromolecules to decrease their recognition by the immune system, is not characterized with sufficient accuracy. It is now known that a subtle modification at the NM surface will be at the root of major changes with biological components. In this article, we developed a capillary electrophoresis method using molecular probes to characterize NMs' surface coverage. A series of proteins with different molecular weight were screened for their adsorption behavior towards nanoparticles bearing different shell conformations. This novel strategy of characterization can bring new information about NMs shell grafting and might allow for a better perception of their behavior in the presence of biological components. The developed method has the potential for further standardization and automation for a routine use.

Keywords: Nanomedicine, capillary electrophoresis, molecular architecture, surface coverage, protein adsorption, molecular probe, shield-effect

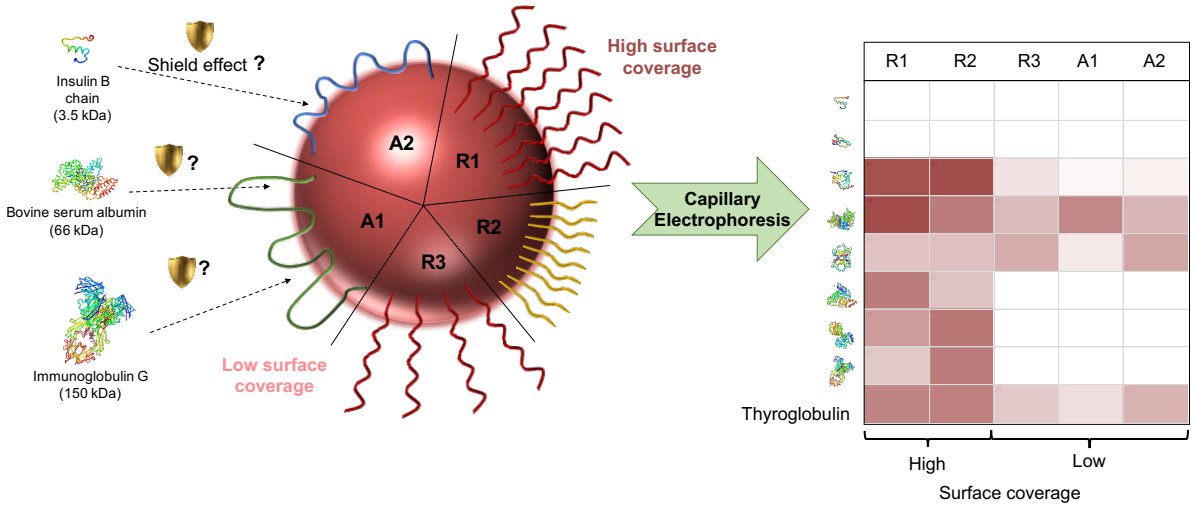

I. Introduction

The number of nanoparticle-based medicinal products that has reached clinical development has increased over the last years [1]. This is a positive signal acknowledging major general advances. However, several challenges remain unanswered [2-5]. Among them, the next important step in nanomedicine (NM) development is expected to come from the comprehension of their interactions with biological components encountered *in vivo* [6]. This progress is pending and unequal efforts are needed to improve the physicochemical characterization of nanomaterials. These efforts are worth made because incomplete or inappropriate characterization of important parameters was identified as critical in project failures by actors involved in the development of NMs [7]. Besides, the lack of characterization is recognized to delay and even inhibit the development of projects involving nanomaterials on a more general level [8-10].

Nanomaterials composing NMs include a wide range of components and their intended use suits for many applications considering different routes of administration, hence facing various delivery and safety challenges [2,11]. Understanding the characteristics of the formulation is an important process in the understanding of their biological activity and safety. This is also needed for quality control analysis to ensure batch to batch consistency of NMs and evaluate nano-similarity in generic version of NMs that has appeared on the market since 2013 [12]. Compared to a therapeutic molecule that can be characterized from a well-defined signature deduced from its NMR spectra, NMs are complex structures resulting from the combination of multiple components. The biological activity and safety depends on many parameters that include fine-tuned chemical and physical traits for each application [12,13]. Characterization of these nanomaterials is complex and parameters to characterize remains the subject of open discussions. They are often decided on a case by case basis from discussion between companies and health authorities' actors [14-16].

Today, properties such as size and surface charge are well controlled and validated to ensure batch to batch reproducibility, but they are not sufficient to warrant NMs' *in vivo* fate reproducibility. A short list proposed by Crist and McNeil [12] from the National Characterization Laboratory of the National Institute of Health includes "the level of surface coverage required for optimal biological performance". This parameter regulates the way

nanomaterials interact with proteins that is a major phenomenon occurring *in vivo* in biological fluids containing proteins, with a tremendous impact on the biological activity of nanomaterials. It includes the density, length, architecture and/or conformation of macromolecules grafted on NM's surface whose small variations have an important impact on interactions with proteins in biological fluids [17-21]. This suggests that characterization methods of the nanomaterial surface coverage should reach the molecular level, degree of precision needed for the intended use. So far, such evaluations require the use of highly specialized methods that are not generally available [7]. The characterization of surface properties has been identified to be not optimal and regulatory agencies emphasizes the need for new methods on this purpose [15,22,23].

As the precise synthetic identity of the nanomaterial is highly difficult to evaluate, an indirect approach consists in identifying proteins that adsorb on nanomaterial surface after incubation in biological fluids containing proteins. In many of these studies, plasma is used to provide with a screenshot of what happens after injection of the NM into the blood [24-27]. The profile of adsorbed proteins deduced from this analysis corresponds to the protein corona and determines the so called "biological identity" of the nanomaterial [28]. It is very sensitive to the surface coverage properties of the nanomaterial. Its determination raised interests to develop predictive models for the *in vivo* behavior of NMs including their cellular uptake, stability and biodistribution [27,29-31]. The determination of the "biological identity" of a nanomaterial would be a very relevant parameter to determine. However, current studies are based on the most advanced techniques applied in proteomic analysis using last generation liquid chromatography - mass spectrometry (LC-MS) instruments and a high expertise is needed to interpret the data [24,25,32]. The preparation of samples prior to the proteomic analysis is also based on many manipulations that may introduce bias in the determination of the protein corona [33,34]. These possibly disturbing steps might be at the root of the major hurdles encountered for a clear correlation of predictive model between synthetic identity, biological identity formed after administration and outcome of NPs. Thus, it is unrealistic to use such a method at a large scale to characterize nanomaterials on a routine basis.

Simpler methods are urgently needed and the present work aimed to explore the potential of a method proposing the analysis of the adsorption of a series of model proteins serving as

molecular probes to sense the surface coverage properties of a NM. The method is based on the determination of the free protein fraction remaining after incubation of a nanoparticle (NP) with a given protein in well controlled conditions. Capillary electrophoresis (CE) was selected as the analytical method. It has recently attracted interest in studies dealing with protein-nanomaterials interactions [35-39]. CE provides several advantages such as low sample consumption, high-throughput, automatable, *in situ* conditions and being highly adaptable to different purposes. In general, it is a method of dosage well implanted in analytical laboratories. Here, CE was selected for the previously mentioned reasons and for its assumed suitability to analyze samples without the need to remove the NPs. The potential of the method to discriminate NMs' grafting coverage was evaluated from the individual response to adsorption given by 9 proteins on 5 types of dextran-coated poly(isobutylcyanoacrylate) (PIBCA) model NPs that differed from the density and architecture of the dextran chains on their surface [18,40-42]. These model NPs were of larger size compared to the size of the proteins. So, the NPs could be viewed as multivalent receptors for the protein to adsorb on their surface that is not the case when nanomaterials are of the same order of magnitude as proteins.

The purpose of this work was to develop a novel accessible method for the characterization of NMs' surface allowing assumptions on its coverage and behavior towards protein adsorption. The development of the method included different parts: (i) the performance of the capillary electrophoresis method was evaluated in terms of its selectivity to determine the free fraction of the different proteins in a sample containing NPs, (ii) an optimal ratio between NPs and protein concentration was determined from adsorption behaviors investigated with 2 proteins (bovine serum albumin (BSA) and immunoglobulin G (IgG)) and (iii) the method was finally applied to investigate the response to adsorption of 9 proteins on each type of the NPs prior to data analysis.

II. Materials and methods

II.1. Materials

Reagents and buffer components: Agarose, polyethylene oxide (PEO) (200,000 Da), ammonium hydroxide, hexadimetrine bromide (Polybrene®), tricine, tris Base (Sigma 7-9®), benzoic acid, sodium chloride and sodium dodecyl sulfate (SDS) were purchased from Sigma

(Saint-Quentin-Fallavier, France). Hydrochloric acid 1M and sodium hydroxide 1M were supplied by Prolabo (Paris, France). Sodium dihydrogenophosphate monohydrate was obtained from Carlo Erba (Val-de-Reuil, France). Calcium lactate, glacial acetic acid, coomassie brilliant blue R-250 were supplied by Thermo Fisher Scientific (Villebon-sur-Yvette, France). Gel-Fix™ for agarose (265x150 mm) was obtained from Serva Electrophoresis (Heidelberg, Germany). All chemicals were of reagent grade and used as purchased. Water used during the study was ultrapure water from a MilliQ® system (Merck, Fontenay-sous-bois, France).

Proteins and antibodies: Goat anti-human IgG, apo-transferrin from human plasma, human immunoglobulin G and transthyretin from human plasma were provided by Merck (Fontenay-sous-bois, France) with a purity > 95%. Aprotinin from bovine lung (purity = 80%), bovine serum albumin (purity > 96%), insulin B chain from bovine pancreas (puritiy > 80%), orosomucoïd from human plasma (purity > 99%), ovalbumin from chicken egg white (purity > 98%), thyroglobulin from bovine thyroid (purity > 90%), fibrinogen fraction I type 1 from human plasma (purity = 66%) and rabbit anti-bovine serum albumin were purchased from Sigma (Saint-Quentin-Fallavier, France).

II.2. Methods

II.2.1. NPs synthesis and characterization

Model nanoparticles made of PIBCA and dextran were used in this work. Three types of NPs were prepared according to the radical redox emulsion polymerization method described by Bertholon et al. (R1, R2 and R3) [40]. Two types of NPs were prepared via anionic emulsion polymerization method (A1 and A2) [40,43]. Aqueous dispersions were obtained after purification by dialysis against water. NPs were then characterized in terms of hydrodynamic diameter, zeta potential, concentration and complement activation as previously described [18,44]. Characteristics of the NPs are given in table 1.

II.2.2. Sample preparation

All samples were prepared as follow prior to analysis. The tested protein (250 µg/mL) was incubated with NPs in phosphate buffer (Sodium dihydrogenophosphate monohydrate: 21mM, adjusted to pH 7.4 with ammonium hydroxide). The final volume of incubation was 300 µL. NPs concentration was expressed in surface area (cm^2/mL) and varied from 0 to 6000 cm^2/mL for the investigation of adsorption trends. The concentration of NPs was fixed at 2000

cm^2/mL for the shield-effect study. Samples were prepared in Eppendorf® Protein LoBind tubes of 0.5 mL and incubated on a wheel at 30 rpm for 2 h 30 min at 25°C (room temperature). At the end of the incubation, the sample was immediately analyzed by capillary zone electrophoresis or gel immunoprecipitation. The absence of aggregates was studied by optical microscopy (microscope Olympus BH-2, magnification x 40) and dynamic light scattering (DLS) (ZetaSizer Nano ZS 90, Malvern Instruments, Orsay, France) with the measurement of NPs' size and the autocorrelation function.

II.2.3. Sample analysis

II.2.3.1. Capillary zone electrophoresis analysis

CE experiments were performed on a PACE MDQ from Beckman Coulter (Villepinte, France). Peak analysis was performed with 32 Karat software. Free proteins were detected and quantified by capillary electrophoresis using a UV detector at 200 nm. Analysis were performed in a 50 cm Poly Microtechnologies™ silica capillary, 50 µm id, from Molex (Bièvres, France). Three methods were used depending on the isoelectric point (pI) of the protein to be analyzed. The different steps and information of these methods are summarized in table 2.

CE electrolyte was Sodium dihydrogenophosphate monohydrate (21 mM in water), adjusted to pH 7.4 with ammonium hydroxide or pH 3 with sodium hydrochloride depending on the method used. PEO coating was prepared at 2 mg/mL in hydrochloric acid at 0.1 M. Polybrene® was prepared at 2 mg/mL in water. At the end of each day of analysis, the capillary was rinsed at 20 psi successively with NaOH 0.1 M (10 min) and water (20 min). Benzoic acid at 1 mg/mL in water was used as migration marker in method 1.

NPs	Hydrodynamic diameter * (nm)	Zeta potential ** (mV)	Concentration *** (mg/mL)	Shell configuration (density, length) [40-42]	Complement activation (pathway) [18,44]	Schematic representation
R1	286	-4	38	Dense long brush (1.3%, 66kDa)	No	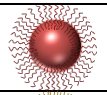
R2	208	-10	44	Dense short brush (1.3%, 17kDa)	Yes (Alternative)	
R3	281	-5	47	Loose long brush (0.5%, 66kDa)	Yes (Classical, lectin and alternative)	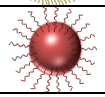
A1	88	-5	37	Loose Loops (1.3%, 66kDa)	Yes (Classical and alternative)	
A2	159	-4	13	Tight Loops (1.3%, 66 kDa)	Yes (Classical and alternative)	
***by DLS (90°) ; **by ELS ; ***by gravimetry.**						

Table 1: Characteristics of the NPs used in this study.

	Method 1: pI < 7	**Method 2: 7 < pI < 8**	**Method 3: pI > 8**
1°) Capillary conditioning	Rinse: Water – 2 min – 20 psi		
	Rinse: HCl 1 M – 5 min – 20 psi	Rinse: NaOH 0.1 M – 5 min – 20 psi	
	Rinse: Coating PEO – 5 min – 20 psi	Rinse: Coating Polybrene® – 5 min – 20 psi	
	Rinse: Electrolyte Phosphate pH 7.4 – 5 min – 20 psi	Rinse: Electrolyte Phosphate pH 3 – 5 min – 20 psi	Rinse: Electrolyte Phosphate pH 7.4 – 5 min – 20 psi
2°) Sample analysis	Sample Injection: Hydrodynamic injection – 5 sec – 0.5 psi		
	Separation: Electrolyte phosphate pH 7.4 – 20 min – 25 kV – Reverse polarity	Separation: Electrolyte phosphate pH 3 – 20 min – 20 kV – Reverse polarity	Separation: Electrolyte phosphate pH 7.4 – 20 min – 20 kV – Reverse polarity
3°) Capillary washing	Rinse: Water – 2 min – 20 psi		
	Rinse: NaOH 1 M – 3 min – 20psi	Rinse: SDS 50 mM – 3 min – 20 psi	
	Rinse: Water – 2 min – 20 psi		

Table 2**:** Conditions of CE methods used for protein detection with pI < 7 (method 1), 7 < pI < 8 (method 2) and pI > 8 (method 3).

II.2.3.2. Gel immunoprecipitation

Rocket immunoelectrophoresis (IE) [45] was used to study BSA adsorption on NPs. Briefly, 13 mL of 1% agarose gel containing Rabbit anti-bovine serum albumin (0.07 mg/mL) and prepared with tricine buffer as described previously [44] was casted at 50°C on a 10 x 7 cm Gel-Fix™ film. 19 wells were formed and 5 µL of incubated samples were deposited. Calibration samples ranging from 25 µg/mL to 250 µg/mL of BSA were also deposited on each gel. They were submitted to electrophoresis (12 mA, 500 V) for 16 hours.

Radial immunodiffusion (ID) [46] was used to evaluate IgG adsorption on NPs. 11 mL of 0.7% agarose gel made in tricine buffer previously mentioned containing Goat anti-Human IgG (10 µL) was casted at 50°C on a 8 x 10 cm Gel-Fix™ film. 20 wells were formed and 5 µL of incubated samples were deposited. Calibration samples ranging from 25 µg/mL to 250 µg/mL of IgG were also deposited on each gel. They were left for migration in a humid chamber for 24 hours before drying and staining steps.

Gels were dried and stained with coomassie brilliant blue as described previously [44]. Then, they were scanned and processed with ImageJ.

II.2.4. Data treatment and method precision

The amount of adsorbed protein onto NPs was deduced from the determination of free protein fraction remaining in the sample after incubation. Protein adsorption was thus monitored via the decrease of the free protein amount in the medium. This corresponded to the area of the protein peak detected by CE-UV, to the height of the rocket for rocket IE and to the area of the circle of diffusion obtained from Radial ID. $\%_{ads}$, the % of adsorbed protein was then calculated as described in Eq.1:

$$\%_{ads} = \frac{(\text{Acontrol} - \text{Asample})}{\text{Acontrol}} * 100 \qquad \textit{(Eq.1)}$$

with $A_{control}$ corresponding to the value of area/height obtained for the protein injected at 250 µg/mL after 2 h 30 min of incubation without NPs and A_{sample} the value obtained for the protein detected in the tested sample after incubation with NPs.

The linearity of response to protein detection was assessed by a calibration curve established for each capillary coating (PEO and Polybrene®) using BSA and IgG respectively. The protein concentration of the calibration curves ranged from 25 µg/mL to 250 µg/mL. The linearity was

evaluated in terms of correlation coefficient (R^2) of the calibration curves. The precision of the CE methods was tested in terms of detection and quantification of proteins. Repeated injection of BSA and IgG at 250 µg/mL were made in order to evaluate their inter-day (intermediate precision) and intra-day (repeatability) variations. These parameters were evaluated through relative standards variations (RSDs) of the area and migration times of protein peaks. Due to the similarity between methods 2 and 3, the results of performance of IgG obtained for method 2 were acknowledged to account for method 3 too.

III. Results

III.1. Development of the method

III.1.1. Methods' performance

CE methods were developed to study the adsorption of 9 different proteins onto NPs, evaluating the capacity of the NPs to repel or allow adsorption of these proteins based on shield properties of their surface coverage. This part aimed to demonstrate (i) the methods suitability to separate the fraction of free protein from NPs contained in the sample as well as (ii) the linearity of response as the function of protein concentration and (iii) the ability to perform a precise quantitation of proteins.

(i) CE conditions to achieve a separation between free proteins and NPs were adapted according to the pI of the proteins, which determined their charge relatively to the pH of the CE electrolyte. Three methods were needed to separate free proteins from NPs. The behavior of the NPs observed in the different methods could be explained by the different coatings used in the capillary.

Method 1: For negatively charged proteins at working conditions (pI of the protein < 7), a neutral coating of PEO was used in order to limit adsorption of proteins on the bare silica capillary wall. This led to the absence of the counter-ions layer on the negatively charged capillary wall (Stern layer) and thus the loss of the electroosmotic flow (EOF) (μ_{EO}=0). In this method, migration was only dependent on the electrophoretic mobility of the entities (μ_{EP}) (Fig. 1B and 1C, left). This explained the migration of proteins towards the anode (positive pole) while NPs were only flushed during the washing step due to their quasi null μ_{EP} value (Fig. 1A left).

Methods 2 and 3: For positively charged proteins in working conditions, the cationic coating of Polybrene® led to the deposition of a compact anionic Stern layer next to the coating. The diffuse layer of anions (Gouy-Chapman layer) was then responsible for the electroosmotic flow directed towards the anode (Fig. 1B, right). Conversely, the electrophoretic mobility of positive proteins was directed to the cathode, thus reducing the apparent mobility ($\mu_{app} = \mu_{EO} + \mu_{EP}$) (Fig. 1C, right). It allowed a separation between NPs directed by the EOF only and proteins with a decreased apparent mobility that migrated slower to the anode (Fig. 1A, right). Proteins with pI > 8 were positively charged at the working pH of 7.4 and could be analyzed with method 3. However, proteins with 7 < pI < 8 were almost neutral at pH 7.4 and must be analyzed with method 2. In this method, the CE electrolyte was lowered to pH 3 to deal with positively charged proteins, which is necessary for the separation. In our study, IgG fell in this situation, being poorly charged at pH 7.4 (6.6 < pI < 7.4).

(ii) The linearity of protein quantitation was assessed by calibration curves performed using BSA (method 1) and IgG (methods 2 and 3) as protein examples for the two types of capillary coating. The good correlation coefficients of calibration curves allowed for a quantitation using protein peak area (R^2= 0.998 for BSA; R^2= 0.995 for IgG).

(iii) The inter-day fidelity and intra-day repeatability of the methods were tested by measurements of protein areas and migration times for BSA and IgG. Results shown in figure 1D indicated good RSDs for the different methods. As an example for area measurement, inter-day fidelity gave RSDs of 7.2 % and 4.7 % for BSA and IgG respectively. Repeatability of intra-day injections gave RSDs of 5.0 % and 5.1 % for BSA and IgG respectively.

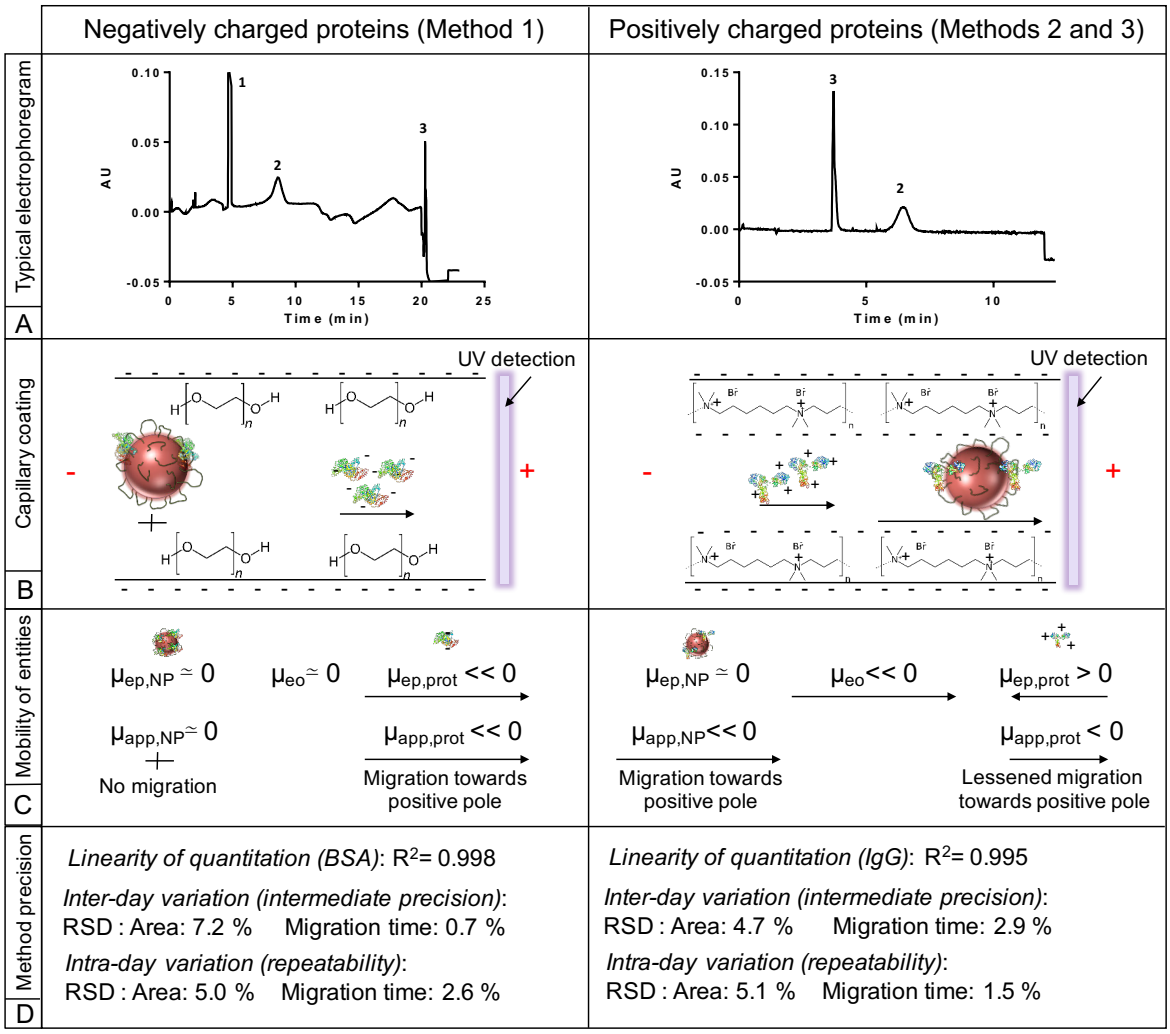

Figure 1: Precision and principles of separation of NPs and free proteins by the developed CE methods. 1A: Typical electrophoregrams obtained for negatively charged proteins at pH 7.4 (Method 1 – left) and positively charged proteins (methods 2 and 3 – right). 1: migration marker, 2: protein peak, 3: NPs peak. 1B: Principle of separation of the mixture free proteins/ NPs according to the capillary coating. 1C: Explanation of migration behavior taking in to account electrophoretic mobility (μ_{EP}) and electroosmotic mobility (μ_{EO}). 1D: Performance of the methods in terms of linearity, intermediate precision and repeatability.

III.1.2. Optimal NP/protein ratio seeking

The purpose of this part was to identify a NP to protein concentration ratio that could be used to characterize the adsorption behavior for a couple NP/protein suitable to discriminate NMs depending on their surface coverage properties. This ratio should allow for a representative evaluation of NPs' repellent power towards adsorption of the tested protein. This optimal ratio was determined from adsorption trends that were investigated with 2 proteins: BSA and IgG. These two proteins were chosen because they were easily available and can be purchased in a large quantity at a reasonable price. This choice was also consistent with the development

of the method as BSA could be determined with method 1 and IgG with method 2. The study was carried out using increasing concentrations of NPs (expressed in cm^2/mL) incubated with a constant concentration of protein (250 µg/mL). The percentage of adsorbed protein as a function of the surface of NPs present in the incubation medium was determined using the corresponding CE method. The adsorption profile of the 2 proteins was investigated on the five NPs.

A strong adsorption of both BSA and IgG was observed on NPs A1, A2 and R3 (cf. Fig.2 left part). The results highlighted that a surface concentration of 2000 cm^2/mL of NPs was enough to adsorb almost all proteins present in the incubation medium while the adsorption of the protein on NPs R1 and R2 was much lower. For the latter, the adsorption was not proportional to the amount of NP introduced. For instance, with NPs R1, the amount of IgG adsorbed increased until it reached a plateau near 60% of adsorption whatever the increase in the amount of NP introduced in the sample. Working at a concentration in NPs of 2000 cm^2/mL and at a concentration in protein of 250 µg/mL allowed a first ranking of the NPs into 2 groups, one allowing a high adsorption of the proteins including NPs A1, A2 and R3 and another including NPs that seem to exclude the studied proteins from adsorption (R1 and R2).

Results and conclusions drawn from determinations achieved using the CE methods were confirmed performing protein determinations by rocket gel electrophoresis according to Laurell's rocket IE method for BSA and by Mancini's radial ID for IgG. Results were depicted in figure 2 (right part). An example of analysis with each gel method was presented in supplementary information (S1 and S2). The consistency of results obtained from the different methods used to evaluate the free fraction of proteins suggested that the high voltage applied in CE did not introduce bias in this determination of free proteins.

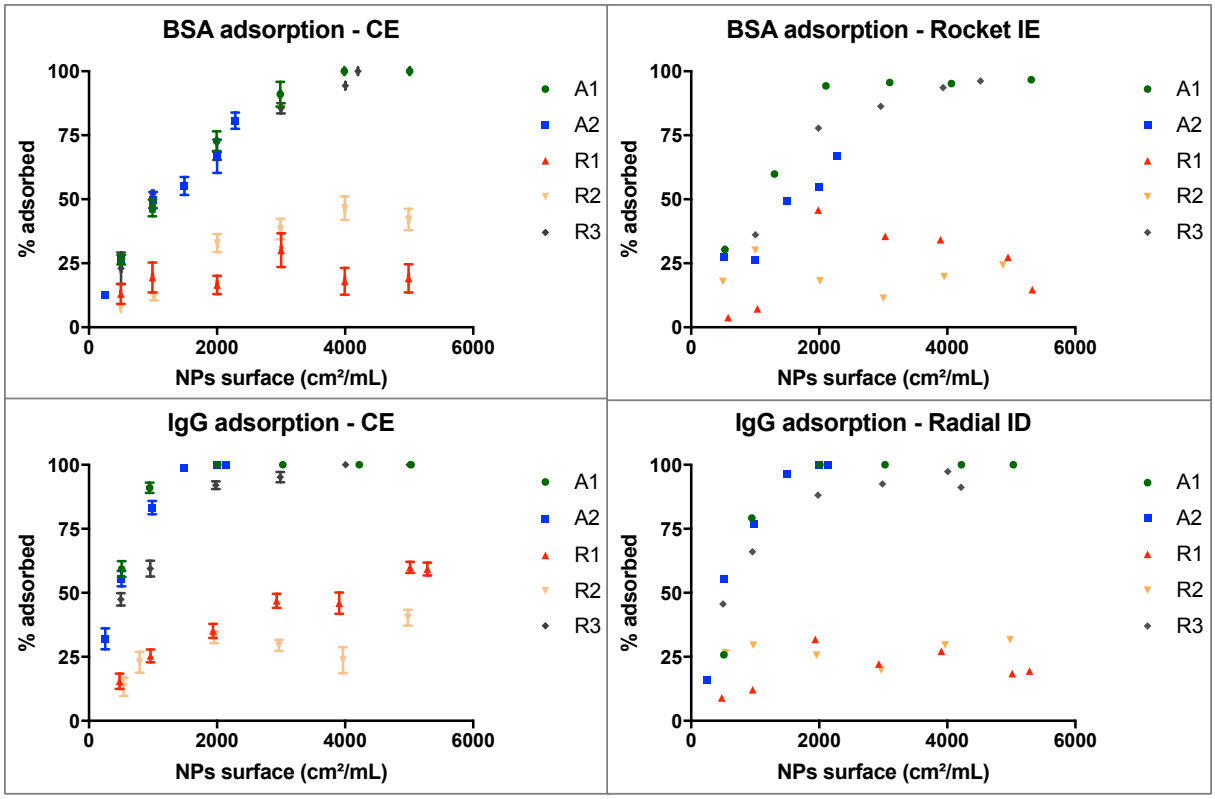

Figure 2: Adsorption trends for BSA and IgG adsorption onto the five NPs evaluated by CE (left part), rocket IE (upper right) and radial ID (lower right).
A1 (●), A2 (■), R1 (▲), R2 (▼) and R3 (◆).

III.2. Application of the method to evaluate surface coverage of NMs through the shield-effect towards protein adsorption

The adsorption of 9 proteins was tested on the five NPs. The main properties of the proteins were reported in table 3. They mainly differed from their size, charge, overall hydrophobicity and only slightly from their shape which was generally globular. Adsorption of these proteins was studied incubating 250 µg/mL of protein with 2000 cm^2/mL of NP as previously determined to provide with possibility to discriminate NPs allowing high or low adsorption of a given protein. No aggregation occurred during incubation of NP with each protein, as it was observed by direct visual observation and optical microscopy. Additionally, size obtained by DLS as well as autocorrelation curves showed no traces of aggregation in samples after incubation (example of data shown in supplementary information S3).

Raw data giving the percentage of adsorption of each protein on the different NPs were plotted on figure 3A. Typically, small proteins massively adsorbed on all types of NPs (Insulin chain B, aprotinin). Adsorption of medium sized proteins (from 44 kDa to 55 kDa) on the five types of NPs was generally low. A marked difference in the adsorption behavior of proteins

on the 5 types of NPs can be highlighted with proteins of the larger size (apo transferrin, IgG, thyroglobulin). These proteins were totally adsorbed on NPs A1, A2 and R3 while they showed only a low adsorption on NPs R1 and R2 suggesting that they were repeled from the surface of these NPs. These results were emphasized from the adsorption heatmap drawn from the raw data where dark blue represents a strong adsorption (Fig. 3B). This representation clearly emphasizes the difference of behavior between A1, A2, R3 and R1, R2 NPs, showing a global decreased adsorption on R1 and R2. Results were consistent with those that could be expected considering the difference in the architecture and density of the dextran chains grafted on the surface of the NPs used as models in the present study. Radical redox polymerized NPs (especially R1, R2) showed a lower adsorption profile than anionic polymerized NPs (A1 and A2). The influence of the density of grafting was also revealed by the difference of adsorption between R1 (dense brush 1.3%) and R3 (loose brush (0.5%).

This adsorption data was then expressed as the remaining free surface of NPs after incubation with proteins. This is in fact the part of the NPs where the repellent capacity (RC) is enough to prevent from the accessibility of proteins. It was called percentage of repellent capacity ($\%_{RC}$). On this purpose, the number of adsorbed proteins (N_{prot}) was first deduced from the % of protein adsorbed ($\%_{ads}$) thanks to the following equation.

$$N_{prot} = \frac{\%ads * Cprot * Vsample * N_A}{100 * MW} \quad \textit{(Eq. 2)}$$

where C_{prot} is the initial protein concentration (in g/L), V_{sample} is the total volume of sample (L), N_A is the Avogadro constant ($N_A = 6.022140857*10^{23}$ mol^{-1}) and MW the molecular weight of the considered protein (g/mol).

Then, the estimated surface area occupied by these adsorbed proteins (S_{prot}, in nm^2) is calculated using the hydrodynamic diameter of proteins depicted in table 3 (Dh, in nm):

$$S_{prot} = Nprot * 4 * \pi * (\frac{Dh}{2})^2 \quad \textit{(Eq. 3)}$$

From this value obtained in Eq.3, $\%_{RC}$ was calculated:

$$\%_{RC} = \left(1 - \frac{S_{prot}}{S_{NP}}\right) * 100 \ ^{\dagger} \quad \textit{(Eq. 4)}$$

with S_{NP} the total surface area of NPs in the incubation medium (nm^2).

† when $S_{prot} > S_{NP}$, $\%_{RC}$ was set by default to 0%.

The % of repellent capacity was plotted on figure 4A with the corresponding heatmap presented on figure 4B. Although no difference between the nanoparticles can be depicted from the data obtained with the smallest proteins (Insulin B chain and aprotinin) that fully covered all NPs surface, a very clear difference in repellent capacity can be highlighted from the data of the adsorption of the larger proteins (MW > 44 kDa). The heatmap clearly depicts a series of NPs keeping free surface area upon incubation with large proteins (R1 and R2), whereas the other NPs showed a high tendency to be almost fully covered with large proteins too.

Protein	**PDB**	**MW (kDa)**	**pI**	**a.a number**	**Dh size (nm)**	**Cristallographic size (nm)**	**GRAVY****	**Charged residues****	**Carbohydrate %**	**Protein shape** (not at scale)
Insulin B chain	4IHN	3.5	5.3	30	< 2.7 [47]	3.7 x 2.6 x 2.4 *	0.303	2+ ; 2-	No	Globular
Aprotinin	3LDJ	6.5	10.5	58	3.2 [48]	3.4 x 2.7 x 2.7 *	-0.479	10+ ; 4-	No	Globular
Orosomucoïd	3KQ0	44.1	2.8	183	7.3 [49]	4.6 x 4.5 x 4.0 *	-0.764	22+ ; 30-	45% [50]	Globular
Ovalbumin	1OVA	44.3	4.6	385	5.6 [51]	7 x 3.6 x 3 [52]	-0.006	35+ ; 47-	3.5% [53]	Globular 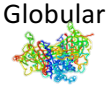
Transthyretyn	4TLT	55	4.6 – 4.9	508 (127 x 4 subunits)	8 [54]	6.9 x 5.5 x 4.8*	-0.274	12+ ; 17-	No	Ovoïd
BSA	4F5S	66.4	4.8	583	7.7 [55]	14.1 x 4.2 x 4.2 [56]	-0.475	82+ ; 99-	No	Globular
Apo Transferrin	2HAU	80	5.8	679	7.3 [57]	7.5 x 7.5 x 7.4	-0.411	84+ ; 87-	5.9% [58]	Globular
Human IgG	1HZH	150	6.6 – 7.4	1344 (457 - *heavy* x 2 ; (215 - *light* x2)	10.6 [49]	14.5 x 8.5 x 4 [59]	-0.483	144+ ; 122-	3% [58]	Y - shaped
Thyroglobulin	P01267	669	4.5	5500 (2750 x2 subunits)	17.2 [60]	n.d	-0.257	510+ ; 592-	10% [61]	n.d

Table 3**:** Summary of the characteristics of tested proteins for the shield-effect study. PDB: Protein Data Bank reference, MW: Molecular weight, pI: isoelectrical point, a.a number: number of amino acids in the protein sequence, Dh size: Hydrodynamic diameter, GRAVY: Hydrophaticity, n.d: not determined. *determined with Jmol **determined via Expasy Protparam tool.

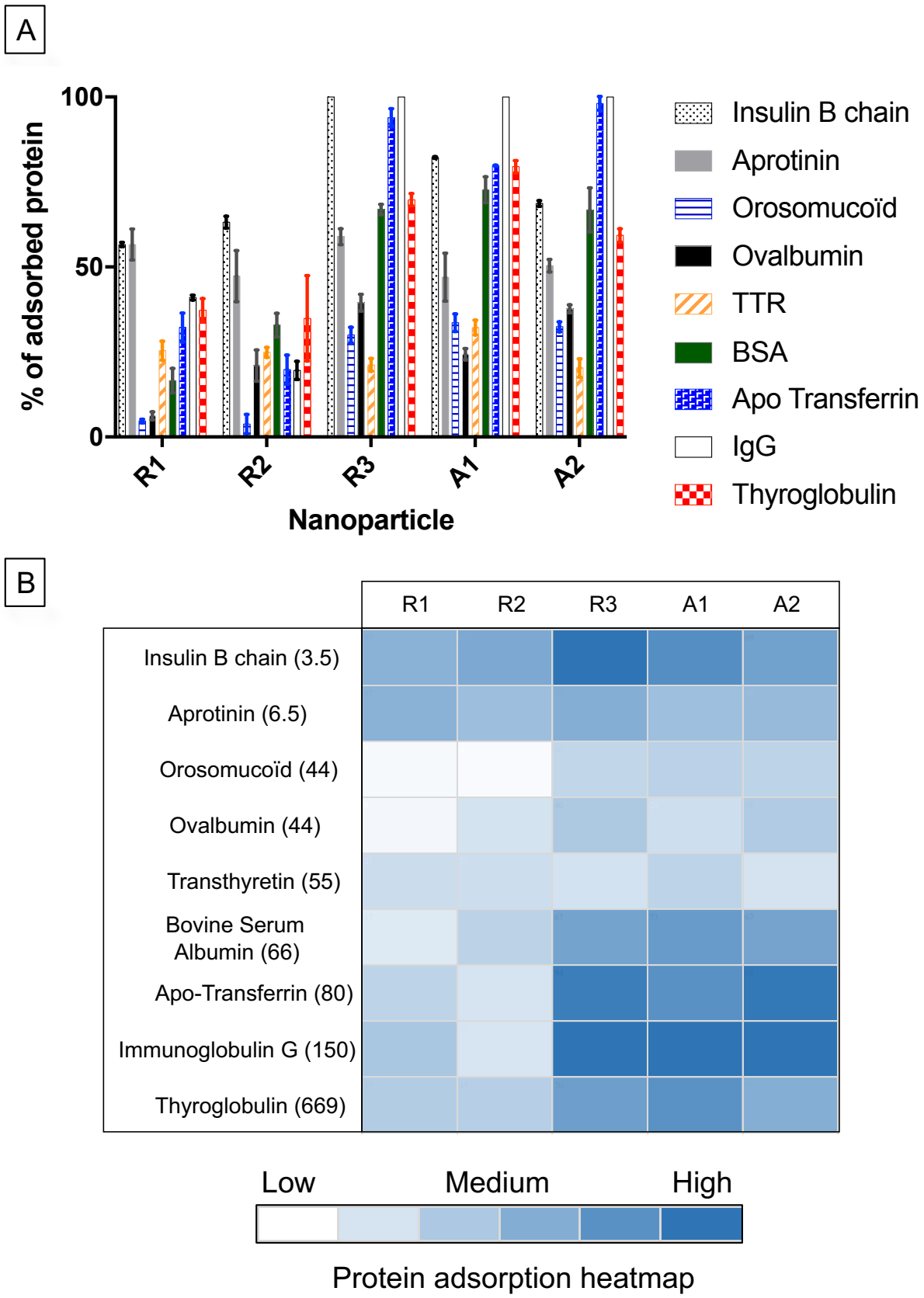

Figure 3: Shield-effect study: A- % of adsorption of the 9 tested proteins on the five type of NPs. B- Heatmap representation of protein adsorption on the five types of NPs (White: 0% to dark blue: 100% of protein adsorbed).

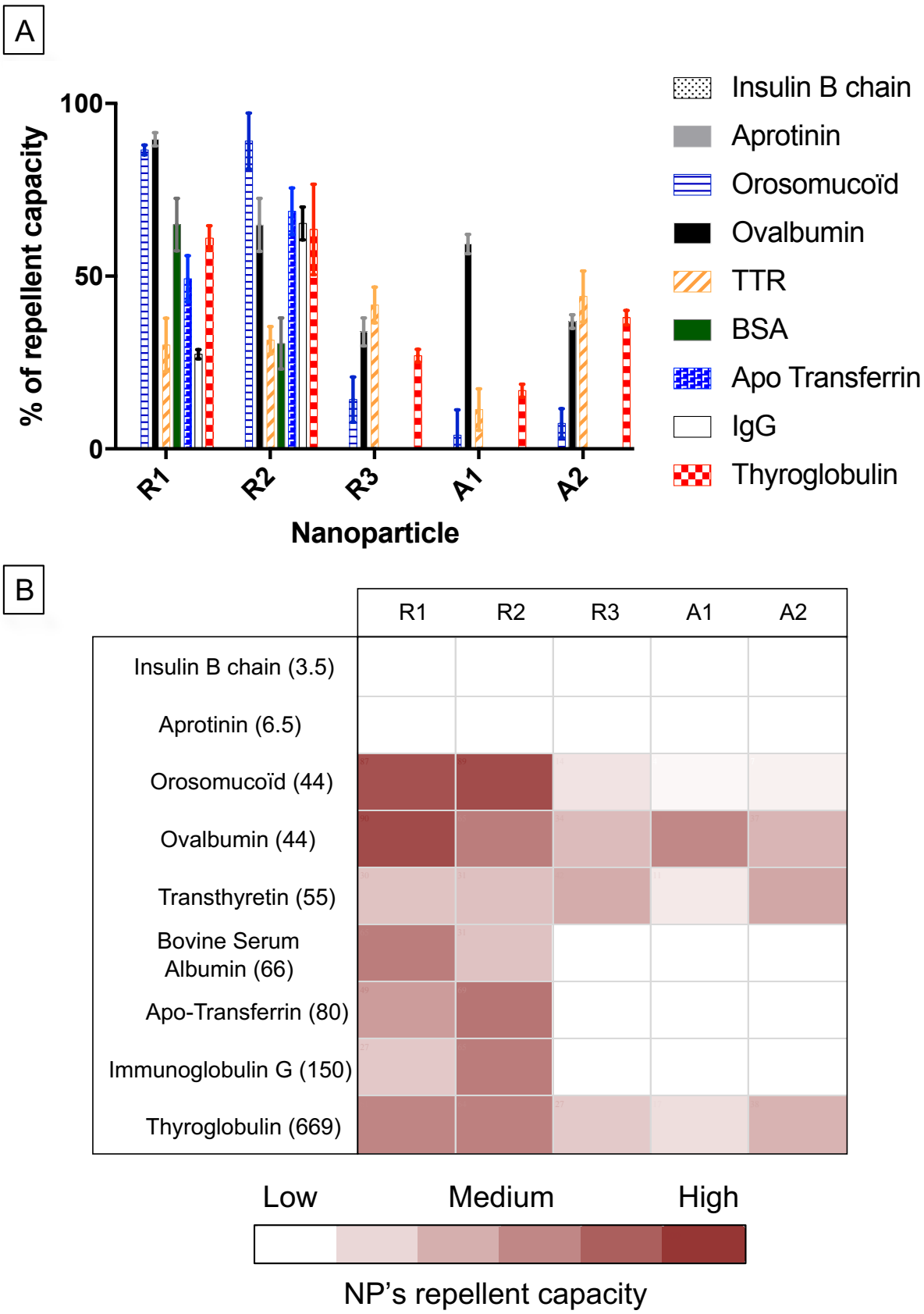

Figure 4: Shield effect study: A- % of repellent capacity of NPs after incubation with the different proteins. B- Heatmap representation of NPs repellent capacity after incubation with the different proteins (White: low RC (0%) to dark red: high RC (100%)).

IV. Discussion

A CE method was developed to quantify the amount of free protein in samples incubated with NPs in experiments designed to evaluate the adsorption of well-defined proteins on NPs surface. This method aimed to determine a new parameter characterizing the NM surface, the surface coverage, that is assumed to control the protein adsorption phenomena. In general, the mode of CE to be used to perform analysis is chosen depending on the kinetics of the studied interaction, here interactions leading to the adsorption of the protein onto NPs. Fast association-dissociation systems are studied by affinity capillary electrophoresis (ACE), Hummel Dreyer method, or frontal analysis capillary electrophoresis (FACE). On the contrary, slow kinetics of interactions are studied via capillary zone electrophoresis (CZE) or FACE [35,37,39]. In our model, determination of the amount of free protein remaining in the sample was achieved after incubation with NPs during 2 h 30 min to reach the equilibrium, according to a slow kinetics of interactions. CZE was then selected using the non-equilibrium capillary electrophoresis of equilibrium mixtures (NECEEM) [62]. This mode is easy-to-use and allows protein quantification directly from the evaluation of the area under the peak. The technique presents other advantages: (i) a low consumption of sample, (ii) a separation and determination of the amount of free proteins without any need of pre-treatment of the sample which includes both the protein and the NPs, and (iii) its automatability.

The optimal duration of incubation was determined through a kinetics study of BSA adsorption onto NPs (data not shown) and was consistent with previous works optimized with these NPs [41,63,64]. As the kinetics of association and dissociation were slow and the equilibrium reached after a period of incubation of 2 h 30 min, the variation of pH introduced by the CE electrolyte in method 2 (pH = 3) was supposed not to modify the equilibrium of adsorption during the short duration of the analysis. This assumption was supported by a prior study made on the comparable NP-protein system, where adsorption equilibrium showed no major modification in a short period upon a pH modification [63]. The three methods could be used to investigate the adsorption of nine proteins on five types of NPs used as models. The precision of the method was verified in terms of intra-day and inter-day repeatability. The results included the deviation due to the different preparations of the samples, as a new sample was prepared and incubated for each inter-day determination. It was also verified that the results obtained by CE was not biased due to the high voltage used

during analysis. The similar results obtained using two other methods of evaluation of free proteins in the same samples acknowledged that the presently developed CE methods could be used to determine the amount of free proteins in samples containing NPs, without need to remove the NPs prior to analysis. An optimal ratio between the concentration of protein and NPs was determined from adsorption trends established with two proteins. It was selected in order to discriminate different responses to protein adsorption between NPs. A high surface coverage of NPs allowed a low adsorption profile of proteins while those bearing a low surface coverage allowed a high adsorption of proteins. The CE methods were then applied to screen the adsorption of the 9 different selected proteins on the five types of NPs after incubation at the previously selected ratio. The five types of NPs could be classified in two groups based on the obtained raw data of adsorption. The proposed method could discriminate NPs with surfaces accessible to the larger proteins from NPs which surface properties seemed to exclude these proteins. These raw data took into consideration the difference in size between NPs because their concentration was expressed in surface area/mL. However, they did not take into account the difference in size of the proteins. Considering this parameter, the amount of surface occupied by the adsorbed proteins on the NP surface was calculated and in turn the amount of NP surface that remained free of adsorption. This last parameter can be viewed as the repellent capacity of the NP creating an efficient shield-effect against the adsorption of a given protein. The surface coverage was estimated from the overall tendency of repellent capacity. We could distinguish NP with a high surface coverage, showing a high repellent capacity for large proteins (NPs R1 and R2). On the contrary, NPs showing a low repellent capacity for main proteins were qualified as bearing a low surface coverage (A1, A2 and R3).

The difference was confirmed with the data representation of the RC which even emphasized the fact that the surface of NPs A1, A2 and R3 were almost fully accessible to tested proteins whatever their size. These observed behaviors are consistent with the results expected from surface characteristics shown by our model NPs (table 1). The dense brushes present on R1 and R2 repeled large proteins while loose R3 brush as well as loops conformations of A1 and A2 allowed the adsorption of these large proteins. These critical parameters have also been identified in a recent study, were both chain length and density were strongly involved in the steric repulsion of molecules [19].

These results demonstrate the interest of the present approach to assess a new parameter characterizing NMs based on the monitoring of protein adsorption in very well-defined conditions, suitable for a further standardization of the method.

Directly linked to its surface properties, the complement activation behavior of a nanomaterial is an important characteristic that depicts its ability to escape the recognition by the innate immune system. At the same time, it gives information about the stealth property of the NM. The triggering of this cascade is mainly driven by the adsorption of complement proteins to NPs. Thus, results of adsorption and coverage properties obtained in this study were crossed with known results of complement activation given by the same model NPs in a previous work [18]. It allowed the identification three classes of NPs. The first class is composed of NPs showing a high surface coverage of their macromolecular grafting, preventing a massive adsorption of protein in the present study, and triggering low complement activation. This is the case for R1 NP, which seems to be very selective in terms of protein interactions thanks to its dense and long brush coverage, limiting at the same time interactions with proteins of the complement system (CS).

Then, a second class includes NPs showing high surface coverage capabilities coupled to a high complement activation. This is the behavior observed for R2. This NP has been found to mainly activate the CS through the alternative pathway. This pathway involves the opsonization process and the activation of the complement cascade by the adsorption of complement proteins to the NP [65]. As hypothesized in a previous work, adsorption of small proteins on the NP core that remains visible due to the short brush conformation of the grafted polysaccharide may allow the adsorption of bigger protein such as complement C3. This phenomenon has also been described by Chen et al. [66]. This phenomenon was not observed with R1 thanks to the longer brush length that covers the small adsorbed proteins which remain invisible to other larger proteins for protein-protein interactions.

Finally, the third class of NP comprises NPs with low coverage capabilities of their shell grafting, allowing a massive adsorption of proteins and triggering a high complement activation. These NPs are A1, A2 and R3 and were assumed to activate the complement system via diverse pathways (classical, alternative, lectin) [18]. The freedom left by their loop and/or loose grafting allows for a higher accessibility of proteins to the hydrophobic core of NPs. As seen in this work, high adsorption of large protein was possible on these NPs. Thus, it

allows recognition by the complement system via different markers (opsonins, immunoglobulins).

The convergence and complementary given by these studies underlines the importance of the understanding of NP characteristics that master interactions with biological elements such as proteins. The method presented in this article could be used to increase the understanding and control of NMs surface properties and reactivity towards biological elements such as blood proteins by evaluating the surface coverage as a new parameter.

V. Conclusion

The method developed in the present work provides a tool to access a new characteristic of a NM, its surface coverage property. This parameter is critical to control protein adsorption phenomenon which is determinant on the *in vivo* fate, activity and safety of NMs. The use of CE allows for a direct analysis of the samples without pre-treatment steps. The method can be standardized as it is based on the use of very well defined conditions and proteins serving as molecular probes that are marketed at a high degree of purity. Being automatable, this CE method is also attractive for a systematic analysis of NMs. Crossed with other parameters such as the status of the complement activation given by the NMs, results produced by this method could be of interest in the future as analytical method to perform quality control analysis of NMs. All in all, the method developed in this work proves the potential for assessing molecular parameters of the NM surface not enough characterized so far.

Acknowledgements

The authors acknowledge the financial support from BPI-France, Project NICE.

VI. Bibliography

1) Anselmo, A. C. & Mitragotri, S. Nanoparticles in the clinic: Nanoparticles in the Clinic. *Bioengineering & Translational Medicine* **1,** 10–29 (2016).
2) Finch, G., Havel, H., Analoui, M., Barton, R. W., Diwan, A. R., Hennessy, M., Reddy, V., Sadrieh, N., Tamarkin, L., Wolfgang, M., Yerxa, B., Zolnik, B. & Liu, M. Nanomedicine Drug Development: A Scientific Symposium Entitled 'Charting a Roadmap to Commercialization'. *The AAPS Journal* **16,** 698–704 (2014).
3) Agrahari, V. & Hiremath, P. Challenges associated and approaches for successful translation of nanomedicines into commercial products. *Nanomedicine* **12,** 819–823 (2017).
4) Ragelle, H., Danhier, F., Préat, V., Langer, R. & Anderson, D. G. Nanoparticle-based drug delivery systems: a commercial and regulatory outlook as the field matures. *Expert Opinion on Drug Delivery* **14,** 851–864 (2017).
5) Landesman-Milo, D. & Peer, D. Transforming Nanomedicines From Lab Scale Production to Novel Clinical Modality. *Bioconjugate Chemistry* **27,** 855–862 (2016).
6) Halappanavar, S., Vogel, U., Wallin, H. & Yauk, C. L. Promise and peril in nanomedicine: the challenges and needs for integrated systems biology approaches to define health risk: Systems biology for nanomedicine and nanotoxicology. *Wiley Interdisciplinary Reviews: Nanomedicine and Nanobiotechnology* e1465 (2017).
7) Baer, D. R., Engelhard, M. H., Johnson, G. E., Laskin, J., Lai, J., Mueller, K., Munusamy, P., Thevuthasan, S., Wang, H., Washton, N., Elder, A., Baisch, B. L., Karakoti, A., Kuchibhatla, S. V. N. T. & Moon, D. Surface characterization of nanomaterials and nanoparticles: Important needs and challenging opportunities. *Journal of Vacuum Science & Technology A: Vacuum, Surfaces, and Films* **31,** 050820 (2013).
8) Salvador Morales, C., Khorasani, A. A. & Weaver, J. Closing the gap: accelerating the translational process in nanomedicine by proposing standardized characterization techniques. *International Journal of Nanomedicine* 5729 (2014).
9) Wei, A., Mehtala, J. G. & Patri, A. K. Challenges and opportunities in the advancement of nanomedicines. *Journal of Controlled Release* **164,** 236–246 (2012).
10) Shiekh, F. A., Farooq, O., Mian, S. H., Bautista, R. L., Arja, S. B. & Andrabi, K. I. The pitfalls of growing nanomaterials. *Nanomedicine (Lond)* **11,** 1635–1638 (2016).
11) Nyström, A. M. & Fadeel, B. Safety assessment of nanomaterials: Implications for nanomedicine. *Journal of Controlled Release* **161,** 403–408 (2012).
12) Crist, R. & McNeil, S. Nanotechnology for Treating Cancer: Pitfalls and Bridges on the Path to Nanomedicines.https://www.cancer.gov/research/key-initiatives/ras/rascentral/blog/2015/nanomedicines (2015). *Consulted on August 2017*
13) Fadeel, B., Feliu, N., Vogt, C., Abdelmonem, A. M. & Parak, W. J. Bridge over troubled waters: understanding the synthetic and biological identities of engineered nanomaterials: Bridging nanotoxicology and nanomedicine. *Wiley Interdisciplinary Reviews: Nanomedicine and Nanobiotechnology* **5,** 111–129 (2013).
14) Xu, X. & Khan, M. A. in *Polymer Nanoparticles for Nanomedicines: A Guide for their Design, Preparation and Development* (eds. Vauthier, C. & Ponchel, G.) 615–633 (Springer International Publishing, 2016).
15) Borgos, S. E. F., Cornier, J., Owen, A., Kwade, A. & Van de Voorde, M. in *Pharmaceutical Nanotechnology: Innovation and Production* 135–156 (Wiley-VCH Verlag GmbH & Co. KGaA, 2017).
16) FDA Nanotechnology Task Force Report 2007 https://www.fda.gov/ScienceResearch/SpecialTopics/Nanotechnology/ucm2006659.htm (2007). *Consulted on August 2017*
17) Hamad, I., Al-Hanbali, O., Hunter, A. C., Rutt, K. J., Andresen, T. L. & Moghimi, S. M. Distinct Polymer Architecture Mediates Switching of Complement Activation Pathways at the

Nanosphere−Serum Interface: Implications for Stealth Nanoparticle Engineering. *ACS Nano* **4,** 6629–6638 (2010).

18) Coty, J.-B., Eleamen Oliveira, E. & Vauthier, C. Tuning complement activation and pathway through controlled molecular architecture of dextran chains in nanoparticle corona. *International Journal of Pharmaceutics* **532**, 769-778 (2017).
19) Lin, J., Zhang, H., Morovati, V. & Dargazany, R. PEGylation on mixed monolayer gold nanoparticles: Effect of grafting density, chain length, and surface curvature. *Journal of Colloid and Interface Science* **504,** 325–333 (2017).
20) Kurtz-Chalot, A., Villiers, C., Pourchez, J., Boudard, D., Martini, M., Marche, P. N., Cottier, M. & Forest, V. Impact of silica nanoparticle surface chemistry on protein corona formation and consequential interactions with biological cells. *Materials Science and Engineering: C* **75,** 16–24 (2017).
21) Walkey, C. D., Olsen, J. B., Guo, H., Emili, A. & Chan, W. C. W. Nanoparticle Size and Surface Chemistry Determine Serum Protein Adsorption and Macrophage Uptake. *Journal of the American Chemical Society* **134,** 2139–2147 (2012).
22) Clogston, J. D., Crist, R. M. & McNeil, S. E. in *Polymer Nanoparticles for Nanomedicines: A Guide for their Design, Preparation and Development* (eds. Vauthier, C. & Ponchel, G.) 187–203 (Springer International Publishing, 2016).
23) EMA Reflection paper on surface coatings: general issues for consideration regarding parenteral administration of coated nanomedicine products. http://www.ema.europa.eu/docs/en_GB/document_library/Scientific_guideline/2013/08/WC500147874.pdf (2013). *Consulted on August 2017*
24) Walkey, C. D., Olsen, J. B., Song, F., Liu, R., Guo, H., Olsen, D. W. H., Cohen, Y., Emili, A. & Chan, W. C. W. Protein Corona Fingerprinting Predicts the Cellular Interaction of Gold and Silver Nanoparticles. *ACS Nano* **8,** 2439–2455 (2014).
25) Hadjidemetriou, M., Al-Ahmady, Z., Mazza, M., Collins, R. F., Dawson, K. & Kostarelos, K. In Vivo Biomolecule Corona around Blood-Circulating, Clinically Used and Antibody-Targeted Lipid Bilayer Nanoscale Vesicles. *ACS Nano* **9,** 8142–8156 (2015).
26) Nguyen, V. H. & Lee, B.-J. Protein corona: a new approach for nanomedicine design. *International Journal of Nanomedicine* **Volume 12,** 3137–3151 (2017).
27) O'Connell, D. J., Bombelli, F. B., Pitek, A. S., Monopoli, M. P., Cahill, D. J. & Dawson, K. A. Characterization of the bionano interface and mapping extrinsic interactions of the corona of nanomaterials. *Nanoscale* **7,** 15268–15276 (2015).
28) Walkey, C. D. & Chan, W. C. W. Understanding and controlling the interaction of nanomaterials with proteins in a physiological environment. *Chem. Soc. Rev.* **41,** 2780–2799 (2012).
29) Beck, M., Mandal, T., Buske, C. & Lindén, M. Serum protein adsorption enhances active leukemia stem cell targeting of mesoporous silica nanoparticles. *ACS Applied Materials & Interfaces* (2017).
30) Brun, E. & Sicard–Roselli, C. Could nanoparticle corona characterization help for biological consequence prediction? *Cancer nanotechnology* **5,** 7 (2014).
31) Schöttler, S., Becker, G., Winzen, S., Steinbach, T., Mohr, K., Landfester, K., Mailänder, V. & Wurm, F. R. Protein adsorption is required for stealth effect of poly(ethylene glycol)- and poly(phosphoester)-coated nanocarriers. *Nature Nanotechnology* **11,** 372–377 (2016).
32) Bigdeli, A., Palchetti, S., Pozzi, D., Hormozi-Nezhad, M. R., Baldelli Bombelli, F., Caracciolo, G. & Mahmoudi, M. Exploring Cellular Interactions of Liposomes Using Protein Corona Fingerprints and Physicochemical Properties. *ACS Nano* **10,** 3723–3737 (2016).
33) Pisani, C., Gaillard, J. C., Dorandeu, C., Charnay, C., Guari, Y., Chopineau, J., Devoisselle, J. M., Armengaud, J. & Prat, O. Experimental separation steps influence the protein content of corona around mesoporous silica nanoparticles. *Nanoscale* **9,** 5769–5772 (2017).
34) Lundqvist, M., Augustsson, C., Lilja, M., Lundkvist, K., Dahlbäck, B., Linse, S. & Cedervall, T. The nanoparticle protein corona formed in human blood or human blood fractions. *PLOS ONE* **12,** e0175871 (2017).

35) Aleksenko, S. S., Shmykov, A. Y., Oszwałdowski, S. & Timerbaev, A. R. Interactions of tumour-targeting nanoparticles with proteins: potential of using capillary electrophoresis as a direct probe. *Metallomics* **4,** 1141 (2012).
36) Capriotti, A. L., Caracciolo, G., Cavaliere, C., Colapicchioni, V., Piovesana, S., Pozzi, D. & Laganà, A. Analytical Methods for Characterizing the Nanoparticle–Protein Corona. *Chromatographia* **77,** 755–769 (2014).
37) Trapiella-Alfonso, L., Ramírez-García, G., d'Orlyé, F. & Varenne, A. Electromigration separation methodologies for the characterization of nanoparticles and the evaluation of their behaviour in biological systems. *TrAC Trends in Analytical Chemistry* **84,** 121–130 (2016).
38) Li, N., Zeng, S., He, L. & Zhong, W. Probing Nanoparticle−Protein Interaction by Capillary Electrophoresis. *Analytical Chemistry* **82,** 7460–7466 (2010).
39) Ramírez-García, G., d'Orlyé, F., Gutiérrez-Granados, S., Martínez-Alfaro, M., Mignet, N., Richard, C. & Varenne, A. Electrokinetic Hummel-Dreyer characterization of nanoparticle-plasma protein corona: The non-specific interactions between PEG-modified persistent luminescence nanoparticles and albumin. *Colloids and Surfaces B: Biointerfaces* **159,** 437–444 (2017).
40) Bertholon, I., Lesieur, S., Labarre, D., Besnard, M. & Vauthier, C. Characterization of Dextran−Poly(isobutylcyanoacrylate) Copolymers Obtained by Redox Radical and Anionic Emulsion Polymerization. *Macromolecules* **39,** 3559–3567 (2006).
41) Vauthier, C., Lindner, P. & Cabane, B. Configuration of bovine serum albumin adsorbed on polymer particles with grafted dextran corona. *Colloids and Surfaces B: Biointerfaces* **69,** 207–215 (2009).
42) Vauthier, C. in *Biointeractions of Nanomaterials* 365–382 (CRC Press, 2014).
43) Couvreur, P., Kante, B., Roland, M., Guiot, P., BAuduin, P. & Speiser, P. Polycyanoacrylate nanocapsules as potential lysosomotropic carriers: preparation, morphological and sorptive properties. *Journal of Pharmacy and Pharmacology* **31,** 331–332 (1979).
44) Coty, J.-B., Varenne, F., Vachon, J.-J. & Vauthier, C. Serial multiple crossed immunoelectrophoresis at a microscale: A stamp-sized 2D immunoanalysis of protein C3 activation caused by nanoparticles: Proteomics and 2-DE. *ELECTROPHORESIS* **37,** 2401–2409 (2016).
45) Laurell, C.-B. Antigen-antibody crossed electrophoresis. *Analytical biochemistry* **10,** 358–361 (1965).
46) Mancini, G., Carbonara, A. O. & Heremans, J. F. Immunochemical quantitation of antigens by single radial immunodiffusion. *Immunochemistry* **2,** 235–254 (1965).
47) Hovgaard, L., Jacobs, H., Mazer, N. A. & Kim, S. W. Stabilization of insulin by alkylmaltosides. A. Spectroscopic evaluation. *International Journal of Pharmaceutics* **132,** 107–113 (1996).
48) Wilkins, D. K., Grimshaw, S. B., Receveur, V., Dobson, C. M., Jones, J. A. & Smith, L. J. Hydrodynamic Radii of Native and Denatured Proteins Measured by Pulse Field Gradient NMR Techniques. *Biochemistry* **38,** 16424–16431 (1999).
49) Armstrong, J. K., Wenby, R. B., Meiselman, H. J. & Fisher, T. C. The Hydrodynamic Radii of Macromolecules and Their Effect on Red Blood Cell Aggregation. *Biophysical Journal* **87,** 4259–4270 (2004).
50) Fournier, T., Medjoubi-N, N. & Porquet, D. Alpha-1-acid glycoprotein. *Biochimica et Biophysica Acta (BBA) - Protein Structure and Molecular Enzymology* **1482,** 157–171 (2000).
51) Schneider, S. Determination of Protein Molecular Weight and Size Using the Agilent 1260 Infinity Multi-Detector Bio-SEC Solution with Advanced Light Scattering Detection. *Agilent Technologies Application* note (2014).
52) Erickson, H. P. Size and Shape of Protein Molecules at the Nanometer Level Determined by Sedimentation, Gel Filtration, and Electron Microscopy. *Biological Procedures Online* **11,** 32–51 (2009).
53) Lee, Y.C. & Montgomery, R. The carbohydrate of ovalbumin. *Arch Biochem Biophys* **95,** 263–270 (1961).

54) Hou, X., Parkington, H. C., Coleman, H. A., Mechler, A., Martin, L. L., Aguilar, M.-I. & Small, D. H. Transthyretin oligomers induce calcium influx via voltage-gated calcium channels. *Journal of Neurochemistry* **100,** 446–457 (2007).
55) Hawe, A., Hulse, W. L., Jiskoot, W. & Forbes, R. T. Taylor Dispersion Analysis Compared to Dynamic Light Scattering for the Size Analysis of Therapeutic Peptides and Proteins and Their Aggregates. *Pharmaceutical Research* **28,** 2302–2310 (2011).
56) Wright, A. K. & Thompson, M. R. Hydrodynamic structure of bovine serum albumin determined by transient electric birefringence. *Biophysical Journal* **15,** 137–141 (1975).
57) Charlwood, P. A. Differential sedimentation-velocity and gel-filtration measurements on human apotransferrin and iron–transferrin. *Biochemical Journal* **125,** 1019–1026 (1971).
58) Putnam, F. W. in *The Plasma Proteins (Second Edition)* 45–166 (Academic Press, 1984).
59) Tan, Y. H., Liu, M., Nolting, B., Go, J. G., Gervay-Hague, J. & Liu, G. A Nanoengineering Approach for Investigation and Regulation of Protein Immobilization. *ACS Nano* **2,** 2374–2384 (2008).
60) Edelhoch, H. The properties of thyroglobulin. I. The effects of alkali. *J Biol Chem* **235,** 1326–1334 (1960).
61) Di Jeso, B. & Arvan, P. Thyroglobulin From Molecular and Cellular Biology to Clinical Endocrinology. *Endocrine Reviews* **37,** 2–36 (2016).
62) Krylov, S. N. Nonequilibrium Capillary Electrophoresis of Equilibrium Mixtures (NECEEM): A Novel Method for Biomolecular Screening. *J Biomol Screen* **11,** 115–122 (2005).
63) Olivier, J.-C., Vauthier, C., Taverna, M., Ferrier, D. & Couvreur, P. Preparation and characterization of biodegradable poly(isobutylcyano acrylate) nanoparticles with the surface modified by the adsorption of proteins. *Colloids and Surfaces B: Biointerfaces* **4,** 349–356 (1995).
64) Vauthier, C., Persson, B., Lindner, P. & Cabane, B. Protein adsorption and complement activation for di-block copolymer nanoparticles. *Biomaterials* **32,** 1646–1656 (2011).
65) Nilsson, B., Ekdahl, K. N., Mollnes, T. E. & Lambris, J. D. The role of complement in biomaterial-induced inflammation. *Mol Immunol* **44,** 82–94 (2007).
66) Chen, F., Wang, G., Griffin, J. I., Brenneman, B., Banda, N. K., Holers, V. M., Backos, D. S., Wu, L., Moghimi, S. M. & Simberg, D. Complement proteins bind to nanoparticle protein corona and undergo dynamic exchange in vivo. *Nature Nanotechnology* **12,** 387–393 (2016).

Supplementary material

Sharp characterization of nanomedicines' surface with molecular probes by capillary electrophoresis: towards understanding and evaluation of surface coverage

J-B. Coty, F. Varenne, O. Garsaa, I. Le Potier, C. Smadja, M.Taverna, C. Vauthier*

Institut Galien Paris-Sud, CNRS, Univ. Paris-Sud, University Paris-Saclay, Châtenay-Malabry, France

***Correspondence:** Dr. Christine Vauthier, CNRS UMR 8612, Institut Galien Paris Sud, Univ. Paris-Sud, Université Paris-Saclay, 5, rue Jean-Baptiste Clément, 92296 Châtenay-Malabry, France. Fax: +33 146835946. E-mail: christine.vauthier@u-psud.fr

S1: Determination of BSA adsorption on NP A1 via rocket immunoelectrophoresis

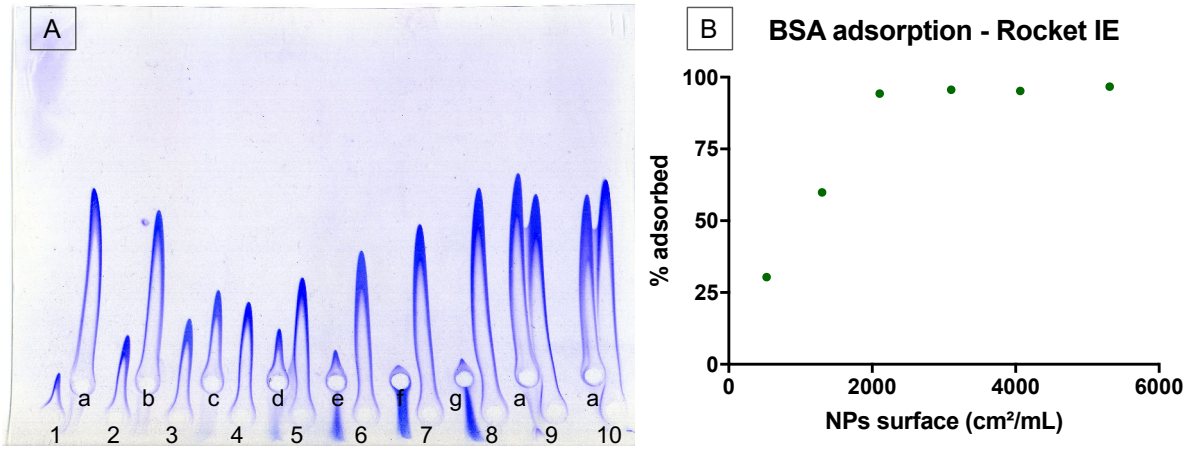

Figure S1: (A) Rocket immunoelectrophoresis gel of BSA adsorption onto nanoparticle A1. 1-10 represents the calibration samples of BSA: 25 µg/mL (1), 50 µg/mL (2), 75 µg/mL (3), 100 µg/mL (4), 125 µg/mL (5), 150 µg/mL (6), 175 µg/mL (7), 200 µg/mL (8), 225 µg/mL (9), 250 µg/mL (10).
a-g represents the free BSA remaining after incubation with A1 at different surface concentrations: 500 cm^2/mL (a), 1000 cm^2/mL (b), 2000 cm^2/mL (c), 3000 cm^2/mL (d), 4000 cm^2/mL (e), 5000 cm^2/mL (f), 6000 cm^2/mL (g).
(B) Corresponding trend of adsorption of BSA on nanoparticle A1.

S2: Determination of IgG adsorption on NP R2 via radial immunodiffusion

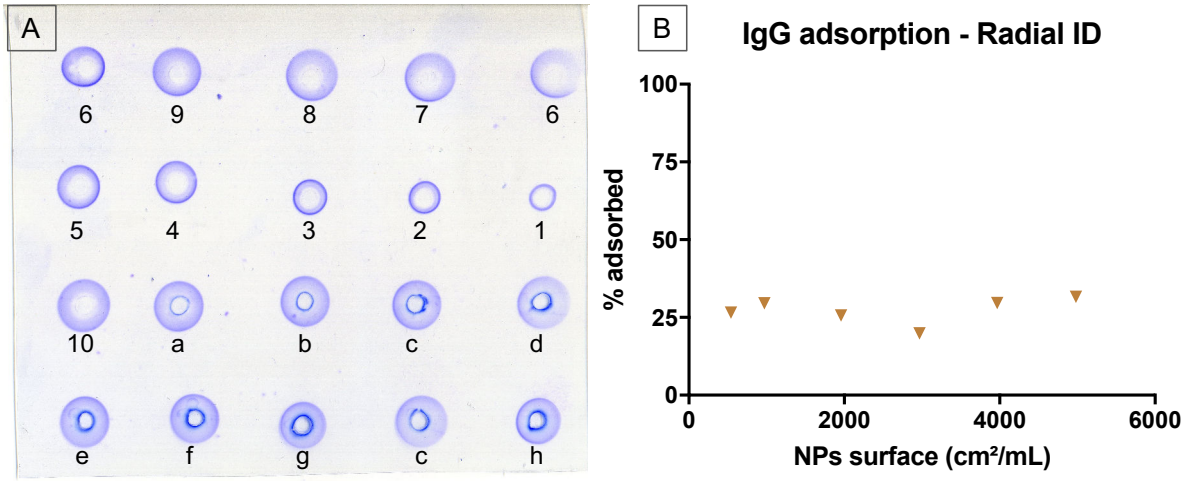

Figure S2: (A) Radial immunodiffusion gel of IgG adsorption onto nanoparticle R2.
1-10 represents the calibration samples of IgG: 25 µg/mL (1), 50 µg/mL (2), 75 µg/mL (3), 100 µg/mL (4), 125 µg/mL (5), 150 µg/mL (6), 175 µg/mL (7), 200 µg/mL (8), 225 µg/mL (9), 250 µg/mL (10).
a-g represents the free IgG remaining after incubation with R2 at different surface concentrations: 500 cm^2/mL (a), 1000 cm^2/mL (b), 2000 cm^2/mL (c), 3000 cm^2/mL (d), 4000 cm^2/mL (e), 5000 cm^2/mL (f), 6000 cm^2/mL (g).
(B) Corresponding trend of adsorption of IgG on nanoparticle R2.

S3: Verification of the absence of aggregates upon NP-proteins incubation

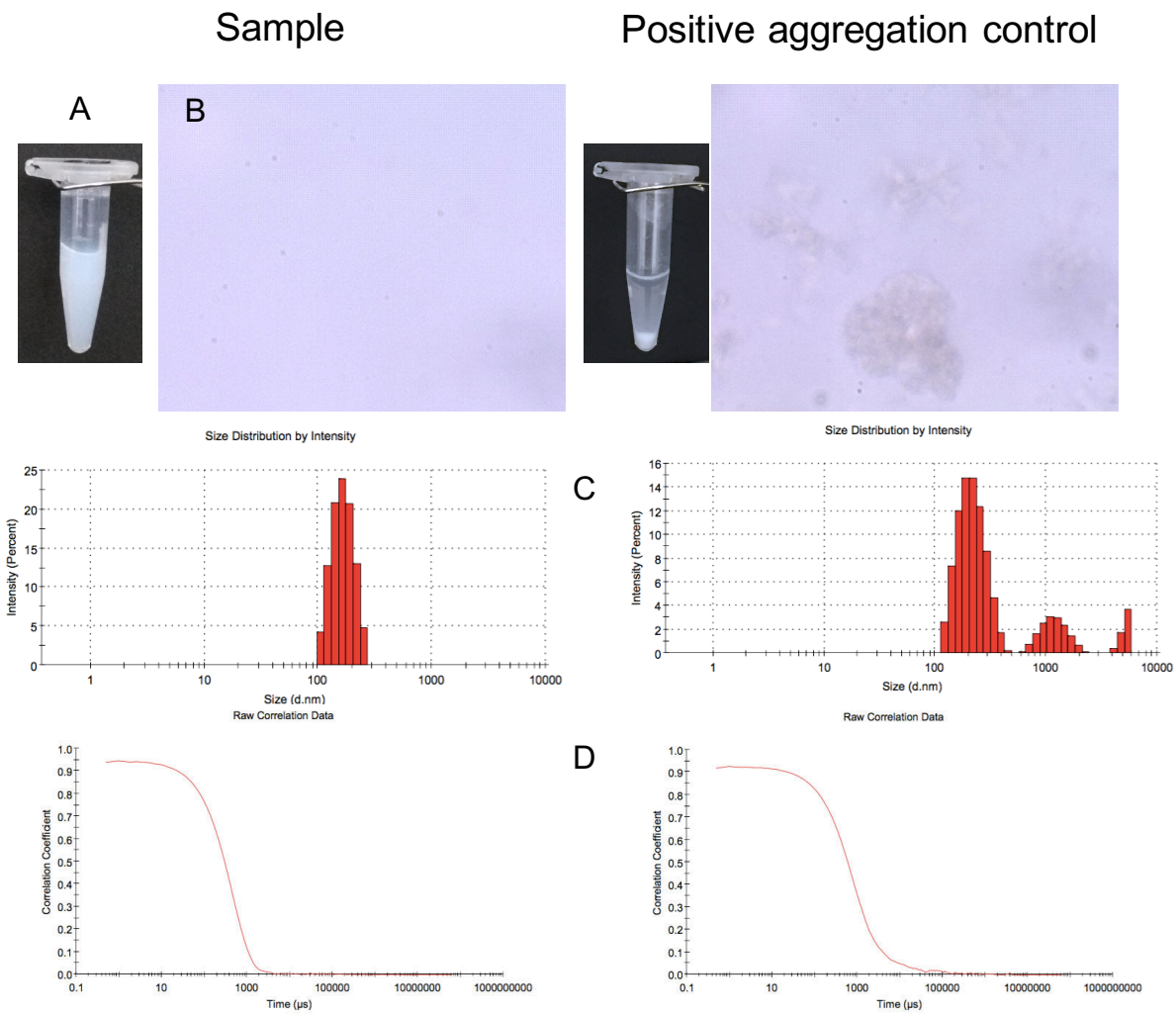

Figure S3: example of aggregation control made on NP A2 after incubation with Apo-Transferrin (left part) compared to a positive control of an aggregated sample of A2 after incubation with fibrinogen (right part).

(A) Verification of the absence of visible aggregates

(B) Optical microscopic verification of the absence of aggregates

(C) Measurement of NP size by dynamic light scattering (DLS)

(D) Autocorrelation curve of DLS measurement

Discussion générale

(see english summary p.217)

Les interactions entre nanomédecines (NMs) et éléments biologiques sont reconnues pour leur forte influence sur la biodistribution des NMs. Plus particulièrement, l'adsorption des protéines plasmatiques sur les nanomatériaux administrés par voie intraveineuse s'avère être déterminante pour le devenir du nanovecteur [1]. Le concept d'identité biologique supplantant l'identité synthétique de la NM après son administration, proposé par Walkey *et al*. et illustré sur la figure 1, est maintenant communément admis dans la communauté scientifique [2-4].

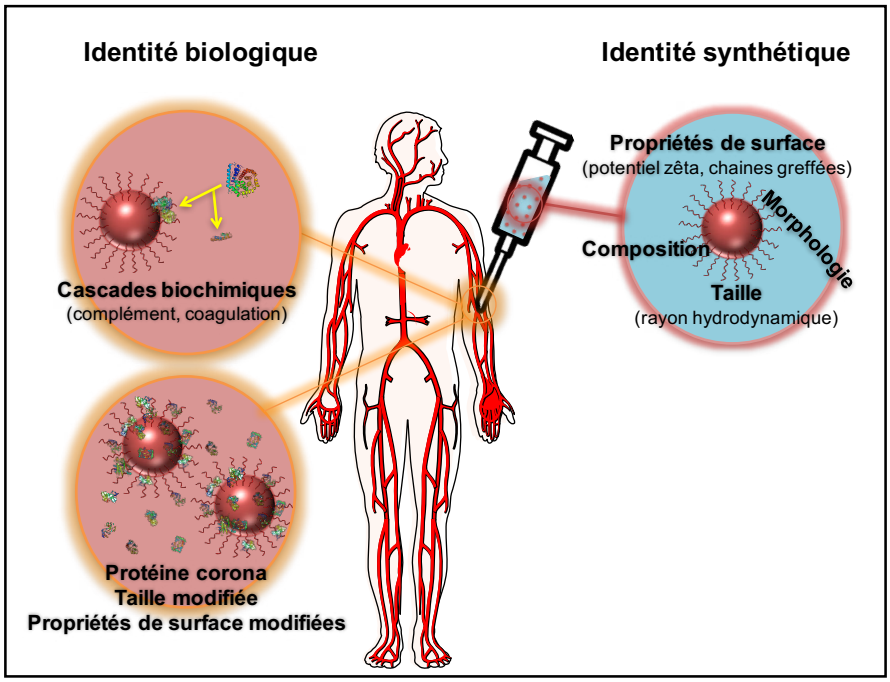

Figure 1 : Concept de l'identité biologique acquise *in vivo* supplantant l'identité synthétique initiale de la nanomédecine.

Actuellement, de nombreux efforts sont tournés vers la compréhension des implications induites par la couche de protéines se formant autour de la NM, la « protéine corona » [4-6]. Il existe en réalité deux niveaux de compréhension à investiguer aujourd'hui, illustrés dans la figure 2 ci-dessous. Dans un premier temps, il s'agit de comprendre quels sont les paramètres physico-chimiques initiaux de la NM (x_i) qui vont influencer les propriétés de l'identité biologique acquise (y_i) par la NM après administration, et plus particulièrement la composition de la protéine corona. Puis, dans un second temps, il est nécessaire d'identifier quels sont les éléments de cette protéine corona responsables du devenir physiologique de ces NMs (z_i), et en particulier de leur biodistribution. Dans ces travaux de thèse, les méthodes développées tendent à répondre à la 1ère partie de cette interrogation. Les travaux concernant la deuxième

partie, visant à établir les corrélations entre identité des protéines adsorbées et devenir *in vivo,* sont en forte expansion avec le développement de modèles de prédiction [4,7,8].

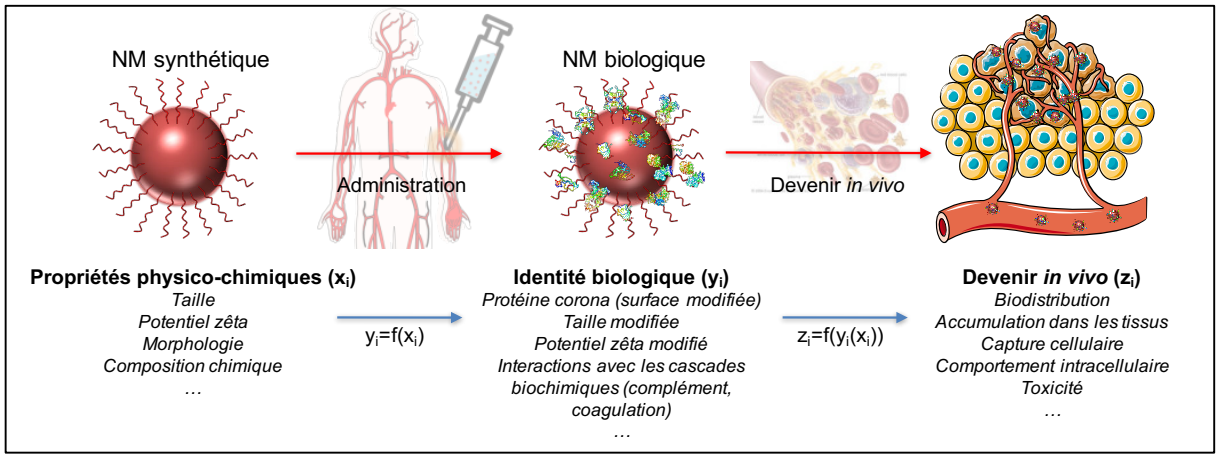

Figure 2 : Paramètres impliqués et relations entre les propriétés physico-chimiques (x_i) et l'identité biologique acquise des nanomédecines (y_i) pour une meilleure compréhension et prédiction de leur devenir *in vivo* (z_i).

Dans cette illustration, qui reprend notamment le modèle de prédiction envisagé dans les travaux de W.C.W. Chan [2,9], on note que les propriétés physico-chimiques des NMs ont un rôle prépondérant pour contrôler l'ensemble des phénomènes régissant leur devenir *in vivo*. Actuellement, lors du développement clinique de NMs, les différences de tolérance ou d'efficacité observées entre plusieurs lots de NMs en phase clinique restent souvent inexpliquées. La caractérisation des NMs a été identifiée comme l'un des points limitant la réussite en phase clinique de ces systèmes pourtant révolutionnaires de par leurs promesses en termes d'amélioration de l'efficacité et de tolérablité de traitements actuellement utilisés [10-12]. Un des points cruciaux de ce challenge serait d'améliorer la compréhension du devenir *in vivo* des NMs, notamment concernant leurs interactions avec les protéines plasmatiques.

Parmi les limites posées par la caractérisation des NMs, nous avons pu identifier un manque de précision dans l'évaluation des paramètres étudiés. En effet, les systèmes biologiques ont la capacité de déceler des différences subtiles au niveau de l'architecture de surface des NMs, que les méthodes de caractérisation actuellement utilisées en routine sont incapables de détecter. Il y a donc un réel besoin de méthodes capables de rivaliser avec la précision des systèmes biologiques. Dans ce contexte, nos travaux de thèse avaient pour objectif de proposer de nouvelles approches pour la caractérisation de NMs, permettant une définition fine des propriétés de surface et tournées vers une démarche de contrôle qualité des lots

cliniques. Le développement de méthodes s'est effectué autour de deux grands axes : l'étude des interactions entre NMs et protéines de la cascade du complément dans une première partie, puis la caractérisation de la surface réactive des NMs dans une seconde partie. Nos travaux se sont appuyés sur l'utilisation d'une série de nanoparticules (NPs) polymère déjà bien caractérisées sur le plan physico-chimique. Ces modèles bien définis ont permis de challenger les méthodes développées et étudier leur capacité à discriminer des NPs de propriétés physico-chimiques différentes. Le terme « nanoparticule » sera généralement utilisé pour désigner ces modèles dans cette discussion.

Interactions des NMs avec le système du complément

Un groupe de protéines important dans la circulation sanguine sont les protéines du système du complément. Comme indiqué plus tôt dans ces travaux (chap II et III) et rappelé dans l'*annexe méthodologique n°4*, ce système constitue la première barrière de l'immunité innée rencontrée par les NMs une fois qu'elles sont injectées dans la circulation sanguine. La reconnaissance des NMs par certaines protéines appelées opsonines peut amener à l'activation de la cascade du complément. Physiologiquement, cette activation génère de nombreuses réactions visant à lutter contre les organismes reconnus comme étrangers. Parmi ces réactions se trouvent l'activation du réseau de cellules phagocytaires ainsi que le déclenchement de réactions d'inflammation via les anaphylatoxines libérées [13]. Ces réactions peuvent être exagérées chez certains patients qui présentent le CARPA (Complement activation related pseudo allergy) [14]. La survenue de ce phénomène observé lors de l'administration de NMs à des patients est encore incomprise et peut mener à de graves réactions jusqu'au décès dans les cas extrêmes. De plus, d'un point de vue thérapeutique, la reconnaissance des NMs par le système du complément induit une forte activité phagocytaire et donc une capture accrue des NMs, notamment par les cellules de Kupffer présentes dans le foie [15]. La biodistribution est alors totalement biaisée et l'efficacité du traitement fortement altérée. L'importance de déterminer la capacité d'un nanomatériau à échapper au système du complément est majeure. Généralement, il est souhaité des NMs dites « furtives » [16], c'est-à-dire non reconnues par le système immunitaire. Il a été démontré que l'attachement de chaines de polymères hydrophiles autour du cœur de la NM pouvait empêcher l'interaction avec les opsonines et ainsi éviter la reconnaissance par le système immunitaire [16-18]. Cependant, des NMs commercialisées et

décrites comme furtives ont montré des réactions d'activation du complément dans certains cas (Doxil®) [19]. Il est donc important de pouvoir contrôler la capacité d'une NM à interagir avec le système du complément. Cela n'est pas réalisé systématiquement aujourd'hui en contrôle qualité clinique, supposant que le comportement d'un lot de NMs vis à vis du système du complément est garanti par ses propriétés testées en routine, à savoir la taille et le potentiel zêta.

Nous avons développé des méthodes qui permettraient une analyse facilitée et de façon plus accessible de l'activation du système du complément par des NPs. Premièrement, la méthode connue d'immunoélectrophorèse bidimensionnelle, dont le principe est rappelé en *annexe méthodologique n°1*, a été modifiée et adaptée pour une analyse en routine (cf. chapitre II). Cette méthode, plutôt simple dans son principe mais de mise en œuvre expérimentale assez lourde a été initialement proposée par Passirani *et al.* en 1998 [20] en utilisant le principe d'immunoélectrophorèse décrit par Laurell [21]. Cependant, compte tenu de la complexité de manipulation demandée et de son très faible débit d'analyse (5 analyses en 24 heures), cette méthode n'était que très peu utilisée. Nous avons repensé son concept en revoyant le processus général de fabrication du gel. La nouvelle conception repose sur un principe de migration en série des différents échantillons, tant lors de la première que de la seconde dimension. Ce principe, déjà utilisé en 1985 par Rochu *et al*. pour la migration en série d'échantillons n'est pourtant que peu utilisé [22]. Ici, il permet d'accroitre significativement le débit d'échantillons analysés. La réalisation du gel s'effectue maintenant entièrement avant le début des électrophorèses, contrairement à ce qui était réalisé avec l'ancienne méthode et dans la méthode de Rochu *et al*. Cela allège considérablement la part de manipulation qui constituait un frein à son utilisation. Enfin, la méthode de multi-crossed IE (µC-IE) a été validée pour sa robustesse (chapitre II ou [23]). Elle permet de déterminer un nouvel indicateur, appelé le $C3A_{50}$, qui correspond à la surface de NP nécessaire pour induire un clivage de 50% de la protéine C3 native. Cet indicateur pourrait, au même titre que l'IC_{50} pour l'étude de la viabilité cellulaire (concentration inhibitrice à 50%), devenir un paramètre incontournable lors de la caractérisation de NMs puisqu'il montre une bonne sensibilité de réponse avec des nanoparticules de caractéristiques physico-chimiques très peu différentes. Un autre avantage de la méthode µC-IE est la possibilité d'estimer d'une façon relative la fraction de protéine C3 clivée. Dans les tests ELISA, la détection d'un fragment spécifique donne une idée précise de

la quantité de ce fragment libéré, sans pour autant avoir d'indication sur la fraction restant inactivée.

La nouvelle version de la méthode d'immunoélectrophorèse 2D a été utilisée au cours de cette thèse dans une étude plus fondamentale de la compréhension des interactions entre nanovecteurs et système du complément. L'objectif était d'étudier la voie d'activation de la cascade du complément empruntée par différentes NPs en modifiant les conditions d'incubation. Alors que les conditions d'incubation utilisées habituellement permettent une activation selon les trois voies connues de la cascade du complément (classique, lectine et alterne), un tampon de composition modifiée inhibe les voies classique et lectine en piégeant les ions calcium, nécessaires au démarrage de ces voies. Nous avons donc pu établir des hypothèses concernant les voies d'activations empruntées par nos NPs modèles au regard de la conformation en surface des chaines de polysaccharides qui les recouvrent, ainsi que de la densité de greffage de ces chaines (chapitre III ou [24]). Ces paramètres ont un fort impact sur la façon dont les NMs vont interagir avec les protéines du complément, influençant non seulement le niveau d'activation du système du complément, mais aussi la voie d'activation empruntée. Cela positionne également la µC-IE développée ici en tant que méthode permettant d'améliorer la compréhension des phénomènes dirigés par la surface des NMs et s'inscrit dans la première partie de la problématique évoquée au début de cette discussion.

La méthode µC-IE a également été utilisée dans d'autres études pour étudier la capacité de différents nanomatériaux à activer ou non le système du complément :

- Pour des complexes albumine de sérum bovin (BSA)-Amphotericine B (AmB) en vue d'une utilisation par voie intraveineuse de ces complexes. Les résultats ont montré que les agrégats d'AmB déclenchaient une activation du système du complément, contrairement à la forme complexée, soulignant l'importance de la stabilisation de l'AmB procurée par les complexes formés avec la BSA [25].
- Pour de nouvelles NPs réalisées par le co-assemblage de cyclodextrines amphiphiles et de lipides, où le système s'est avéré être non activant de la protéine C3 et prometteur comme nanovecteur pour une administration intraveineuse [26].
- Pour des NPs constituées de PolyBenzyl L-Glutamate (PBLG) fonctionnalisées avec différents groupements de ciblage et de marquage. Il a été montré que les NPs

fonctionnalisées avec des anticorps greffés sur une couronne de PEG n'activaient pas le système du complément [27].

- Pour des NPs composées de copolymères PBLG-PEG de différentes morphologies. L'étude de l'activation du complément a démontré que la forme allongée des NPs n'induisait pas un phénomène d'activation de la protéine C3 [28].

Ces différentes études ont pu démontrer la versatilité de la méthode µC-IE qui a été appliquée à l'étude de différents nanomatériaux et sa capacité à donner des résultats robustes sans modification de protocole. Cependant, l'une des limites rencontrées pour une utilisation répandue en routine de cette méthode est la consommation de temps qu'elle suppose, avec un durée d'électrophorèse de 5 heures ajoutée au temps de traitement et lecture du gel.

Une autre technique que nous avons ensuite utilisé pour une évaluation de l'activation du complément directement automatisable est la résonnance plasmonique de surface (SPR), dont le principe de fonctionnement a été rappelé en *annexe méthodologique n°3*. Nous avons développé une puce permettant l'étude de l'activation du complément par la mesure simultanée de la quantité de fragment C3a libéré ainsi que la quantité de protéine C3 native résiduelle. Nous avons pu, par cette méthode, retrouver les mêmes comportements d'activation du complément des NPs modèles utilisées dans l'étude par µC-IE précédemment validée. Le principal avantage de la méthode SPR est sa rapidité et sa capacité à être totalement automatisée ne nécessitant aucune manipulation autre que de placer les échantillons à analyser dans l'appareil directement après l'étape d'incubation.

Le second avantage apporté par la SPR est la possibilité de détecter de façon indépendante plusieurs protéines lors de l'analyse d'un même échantillon. Les 4 canaux indépendants de la puce utilisées dans nos travaux rendent possible ce multiplexage. Dans ces travaux décrits dans le chapitre IV, les canaux de la puce ont été utilisés pour mesurer le signal non-spécifique (2 canaux) et pour mesurer le niveau des protéines C3a et C3 (2 canaux). Lors de ces travaux de thèse, d'autres études ont été menées pour détecter des fragments plus intimement liés à l'une des voies d'activation du complément. Des anticorps spécifiques du fragment C4d libéré lors de l'activation par les voies classique et lectine, du fragment Bb intervenant dans l'amplification de la voie alterne ainsi que du complexe soluble sC5b-9 formé dans la voie terminale de la cascade du complément ont été immobilisés sur la puce pour une détection par SPR (cf. Fig. 3). La puce ainsi constituée d'anticorps spécifiques dirigés contre les fragments

C3a, C4d, Bb et sC5b-9 permet à la fois une mesure globale de l'activation du complément par la détection du C3a et du complexe sC5b-9, mais aussi une identification de la voie d'activation prépondérante en mesurant la quantité de C4d et Bb libérés. Le récapitulatif des différents fragments identifiés par les méthodes SPR et µC-IE sont illustrés sur la figure 3 ci-dessous.

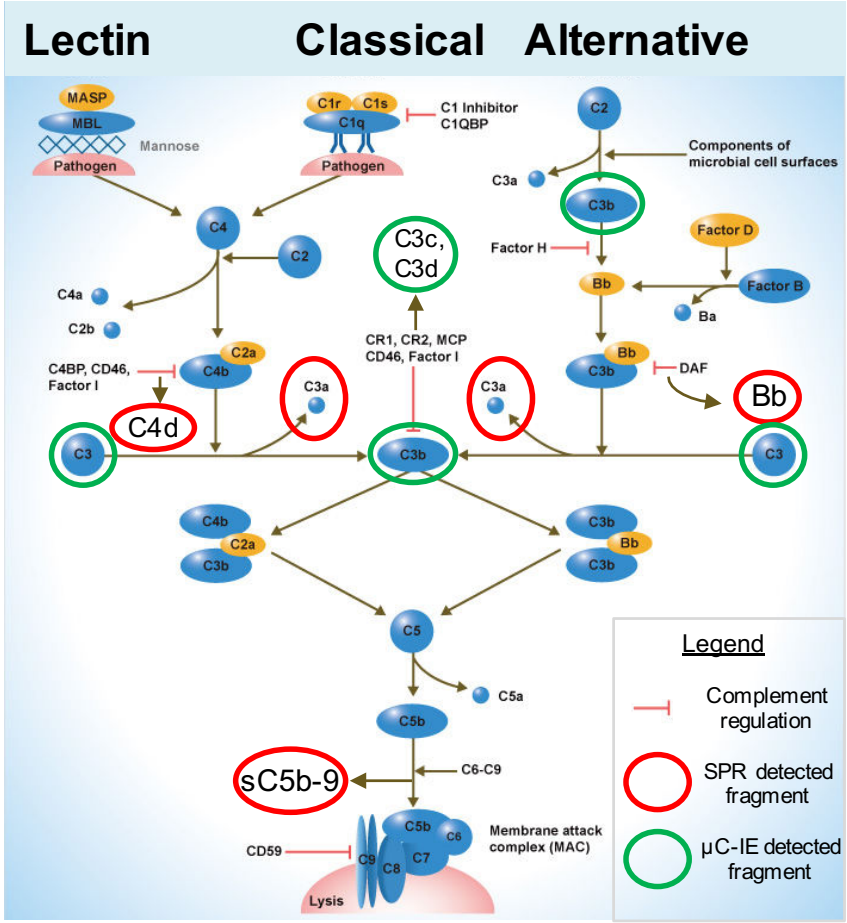

Figure 3 : identification des fragments de la cascade du complément détectés par les méthodes SPR et µC-IE *(adapté depuis http://www.sinobiological.com/Complement-Activation-Pathways-a-1511.html)*.

Cependant, les anticorps spécifiques des voies d'activation utilisés n'ont pas montré de réponse assez spécifique aux différents fragments ciblés (C4d, Bb et SC5b-9), masqués par une forte contribution du signal non-spécifique. Bien qu'étant garantis pour leur néo-spécificité contre les fragments correspondants, nous n'avons pu aboutir à des résultats suffisamment convaincants avec ces anticorps. D'autres études menées sur des anticorps spécifiques contre les fragments de la cascade du complément ont également spécifié le manque de spécificité de certains anticorps néo-spécifiques [29,30], qui sont pourtant utilisés dans des kits ELISA commercialisés. Ce comportement face au signal non-spécifique rejoint d'ailleurs celui

observé lors de l'utilisation du kit ELISA contre le fragment iC3b, pour la comparaison des méthodes d'évaluation de l'activation du complément dans le chapitre IV. Les résultats obtenus par ce kit montraient eux aussi un signal non-spécifique trop important pour permettre une interprétation satisfaisante des résultats. Une optimisation du type d'anticorps ou du sérum utilisé serait nécessaire afin d'aboutir à une puce permettant le diagnostic du niveau d'activation du complément ainsi que du mécanisme d'activation de façon simultanée. Nos travaux sur le développement de la méthode SPR ont permis de développer une puce évaluant de manière globale le phénomène d'activation du complément produit par les NMs. Cela s'est effectué en mesurant la baisse de la quantité de la protéine C3 détectée et l'apparition d'un fragment issu de cette protéine, le C3a.

La préparation de l'échantillon dans l'interaction NM-protéine

L'étude par SPR des conditions de préparation de l'échantillon avant analyse a également levé une interrogation sur la façon d'étudier l'activation du complément après incubation avec des NPs. Les résultats obtenus ici montrent que le retrait des NPs avant analyse peut biaiser la réponse finale en pouvant donner des résultats faussement négatifs. C'est l'un des inconvénients inhérents à l'analyse de l'activation du complément s'attachant à la détection d'un fragment spécifique. Ici, la protéine C3a a démontré une forte affinité pour certaines NPs testées. Le retrait de ces NPs s'est accompagné du retrait du fragment C3a, donnant ainsi une détection biaisée. Cette perte du fragment C3a adsorbé sur les NPs lors de l'étape de centrifugation a clairement été démontrée lors de nos travaux. L'incubation d'un sérum totalement activé, et contenant donc une forte quantité de C3a, avec nos NPs modèles, a montré une déplétion totale de la quantité de C3a entre l'analyse avant et après retrait des NPs. Ce mode d'étude visant à détecter spécifiquement un fragment de protéine est typiquement retrouvé dans le cas de la méthode ELISA. Pour remédier au possible biais inhérent à ce type de détection, il devient important de réaliser des détections sur différents fragments pour valider la cohérence des résultats et avoir une réponse plus robuste. C'est cette démarche qui a été entreprise avec la mise au point de la puce SPR multiplexée, donnant la possibilité de doser plusieurs protéines spécifiquement lors d'un même passage d'échantillon. L'atout de cette méthode résidait également dans la partie économique plus intéressante que l'ELISA. La µC-IE contourne ce biais en donnant une vision globale de l'état du C3 natif et de ses fragments. Nous avons alors plus d'information et de recul afin d'anticiper

ou comprendre un biais quelconque. Ces résultats obtenus en SPR soulignent que l'analyse des échantillons directe sans étape de séparation préalable est la plus fiable dans le cas de l'étude de l'activation du complément. La façon de préparer les échantillons avant analyse conditionne le résultat obtenu pour ce genre d'étude. Ce type de biais incite également à réaliser des contrôles supplémentaires pour vérifier l'innocuité de la présence de NMs ou des étapes de traitement de l'échantillon sur la réponse finale.

Lorsque l'on reprend l'exemple des tests ELISA pour la détection de fragments d'activation du complément après incubation avec des NMs, différentes façons de procéder sont revendiquées. Les protocoles fournisseurs de kits ELISA ainsi que les protocoles du NCL utilisant ces kits n'indiquent pas d'étape de retrait des NMs avant d'effectuer le test [31,32]. Cependant, des études décrites dans la littérature proposent des protocoles où l'étape de retrait des NMs avant évaluation par ELISA est indiquée [33,34]. Une standardisation de ce type de protocole est encore nécessaire aujourd'hui.

Dans l'étude d'autres interactions entre NMs et protéines comme la résolution de la protéine corona, cette étape de séparation est systématiquement appliquée sur les échantillons préalablement à l'analyse des protéines par LC-MS. Aujourd'hui, cette séparation est principalement réalisée par centrifugation/ultracentrifugation, chromatographie d'exclusion stérique (SEC) ou séparation magnétique dans le cas où la nature des NMs le permet. Avec ces méthodes, les équilibres peuvent être fortement perturbés d'un côté par le fait que l'on sépare les NMs de leur milieu d'équilibre, et d'autre part parce que les principes de séparation utilisés ont souvent un fort impact mécanique sur la surface des NMs (centrifugation, SEC) [35,36]. Ces méthodes s'accompagnent également d'une consommation de temps considérable. Des solutions moins perturbantes et moins consommatrices en temps tendent à apparaître mais restent pour l'instant spécifiques aux laboratoires où elles sont mises au point [37,38]. Les méthodes développées dans le cadre de cette thèse ont été conçues en contournant délibérément cette étape de séparation préalable des NMs, soit parce qu'elles ne nécessitaient pas cette étape de séparation avant analyse (SPR), soit en intégrant cette étape dans la méthode d'analyse en elle-même (µC-IE, EC).

Caractérisation de la surface réactive des nanomédecines

Un paramètre qu'il serait intéressant de déterminer pour la caractérisation de NMs est le recouvrement de leur surface par les chaines de polymère hydrophiles qui les constituent [39]. Ce paramètre joue un rôle important dans la sélection des protéines qui s'adsorbent sur la surface des NMs pour former la protéine corona, définissant l'identité biologique de la NM. Pouvoir appréhender cette propriété est devenu une priorité pour améliorer la compréhension des NMs quant à leur capacité à interagir de manière reproductible avec les protéines et ainsi garantir leur comportement *in vivo* [39]. Pour aborder la caractérisation de ce paramètre, nous avons proposé une méthode visant à étudier la réactivité de la surface des NMs vis à vis d'une série de protéines. Ces dernières ont été utilisées comme outils moléculaires pour sonder l'accessibilité de la surface des NMs.

En effet, la plupart des NMs développées actuellement sont destinées à l'administration par voie intraveineuse et sont conçues sur un modèle de structure cœur-couronne. Le greffage de macromolécules hydrophiles (PEG, polysaccharides) sur le cœur de la NM est la stratégie la plus répandue afin de conférer la propriété de furtivité au nanomatériau. Cette approche permet de réduire l'accessibilité aux protéines plasmatiques et notamment aux opsonines qui déclenchent la réponse immunitaire. Des études ont prouvé l'efficacité de ces revêtements [40,41]. Ce greffage n'empêche pas totalement le phénomène d'adsorption mais pourrait avoir un rôle dans la sélection des protéines pouvant s'adsorber. Des travaux récents suggèrent que l'architecture moléculaire de cette couronne de polymère joue un rôle dans la réactivité de cette surface vis à vis des protéines [24,41-43]. Dans la pratique, cette couverture polymère ainsi que sa conformation ne sont que très peu caractérisées faute de méthodes adaptées.

Le principe de la méthode que nous avons développé repose sur l'étude de l'adsorption d'une série de protéines de masse molaire différentes, dont les propriétés conformationnelles sont parfaitement définies. Cette méthode s'appuie sur un protocole en deux temps comprenant une incubation des NPs avec chaque protéine dans des conditions contrôlées, puis une analyse de la quantité de protéines adsorbée ne nécessitant aucun traitement préalable de l'échantillon, s'affranchissant des biais discutés précédemment. Pour réaliser ces analyses, nous avons développé des méthodes basées sur l'utilisation de l'électrophorèse capillaire (EC), une technique d'analyse de plus en plus souvent utilisée dans des études de l'interaction

NP-protéines [44-46]. La méthode repose sur l'hypothèse que la couronne formée par les chaines de polymères hydrophiles à la surface des NPs constitue un système de sélection des protéines adsorbées, basé principalement sur un effet d'exclusion stérique. Cette hypothèse s'appuie sur les résultats de travaux antérieurs qui ont montré que l'activation du système du complément par des NPs recouvertes d'une brosse épaisse de polymère hydrophile dépendait de la probabilité d'insertion de la protéine C3 dans cette brosse [47].

La méthode proposée dans le chapitre V a permis d'étudier de façon systématique l'adsorption de protéines de masses molaires différentes sur une nanoparticule donnée. Cela permet de dégager la capacité d'une NP à empêcher l'adsorption de certaines protéines relativement à leurs dimensions, donnant des informations sur l'efficacité de sa couverture polymère en surface. Les résultats montrent que le comportement d'adsorption des protéines ne varie pas de façon linéaire avec la masse molaire des différentes protéines testées, indiquant un phénomène plus complexe que la seule notion d'« effet bouclier » des chaines greffées en surface. Néanmoins, un effet excluant de certaines NPs pour des protéines de haute masse molaire a pu être mis en évidence. Des réponses différentes en termes de comportement d'adsorption ont en effet pu être corrélés aux différents niveaux de couverture de la surface des NPs utilisées comme modèles de travail. Les méthodes d'EC développées dans le cadre de ces travaux permettent l'analyse de l'adsorption de tous types de protéines, en utilisant les conditions adaptées au point isoélectrique de la protéine étudiée. Dans cette étude, une sélection de protéine a été faite sur des critères de disponibilités à grande échelle en vue d'une utilisation pour l'évaluation en routine de la réactivité de la surface des NMs. La démarche établie propose une méthode simple à implémenter pour une application systématique à la caractérisation de la surface des NMs.

Démarche des méthodes développées

Dans nos études, la taille des NPs utilisées (diamètre hydrodynamique (D_H) > 100 nm) est bien supérieure à celle des protéines testées (D_H < 15 nm). Il est important de remarquer ce point qui n'est que très peu commenté dans la littérature tandis que les interactions NMs-protéines relèvent de régimes totalement différents selon l'échelle de taille considérée. D'autres observations pourraient être rapportées avec des NPs dont la taille serait du même ordre de grandeur que les protéines. Les NPs modèles qui ont été utilisées pour le développement de nos méthodes sont de même nature chimique avec différentes configurations de surface

(brosse, boucle) et densités de greffage. La diversité des caractéristiques présentées par ces NPs nous a permis d'identifier les paramètres critiques influençant les différentes propriétés mesurées (activation du complément, accessibilité des protéines). Les méthodes développées nous ont permis d'approfondir cette connaissance des NPs du point de vue de leurs interactions avec les protéines de par la compréhension de phénomènes spécifiques. Cela a notamment été démontré lors d'étude de mécanisme d'activation du complément réalisé par µC-IE ou l'étude d'adsorption de protéines de différents poids moléculaires par EC. Ces méthodes ont également permis de contrôler plus précisément nos différentes synthèses de NPs en ajoutant aux paramètres actuellement contrôlés (taille, potentiel zêta, concentration), des paramètres relevant de leurs interactions avec les systèmes biologiques (activation du complément ($C3A_{50}$), propriétés d'adsorption de protéines données). Elles permettent de détecter des différences au niveau de l'architecture moléculaire des chaines hydrophiles de la couronne. Cela constitue une avancée dans la démarche adoptée dans le cadre de cette thèse, qui était d'apporter des solutions pour améliorer le contrôle qualité de lots de NMs et garantir une meilleure reproductibilité de leur action *in vivo*. Cette démarche est imagée dans la figure 4 ci-dessous.

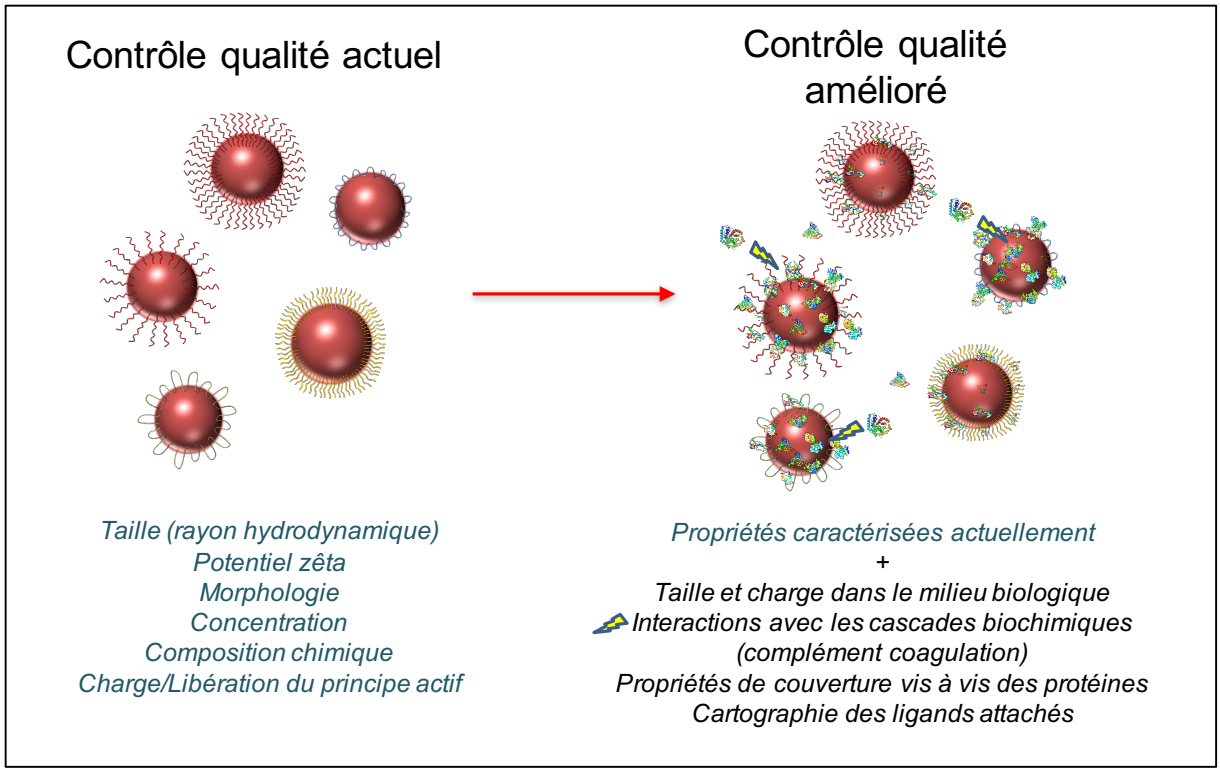

Figure 4: Démarche de contrôle qualité amélioré des nanomédecines. Exemples de paramètres déterminés.

En reprenant la problématique posée initialement sur les niveaux de caractérisation des NMs, ce contrôle qualité amélioré intègre de nouveaux paramètres physico-chimiques initiaux de la NM (x_i), comme la couverture des chaines de polymères recouvrant la NM ou la cartographie des ligands de ciblage greffés sur ces chaines. Cette démarche propose également d'intégrer des éléments de l'identité biologique (y_i) dans le contrôle qualité, afin de garantir directement la reproductibilité de certaines interactions avec les cascades biochimiques ou le changement des paramètres de taille et de potentiel zêta dans ces milieux. De plus, en développant l'analyse de nouveaux paramètres de l'identité initiale des NMs, ces derniers pourront être ajoutés aux propriétés intrinsèques de ces NMs (x_i), offrant une identité synthétique plus détaillée des NMs et améliorant ainsi la compréhension et la modélisation de leurs effets sur l'identité biologique (y_i).

Vision personnelle et perspectives

Les méthodes développées dans le cadre de cette thèse apportent des outils pour un meilleur contrôle et une meilleure compréhension des phénomènes intervenant après l'administration par voie intraveineuse de NMs. C'est un des leviers qui peut mener aux prochaines grandes avancées dans le domaine de la Nanomédecine, vers un meilleur contrôle de l'activité et la sécurité de ces nanovecteurs. Compte tenu des difficultés actuelles rencontrées pour une viabilité des NMs crées, de nouvelles stratégies émergent pour contourner ou mieux appréhender ces obstacles. La fin de cette discussion rend compte de stratégies qui pourraient être intéressantes de suivre pour surpasser les difficultés rencontrées actuellement.

Comme indiqué au début de cette discussion, une première partie importante consiste à comprendre la connexion entre propriétés synthétiques de la NM et interactions avec les éléments biologiques qui lui confèreront son identité biologique. Dans cette optique, l'idée du recrutement contrôlé de protéines spécifiques dans la protéine corona est aujourd'hui une stratégie qui commence à émerger [48,49]. Différentes protéines sont déjà connues pour avoir des effets sur le comportement des nanovecteurs dans l'organisme : la clusterine (ou apolipoprotéine J) a été identifiée comme un acteur principal de la furtivité des NMs [50,51], la transferrine dont les récepteurs sont surexprimés sur les cellules tumorales [52,53], ou encore l'apolipoprotéine E qui permet de franchir la barrière hématoencéphalique et cibler le système nerveux central [54-56]. Alors que des tentatives de greffage de protéines spécifiques avant administration ont été réalisées, elles sont le plus souvent altérées par l'adsorption de

protéines endogènes recouvrant les protéines greffées et altérant ainsi les capacités de ciblage espérées [57,58]. La prochaine étape est de synthétiser des NMs avec des propriétés surfaciques qui favorisent le recrutement de certaines protéines endogènes [59]. Par exemple, des lipoplexes ont montré un enrichissement de leur protéine corona en vitronectine, protéine dont les récepteurs sont surexprimés sur les cellules cancéreuses. Ces vecteurs ont montré un ciblage accru pour ces cellules en présence de leur protéine corona [60]. Plus récemment, Sobot *et al*. ont démontré le recrutement de lipoprotéines endogènes par des nanoparticules de squalène couplées à la gemcitabine, promouvant le ciblage des cellules cancéreuses [61]. La partie la plus complexe est de concevoir la NM avec les propriétés qui favoriseront l'adsorption de la protéine souhaitée avec l'effet escompté. Ce phénomène de ciblage par la protéine corona est cependant encore loin d'être une stratégie courante, étant fortement limité par la compréhension des phénomènes le gouvernant. Une illustration de ce fait est la démonstration de l'effet bénéfique de la protéine corona qui améliore la capture par les cellules cancéreuses d'une nanomédecine actuellement sur le marché (Onyvide®), sans que l'on sache quelle propriété intrinsèque de la NM ni quelle protéine de la corona induisent cet effet [62].

Il existe d'autres stratégies actuellement développées pour améliorer l'efficacité des NMs en contournant les limitations liées à la caractérisation et à la compréhension des interactions de NMs synthétiques dans les milieux biologiques. L'une d'entre elle consiste en l'utilisation d'éléments biomimétiques en guise de nanovecteurs [63]. Etant déjà connus par les systèmes biologiques, ces éléments ne posent à priori pas de problèmes de toxicité ou de biocompatibilité et leur comportement *in vivo* est déjà connu de par leur fonctionnement dans l'organisme. On lève alors deux principaux obstacles qui barrent pour l'instant le développement des NMs de synthèse : la toxicité et la compréhension de leur devenir *in vivo*. Le tout est de pouvoir utiliser un élément biologique qui corresponde à la fonction visée pour la problématique étudiée. Plusieurs exemples existent comme la fabrication des « leukosomes », qui sont des liposomes incluant dans leur bicouche lipidique des protéines membranaires retrouvées dans les membranes des leucocytes. Ces vecteurs, non reconnus par le système immunitaire, ont la capacité de cibler les tissus enflammés [64]. D'autres NPs utilisant la membrane d'érythrocytes ont récemment été développées montrant un ciblage accru de cellules tumorales [65]. Enfin, dans le même ordre d'idée, une stratégie de cheval de

Troie utilisant la membrane de plaquettes activées a été décrite. Des NPs de silice ont été recouvertes par cette membrane de plaquette conjuguée à des cytokines capables de tuer les cellules tumorales circulantes dans la circulation sanguine [66].

Toutes ces pistes développant de nouvelles stratégies de nanovecteurs prenant en compte les obstacles rencontrés *in vivo* sont très excitantes dans l'optique d'une amélioration significative de l'efficacité et de la sécurité des traitements par les nanomédecines. Elles sont la preuve d'un enthousiasme et d'une évolution dans la pensée et la conception des nanosystèmes depuis le concept de « magic bullet » [67]. La problématique de leur caractérisation restera cependant un souci majeur pour garantir la reproductibilité de leur comportement *in vivo* pour une utilisation clinique.

Références bibliographiques :

1) Aggarwal, P., Hall, J. B., McLeland, C. B., Dobrovolskaia, M. A. & McNeil, S. E. Nanoparticle interaction with plasma proteins as it relates to particle biodistribution, biocompatibility and therapeutic efficacy. *Advanced Drug Delivery Reviews* **61,** 428–437 (2009).
2) Walkey, C. D. & Chan, W. C. W. Understanding and controlling the interaction of nanomaterials with proteins in a physiological environment. *Chem. Soc. Rev.* **41,** 2780–2799 (2012).
3) Fadeel, B., Feliu, N., Vogt, C., Abdelmonem, A. M. & Parak, W. J. Bridge over troubled waters: understanding the synthetic and biological identities of engineered nanomaterials: Bridging nanotoxicology and nanomedicine. *Wiley Interdisciplinary Reviews: Nanomedicine and Nanobiotechnology* **5,** 111–129 (2013).
4) Caracciolo, G., Farokhzad, O. C. & Mahmoudi, M. Biological Identity of Nanoparticles In Vivo: Clinical Implications of the Protein Corona. *Trends in Biotechnology* **35,** 257–264 (2017).
5) Hadjidemetriou, M. & Kostarelos, K. Nanomedicine: Evolution of the nanoparticle corona. *Nature Nanotechnology* **12**, 288–290 (2017).
6) Pederzoli, F., Tosi, G., Vandelli, M. A., Belletti, D., Forni, F. & Ruozi, B. Protein corona and nanoparticles: how can we investigate on?: Protein corona and nanoparticles. *Wiley Interdisciplinary Reviews: Nanomedicine and Nanobiotechnology* e1467 (2017).
7) Bai, X., Liu, F., Liu, Y., Li, C., Wang, S., Zhou, H., Wang, W., Zhu, H., Winkler, D. A. & Yan, B. Toward a systematic exploration of nano-bio interactions. *Toxicology and Applied Pharmacology* **323,** 66–73 (2017).
8) Lynch, I., Afantitis, A., Leonis, G., Melagraki, G. & Valsami-Jones, E. in Advances in QSAR Modeling: Applications in Pharmaceutical, Chemical, Food, Agricultural and Environmental Sciences (ed. Roy, K.) 385–424 (Springer International Publishing, 2017).
9) Walkey, C. D., Olsen, J. B., Song, F., Liu, R., Guo, H., Olsen, D. W. H., Cohen, Y., Emili, A. & Chan, W. C. W. Protein Corona Fingerprinting Predicts the Cellular Interaction of Gold and Silver Nanoparticles. *ACS Nano* **8,** 2439–2455 (2014).
10) Desai, N. Challenges in Development of Nanoparticle-Based Therapeutics. *The AAPS Journal* **14,** 282–295 (2012).
11) Salvador Morales, C., Khorasani, A. A. & Weaver, J. Closing the gap: accelerating the translational process in nanomedicine by proposing standardized characterization techniques. *International Journal of Nanomedicine* 5729 (2014).
12) Agrahari, V. & Hiremath, P. Challenges associated and approaches for successful translation of nanomedicines into commercial products. *Nanomedicine* **12,** 819–823 (2017).
13) Merle, N. S., Noe, R., Halbwachs-Mecarelli, L., Fremeaux-Bacchi, V. & Roumenina, L. T. Complement System Part II: Role in Immunity. *Frontiers in Immunology* **6,** (2015).
14) Szebeni, J. Complement activation-related pseudoallergy: A new class of drug-induced acute immune toxicity. *Toxicology* **216,** 106–121 (2005).
15) Samuelsson, E., Shen, H., Blanco, E., Ferrari, M. & Wolfram, J. Contribution of Kupffer cells to liposome accumulation in the liver. *Colloids and Surfaces B: Biointerfaces* **158,** 356–362 (2017).
16) Bazile, D., Prud'homme, C., Bassoullet, M.-T., Marlard, M., Spenlehauer, G. & Veillard, M. Stealth Me. PEG-PLA nanoparticles avoid uptake by the mononuclear phagocytes system. *Journal of pharmaceutical sciences* **84,** 493–498 (1995).
17) Gref, R., Domb, A., Quellec, P., Blunk, T., Müller, R. H., Verbavatz, J. M. & Langer, R. The controlled intravenous delivery of drugs using PEG-coated sterically stabilized nanospheres. *Advanced Drug Delivery Reviews* **16,** 215–233 (1995).
18) Verrecchia, T., Spenlehauer, G., Bazile, D. V., Murry-Brelier, A., Archimbaud, Y. & Veillard, M. Non-stealth (poly (lactic acid/albumin)) and stealth (poly (lactic acid-polyethylene glycol)) nanoparticles as injectable drug carriers. *Journal of Controlled Release* **36,** 49–61 (1995).

19) Chanan-Khan, A. Complement activation following first exposure to pegylated liposomal doxorubicin (Doxil(R)): possible role in hypersensitivity reactions. *Annals of Oncology* **14,** 1430–1437 (2003).
20) Passirani, C., Barratt, G., Devissaguet, J.-P. & Labarre, D. Interactions of nanoparticles bearing heparin or dextran covalently bound to poly (methyl methacrylate) with the complement system. *Life sciences* **62,** 775–785 (1998).
21) Laurell, C.-B. Antigen-antibody crossed electrophoresis. *Analytical biochemistry* **10,** 358–361 (1965).
22) Rochu, D. & Fine, J.-M. Multiple crossed immunoelectrophoresis on agarosecoated GelBond film. *Electrophoresis* **6,** 388–391 (1985).
23) Coty, J.-B., Varenne, F., Vachon, J.-J. & Vauthier, C. Serial multiple crossed immunoelectrophoresis at a microscale: A stamp-sized 2D immunoanalysis of protein C3 activation caused by nanoparticles: Proteomics and 2-DE. *ELECTROPHORESIS* **37,** 2401–2409 (2016).
24) Coty, J.-B., Eleamen Oliveira, E. & Vauthier, C. Tuning complement activation and pathway through controlled molecular architecture of dextran chains in nanoparticle corona. *International Journal of Pharmaceutics* **532**, 769-778 (2017).
25) Marcelino, H.R., Coty, J.-B., Chéron, M., Vauthier, C., Egito, E.S.T. & Ponchel G. Amphotericin B and bovine serum albumin interactions: Physicochemical characterization and in vitro immunogenic activity. Article in preparation.
26) Nguyễn, C. H., Putaux, J.-L., Santoni, G., Tfaili, S., Fourmentin, S., Coty, J.-B., Choisnard, L., Gèze, A., Wouessidjewe, D., Barratt, G., Lesieur, S. & Legrand, F.-X. New nanoparticles obtained by co-assembly of amphiphilic cyclodextrins and nonlamellar single-chain lipids: Preparation and characterization. *International Journal of Pharmaceutics* **531**, 444-456 (2017).
27) Palácio, S.B, Taylor Sarahi, A.Y., Coty, J.-B., Egidy, G., Vauthier, C. & Ponchel, G. Functionalized Poly(γ-benzyl-L-glutamate)-PEG-Bt-MART-1 nanoparticles for melanoma targeting. Article in preparation.
28) Taylor Castillo, A.Y., Papagna, F., Coty, J.-B., Khoubai, F.Z., Vergnaud, J., Vauthier, C., Martinez Barbosa, M.E. & Ponchel, G. Rational designed Poly(γ-benzyl-L-glutamate) nanoparticles for nanomedicine applications in cancer treatment. Article in preparation.
29) Blom, A. M., Österborg, A., Mollnes, T. E. & Okroj, M. Antibodies reactive to cleaved sites in complement proteins enable highly specific measurement of soluble markers of complement activation. *Molecular Immunology* **66,** 164–170 (2015).
30) Bansal, R. Neoantibodies for diagnosing tissue injury. Patent WO2012075023A2. (2012).
31) Neun, B.W, Ilinskaya, A., & Dobrovolskaia, M.A. NCL Method ITA-5.2: Analysis of Complement Activation by EIA. https://ncl.cancer.gov/sites/default/files/protocols/NCL_Method_ITA-5.2.pdf (2015). *Consulted on August 2017*
32) An enzyme immunoassay for the quantitation of the C4d-containing fragments of activated C4 of the Classical Complement Pathway. https://www.quidel.com/sites/default/files/product/documents/a008_microvue_c4d_english.pdf (2009). *Consulted on August 2017*
33) Moghimi, S. M. & Hamad, I. Liposome-Mediated Triggering of Complement Cascade. *Journal of Liposome Research* **18,** 195–209 (2008).
34) Wibroe, P. P. & Moghimi, S. M. in *Functional Nanoparticles for Bioanalysis, Nanomedicine, and Bioelectronic Devices Volume 2* (eds. Hepel, M. & Zhong, C.-J.) **1113,** 365–382 (American Chemical Society, 2012).
35) Lundqvist, M., Augustsson, C., Lilja, M., Lundkvist, K., Dahlbäck, B., Linse, S. & Cedervall, T. The nanoparticle protein corona formed in human blood or human blood fractions. *PloS one* **12,** e0175871 (2017).
36) Pisani, C., Gaillard, J. C., Dorandeu, C., Charnay, C., Guari, Y., Chopineau, J., Devoisselle, J. M., Armengaud, J. & Prat, O. Experimental separation steps influence the protein content of corona around mesoporous silica nanoparticles. *Nanoscale* **9,** 5769–5772 (2017).
37) Ashby, J., Schachermeyer, S., Pan, S. & Zhong, W. Dissociation-Based Screening of Nanoparticle–Protein Interaction via Flow Field-Flow Fractionation. *Analytical Chemistry* **85,** 7494–7501 (2013).

38) Ibsen, S., Sonnenberg, A., Schutt, C., Mukthavaram, R., Yeh, Y., Ortac, I., Manouchehri, S., Kesari, S., Esener, S. & Heller, M. J. Recovery of Drug Delivery Nanoparticles from Human Plasma Using an Electrokinetic Platform Technology. *Small* **11,** 5088–5096 (2015).
39) Crist, R. & McNeil, S. Nanotechnology for Treating Cancer: Pitfalls and Bridges on the Path to Nanomedicines.https://www.cancer.gov/research/key-initiatives/ras/rascentral/blog/2015/nanomedicines (2015). *Consulted on August 2017*
40) Hong Du, H., Chandaroy, P., & Hui, S.W. Grafted poly-(ethylene glycol) on lipid surfaces inhibits protein adsorption and cell adhesion. *Biochima et Biophysica Acta (BBA) – Biomembranes* **1326(2)**, 236-248 (1997).
41) Walkey, C. D., Olsen, J. B., Guo, H., Emili, A. & Chan, W. C. W. Nanoparticle Size and Surface Chemistry Determine Serum Protein Adsorption and Macrophage Uptake. *Journal of the American Chemical Society* **134,** 2139–2147 (2012).
42) Hamad, I., Al-Hanbali, O., Hunter, A. C., Rutt, K. J., Andresen, T. L. & Moghimi, S. M. Distinct Polymer Architecture Mediates Switching of Complement Activation Pathways at the Nanosphere−Serum Interface: Implications for Stealth Nanoparticle Engineering. *ACS Nano* **4,** 6629–6638 (2010).
43) Lin, J., Zhang, H., Morovati, V. & Dargazany, R. PEGylation on mixed monolayer gold nanoparticles: Effect of grafting density, chain length, and surface curvature. *Journal of Colloid and Interface Science* **504,** 325–333 (2017).
44) Trapiella-Alfonso, L., Ramírez-García, G., d'Orlyé, F. & Varenne, A. Electromigration separation methodologies for the characterization of nanoparticles and the evaluation of their behaviour in biological systems. *TrAC Trends in Analytical Chemistry* **84,** 121–130 (2016).
45) Aleksenko, S. S., Matczuk, M. & Timerbaev, A. R. Characterization of interactions of metal-containing nanoparticles with biomolecules by CE: An update (2012-2016): Nanoanalysis. *ELECTROPHORESIS* **38,** 1661–1668 (2017).
46) Ramírez-García, G., d'Orlyé, F., Gutiérrez-Granados, S., Martínez-Alfaro, M., Mignet, N., Richard, C. & Varenne, A. Electrokinetic Hummel-Dreyer characterization of nanoparticle-plasma protein corona: The non-specific interactions between PEG-modified persistent luminescence nanoparticles and albumin. *Colloids and Surfaces B: Biointerfaces* **159,** 437–444 (2017).
47) Vauthier, C., Persson, B., Lindner, P. & Cabane, B. Protein adsorption and complement activation for di-block copolymer nanoparticles. *Biomaterials* **32,** 1646–1656 (2011).
48) Nguyen, V. H. & Lee, B.-J. Protein corona: a new approach for nanomedicine design. *International Journal of Nanomedicine* **Volume 12,** 3137–3151 (2017).
49) Müller, J., Bauer, K. N., Prozeller, D., Simon, J., Mailänder, V., Wurm, F. R., Winzen, S. & Landfester, K. Coating nanoparticles with tunable surfactants facilitates control over the protein corona. *Biomaterials* **115,** 1–8 (2017).
50) Schöttler, S., Becker, G., Winzen, S., Steinbach, T., Mohr, K., Landfester, K., Mailänder, V. & Wurm, F. R. Protein adsorption is required for stealth effect of poly(ethylene glycol)- and poly(phosphoester)-coated nanocarriers. *Nature Nanotechnology* **11,** 372–377 (2016).
51) Schöttler, S., Landfester, K. & Mailänder, V. Controlling the Stealth Effect of Nanocarriers through Understanding the Protein Corona. *Angewandte Chemie International Edition* **55,** 8806–8815 (2016).
52) Gatter, K. C., Brown, G., Trowbridge, I. S., Woolston, R. E. & Mason, D. Y. Transferrin receptors in human tissues: their distribution and possible clinical relevance. *Journal of Clinical Pathology* **36,** 539–545 (1983).
53) Tortorella, S. & Karagiannis, T. C. Transferrin Receptor-Mediated Endocytosis: A Useful Target for Cancer Therapy. *The Journal of Membrane Biology* **247,** 291–307 (2014).
54) Garcia-Garcia, E., Andrieux, K., Gil, S. & Couvreur, P. Colloidal carriers and blood–brain barrier (BBB) translocation: A way to deliver drugs to the brain? *International Journal of Pharmaceutics* **298,** 274–292 (2005).
55) Kim, H. R., Andrieux, K., Delomenie, C., Chacun, H., Appel, M., Desmaële, D., Taran, F., Georgin, D., Couvreur, P. & Taverna, M. Analysis of plasma protein adsorption onto PEGylated nanoparticles by

complementary methods: 2-DE, CE and Protein Lab-on-chip® system. *Electrophoresis* **28,** 2252–2261 (2007).
56) Wohlfart, S., Gelperina, S. & Kreuter, J. Transport of drugs across the blood–brain barrier by nanoparticles. *Journal of Controlled Release* **161,** 264–273 (2012).
57) Mirshafiee, V., Mahmoudi, M., Lou, K., Cheng, J. & Kraft, M. L. Protein corona significantly reduces active targeting yield. *Chemical Communications* **49,** 2557 (2013).
58) Salvati, A., Pitek, A. S., Monopoli, M. P., Prapainop, K., Bombelli, F. B., Hristov, D. R., Kelly, P. M., Åberg, C., Mahon, E. & Dawson, K. A. Transferrin-functionalized nanoparticles lose their targeting capabilities when a biomolecule corona adsorbs on the surface. *Nature Nanotechnology* **8,** 137–143 (2013).
59) Caracciolo, G. Liposome–protein corona in a physiological environment: Challenges and opportunities for targeted delivery of nanomedicines. *Nanomedicine: Nanotechnology, Biology and Medicine* **11,** 543–557 (2015).
60) Caracciolo, G., Cardarelli, F., Pozzi, D., Salomone, F., Maccari, G., Bardi, G., Capriotti, A. L., Cavaliere, C., Papi, M. & Laganà, A. Selective Targeting Capability Acquired with a Protein Corona Adsorbed on the Surface of 1,2-Dioleoyl-3-trimethylammonium Propane/DNA Nanoparticles. *ACS Applied Materials & Interfaces* **5,** 13171–13179 (2013).
61) Sobot, D., Mura, S., Yesylevskyy, S. O., Dalbin, L., Cayre, F., Bort, G., Mougin, J., Desmaële, D., Lepetre-Mouelhi, S., Pieters, G., Andreiuk, B., Klymchenko, A. S., Paul, J.-L., Ramseyer, C. & Couvreur, P. Conjugation of squalene to gemcitabine as unique approach exploiting endogenous lipoproteins for drug delivery. *Nature Communications* **8,** 15678 (2017).
62) Papi, M., Caputo, D., Palmieri, V., Coppola, R., Palchetti, S., Bugli, F., Martini, C., Digiacomo, L., Pozzi, D. & Caracciolo, G. Clinically approved PEGylated nanoparticles are covered by a protein corona that boosts the uptake by cancer cells. *Nanoscale* **9,** 10327–10334 (2017).
63) Yoo, J.-W., Irvine, D. J., Discher, D. E. & Mitragotri, S. Bio-inspired, bioengineered and biomimetic drug delivery carriers. *Nature Reviews Drug Discovery* **10,** 521–535 (2011).
64) Molinaro, R., Corbo, C., Martinez, J. O., Taraballi, F., Evangelopoulos, M., Minardi, S., Yazdi, I. K., Zhao, P., De Rosa, E., Sherman, M. B., De Vita, A., Toledano Furman, N. E., Wang, X., Parodi, A. & Tasciotti, E. Biomimetic proteolipid vesicles for targeting inflamed tissues. *Nature Materials* **15,** 1037–1046 (2016).
65) Rao, L., Meng, Q.-F., Bu, L.-L., Cai, B., Huang, Q., Sun, Z.-J., Zhang, W.-F., Li, A., Guo, S.-S., Liu, W., Wang, T.-H. & Zhao, X.-Z. Erythrocyte Membrane-Coated Upconversion Nanoparticles with Minimal Protein Adsorption for Enhanced Tumor Imaging. *ACS Applied Materials & Interfaces* **9,** 2159–2168 (2017).
66) Li, J., Ai, Y., Wang, L., Bu, P., Sharkey, C. C., Wu, Q., Wun, B., Roy, S., Shen, X. & King, M. R. Targeted drug delivery to circulating tumor cells via platelet membrane-functionalized particles. *Biomaterials* **76,** 52–65 (2016).
67) Strebhardt, K. & Ullrich, A. Paul Ehrlich's magic bullet concept: 100 years of progress. *Nature Reviews Cancer* **8,** 473–480 (2008).

Summary of the General discussion

Numerous efforts are being made for a better characterization and understanding of the relations between synthetic identity, biological identity and physiological outcomes of nanomedicines (NMs) (cf. Figures 1 and 2). In this thesis, we focused on the development of methods for a better control of synthetic nanomaterials and of their interactions with blood proteins.

First, we could identify through a bibliographic study of current NMs characterization a lack of precision of current methods used to control nanomaterials (cf. Chapter I). When compared to the sharpness of biological systems, current properties of NMs characterized on a daily basis are not fine enough to ensure a reproducibility of interactions with biological components. We thus developed methods to improve this characterization following two main orientations: methods for the study of complement activation triggered by NMs and a method to characterize the surface coverage of NMs using proteins.

The complement system is known to be of importance for NMs safety and efficacy, as it can completely modify the biodistribution and the stealthiness of the NM. However, today the tendency of a NM batch to activate the complement system is not assessed on a daily basis, due to the complexity of existing method or the cost associated to these methods.

We thus developed methods that could make easier the routine analysis of complement activation by NMs. A known method of bidimensional immunoelectrophoresis has been totally renovated for a use at a higher throughput and requiring less manipulations. A system of serial migration of samples in both first and second dimensions of electrophoresis was optimized: the MultiCrossed-immunoelectrophoresis (µC-IE) (cf. Chapter II). The novel method allows for the analysis of up to 35 samples in 6 hours. It opens new possibilities of characterization such as the determination of the amount of NMs necessary to cleave 50% of the native C3 protein ($C3A_{50}$) or for deeper studies to elucidate which pathways are involved in complement activation (cf. Chapter III). This method has also been used in collaborative studies applied to different kind of nanosystems (cf. refs [25-28]).

Then, the potential of surface plasmon resonance (SPR) has been explored for an automated and multiplexed assessment of complement activation by NMs. The possibility to investigate the level of different complement fragments at the same time has been explored (cf. Figure 3). This would be a possibility of choice when controlling complement activation and resolving the complement pathway at the same time. Non-specific binding interactions hampered the development of this ideal chip. However, consistent results with those found with the previously mentioned µC-IE method were found when working on C3 and C3a fragments. Moreover, a possible bias on the evaluation of complement activation related to sample preparation (here, centrifugation and NM removal) has been demonstrated from analyses performed with the SPR method (cf. Chapter IV).

Finally, a method assessing the level of surface coverage provided by polymer chains composing NMs' shell was developed. This method, using capillary electrophoresis (CE), used selected proteins as molecular tools to probe the surface of nanomaterials. The capacity of a NM to repel proteins has thus been explored through the determination of the amount of adsorbed proteins. The method was challenged with five polymer nanoparticles (NPs) for which the surface coverage characteristics were already known. The method could distinguish two kinds of surface coverage among our model NPs. Those bearing dense brushes on their surface were able to repel more efficiently proteins of larger size, while NPs with loops or loose grafting were more accessible to proteins. This CE method offers the advantages to realise an *in situ* separation between NMs and proteins, without the need for preliminary sample treatment prior to anlaysis. This method that uses standardized conditions is also applicable on a routine basis and can be automated.

The methods developed in this thesis could be used to control the quality of our differents NPs batches, added to conventional determination of size and zeta potential. The introduction of the control of their interaction with biological elements could be an approach to expand in routine quality control of NMs clinical batches (cf. Figure 4). In parallel, a more systematic and precise characterization of such interactions will increase our knowledge about NPs and their interactions with proteins. These new information are certainly helpful for the development of better predictive models.

As it tends to emerge from the world of Nanomedicine, I think that next step for NMs success in real life is possible at the expense of an improved comprehension of phenomenon occurring

after administration. The black box of what is happening *in vivo* needs to be rip opened, notably through the development of a better characterization of NMs.

In parallel, new approaches that take into account these difficulties directly into the conception of the NMs are developed. The rational design of nanocarrier able to recruit specific endogen proteins in their protein corona are emerging. As the role of some protein have been evidenced to influence the biodistribution (Apo-E to the brain, transferrin to tumor cells), some systems able to enrich their protein corona in such proteins were designed [60,61]. Also, the use of biomimetic vectors is under development. Nanocarriers made of lipids bilayers containing leucocyte transmembrane proteins were developed (leukosomes [64]), others were covered of erythrocytes or platelets membranes to act as Trojan horses [65,66].

All these strategies trying to deal with natural obstacles found in vivo are the proof of a constant evolution and questioning of nanomedicine field. They are exciting in the perspective of future nanomedicine achievements. The matter of their characterization will nonetheless remain a major concern for their safety and efficacy reproducibility.

Conclusion générale

The characterization of nanomedicines (NMs) has been pointed out as one of the main barrier for a higher success of their clinical translation. While discrete changes of NMs properties are accurately detected by biological systems, current characterization methods are much less precise and these slight modifications are often unperceived. For NMs destined to an intravenous injection, it is known that the contact with blood proteins will dictate their *in vivo* behavior. On one hand, the raw comprehension of the becoming of the nanomedicine *in vivo* has to be improved, starting from a better knowledge of its pristine properties. On the other hand, today's methods used for the daily characterization of NMs to ensure batches reproducibility are poorly sensitive. Current controlled properties prior to clinical use are largely insufficient, but awaited improvements are pending to the introduction of new methods providing sharper information about the NM. The aim of the thesis was to develop methods that could help filling this gap and provide methods allowing a more precise routine characterization of nanomedicines.

First, the interactions of NMs with proteins of the complement system were studied in this work. An immunoelectrophoresis method was renovated to improve the throughput and accessibility of this method. The new method considerably increased the number of samples to be analyzed while reducing the manipulation complexity and time. The method was also validated for its robustness and precision. These improvements allowed for new studies of complement activation by nanoparticles, notably with the creation of the $C3A_{50}$ indicator which reflects the capacity of a NM to trigger the complement cascade. Another study was done to explore the mechanistic pathways triggered regarding the molecular architecture of tested nanoparticles. This study showed that this parameter was of paramount importance, governing the interactions between complement proteins and nanoparticle's surface. This method was also used in collaborative studies to assess the complement activation behavior of various nanosystems.

Then, surface plasmon resonance (SPR) was employed to study the complement system activation by NMs. This technique was selected for its capacity to automatize analysis and allow for a straightforward detection of complement fragments. Conditions of flow, antibodies' immobilization on the chip, regenerations steps and sample preparation were optimized to give quality results. The non-specific binding, which is SPR Achill's heel, has been mastered in our study. The complement activation behaviors of model nanoparticles found

with the developed chip were consistent with those defined by the previously mentioned immunoelectrophoresis method. This method proved to be reproducible and become a possible tool for an automated assessment of complement activation in routine. The potential for further multiplexing of detected fragments shows high promises for the simultaneous detection of up to four complement fragments at the same time. Finally, this method allowed to detect a bias in sample preparation when nanoparticles were removed before analysis, alerting from the necessity to check every procedure step when dealing with NMs and protein detection.

Finally, a novel approach for probing the NM surface architecture was developed. A capillary electrophoresis method allowed to study separately the adsorption of nine proteins on different model nanoparticles. These proteins, used as molecular probes were well defined in terms of size and spatial structure. This work showed that such a surface screening could allow for a discrimination in the NM surface coverage by assessing the efficacy of the hydrophilic chain grafted on its surface. This parameter is of importance since it is now appearing that polymer shell around NP core has the role to select the adsorption of proteins in the bloodstream rather than fully block protein adsorption. This capillary electrophoresis method allowed to class our model nanoparticles for their adsorption behavior. Results confirmed that dense brushes grafting were better for prevent adsorption of high molecular weight proteins. Besides, these results were further compared with complement activation behaviors and showed that previously made hypotheses could be supported by this study. The accessibility and automatable character of the capillary electrophoresis put this method as a possible candidate for the screening of NM surface coverage properties.

The approach followed in this thesis brings an opening for a sharper characterization of nanomedicines regarding their interactions with blood proteins. The wish of improved throughput and methods accessibility was a primordial criterion in our method development. The interests of the developed method not only lie in the new knowledge they bring about NM properties and interactions with blood proteins, but also in their possibility to be included in a procedure of quality control to ensure a better reproducibility of NMs' safety and efficacy between different batches.

Annexes méthodologiques

Annexe 1 : Principe de l'immunoélectrophorèse bidimensionnelle

L'immunoélectrophorèse bidimensionnelle (ou immunoélectrophorèse croisée) est une méthode combinant les principes de l'électrophorèse simple et de la méthode d'immunoélectrophorèse de Laurell [1]. Cette méthode permet une analyse semi quantitative d'antigènes d'intérêt dans un mélange complexe.

Comme son nom l'indique, cette méthode s'effectue en deux étapes. Elle consiste à séparer dans un premier temps dans un gel d'agarose des protéines selon leur poids moléculaire et leur densité de charge (cf Fig. 1A). La majorité des protéines étant chargées négativement au pH d'électrophorèse (pH : 7-8), la séparation s'effectue généralement selon le poids moléculaire, laissant les protéines les plus petites migrer plus rapidement que les protéines de haut poids moléculaire.

Dans un second temps, ces protéines vont migrer dans un second gel d'agarose contenant un anticorps spécifique dirigé contre la ou les protéine(s) d'intérêt (cf. Fig. 1B). Cela va aboutir à la formation de complexes antigènes-anticorps et à l'apparition de fusées de précipitation. La hauteur, et donc l'aire, de ces fusées, sont proportionnelles à la quantité d'antigène initialement présent dans l'échantillon.

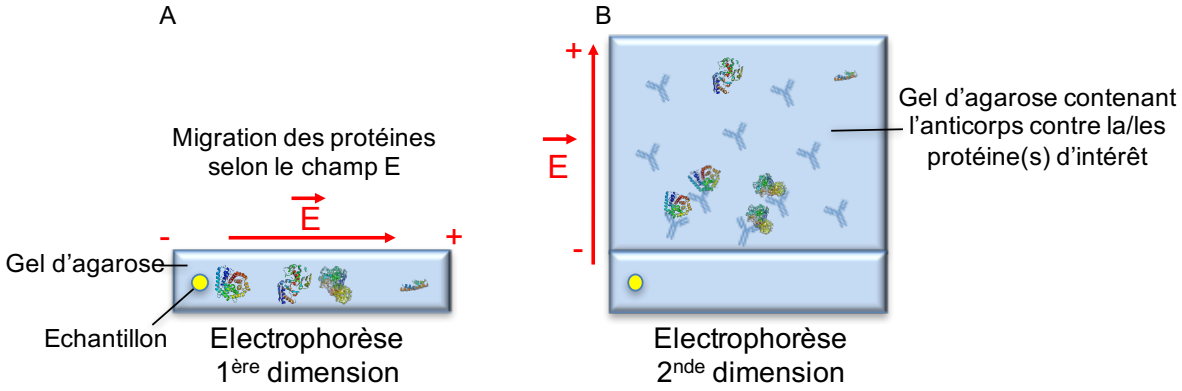

Figure 1: Principe de l'immunoélectrophorèse bidimensionnelle. A: principe de la première dimension séparant les protéines selon leur MW et charge, B: principe de la seconde dimension où les protéines spécifiques sont précipités par l'anticorps incorporé dans le gel en formant des complexes antigènes-Anticorps.

Cette méthode est adaptée à la détection de protéines d'intérêt dans des mélanges complexes grâce à la sélectivité apportée par la présence d'anticorps spécifiques dans le gel de seconde dimension. Dans le cas de notre méthode pour la détection de protéines du complément, le gel de seconde dimension contient un anticorps polyclonal dirigé contre la protéine C3. Il reconnaît donc la protéine C3 native ainsi que ses fragments de haut poids moléculaires (C3b, C3c) (cf.Fig. 2).

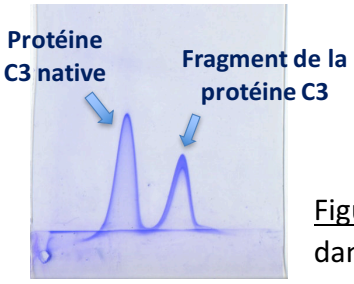

Figure 2: Exemple d'électrophorégramme obtenu dans le cas de la détection de la protéine C3.

[1] Laurell, C. B., *Anal. Biochem.* 1965, *10*, 358–361.

Annexe 2 : Principe de l'électrophorèse capillaire

L'électrophorèse capillaire (EC) est une technique permettant la séparation d'entités sous l'effet d'un champ électrique selon leur mobilités respectives. Cette méthode reprend le principe de l'électrophorèse traditionnelle en remplaçant le support gel par un électrolyte dans un tube capillaire. La détection des analytes s'effectue peu avant la sortie de capillaire, le plus souvent par UV ou fluorescence. L'EC permet entre autres de réduire la consommation des échantillons et réactifs, réduire le temps d'analyse, améliorer la résolution de séparation et faciliter la manipulation par rapport à l'électrophorèse sur gel.

La migration des entités introduites dans l'EC est soumise à deux phénomènes : l'électroosmose et l'électromigration.

L'électroosmose, caractérisée par le flux électroosmotique (FEO), correspond à la force d'entrainement créée par l'écoulement de l'électrolyte dans le capillaire. Ce FEO est dû à la présence de charges à la surface du capillaire (charges négatives dans le cas du capillaire de silice) qui entraine la formation d'une double-couche de contre ions (ici cations) de l'électrolyte proche de cette surface. Lors de l'application du champ électrique, les cations de la couche diffuse vont migrer vers la cathode, ce qui va entrainer un mouvement de tous les composés présents dans le capillaire vers ce pôle, c'est l'électroosmose. Ce phénomène est d'intensité égale pour tous les composés se trouvant dans le capillaire, qui vont donc avoir une certaine valeur de mobilité électroosmotique (µEO).

Le deuxième phénomène régissant la migration des entités dans le capillaire est l'électromigration. Cette composante résulte du déplacement d'une espèce chargée sous l'application d'un champ électrique. C'est l'équivalent du phénomène de migration d'espèces chargées utilisé en électrophorèse classique. L'électromigration est fonction de la charge et du rayon hydrodynamique propres à chaque entité, qui définissent sa valeur de mobilité électrophorétique (µEP).

En électrophorèse capillaire de zone (ECZ), mode utilisé dans ces travaux, la migration des entités s'effectue selon leur rapport charge/rayon hydrodynamique dans un électrolyte de pH et force ionique constants. La migration s'effectue selon la combinaison des phénomènes d'électroosmose et d'électromigration. Chaque entité est caractérisée par ce que l'on appelle une mobilité apparente (µapp), avec µapp = µEO + µEP. Le principe général de la migration par ECZ est illustré sur la figure 1 en page suivante.

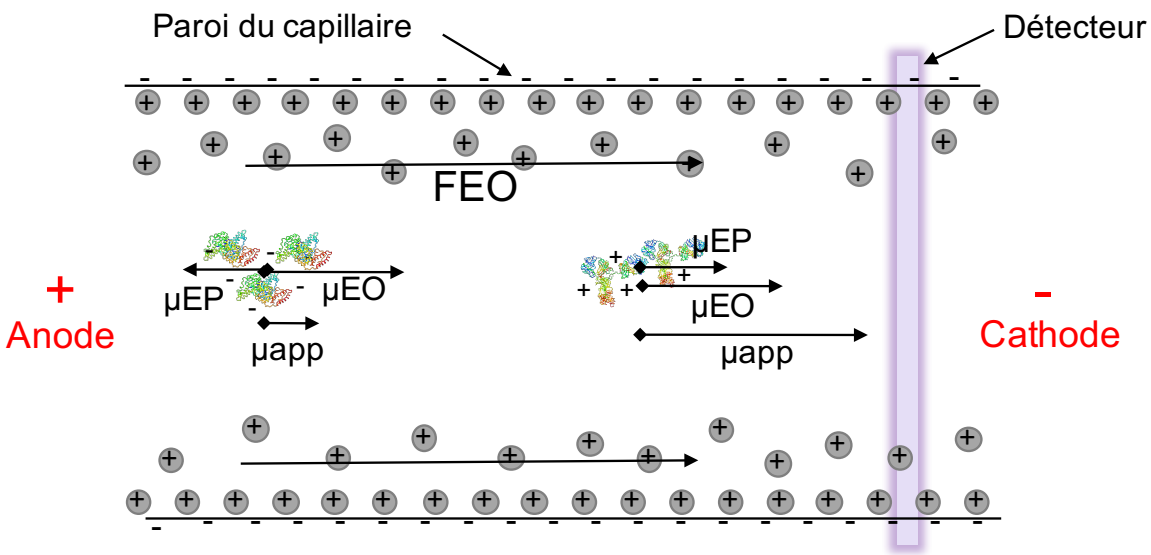

Figure 1: Principe de la migration d'entités chargées par ECZ. Cas d'un capillaire de silice (FEO : Flux électroosmotique ; μEP : mobilité électrophorétique ; μEO : mobilité électroosmotique ; μapp : mobilité apparente).

Dans le cas de la séparation de deux protéines de charges différentes comme illustré sur la figure 1, le type d'électrophorégramme obtenu est représenté sur la figure 2.

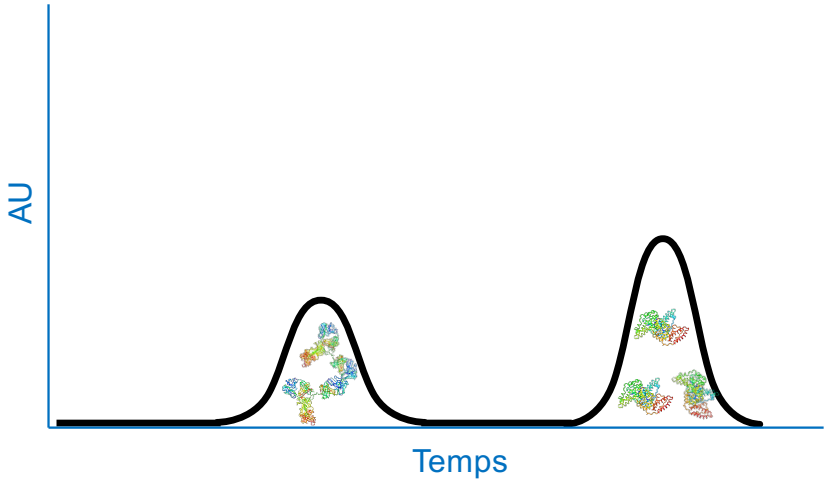

Figure 2: exemple d'électrophorégramme obtenu pour la séparation de deux protéines par ECZ (AU : Unité arbitraire).

Annexe 3 : Principe de la résonance plasmonique de surface

La résonance plasmonique de surface (SPR) est une technique utilisée pour détecter l'interaction survenant entre un récepteur immobilisé sur une surface métallique et un ligand s'adsorbant sur ce récepteur. La variation de l'angle de résonance plasmonique en fonction du temps permet la visualisation des interactions en temps réel sans marquage des molécules. Cette méthode est généralement utilisée pour étudier les interactions de cinétique ou d'affinités entre biomolécules.

La surface métallique utilisée est souvent une fine couche d'or, riche en électrons libres. Le déplacement de ces électrons à la surface du métal aboutit à la propagation d'ondes oscillantes appelées plasmons. En pratique, un rayon lumineux de longueur d'onde donnée est envoyé vers cette surface métallique. A une valeur critique de l'angle d'incidence, la réflexion du rayon est totale et on observe la propagation d'une onde évanescente dans la surface métallique, capable d'entrer en résonance avec l'onde du plasmon de surface. L'énergie absorbée par le plasmon de surface conduit à une diminution de l'intensité de l'onde réfléchie. L'angle qui correspond à ce minimum d'intensité réfléchie est appelé angle de résonance plasmonique [1].

Lors de la fixation d'un ligand sur un récepteur greffé sur la surface métallique, l'indice de réfraction de cette dernière va changer et donner lieu à une modification de la valeur de l'angle de résonnance plasmonique (cf Fig. 1). Plus la quantité de ligand accrochée sur la surface est élevée, plus la variation de l'angle de résonance est importante.

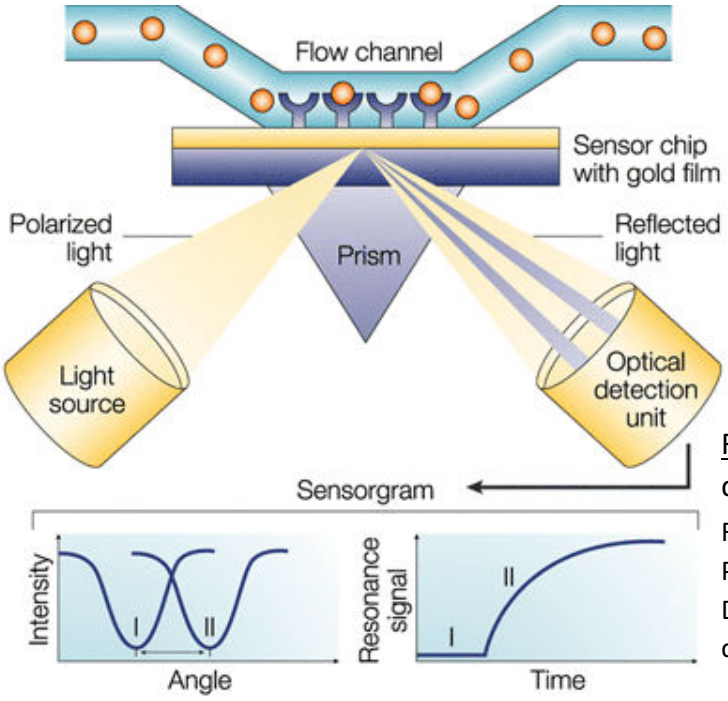

Figure 1: Principe général de la détection SPR.

Reproduit avec autorisation de Macmillan Publishers Ltd: Nature Reviews Drug Discovery 1, 515-528 (July 2002) | doi:10.1038/nrd838. copyright 2002.

[1] Sébastien Laurent. Détections d'interactions biologiques par imagerie de résonance plasmonique de surface : applications au criblage pharmaceutique de chimiothèques & à la détection de toxines. Biotechnologie. Université Joseph-Fourier - Grenoble I, 2007. Français. <tel-00731249v1>

Annexe 4 : Introduction au système du complément

Le système du complément est le principal acteur de la réponse humorale du système immunitaire. Il est composé d'un ensemble de protéines se trouvant dans le plasma sanguin et dont l'activation fonctionne en une cascade de réactions biochimiques. L'activation de cette cascade est généralement produite par l'interaction de protéines sanguines appelées opsonines, avec le corps étranger. Cela conduit, dans le cas des nanoparticules, à l'opsonisation de ces dernières, déclenchant une cascade de réactions biochimiques. L'agent étranger ainsi reconnu est marqué par des fragments protéiques qui favoriseront sa clairance par les cellules du système reticulo-endothélial (e.g. macrophages). Dans le cas des nanomédecines (NMs), une reconnaissance par le système du complément peut entrainer des réactions brutales d'hyper-allergie, menaçant la santé du patient, mais aussi biaiser le temps de circulation et la biodistribution des NMs. Une façon de doser ce degré de reconnaissance des NMs par le système immunitaire est de déterminer la quantité de protéine C3 clivée, cette protéine étant au coeur de la cascade du complément (cf. Figure 1).

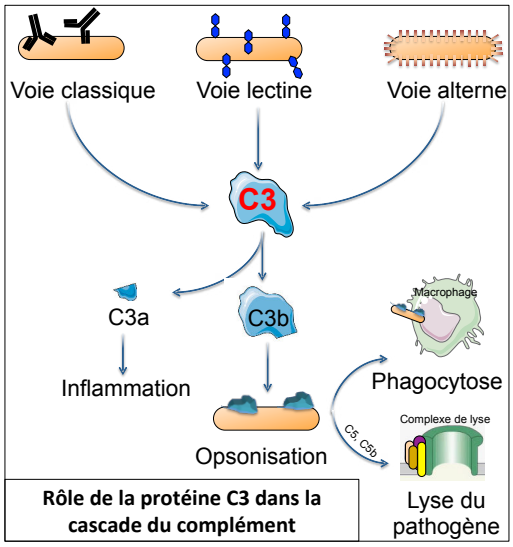

Figure 1: schéma simplifié de la cascade d'activation du complément soulignant le rôle central de la protéine C3.

Aujourd'hui, trois voies d'activation sont connues. La voie classique est déclenchée par l'interaction du module de reconnaissance C1q avec des complex immuns formés en surface de l'agent pathogène. La voie alterne est déclenchée par l'attachement de fragments résiduels de la protéine C3 à la surface de l'agent étranger. Enfin la voie lectine intervient suite à la reconnaissance de certains motifs carbohydrates à la surface du système par la mannose-binding lectine (MBL) [1].

Les conséquences de l'activation sont multiples, allant de réactions inflammatoires par la libération d'anaphylatoxines, jusqu'à la formation du complexe de lyse pour éliminer les agents présentant une membrane lipidique, et le marquage des entités pour leur prise en charge par les cellules phagocytaires. D'autres implications dans la reponse immunitaire adaptative sont maintenant reconnues [2].

[1] Merle, N. S., Church, S. E., Fremeaux-Bacchi, V. & Roumenina, L. T. Complement System Part I: Molecular Mechanisms of Activation and Regulation. *Frontiers in Immunology* **6,** (2015).
[2] Merle, N. S., Noe, R., Halbwachs-Mecarelli, L., Fremeaux-Bacchi, V. & Roumenina, L. T. Complement System Part II: Role in Immunity. *Frontiers in Immunology* **6,** (2015).

Annexe bibliographique

G Model
IJP 16822 No. of Pages 13

ARTICLE IN PRESS

International Journal of Pharmaceutics xxx (2017) xxx–xxx

Contents lists available at ScienceDirect

International Journal of Pharmaceutics

journal homepage: www.elsevier.com/locate/ijpharm

New nanoparticles obtained by co-assembly of amphiphilic cyclodextrins and nonlamellar single-chain lipids: Preparation and characterization

Cảnh Hưng Nguyễn[a,1], Jean-Luc Putaux[b], Gianluca Santoni[c], Sana Tfaili[d], Sophie Fourmentin[e], Jean-Baptiste Coty[a], Luc Choisnard[f], Annabelle Gèze[f], Denis Wouessidjewe[f], Gillian Barratt[a], Sylviane Lesieur[a], François-Xavier Legrand[a,*]

[a] Institut Galien Paris-Sud, CNRS UMR 8612, Univ. Paris-Sud, Université Paris-Saclay, 5 rue Jean-Baptiste Clément, F-92290 Châtenay-Malabry, France
[b] Centre de Recherches sur les Macromolécules Végétales, CNRS UPR 5301, Univ. Grenoble Alpes, BP 53, F-38401 Grenoble Cedex 9, France
[c] European Synchrotron Radiation Facility, 71 avenue des Martyrs, F-38000 Grenoble, France
[d] Lip(Sys)^2, EA 7357, Chimie Analytique Pharmaceutique, Univ. Paris-Sud, Université Paris-Saclay, 5 rue Jean-Baptiste Clément, F-92290 Châtenay-Malabry, France
[e] Unité de Chimie Environnementale et Interactions sur le Vivant, EA 4492, SFR Condorcet FR CNRS 3417, Université Littoral Côte d'Opale, 145 avenue Maurice Schumann, F-59140 Dunkerque, France
[f] Département de Pharmacochimie Moléculaire, CNRS UMR 5063, Univ. Grenoble Alpes, F-38000 Grenoble, France

ARTICLE INFO

Article history:
Received 10 April 2017
Received in revised form 30 June 2017
Accepted 2 July 2017
Available online xxx

Keywords:
Amphiphilic cyclodextrin
Monoolein
Nanoparticles
Small-angle X-ray scattering
Transmission electron microscopy
Complement activation

ABSTRACT

This work aimed at preparing new nanoscale assemblies based on an amphiphilic bio-esterified β-cyclodextrin (β-CD), substituted at the secondary face with *n*-decanoic fatty acid chains (β-CD-C_{10}), and monoolein (MO) as new carriers for parenteral drug delivery. Stable binary (β-CD-C_{10}/MO) and ternary (β-CD-C_{10}/MO/stabilizer) nanoscale assemblies close to 100 nm in size were successfully prepared in water by the solvent displacement method. The generated nanoparticles were fully characterized by dynamic light scattering, transmission electron microscopy, small-angle X-ray scattering, residual solvent analysis, complement activation and the contribution of each formulation parameter was determined by principal component analysis. The β-CD-C_{10} units were shown to self-organize into nanoparticles with a hexagonal supramolecular packing that was significantly modulated by the molar ratio of the constituents and the presence of a steric or electrostatic stabilizer (DOPE-PEG_{2000} or DOPA/POPA, respectively). Indeed, nanoparticles differing in morphology and in hexagonal lattice parameters were obtained while the co-existence of multiple mesophases was observed in some formulations, in particular for the β-CD-C_{10}/MO/DOPA and β-CD-C_{10}/MO/POPA systems. The mixed β-CD-C_{10}/MO/DOPE-PEG_{2000} nanoparticles (49:49:2 in mol%) appeared to be the most suitable for use as a drug delivery system since they contained a very low amount of residual solvent and showed a low level of complement C3 activation.

© 2017 Elsevier B.V. All rights reserved.

1. Introduction

Non-lamellar liquid crystalline phases formed by lyotropic lipids are particularly attractive for the formulation of active pharmaceutical ingredients because of their unique structure of lipid assembly interpenetrated with nanoscale water channels that provide multiple compartments for the efficient loading and sustained release of hydrophilic, lipophilic or amphiphilic molecules (Guo et al., 2010; Kulkarni, 2012). In recent years, nano-assemblies generated from these phases, referred to as ISAsomes (Internally Self-Assembled "somes" or particles), and in particular cubosomes and hexosomes, have been increasingly investigated as

Abbreviations: β-CD-C_{10}, β-cyclodextrin *n*-decanoic ester; MO, monoolein; DOPE-PEG_{2000}, ammonium salt of 1,2-dioleoyl-*sn-glycero*-3-phosphoethanolamine-*N*-[methoxy(polyethylene glycol)-2000]; DOPA, sodium salt of 1,2-dioleoyl-*sn-glycero*-3-phosphate; POPA, sodium salt of 1-palmitoyl-2-oleoyl-*sn-glycero*-3-phosphate.

* Corresponding author.
E-mail address: francois-xavier.legrand@u-psud.fr (F.-X. Legrand).
[1] Present address: Department of Pharmaceutics, Hanoi University of Pharmacy, Hanoi, Vietnam.

http://dx.doi.org/10.1016/j.ijpharm.2017.07.007
0378-5173/© 2017 Elsevier B.V. All rights reserved.

Please cite this article in press as: C.E.A.H.B. Nguy n, et al., New nanoparticles obtained by co-assembly of amphiphilic cyclodextrins and nonlamellar single-chain lipids: Preparation and characterization, Int J Pharmaceut (2017), http://dx.doi.org/10.1016/j.ijpharm.2017.07.007

promising alternatives to other lipid-based drug nanocarriers such as liposomes or lipid nanoparticles (Azmi et al., 2015; Ganem-Quintanar et al., 2000; Guo et al., 2010; Milak and Zimmer, 2015; Mulet et al., 2013; Shah et al., 2001). The majority of these studies have chosen 1-oleylglycerol or monoolein as the main component. Monoolein is indeed a versatile lyotropic lipid since it forms different mesophases in water, the topology of which can vary as a function of hydration and temperature to include lamellar, bicontinuous cubic and hexagonal molecular packings whose lattice parameters can be adapted to incorporate co-lipids or other guest molecules. As a result of this reverse bicontinuous cubic phases consisting of a highly twisted lipid bilayer delimiting two non-intersecting water channels, these nano-assemblies can accommodate a wide range of therapeutic substances varying in water solubility and molecular mass, from traditional active molecules to biological macromolecules, notably peptides and proteins (Boyd et al., 2007; Chen et al., 2012; Lee et al., 2009; Peng et al., 2010; Rizwan et al., 2010; Wyatt and Dorschel, 1992; Zhen et al., 2012). In the same way, inverse hexagonal phases based on monoolein organized as juxtaposed cylindrical aqueous cores delimited by lipid monolayer shells have been attracting increasing attention for the delivery of drugs (Duttagupta et al., 2016; Guo et al., 2010; Meli et al., 2017). The particular interest of these liquid crystalline mesophases lies in the fact that their hierarchical nanostructure can determine the release kinetics and bioavailability of drugs while protecting them and reducing their toxicity. Effective sustained release and improvement of oral or topical absorption of incorporated hydrophilic model drugs have been clearly demonstrated in vitro and in vivo (Boyd et al., 2007; Guo et al., 2010; Lopes et al., 2006; Meli et al., 2017; Nazaruk et al., 2015; Peng et al., 2010; Rizwan et al., 2010; Wyatt and Dorschel, 1992; Zhen et al., 2012).

Most studies conducted to date have focused on the use of non-lamellar lipid mesophases for oral or topical administration rather than for parenteral routes, due to the rather high viscosity of the formulations (Milak and Zimmer, 2015; Shah et al., 2001). As far as intravenous administration is concerned, some modifications have to be made to the formulation. Most importantly, the mesophases must be dispersed as particles with a size in the submicron range and furthermore be stabilized so as to have long-circulating properties in the cardiovascular system. Nanoscale cubosome or hexosome formulations have been tested over the last twenty years and special efforts have been made to ensure that they retain a stable colloidal state in physiological fluids (Guo et al., 2010; Guo et al., 2010; Mulet at al., 2013). Steric stabilization by hydrophilic polymer coating has been preferred to electrostatic stabilization since rapid elimination of charged nanoparticles from the systemic circulation as a result of complement activation has been reported (Fraser et al., 2013; Han et al., 2010; Hartnett et al., 2014; Lindell et al., 1998). However, the introduction of polymer stabilizers such as amphiphilic triblock copolymers based on ethylene oxide or poly(ethylene glycol)-grafted lipids can induce structural changes that can modify the encapsulation yields and release processes of drugs (Cervin et al., 2009; Johnsson et al., 2006; Zeng et al., 2012).

Furthermore, the reduced size of the mesophase dispersions significantly increases the surface area of the particles in direct contact with the external dispersion medium, increasing the risk of both reduced drug loading efficiency and loss of sustained release action. To address these issues, the addition of components able to reinforce the nanoporosity of ISAsomes while preserving their original liquid crystalline state can be envisaged. An attractive possibility is to use hollow deep vase-like building blocks based on cyclodextrins (CDs): cyclic oligosaccharides able to form host-guest inclusion complexes with a wide range of hydrophobic compounds (Kfoury et al., 2015; Uzqueda et al., 2009). CDs are already in use for some pharmaceutical applications, mainly to enhance bioavailability and stability of drugs and to reduce some of their undesirable properties such as volatility and taste. Nanoscale CD assemblies for multi-drug delivery have been developed from amphiphilic derivatives that have been synthesized by enzymatic transesterification with long-chain fatty acids on hydroxyl groups at one or both faces of the native CDs (Choisnard et al., 2011). These bio-esterified CD molecules can self-assemble or be incorporated into lipid-based reverse cubic mesophases, playing the role of structural stabilizer while their cavity enhances the incorporation yield of hydrophobic substances, as demonstrated by a recent study (Zerkoune et al., 2016). More precisely, nanodispersions composed of monoolein, polysorbate-80 and a bio-transesterified CD with C10 chains grafted mostly on the secondary face (referred to as β-CD-C_{10}) with a total degree of substitution (TDS) of 7.3 were formed by hydration of a three-component film in excess water followed by sonication. Small-angle X-ray scattering (SAXS) characterization revealed that, in the absence of the amphiphilic CD, no inner ordered structure was observed while, in contrast, the presence of 4 mol% β-CD-C_{10} induced reverse cubic molecular packing. Moreover, it was shown that the CD-containing nanostructures could entrap up to 94% of the hydrophobic Oil Red model molecule (Zerkoune et al., 2016).

Following on from these promising results, the present work focuses on the preparation, and characterization of mixed β-CD-C_{10}/monoolein nanoscale assemblies, and their evaluation as drug carriers for parenteral administration. For this purpose, nanodispersions with or without steric stabilizers were prepared by the well-known solvent displacement method, while accurately monitoring the amount of residual solvent using appropriate techniques. Systematic investigations were undertaken to determine the influence of the composition on the feasibility of forming mesoporous nano-objects in isotonic media with a well-defined size distribution as well as on the structural variability of their inner molecular organization. Furthermore, the interaction of the multicompartment nanoscale systems prepared by this method with blood components was examined in detail to predict their systemic behavior.

2. Material and methods

2.1. Materials

The β-CD-C_{10} amphiphilic cyclodextrin (MM = 2293.7 g mol^{-1}; TDS = 7.5) was synthesized by an enzymatically-assisted pathway using thermolysin as catalyzer and decanoic vinyl esters (C_{10}) as acyl donors (Choisnard et al., 2006, 2007). It was obtained as a white powder which was analyzed by matrix-assisted laser desorption/ionization mass spectroscopy (MALDI-MS) to determine the mean molecular mass and the mean substitution degree of the batch (Choisnard et al., 2011). Monoolein (MO) was obtained from Sigma-Aldrich at its highest purity and was used without any recrystallization. The ammonium salt of 1,2-dioleoyl-*sn-glycero*-3-phosphoethanolamine-N-[methoxy(polyethylene glycol)-2000] (DOPE-PEG_{2000}) and sodium salts of 1,2-dioleoyl-*sn-glycero*-3-phosphate (DOPA) or of 1-palmitoyl-2-oleoyl-*sn-glycero*-3-phosphate (POPA) were purchased from Avanti Polar Lipids. Anhydrous organic solvents (HPLC grade) were purchased from Carlo-Erba and used without further purification. Ultrapure water (γ = 72.2 mN. m^{-1} at 22 °C, resistivity 18.2 MΩ·cm) was produced by a Millipore Milli-Q Direct 8 water purification system and sterile isotonic 5% glucose aqueous solution was purchased from C.D.M. Lavoisier.

2.2. Nanoparticle preparation

The nanoparticle suspensions were prepared using the solvent displacement technique. Five milligrams of amphiphilic

compounds (at the desired molar proportions of the various compounds) were dissolved in 2.5 mL of anhydrous acetone in the case of β-CD-C_{10}, MO/β-CD-C_{10} and MO/β-CD-C_{10}/DOPE-PEG_{2000} nanoparticles or in 2.5 mL of anhydrous THF in the case of MO/β-CD-C_{10}/DOPA and MO/β-CD-C_{10}/POPA nanoparticles, at a final concentration of 2 mg mL^{-1}. Two milliliters of this solution were slowly added into 5 mL of ultrapure water (or 5 mL of 1% glucose aqueous solution) under magnetic stirring (1000 rpm). Nanoparticles were formed spontaneously and the colloidal suspension was submitted to evaporation under reduced pressure to remove the organic solvent. To ensure that the majority of the organic solvent was removed, the suspension was concentrated at 40 °C under vacuum down to a final aqueous volume equal to 20% of initial aqueous volume. All suspensions were stored at 4 °C until further investigation.

2.3. Quantification of residual solvent

The amount of residual organic solvents in each nanoparticle preparation was thoroughly investigated by Static-Headspace Gas Chromatography (SH-GC). Aliquots of each preparation (100 μL) were added to 10 mL of water in a 22-mL headspace glass vial. The vials were then sealed with a silicone septa and aluminum foil and maintained at 25.0 ± 0.1 °C. After 1 h of equilibration, solvents were analyzed with a G1888 Agilent headspace autosampler coupled to a Perkin Elmer Autosystem XL equipped with a flame ionization detector using a DB624 column. The temperature conditions were set as follows: detector temperature, 280 °C; column temperature, 40 °C for 8 min; carrier gas, nitrogen. The amount of residual acetone or THF was determined using a calibration curve.

2.4. Dynamic light scattering (DLS)

The hydrodynamic diameter (d_H) distribution of the nanoparticles was determined at 25 °C by DLS using a Zetasizer Nano ZS90 (Malvern Instruments) operating at a fixed scattered angle of 90° and equipped with a Helium-Neon laser source of wavelength of 633 nm. Measurements were performed in macrocuvettes with 1-cm optical pathway and four optical faces (Sarstedt) containing an appropriate volume (1 mL) of sample, prepared as described above, after dilution to 0.8 mg mL^{-1}. The d_H values were calculated using the Stokes-Einstein equation assuming a spherical shape of the nanoparticles. The nanoparticle size profile was obtained from the intensity-weighted distribution and corresponded to the median diameter derived from the cumulative distribution curve. The polydispersity index (PI) was deduced from cumulant analysis. All measurements were performed in triplicate. Values are given as mean values of three measurements.

2.5. Small-angle X-ray scattering (SAXS)

SAXS experiments were performed on the BioSAXS beamline BM29 (Pernot et al., 2013) at the European Synchrotron Radiation Facility (ESRF, Grenoble, France) using the standard automated setup for high throughput solution studies (Round et al., 2015). A few microliters of samples were injected via an automated sample exchanger at a slow and very reproducible flow rate into a quartz capillary (1.8 mm internal diameter), which was then placed in front of the X-ray beam. The quartz capillary was enclosed in a vacuum chamber, in order to avoid parasitic scattering. All samples were analyzed at 20.0 ± 0.1 °C using a lipid concentration of 4 mg mL^{-1} to avoid multiple scattering artifacts in the scattering pattern, with background buffer measurements before and after each sample. All data were collected at 12.5 keV, corresponding to a wavelength of 0.0992 nm, with a sample-to-detector distance of 2.867 m. For each sample, 30 successive time frames with 1 s exposure were acquired using a Pilatus 1 M detector in the scattering vector q-range $0.04 < q < 5\ nm^{-1}$. In addition, the sample was streamed through the beam to make sure that no part of sample was overexposed. The dedicated beamline software BsxCuBe was used for data collection and processing (radial averaging and q-conversion of the normalized 2D data) was performed using EDNA (Brennich et al., 2016). The detector q-axis was calibrated using the diffraction pattern of silver behenate and the scattering of pure water was used to calibrate the intensity to absolute units. Sample scattering intensity was normalized with respect to the incident beam decay and acquisition time. SAXS profiles are shown as the intensity function $q = 4\pi\sin(\theta)/\lambda$, where 2θ is the scattering angle and λ the wavelength of the incident beam.

2.6. Transmission electron microscopy (TEM)

Drops of dilute nanoparticle suspensions were deposited onto freshly glow-discharged carbon-coated Cu/Pd grids. The specimens were negatively stained with 2 wt% uranyl acetate or Uranyless™ (Delta Microscopies) and observed with a Philips CM200 microscope (FEI) operating at 200 kV. Images were recorded with a TemCam F216 (TVIPS) camera.

With the exception of the preparations in which the nanoparticles were highly aggregated, deformed or with too complex shapes (formulations 11, 13 and 14), the particle size distribution was determined from TEM images using the Image J software and calculating the average diameter of up to 500 spheroidal particles (350 in the case of formulation 7). Number-weighted mean diameter ($d_{1,0}$), number-weighted median diameter (d_{TEM}), volume-weighted mean diameter ($d_{4,3}$), intensity-weighted mean diameter, also referred to as harmonic z-average diameter ($d_{6,5}$), and polydispersity index were calculated from the particle size distributions as described in Schmiele et al. (2016) (Supporting information, Table S2), $d_{1,0}$, $d_{4,3}$ and $d_{6,5}$ were calculated using the formula $d_{k,l} = \left(\frac{\sum n_i \cdot d_i^k}{\sum n_i \cdot d_i^l}\right)^{\frac{1}{k-l}}$. For a few formulations (1, 5, 6 and 7) exhibiting a distinct population of barrel-shaped particles, the average length, width and aspect ratio (length-to-width ratio) were determined as well.

2.7. Differential scanning calorimetry (DSC)

DSC experiments were carried out using a Perkin-Elmer DSC Diamond apparatus equipped with a Intracooler 2P cooling device and connected to a Pyris Thermal Analysis Software System (version 9.1). The calorimeter was calibrated as described in IUPAC recommendations (Della Gatta et al., 2006). The samples (hydrated at 90% w/w with pure water), in the range of 14–17 mg, were accurately weighed and hermetically sealed into 50 μL aluminum pans (pan, part BO143017 and cover, part BO143003); an empty pan was used as a reference. The samples were cooled from 14 to −14 °C in the case of DOPA and from 35 to 5 °C for POPA at a constant rate, $|dT/dt| = 5\ °C\ min^{-1}$ and heated from −14 to 14 °C in the case of DOPA or from 5 to 35 °C for POPA at different rates, $dT/dt = 2$, 3, 4 and 5 °C min^{-1}. The first scan was preceded by a 10 min isotherm at 25 °C to allow the samples to reach thermal equilibrium. All the transitions were found to be reversible and reproducible in the repeated scans. The transition temperatures were taken at the onset of the transitions (T_{onset}) i.e., the intersection of the tangent to the left side of the endothermic peak with the baseline. The end temperature (T_{end}), corresponding to the completion of transition, was also reported. This temperature was taken at the intercept of the baseline with the tangent to the right-hand side of the heating curve. To eliminate the effects of

the heating rate on the temperature, determinations were carried out at different rates, and the temperature was extrapolated to a zero rate. The transition enthalpy was determined from the area under the peaks and normalized by the phospholipid content. To calculate the area under the peak, a baseline connecting the linear segments of the heat capacity curve between the onset and endpoint of the transition was subtracted.

2.8. Evaluation of complement protein C3 activation

The method of multi-crossed 2D immunoelectrophoresis (μC-IE) described by Coty et al. (2016) was employed to evaluate the cleavage of complement protein C3. Briefly, the nanoparticle preparations (50 μL) were incubated with human serum (25 μL) in Veronal Buffered Saline (VBS^{2+}, 25 μL) for 1 h at 37 °C, followed by rapid cooling to 4 °C in an ice bath for immediate analysis by μC-IE.

An agarose gel at 1% containing a polyclonal anti-C3 antibody (goat, Fitzgerald) was prepared in Tricine buffer (1 mM Calcium Lactate, 63 mM Tris, 27 mM Tricine, in milliQ® water, pH 8.6) and then cast on a Gel-Fix™ film. Bands of gel were cut and filled with 1% agarose gel prepared in Tricine buffer for the 1st dimension. Wells were formed at the same time using a homemade comb. The gel was placed in Multiphor II electrophoresis system (GE Healthcare, Velizy-Villacoublay, France) and the wells were filled with 2.5 μL of sample. The samples were then subjected to the first-dimension electrophoresis (600 V, 16 mA, 100 W, 75 min), migrating freely in the agarose gel band according to their molecular weight. Then, the gel was rotated through a 90° angle to proceed with the second-dimension rocket immunoelectrophoresis (500 V, 12 mA, 100 W, 3 h 30 min). Gels were dried and stained with Coomassie brilliant blue. The gels were numerically scanned and the area under the peaks was integrated using ImageJ software. The first peak on the left side was identified as native C3 while the second peak from the left was attributed to protein fragments derived from C3 cleavage. Percentage activation was calculated as the ratio of the surface area of the peak of the cleaved protein fragments to that of the sum of the surface areas of the peaks corresponding to native C3 and the fragments. This ratio was then normalized on a scale ranging from 0 to 100 in which 100 indicated total activation and 0 the spontaneous activation, measured in absence of nanoparticles.

2.9. Principal component analysis (PCA)

PCA was carried out for the 14 formulations and the 14 variables (Supporting information, Table S3) using Simca P+ software (version 12.0.1.0). Prior to analysis, our data set was centered and normalized. The variation of each variable was centered so that the mean of each column was equal to 0 and scaled to the unit variance 1/(standard deviation).

3. Results and discussion

All the studies described in the present work were carried out by using the same batch of amphiphilic β-cyclodextrin (β-CD-C_{10}) synthesized by enzymatic transesterification with *n*-decanoic vinyl esters (C_{10}) as acyl donors and characterized by a degree of substitution of 7.5 ± 0.8, the C_{10} hydrocarbon chains being almost entirely attached to the secondary hydroxyl groups. This confers a skirt-like shape to the molecule that predisposes it for mesoscopic self-assembling properties in aqueous media (Choisnard et al., 2006, 2007, 2011; Gèze et al., 2007). Previous results have demonstrated that β-CD-C_{10} can form a mixed reverse cubic mesophase at 4 mol% ratio in association with monoolein (91 mol %) and polysorbate-80 (5 mol%) that can be dispersed as cubosomes by sonication (Zerkoune et al., 2016). Here, we have explored a wider range of compositions in order to optimize the incorporation level of β-CD-C_{10}. Furthermore, we have developed an alternative preparation protocol by solvent displacement with a view to future scale-up. Preliminary experiments aimed at obtaining stable nano-assemblies using the methodology of Zerkoune et al. (2016) with isotonic buffered solutions as the aqueous phase resulted in particle aggregation (results not shown). Therefore, stabilizing additives other than polysorbate-80 were evaluated: the poly(ethylene glycol)-grafted phospholipid DOPE-PEG_{2000} that has already been shown to stabilize lipid-based nanocarriers in blood (Che et al., 2015; Dos Santos et al., 2007), and anionic phospholipids, DOPA or POPA, that can act as physical stabilizers to prevent particle aggregation (Bozzuto and Molinari, 2015; Crommelin, 1984).

Several series of samples were prepared in order to determine the best proportions of MO, β-CD-C_{10} and stabilizer. In particular, the maximum β-CD-C_{10} loading that could yield stable nano-objects with well-defined internal structure was determined. For comparison, preparations made from β-CD-C_{10} alone or in binary mixtures with MO were also studied. A previous screening of operational conditions has shown that smaller and monodisperse β-CD-C_{10} nano-assemblies could be obtained by solvent displacement when acetone was used as the organic phase, with acetone-to-water volume ratios lower than 1 giving optimal production yields (Choisnard et al., 2005, 2006). Therefore, when possible, all the preparations were made by using acetone as the organic solvent, with a total concentration of 2 mg mL^{-1} of nanoparticle components and an acetone-to-aqueous-phase volume ratio of 0.4. Under these conditions, in all cases, a colloidal dispersion was formed immediately upon slow addition of the organic solution into water and remained stable when the acetone was removed by evaporation under reduced pressure. The amount of residual acetone was determined for all the samples. Moreover, all dispersions were analyzed in parallel by DLS and TEM in order to obtain complementary information about the shape, size and

Table 1
Properties of β-CD-C_{10} and binary β-CD-C_{10}/MO nanoparticles.

Formulation	MO (mol%)	CD (mol%)	d_H (nm)[a]	PI[b]	d_{TEM} (nm)[c]	$d_{6,5}$ (nm)[d]	RS ($g.L^{-1}$)[e]	a_{hex} (nm)[f]	C3b (%)[g]
1	–	100	80 ± 35	0.214	68 ± 18	93	1.1	4.39 ± 0.03	19
2	25.0	75.0	93 ± 26	0.079	75 ± 18	101	0.4	4.48 ± 0.02	13
3	50.0	50.0	92 ± 24	0.070	75 ± 16	96	2.4	4.52 ± 0.01	12
4	75.0	25.0	91 ± 21	0.055	74 ± 15	97	1.5	4.58 ± 0.02	17

[a] Intensity-weighted median hydrodynamic diameter (DLS).
[b] Polydispersity index (DLS).
[c] Number-weighted median diameter for spheroidal particles (TEM).
[d] Harmonic *z*-average diameter for spheroidal particles (TEM).
[e] Residual content of acetone.
[f] Hexagonal lattice structure parameter.
[g] Activation of C3 protein.

Please cite this article in press as: C.E.A.H.B. Nguy n, et al., New nanoparticles obtained by co-assembly of amphiphilic cyclodextrins and nonlamellar single-chain lipids: Preparation and characterization, Int J Pharmaceut (2017), http://dx.doi.org/10.1016/j.ijpharm.2017.07.007

size distribution of the nanoparticles. However, the results obtained with the two techniques have to be compared with care. While DLS data are collected from a large number of particles in suspension, TEM images only show a limited number of particles (with possible drying/staining artefacts) which may not represent the whole suspension faithfully. On the other hand, TEM provides useful information about anisometric particle shape that is not taken into account in the DLS analysis. This may affect the result when populations of particles with different shapes coexist in suspension. In addition, in polydisperse suspensions, the method of preparation of negatively stained TEM specimens may influence the relative number of particles with different sizes, while DLS may give more weight to large particles with respect to smaller ones in the statistical analysis.

3.1. β-CD-C_{10} and binary β-CD-C_{10}/MO nano-assemblies

Nanoprecipitation in water of the β-CD-C_{10} alone in acetone solution produced nanoparticles with a mean hydrodynamic diameter d_h close to 80 nm. The addition of MO at 25.0, 50.0 and 75.0 mol% also allowed nanoparticles to be formed. However, the d_h values slightly increased up to about 90 nm while the polydispersity indexes dramatically decreased with increasing MO content (Table 1). It is remarkable that, despite extensive rotary evaporation, residual acetone ranging from 0.4 to 2.4 g L^{-1} was found in all the samples and was probably entrapped within the nanoparticles. TEM images of negatively stained preparations (Fig. 1) reveal that the β-CD-C_{10} suspension contains a mixture of spheroidal and barrel-like nanoparticles in agreement with previous observations (Fig. 1a) (Gèze et al., 2009; Putaux et al., 2017; Yameogo et al., 2012) and that the addition of MO, whatever the concentration, did not significantly change the particle shape distribution (Fig. 1b–d). For spheroidal nanoparticles, number-weighted median diameters were calculated from the size distributions obtained from a series of low-magnification TEM images. As the diameter determined by DLS is an intensity-weighted median hydrodynamic diameter and that obtained by TEM is a number-weighted median diameter, it is difficult to directly compare the values obtained with the two techniques, which depend on different physical properties of the particles. For a more reliable comparison, harmonic *z*-average diameters that can be considered as intensity-weighted diameters were calculated from the TEM size distributions. In the case of β-CD-C_{10} nanoparticles, an average aspect ratio could be calculated by measuring the length and width of 100 nanoparticles and was equal to about 2.0.

The internal structure of the different batches of β-CD-C_{10} or β-CD-C_{10}/MO nanoparticles was investigated by SAXS using synchrotron radiation. The scattering intensity profile recorded from MO-free nanoparticles (Fig. 2, curve 1) is in agreement with the form factor of three-dimensional assemblies of finite submicronic size for which the Bragg reflections are superimposed, indicating an inner periodic structure of these assemblies. No oscillation is visible on the SAXS profile, confirming the high polydispersity for these nanoparticles. The Kratky plot $q^2.I(q)$ versus q (Supporting information, Fig. S1) reveals a bell shape typical of globular particles with a q value at the maximum of the curve $q_{max} = 0.0478\ nm^{-1}$. Moreover, in the larger q-region that corresponds to the right-hand side of the Kratky bell-shaped curve ($q > 0.1\ nm^{-1}$, Supporting information, Fig. S1), the scattering intensity decreases as q^{-4} according to ideal Porod behavior for individual globular structures with a solvent-accessible smooth surface. By assuming a spherical geometry of the particles, the q_{max} value gives to an estimate of the particle radius of 36 nm as deduced from the pseudo-Guinier radius $R_g = \sqrt{3}/q_{max}$.. This result is in good agreement with the mean hydrodynamic radius of 40 ± 3 nm determined by DLS, considering that the SAXS analysis determines the geometric size while the DLS measurement

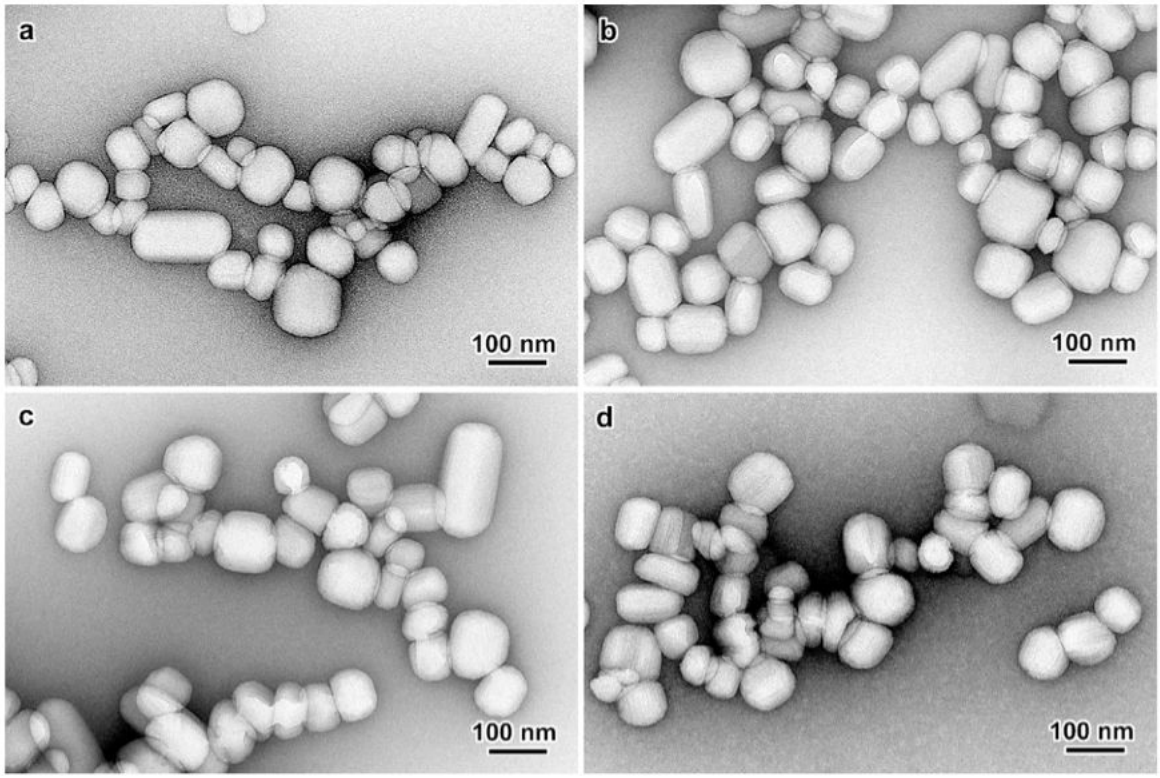

Fig. 1. TEM images of negatively stained nanoparticles prepared from amphiphilic β-cyclodextrin β-CD-C_{10} with different molar proportions of monoolein: (a) formulation 1 (0 mol%), (b) formulation 2 (25.0 mol%), (c) formulation 3 (50.0 mol%) and (d) formulation 4 (75.0 mol%).

Please cite this article in press as: C.E.A.H.B. Nguy n, et al., New nanoparticles obtained by co-assembly of amphiphilic cyclodextrins and nonlamellar single-chain lipids: Preparation and characterization, Int J Pharmaceut (2017), http://dx.doi.org/10.1016/j.ijpharm.2017.07.007

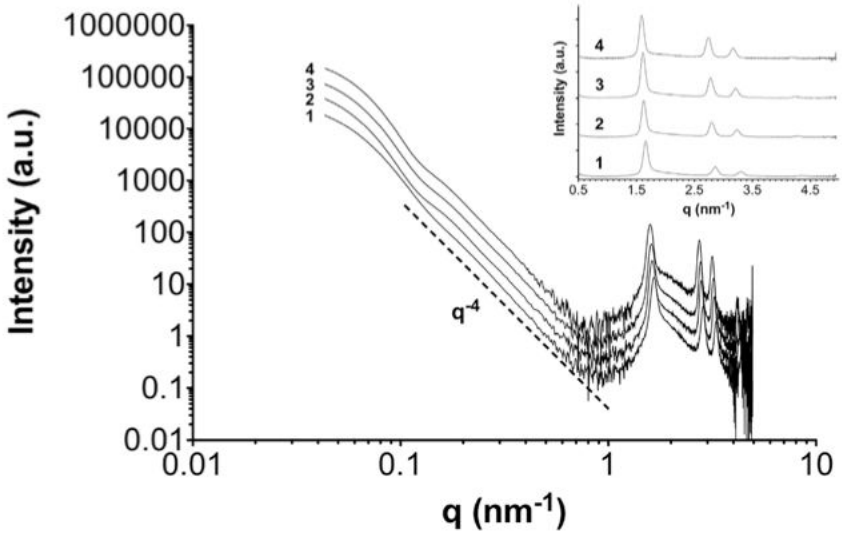

Fig. 2. SAXS profiles on a double logarithm scale of β-CD-C_{10} nanoparticle suspensions and of binary β-CD-C_{10}/MO nanoparticle suspensions (the formulation number is indicated beside the corresponding pattern). The inset shows the enlarged patterns at high angle on a linear scale.

includes the water layer carried by the particles during their Brownian motion. The internal structure of the particles generates four Bragg reflections at $q = 1.66$, 2.86, 3.31 and 4.38 nm^{-1}, corresponding to the ratio sequence $1 : \sqrt{3} : \sqrt{4} : \sqrt{7}$. This corresponds to a hexagonal molecular packing with a lattice parameter $a = 4.39$ nm. This type of supramolecular organization has already been reported for nanoparticles made of β-CD-C_{10} derivatives (Choisnard et al., 2011; Putaux et al., 2017). The association of MO with β-CD-C_{10} in molar proportions of 25.0, 50.0 and 75.0 mol% (formulations 2, 3 and 4, respectively), yielded mixed nanoparticles with structural properties similar to those observed for the amphiphilic cyclodextrin used alone. The corresponding SAXS patterns are shown in Fig. 2. Interestingly, curve oscillation is detectable on each SAXS profile, supporting a rather narrow size distribution for these nanoparticles. Bell-shaped Kratky plots and q^{-4}-decrease of scattering intensity in the Porod region clearly indicate the formation of smooth-surface globular particles. As for β-CD-C_{10} nanoparticles, nanoparticle radii determined using the Kratky plot are smaller than those determined by DLS. The existence of an inner hexagonal packing of the component molecules is shown by a series of four Bragg reflections in a ratio sequence of $1 : \sqrt{3} : \sqrt{4} : \sqrt{7}$. , present for all β-CD-C_{10}/MO nanoparticles whatever their composition, only slightly differing from each other by the position of the diffraction peaks. The first-order Bragg reflection was centered at $q = 1.63$, 1.61 and 1.59 nm^{-1} (i.e., hexagonal-lattice parameters $a = 4.48$, 4.52 and 4.58 nm) for nanoparticles containing 25.0, 50.0 and 75.0 mol% of MO respectively. The hexagonal lattice periodicity progressively increased with increasing MO content, with an almost linear increment of 0.0024 nm for a 1 mol% increase in MO. This result and the absence of secondary Bragg reflections in the SAXS patterns indicate that the lipid molecules do not form a separate phase during the nanoprecipitation process.

Finally, in order to characterize the nanoparticle surface and its interaction with proteins, β-CD-C_{10} and β-CD-C_{10}/MO nanoparticles were investigated for their ability to activate the complement C3 protein, which is a key protein in the complement activation cascades. It was observed that both types of nanoparticles were weak activators of the complement C3 component in human serum. A low activation by β-CD-C_{10} and β-CD-C_{10}/MO nanoparticles, even at high specific surface area ($S \approx 1000\ cm^2\ mL^{-1}$) was observed (Fig. S2). This could be explained by an efficient inhibition of serum protein adsorption by the hydrophilic head groups which prevents the triggering of the cascade reaction leading to C3 cleavage.

3.2. Ternary β-CD-C_{10}/MO/DOPE-PEG_{2000} nano-assemblies

Since DOPE-PEG_{2000} is able to stabilize MO-based cubosomes at very low molar proportions (Angelov et al., 2012, 2015), 2 mol% of DOPE-PEG_{2000} was introduced in the preparations by co-solubilization in acetone before nanoprecipitation in water in the same conditions as those described above. Similar mean hydrodynamic diameters in the 80–90 nm range with rather high polydispersity indexes, as observed for β-CD-C_{10}/MO nanoparticles, were measured by DLS (Table 2). This is in accordance with the TEM images shown in Fig. 3 demonstrating the coexistence of spheroidal and barrel-like nano-objects with a wide size distribution ranging from 40 nm to 300 nm. As for β-CD-C_{10} and β-CD-C_{10}/MO nanoparticles, number-weighted median diameters and harmonic *z*-average diameters determined for spheroidal nanoparticles by TEM were very different from those measured by DLS, especially for formulations 7 and 8. In the case of formulation 7, as a majority of barrel-shaped particles were observed, the comparison between the hydrodynamic diameter obtained by DLS and the diameter of spheroidal particles measured by TEM is not suitable. In this system, a median length equal to 91 ± 32 nm and a median width equal to 52 ± 17 nm were found and these values lead to an equivalent spherical diameter of 72 ± 24 nm for the elongated particles which is very close to the hydrodynamic diameter determined by DLS. For formulation 8, the higher viscosity of the medium (i.e., containing 5% glucose) could probably restrict the selection to bigger particles during the blotting. Moreover, the average aspect ratio of elongated nanoparticles was about 2.1, 2.1 and 1.8 for formulations 5, 6 and 7 respectively.

The SAXS profiles of the β-CD-C_{10}/MO/DOPE-PEG_{2000} nanoparticles are consistent with the presence of nanoscale objects of finite size and shows Bragg reflections indicating the formation of an inner molecular organization with a periodically ordered hexagonal lattice (Fig. 4). The nanoparticle diameters determined with the Kratky plot (about 73 nm for the three samples) were smaller than those determined by DLS (83, 87 and 88 nm for nanoparticles containing 24.5, 49.0 and 73.5 mol% of MO respectively) and the larger difference between the gyration and

Table 2
Properties of ternary β-CD-C_{10}/MO/DOPE-PEG_{2000} nanoparticles (DOPE-PEG_{2000}: 2.0 mol%).

Formulation	MO (mol%)	CD (mol%)	d_H (nm)[c]	PI[d]	d_{TEM} (nm)[e]	$d_{6,5}$ (nm)[f]	RS ($g.L^{-1}$)[g]	a_{hex} (nm)[h]	a_{hex} (nm)[i]	C3b (%)[j]
5[a]	24.5	73.5	83 ± 36	0.223	47 ± 18	79	0.1	4.54 ± 0.02	–	20
6[a]	49.0	49.0	87 ± 32	0.136	50 ± 21	88	0.1	4.64 ± 0.04	–	22
7[a]	73.5	24.5	88 ± 27	0.095	30 ± 9	44	0.1	4.75 ± 0.14	5.42 ± 0.11	20
8[b]	49.0	49.0	63 ± 18	0.093	51 ± 29	129	2.8	4.64 ± 0.02		29

[a] Prepared in pure water.
[b] Prepared in glucose 5% adjusted to pH 7.4 (10 mM of HEPES).
[c] Intensity-weighted median hydrodynamic diameter (DLS).
[d] Polydispersity index (DLS).
[e] Number-weighted median diameter for spheroidal particles (TEM).
[f] Harmonic *z*-average diameter for spheroidal particles (TEM).
[g] Residual content of acetone.
[h] Hexagonal lattice structure parameter (first phase).
[i] Hexagonal lattice structure parameter (second phase).
[j] Activation of C3 protein.

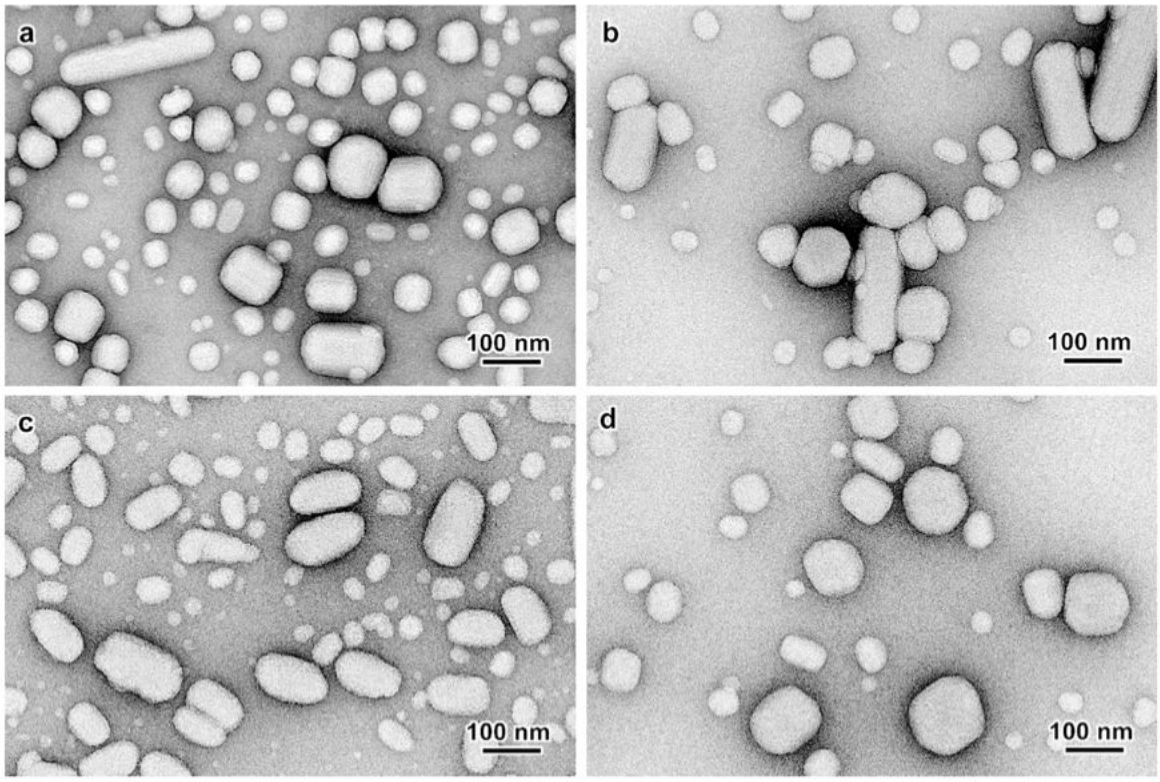

Fig. 3. TEM images of negatively stained β-CD-C_{10}/MO/DOPE-PEG_{2000} nanoparticles with different proportions of MO and prepared in different media: (a) formulation 5 (24.5 mol%; water), (b) formulation 6 (49.0 mol%; water), (c) formulation 7 (73.5 mol%; water) and (d) formulation 8 (49.0 mol%; glucose 5%).

hydrodynamic diameters can be explained by the presence on of PEG the nanoparticle surface, which is not taken into account by SAXS measurements (Garcia-Diez et al., 2016). Moreover, in the presence of DOPE-PEG_{2000}, the decrease of the scattering intensity at wider angles could not be successfully described by a simple q^{-4} power law. A linear fit of log I(q) *vs.* log q results in coefficient $\alpha \approx -4.3$, -4.5 and -4.8 for β-CD-C_{10}/MO/DOPE-PEG_{2000} nanoparticles containing 24.5, 49.0 and 73.5 mol% of MO respectively, taking into account that the scattering intensity could be fitted by $I(q) \propto q^{\alpha}$. The deviation from the q^{-4} law may be explained by differences in surface roughness (Hertle, 2010), probably caused by dangling PEG chains at the nanoparticle/water interface. For β-CD-C_{10}/MO/DOPE-PEG_{2000} nanoparticles containing 24.5 or 49.0 mol% of MO, one hexagonal lattice was observed with the first Bragg peak centered at $q = 1.60$ and $1.57\ nm^{-1}$ respectively, corresponding to hexagonal lattice parameters of 4.54 and 4.64 nm, respectively. In contrast, two co-existing hexagonal phases were observed for β-CD-C_{10}/MO/DOPE-PEG_{2000} nanoparticles containing 73.5 mol% of MO and, after fitting the SAXS profile, the two first Bragg peaks were positioned at $q = 1.35$ and $1.49\ nm^{-1}$, leading to hexagonal lattice parameters of 4.75 and 5.42 nm. By dismissing the phase which has the larger lattice parameter, a linear relationship between the hexagonal lattice parameter and the quantity of MO can be observed, with a slope equal to about 0.0042 nm for a MO increment of 1 mol%. As a first conclusion, the addition of 2 mol% of DOPE-PEG_{2000} leads to the formation of rough nanoparticles and to a phase separation at high MO content.

Finally, complement activation experiments were performed to study the impact of PEG chain coating on the nanoparticle surface. Whereas about 14% of C3 protein present in the serum was activated by β-CD-C_{10}/MO nanoparticles, β-CD-C_{10}/MO/DOPE-PEG_{2000} nanoparticles led to complement activation of about 20%,

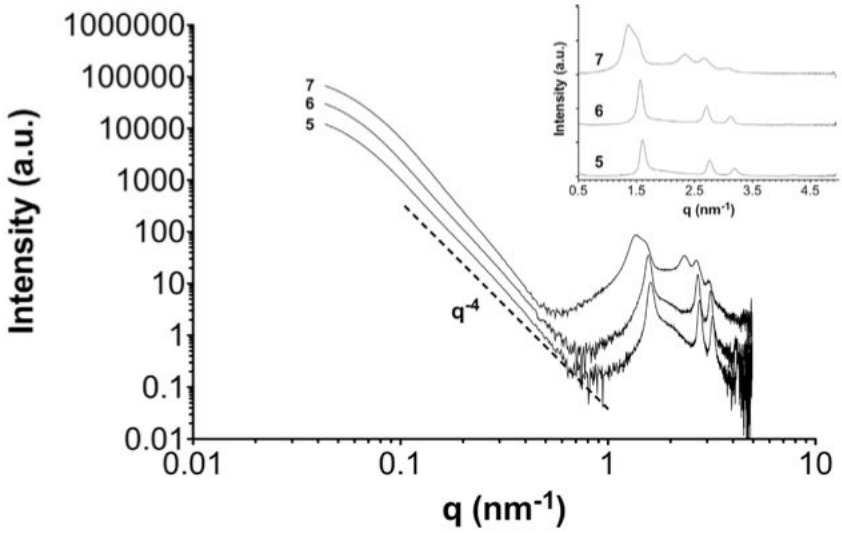

Fig. 4. SAXS profiles on a double logarithm scale of ternary β-CD-C_{10}/MO/DOPE-PEG_{2000} nanoparticle suspensions (the formulation number is indicated beside the corresponding pattern). The inset shows the enlarged patterns at high angle on a linear scale.

which was identical to the activation of the serum measured in the presence of β-CD-C_{10} nanoparticles under identical experimental conditions (about 19%). The same trend was observed by Mosqueira et al. (2001) with PLA and PLA-PEG nanocapsules. In particular, these authors observed an increase in the activation of the complement for nanocapsules coated with a low surface density of PEG compared with naked PLA nanocapsules. An explanation is that the presence of a low PEG density probably contributes to trapping plasma proteins on the nanoparticle surface and thereby increasing complement activation.

Since our attempt to prepare β-CD-C_{10}/MO/DOPE-PEG_{2000} nanoparticles in isotonic saline led to aggregation, we prepared β-CD-C_{10}/MO/DOPE-PEG_{2000} nanoparticles in 5% glucose, another isotonic medium, adjusted to pH 7.4 by addition of 10 mM HEPES. As the β-CD-C_{10}/MO/DOPE-PEG_{2000} system with 49.0 mol% of MO gave stable nanoparticles with high β-CD-C_{10} loading with only one hexagonal structure, this composition was chosen to compare the results obtained in pure water and in 5% glucose. In the latter medium, stable nanoparticles were produced with a lower size, a lower polydispersity and a higher acetone content than those produced in pure water (formulation 8 in Table 2). The TEM images of negatively stained PEGylated nanoparticles (Fig. 3d) show a polydisperse distribution of bulky faceted particles. These results may be explained by the higher viscosity of 5% glucose solution compared with pure water, influencing the nanoprecipitation process. It is also possible that the presence of glucose limits the growth of the particles in specific directions of the hexagonal organization. More precisely, the higher viscosity may prevent the axial growth of particles, leading to a bulkier shape. Moreover, it should be noted that the preparation of β-CD-C_{10}/MO/DOPE-PEG_{2000} nanoparticles containing 49.0 mol% of MO in isotonic glucose solution instead of pure water did not change the internal structure of the nanoparticles. The same hexagonal lattice parameter, i.e. 4.64 nm, was found for this system (Supporting information, Fig. S2).

3.3. Ternary β-CD-C_{10}/MO/DOPA nano-assemblies

Since our initial aim was to produce stable nanoparticles in buffered saline medium, we decided to prepare mixed nanoparticles including the sodium salt of dioleylphosphatidic acid (DOPA) which is known to stabilize both liposomes (Yohannes et al., 2006) and monoolein cubic phases (Li et al., 2001) in buffered saline media. The percentage of added DOPA was chosen on the basis of the results published by Li et al. (2001) in which they observed, in presence of 10 mol% of DOPA, the formation of a stable cubic phase with an Im3m space group for sodium chloride concentrations between 0 and 60 mM and another stable cubic phase with an Pn3m space group for sodium chloride concentrations between 70 and 1000 mM. In the light of these results, the addition of 10 mol% of DOPA was retained for our studies. The same nanoprecipitation protocol was used. However, as DOPA is not soluble in acetone, other organic solvents, miscible with water and with boiling points lower than that of water, were tested (data not

Table 3
Properties of ternary β-CD-C_{10}/MO/DOPA nanoparticles (DOPA: 10.0 mol%).

Formulation	MO (mol%)	CD (mol%)	d_H (nm)[a]	PI[b]	d_{TEM} (nm)[c]	$d_{6,5}$ (nm)[d]	RS ($g.L^{-1}$)[e]	RS ($g.L^{-1}$)[f]	a_{hex} (nm)[g]	a_{hex} (nm)[h]	C3b (%)[i]
9	22.5	67.5	114 ± 30	0.072	75 ± 25	114	0.1	2.3	4.68 ± 0.04	–	44
10	45.0	45.0	96 ± 32	0.113	72 ± 21	101	0.2	1.9	4.68 ± 0.04	5.15 ± 0.12	39
11	67.5	22.5	118 ± 29	0.063	–	–	0.1	1.1	–	5.59 ± 0.06	37

[a] Intensity-weighted median hydrodynamic diameter (DLS).
[b] Polydispersity index (DLS).
[c] Number-weighted median diameter for spheroidal particles (TEM).
[d] Harmonic z-average diameter for spheroidal particles (TEM).
[e] Residual content of acetone.
[f] Residual content of THF.
[g] Hexagonal lattice structure parameter (first phase).
[h] Hexagonal lattice structure parameter (second phase).
[i] Activation of C3 protein.

Please cite this article in press as: C.E.A.H.B. Nguy n, et al., New nanoparticles obtained by co-assembly of amphiphilic cyclodextrins and nonlamellar single-chain lipids: Preparation and characterization, Int J Pharmaceut (2017), http://dx.doi.org/10.1016/j.ijpharm.2017.07.007

shown). Tetrahydrofuran was selected because of its capacity to solubilize the three components of the system (i.e. β-CD-C_{10}, MO and DOPA). Using the previous experimental conditions with this change of organic solvent, stable nanoparticles were prepared and were characterized as above. Residual THF was quantified (Table 3) and residual acetone from the β-CD-C_{10} powder was also detected. Of the three formulations prepared with DOPA, formulations 9 and 11 gave larger nanoparticles than formulation 10, but these larger nanoparticles were more monodisperse. TEM images recorded after negative staining (Fig. 5) confirmed the size analysis: a large variety of β-CD-C_{10}/MO/DOPA nanoparticles (Fig. 5b) was observed for a β-CD-C_{10}/MO ratio equal to 1. In the case of β-CD-C_{10}/MO/DOPE-PEG_{2000} nanoparticles containing a high proportion of MO (Fig. 5b and c), a large population of elongated particles was observed with striations on their surfaces, probably caused by the presence of DOPA. Harmonic *z*-average diameter determined by TEM for spheroidal nanoparticles of formulations 9 and 10 were very close to those measured by DLS. For these three formulations, the aspect ratio could not be determined due to the compact and facetted shape of the nanoparticles.

As observed for β-CD-C_{10}/MO/DOPE-PEG_{2000} nanoparticles, β-CD-C_{10}/MO/DOPA nanoparticles displayed a complex SAXS signal and nanoparticle diameters determined with the Kratky plot were lower than those determined by DLS (111, 96 and 118 nm for nanoparticles containing 22.5, 45.0 and 67.5 mol% of MO respectively) (Fig. 6). The fitting of the SAXS profiles in the Porod region by $\log I(q) = \beta + \alpha \times \log q$ showed that the decrease of the scattering intensity could not be adequately described by a simple q^{-4} law ($\alpha \approx -4.2$, -4.3 and -4.4 for β-CD-C_{10}/MO/DOPA nanoparticles containing 22.5, 45.0 and 67.5 mol% of MO respectively). As for β-CD-C_{10}/MO/DOPE-PEG_{2000} nanoparticles, this deviation could be explained by the presence of phosphate groups at the nanoparticle/water interface conferring roughness to the surface. β-CD-C_{10}/MO/DOPA nanoparticles containing 22.5 and 67.5 mol% of MO displayed a single hexagonal phase with lattice parameters equal to 4.68 and 5.59 nm respectively, while nanoparticles containing 45.0 mol% of MO were a mixture of these two hexagonal phases with lattice parameters equal to 4.68 and 5.15 nm. In the presence of DOPA, a β-CD-C_{10}/MO ratio greater than 1 resulted in more condensed particles than those prepared with a β-CD-C_{10}/MO ratio less than 1.

Although it is already known that liposomes containing phosphatidic acid activate the complement system (Chonn et al., 1991; Liu et al., 1999; Malmsten et al., 1996), we wanted to verify this phenomenon with our mixed β-CD-C_{10}/MO/DOPA nanoparticles. Indeed, a significant increase in complement activation was observed in the presence of our mixed β-CD-C_{10}/MO/DOPA nanoparticles, with a 2.5 and 2-fold increase compared with β-CD-C_{10}/MO and β-CD-C_{10}/MO/DOPE-PEG_{2000} nanoparticles respectively. Nevertheless, all tested formulations displayed complement activation percentages under 50%, which can be considered as a low level of activation.

3.4. Ternary β-CD-C_{10}/MO/POPA nano-assemblies

Since the β-CD-C_{10}/MO/DOPA system displayed an atypical behavior, we wished to know whether this was specific to the use of DOPA or to the inclusion of a phosphatidic acid in general. Therefore, the sodium salt of palmitoyloleylphosphatidic acid (POPA) was used instead of the sodium salt of DOPA. The same nanoprecipitation process as that used for the preparation of β-CD-C_{10}/MO/DOPA nanoparticles yielded stable β-CD-C_{10}/MO/POPA nanoparticles. A similar behavior to that of β-CD-C_{10}/MO/DOPA nanoparticles was observed. Namely, smaller nanoparticles were obtained for a β-CD-C_{10}/MO ratio equal to 1 but in all cases, β-CD-C_{10}/MO/POPA nanoparticles were smaller than β-CD-C_{10}/MO/DOPA nanoparticles (Table 4). Moreover, for nanoparticles containing a high proportion of MO (Fig. 7b and c), elongated particles with very marked striations

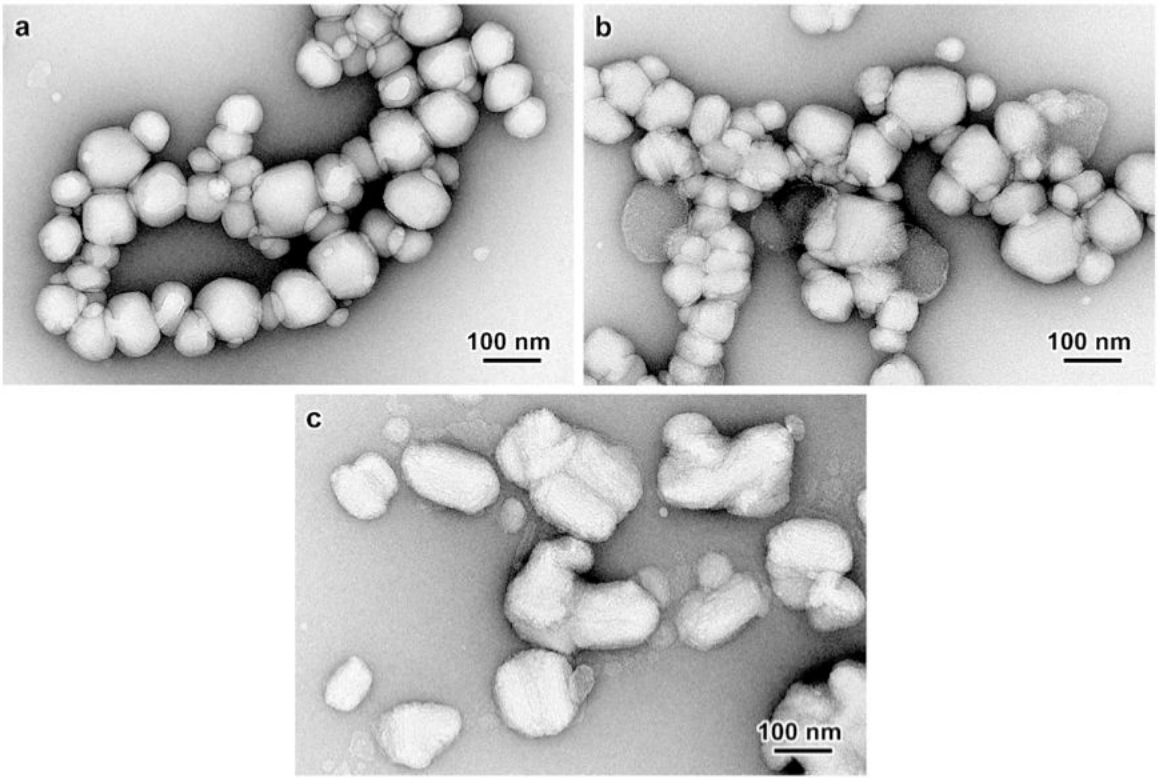

Fig. 5. TEM images of negatively stained β-CD-C_{10}/MO/DOPA nanoparticles with different molar proportions of MO: (a) formulation 9 (22.5 mol%), (b) formulation 10 (45.0 mol%) and (c) formulation 11 (67.5 mol%).

Please cite this article in press as: C.E.A.H.B. Nguy n, et al., New nanoparticles obtained by co-assembly of amphiphilic cyclodextrins and nonlamellar single-chain lipids: Preparation and characterization, Int J Pharmaceut (2017), http://dx.doi.org/10.1016/j.ijpharm.2017.07.007

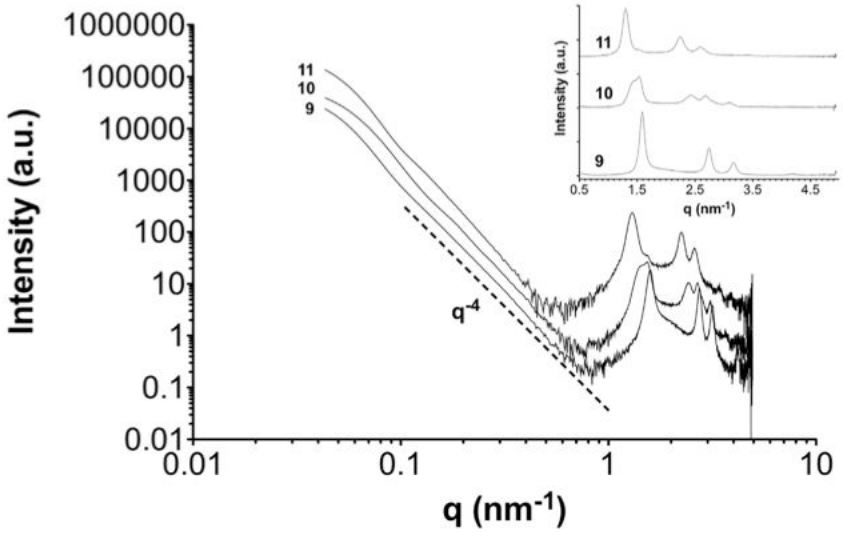

Fig. 6. SAXS profiles on a double logarithm scale of ternary β-CD-C_{10}/MO/DOPA nanoparticle suspensions (the formulation number is indicated beside the corresponding pattern). The inset shows the enlarged patterns at high angle on a linear scale.

Table 4
Properties of ternary β-CD-C_{10}/MO/POPA nanoparticles (POPA: 10.0 mol%).

Formulation	MO (mol%)	CD (mol%)	d_H (nm)[a]	PI[b]	d_{TEM} (nm)[c]	$d_{6,5}$ (nm)[d]	RS ($g.L^{-1}$)[e]	RS ($g.L^{-1}$)[f]	a_{hex} (nm)[g]	a_{hex} (nm)[h]	C3b (%)[i]
12	22.5	67.5	102 ± 29	0.083	69 ± 26	107	0.2	0.3	4.57 ± 0.02	–	21
13	45.0	45.0	89 ± 24	0.076	–	–	0.2	0.7	4.71 ± 0.13	5.19 ± 0.09	54
14	67.5	22.5	106 ± 30	0.082	–	–	0.4	0.9	–	5.64 ± 0.01	33

For footnotes, see Table 3.

were observed, especially for a β-CD-C_{10}/MO ratio less than 1. This more pronounced behavior could result from the higher solid-to-liquid state transition temperature of the phospholipid hydrocarbon chains, which is equal to 19.1 °C in the case of POPA and −8.2 °C for DOPA (Supporting information, Fig. S4 and Table S1). The transition temperatures were very close to those obtained previously for POPA (Basso et al., 2016; Sánchez-Bautista et al., 2007) and DOPA (Smaal et al., 1987).

A similar scattering behavior to that observed with β-CD-C_{10}/MO/DOPA nanoparticles was recorded with β-CD-C_{10}/MO/POPA nanoparticles (Fig. 8). In this case, the α coefficient was −4.2, −4.2 and −4.4 for β-CD-C_{10}/MO/POPA nanoparticles containing 22.5, 45.0 and 67.5 mol% of MO respectively, showing some differences at the level of the water/nanoparticle interface. Like β-CD-C_{10}/MO/DOPA nanoparticles, β-CD-C_{10}/MO/POPA nanoparticles containing 22.5 and 67.5 mol% of MO displayed only one hexagonal phase with lattice parameters of 4.57 and 5.64 nm respectively, while nanoparticles containing 45.0 mol% of MO were made up of a mixture of these two hexagonal phases with lattice parameters of 4.71 and 5.19 nm. Therefore, as was observed for nanoparticles prepared in presence of DOPA, β-CD-C_{10}/MO/POPA nanoparticles exhibit complex behavior as a function of the β-CD-C_{10}/MO ratio.

Finally, complement activation was evaluated to determine the activating capacity of β-CD-C_{10}/MO/POPA nanoparticles. These nanoparticles activated the complement system by about 36%, corroborating the results obtained with the β-CD-C_{10}/MO/DOPA, i.e. a 2.5 and 2-fold increase compared with β-CD-C_{10}/MO and β-CD-C_{10}/MO/DOPE-PEG_{2000} nanoparticles respectively.

3.5. Principal component analysis

Principal component analysis (PCA) was carried out according to the data table that describes the different formulations by the 12 inter-correlated quantitative variables considered in this study. The goal was to extract the important information from this table by representing the data as a set of new orthogonal variables, called principal components, and to display the pattern of similarity of the observations and of the variables as points in 2D-projections (Bishop et al., 2015). After PCA analysis, we determined the most relevant principal components (PC) and the scree plot (Fig. 9a) shows that the first four principal components explained 81.7% of the variance. The first two components accounted for 59.1% of the variance and were considered for the bi-plot of scores (observations in space of PC) and loadings (variables in space of PC). The third component PC3 allowed the contribution of the molar percentage of POPA to be described more accurately. The bi-plot of scores (represented by blue inverted triangles for formulations in acetone and by red triangles for formulations in THF) and loadings (black squares) in the space of PC1 (*x*-axis) and PC2 (*y*-axis) is shown in Fig. 9b. According to PC1, formulations are grouped into 2 clusters: one corresponding to systems formulated in acetone and the second to systems formulated in THF.

The lattice parameter of the second phase, the residual content of THF, the molar percentage of MO, POPA and DOPA, the hydrodynamic diameter and the complement protein C3 activation are positively correlated with PC1. The molar percentages of DOPE-PEG_{2000} and β-CD-C_{10}, the residual content of acetone, the lattice parameter of the first phase and the polydispersity index are inversely correlated with PC1. In summary, this means that a higher percentage of MO combined with POPA and DOPA leads to greater lattice parameters in the second phase, larger hydrodynamic diameters and more complement protein C3 activation. A higher percentage of MO combined with POPA and DOPA results in a lower polydispersity index. Finally, nanoparticles prepared with a higher content of β-CD-C_{10} in the presence or in the absence of DOPE-PEG_{2000} with acetone as the nanoprecipitation solvent, are

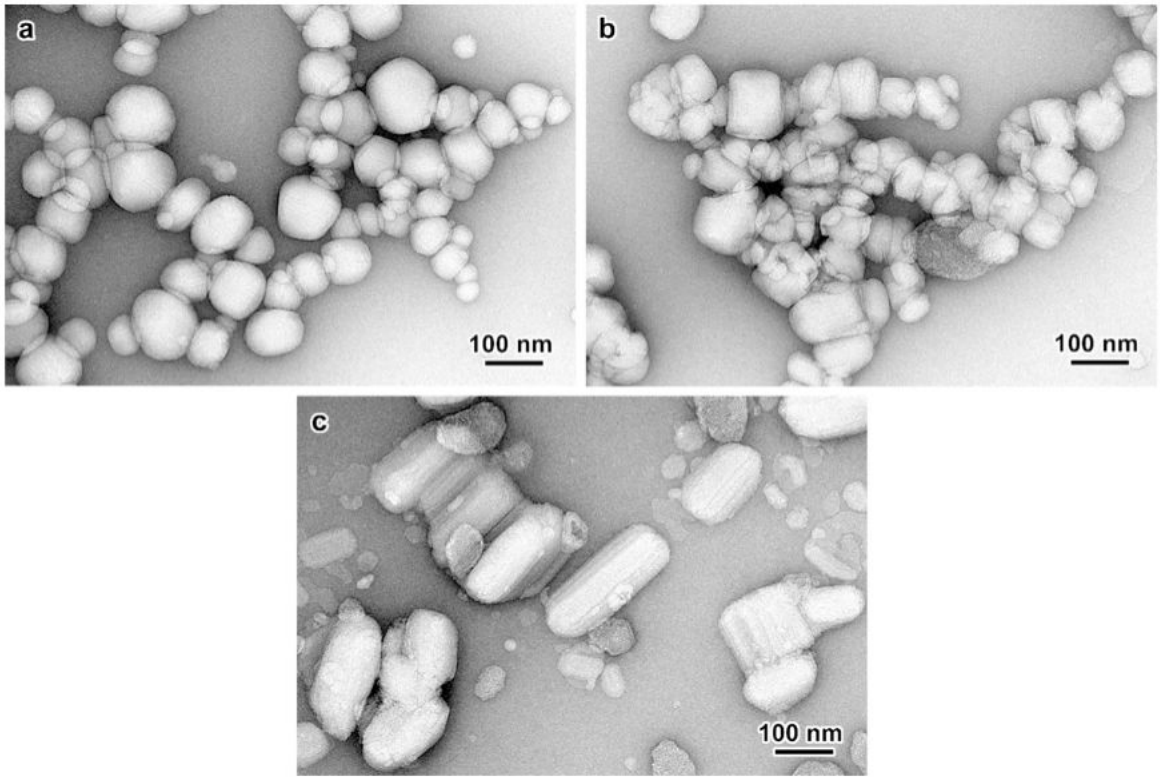

Fig. 7. TEM images of negatively stained β-CD-C_{10}/MO/POPA nanoparticles with different molar proportions of MO: (a) formulation 12 (22.5 mol%), (b) formulation 13 (45.0 mol%) and (c) formulation 14 (67.5 mol%).

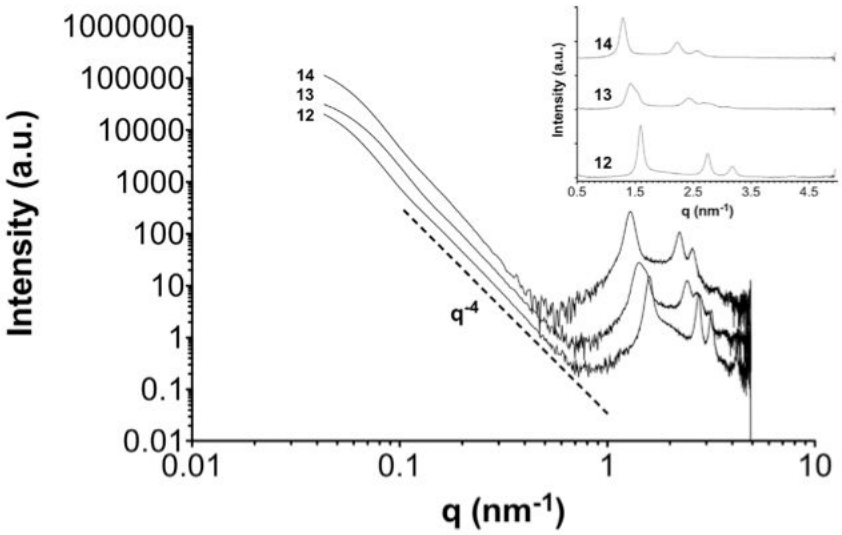

Fig. 8. SAXS profiles on a double logarithm scale of ternary β-CD-C_{10}/MO/POPA nanoparticle suspensions (the formulation number is indicated beside the corresponding pattern). The inset shows the enlarged patterns at high angle on a linear scale.

smaller but more polydisperse nanoparticles and exhibit low complement activation and a single internal structure that is mainly governed by the self-assembly of β-CD-C_{10}.

4. Conclusion

The most important conclusion to come out of this study is that, in all formulations, the β-CD-C_{10} governs the internal inverse hexagonal organization of the nanoparticles. The addition of MO leads to an increase in lattice parameter, thereby indicating a swelling of the hexagonal structure by insertion of the lipid molecules inside the layers. Moreover, due to the amphiphilic nature of MO which is probably adsorbed at the water/nanoparticle interface, we can consider that MO contributes to the good colloidal stability of the porous nanoparticles.

After an extensive screening, our study demonstrates that the structure and properties predicting the in-vivo fate of the β-CD-C_{10}/MO nanoparticles are significantly affected by the addition of a third component. The addition of a phosphatidic acid during the preparation results in the formation of nanoparticles with an

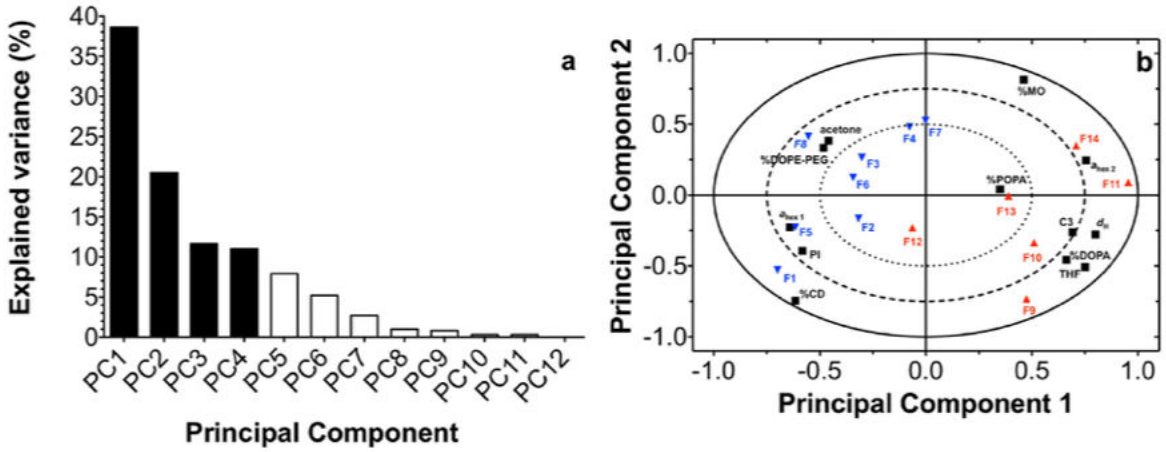

Fig. 9. The scree plot graphic (a) showing that the first four principal components explained 81.7% of the variance. The first two components accounted for 59.1% of the variance. The bi-plot of scores (represented by blue inverted triangles for formulations in acetone and by red triangles for formulations in THF) and loadings (black squares) in the space of PC1 (*x*-axis) and PC2 (*y*-axis) is shown in graphic b. (For interpretation of the references to colour in this figure legend, the reader is referred to the web version of this article.)

uneven surface. A promising system combining the presence of a PEGylated lipid and high β-CD-C_{10} loading has been successfully prepared. Further investigation is necessary to evaluate the capacity of these nanocarriers to incorporate active ingredients as well as their ability to modify drug release. The multicompartment nature of the nanoparticles offers promising solutions for the co-delivery of various drugs, by loading a water-soluble active ingredient in water channels or a lipophilic therapeutic substance in lipid bilayers, or replacing a few mol% of MO by an amphiphilic drug or a lipid prodrug. Finally, this study clearly indicates that detailed characterization by electron microscopy and small-angle X-ray scattering is required to obtain reliable information about the shape and the internal structure of lipid nanoparticles.

Acknowledgements.

We thank Delphine Levilly (DPM, UMR CNRS 5063) for amphiphilic cyclodextrin synthesis, Dr Claudie Bourgaux (IGPS, UMR CNRS 8612) for preliminary SAXS measurements, Maiwenn Tonga Ngatchou and Dr Christine Vauthier (IGPS, UMR CNRS 8612) for their help with complement activation studies and Pr David Landy (UCEIV, EA 4492) for fruitful discussions. We acknowledge the European Synchrotron Radiation Facility for provision of synchrotron radiation facilities (proposal MX-1865) and the NanoBio-ICMG Platform for granting access to the Electron Microscopy facility. The financial support from ANR SIMI10 Nanosciences to the project CYDEXCAR (ANR-11-BS10-0007) is gratefully acknowledged.

Appendix A. Supplementary data

Supplementary data associated with this article can be found, in the online version, at http://dx.doi.org/10.1016/j.ijpharm.2017.07.007.

References

Angelov, B., Angelova, A., Filippov, S., Karlsson, G., Terrill, N., Lesieur, S., Štěpánek, P., 2012. SAXS study of sterically stabilized lipid nanocarriers functionalized by DNA. J. Phys. Conf. Ser. 351, 012004.
Angelov, B., Angelova, A., Drechsler, M., Garamus, V.M., Mutafchieva, R., Lesieur, S., 2015. Identification of large channels in cationic PEGylated cubosome nanoparticles by synchrotron radiation SAXS and Cryo-TEM imaging. Soft Matter. 11, 3686–3692.
Azmi, I.D.M., Wu, L.P., Wibroe, P.P., Nilsson, C., Ostergaard, J., Sturup, S., Gammelgaard, B., Urtti, A., Moghimi, S.M., Yaghmur, A., 2015. Modulatory effect of human plasma on the internal nanostructure and size characteristics of liquid-crystalline nanocarriers. Langmuir 31, 5042–5049.
Basso, L.G.M., Vicente, E.F., Crusca, E., Cilli, E.M., Costa-Filho, A.J., 2016. SARS-CoV fusion peptides induce membrane surface ordering and curvature. Sci. Rep. 6, 37131.
Bishop, C.J., Abubaker-Sharif, B., Guiriba, T., Tzeng, S.Y., Green, J.J., 2015. Gene delivery polymer structure-function relationships elucidated via principal component analysis. Chem. Commun. 51, 12134–12137.
Boyd, B.J., Khoo, S.M., Whittaker, D.V., Davey, G., Porter, C.J., 2007. A lipid-based liquid crystalline matrix that provides sustained release and enhanced oral bioavailability for a model poorly water soluble drug in rats. Int. J. Pharm. 340, 52–60.
Bozzuto, G., Molinari, A., 2015. Liposomes as nanomedical devices. Int. J. Nanomed. 10, 975–999.
Brennich, M.E., Kieffer, J., Bonamis, G., De Maria Antolinos, A., Hutin, S., Pernot, P., Round, A., 2016. Online data analysis at the ESRF bioSAXS beamline, BM29. J. Appl. Cryst. 49, 203–212.
Cervin, C., Vandoolaeghe, P., Nistor, C., Tiberg, F., Johnsson, M., 2009. A combined in vitro and in vivo study on the interactions between somatostatin and lipid-based liquid crystalline drug carriers and bilayers. Eur. J. Pharm. Sci. 36, 377–385.
Che, J., Okeke, C.I., Hu, Z.B., Xu, J., 2015. DSPE-PEG: A distinctive component in drug delivery system. Curr. Pharm. Des. 21, 1598–1605.
Chen, Y., Lu, Y., Zhong, Y., Wang, Q., Wu, W., Gao, S., 2012. Ocular delivery of cyclosporine A based on glyceryl monooleate/poloxamer 407 liquid crystalline nanoparticles: preparation, characterization, in vitro corneal penetration and ocular irritation. J. Drug Target. 20, 856–863.
Choisnard, L., Gèze, A., Bigan, M., Putaux, J.-L., Wouessidjewe, D., 2005. Efficient size control of amphiphilic cyclodextrin nanoparticles through a statistical mixture design methodology. J. Pharm. Pharmaceutic. Sci. 8, 593–600.
Choisnard, L., Gèze, A., Putaux, J.-L., Wong, Y.S., Wouessidjewe, D., 2006. Nanoparticles of β-cyclodextrin esters obtained by self-assembling of biotransesterified β-cyclodextrins. Biomacromolecules 7, 515–520.
Choisnard, L., Gèze, A., Yaméogo, J.B.G., Putaux, J.-L., Wouessidjewe, D., 2007. Miscellaneous nanoaggregates made of β-CD esters synthesised by an enzymatic pathway. Int. J. Pharm. 344, 26–32.
Choisnard, L., Gèze, A., Vanhaverbeke, C., Yaméogo, J.B.G., Putaux, J.-L., Brasme, B., Jullien, L., Boullanger, S., Elfakir, C., Wouessidjewe, D., 2011. Physicochemical characterization of α-, β-, and γ-cyclodextrins bioesterified with decanoate chains used as building blocks of colloidal nanoparticles. Biomacromolecules 12, 3031–3038.
Chonn, A., Cullis, P.R., Devine, D.V., 1991. The role of surface charge in the activation of the classical and alternative pathways of complement by liposomes. J. Immunol. 146, 4234–4241.
Coty, J.-B., Varenne, F., Vachon, J.-J., Vauthier, C., 2016. Serial multiple crossed immunoelectrophoresis at a microscale: a stamp-sized 2D immunoanalysis of protein C3 activation caused by nanoparticles. Electrophoresis 37, 2401–2409.
Crommelin, D.J., 1984. Influence of lipid composition and ionic strength on the physical stability of liposomes. J. Pharm. Sci. 73, 1559–1563.
Della Gatta, G., Richardson, M.J., Sarge, S.M., Stolen, S., 2006. Standards, calibration, and guidelines in microcalorimetry – Part 2: Calibration standards for differential scanning calorimetry. Pure Appl. Chem. 78, 1455–1476.
Dos Santos, N., Allen, C., Doppen, A.M., Anantha, M., Cox, K.A.K., Gallagher, R.C., Karlsson, G., Edwards, K., Kenner, G., Samuels, L., Webb, M.S., Bally, M.B., 2007. Influence of poly(ethylene glycol) grafting density and polymer length on liposomes: relating plasma circulation lifetimes to protein binding. Biochim. Biophys. Acta: Biomembranes 1768, 1367–1377.

Duttagupta, A.S., Chaudhary, H.M., Jadhav, K.R., Kadam, V.J., 2016. Cubosomes: innovative nanostructures for drug delivery. Curr. Drug Deliv. 13, 482–493.
Fraser, S.J., Mulet, X., Hawley, A., Separovic, F., Polyzos, A., 2013. Controlling nanostructure and lattice parameter of the inverse bicontinuous cubic phases in functionalised phytantriol dispersions. J. Colloid Interface Sci. 408, 117–124.
Gèze, A., Choisnard, L., Putaux, J.-L., Wouessidjewe, D., 2009. Colloidal systems made of biotransesterified α, β, and γ cyclodextrins grafted with C10 alkyl chains. Mater. Sci. Eng. C. 29, 458–462.
Ganem-Quintanar, A., Quintanar-Guerrero, D., Buri, P., 2000. Monoolein: a review of the pharmaceutical applications. Drug. Dev. Ind. Pharm. 26, 809–820.
Garcia-Diez, R., Gollwitzer, C., Krumrey, M., Varga, Z., 2016. Size determination of a liposomal drug by small-angle X-ray scattering using continuous contrast variation. Langmuir 32, 772–778.
Guo, C., Wang, J., Cao, F., Lee, R.J., Zhai, G., 2010. Lyotropic liquid crystal systems in drug delivery. Drug Discov. Today 15, 1032–1040.
Han, K., Pan, X., Chen, M., Wang, R., Xu, Y., Feng, M., Li, G., Huang, M., Wu, C., 2010. Phytantriol-based inverted type bicontinuous cubic phase for vascular embolization and drug sustained release. Eur. J. Pharm. Sci. 41, 692–699.
Hartnett, T.E., Ladewig, K., O'Connor, A.J., Hartley, P.G., McLean, K.M., 2014. Size and phase control of cubic lyotropic liquid crystal nanoparticles. J. Phys. Chem. B 118, 7430–7439.
Hertle, Y., 2010. Structure and Dynamics of New Intelligent Copolymer Hydrogels and Hydrogel Nanoparticle Hybrids Ph.D. Dissertation. Bayreuth University, Germany.
Johnsson, M., Barauskas, J., Norlin, A., Tiberg, F., 2006. Physicochemical and drug delivery aspects of lipid-based liquid crystalline nanoparticles: a case study of intravenously administered propofol. J. Nanosci. Nanotechnol. 6, 3017–3024.
Kfoury, M., Balan, R., Landy, D., Nistor, D., Fourmentin, S., 2015. Investigation of the complexation of essential oil components with cyclodextrins. Supramol. Chem. 27, 620–628.
Kulkarni, C.V., 2012. Lipid crystallization: from self-assembly to hierarchical and biological ordering. Nanoscale 4, 5779–5791.
Lee, K.W., Nguyen, T.H., Hanley, T., Boyd, B.J., 2009. Nanostructure of liquid crystalline matrix determines in vitro sustained release and in vivo oral absorption kinetics for hydrophilic model drugs. Int. J. Pharm. 365, 190–199.
Li, S.J., Yamashita, Y., Yamazaki, M., 2001. Effect of electrostatic interactions on phase stability of cubic phases of membranes of monoolein/dioleoylphosphatidic acid mixtures. Biophys. J. 81, 983–993.
Lindell, K., Engblom, J., Engström, S., Jonströmer, M., Carlsson, A., 1998. Influence of a charged phospholipid on the release pattern of timolol maleate from cubic liquid crystalline phases. Prog. Colloid Polym. Sci. 108, 111–118.
Liu, C., Marshall, P., Schreibman, I., Vu, A., Gai, W.M., Whitlow, M., 1999. Interaction between terminal complement proteins C5b-7 and anionic phospholipids. Blood 93, 2297–2301.
Lopes, L.B., Ferreira, D.A., de Paula, D., Garcia, M.T.J., Thomazini, J.A., Fantini, M.C.A., Bentley, M.V.L.B., 2006. Reverse hexagonal phase nanodispersion of monoolein and oleic acid for topical delivery of peptides: in vitro and in vivo skin penetration of cyclosporin A. Pharm. Res. 23, 1332–1342.
Malmsten, M., Lassen, B., Van Alstine, J.M., Nilsson, U.R., 1996. Adsorption of complement proteins C3 and C1q. J. Colloid Interface Sci. 178, 123–134.
Meli, V., Caltagirone, C., Sinico, C., Lai, F., Falchi, A.M., Monduzzi, M., Obiols-Rabasa, M., Picci, G., Rosa, A., Schmidt, J., Talmon, Y., Murgia, S., 2017. Theranostic hexosomes for cancer treatments: an in vitro study. New J. Chem. 41, 1558–1565.
Milak, S., Zimmer, A., 2015. Glycerol monooleate liquid crystalline phases used in drug delivery systems. Int. J. Pharm. 478, 569–587.
Mosqueira, V.C.F., Legrand, P., Gulik, A., Bourdon, O., Gref, R., Labarre, D., Barratt, G., 2001. Relationship between complement activation, cellular uptake and surface physicochemical aspects of novel PEG-modified nanocapsules. Biomaterials 22, 2967–2979.
Mulet, X., Boyd, B.J., Drummond, C.J., 2013. Advances in drug delivery and medical imaging using colloidal lyotropic liquid crystalline dispersions. J. Colloid Interface Sci. 393, 1–30.
Nazaruk, E., Miszta, P., Filipek, S., Górecka, E., Landau, E.M., Bilewicz, R., 2015. Lyotropic cubic phases for drug delivery: diffusion and sustained release from the mesophase evaluated by electrochemical methods. Langmuir 24, 12753–12761.
Peng, X., Wen, X., Pan, X., Wang, R., Chen, B., Wu, C., 2010. Design and in vitro evaluation of capsaicin transdermal controlled release cubic phase gels. AAPS Pharm. Sci. Tech. 11, 1405–1410.
Pernot, P., Round, A., Barrett, R., De Maria Antolinos, A., Gobbo, A., Gordon, E., Huet, J., Kieffer, J., Lentini, M., Mattenet, M., Morawe, C., Mueller-Dieckmann, C., Ohlsson, S., Schmid, W., Surr, J., Theveneau, P., Zerrad, L., McSweeney, S., 2013. Upgraded ESRF BM29 beamline for SAXS on macromolecules in solution. J. Synchrotron Rad. 20, 660–664.
Putaux, J.-L., Lancelon-Pin, C., Legrand, F.-X., Pastrello, M., Choisnard, L., Gèze, A., Rochas, C., Wouessidjewe, D., 2017. Self-assembly of amphiphilic biotransesterified β-cyclodextrins: supramolecular structure of nanoparticles and surface properties. Langmuir . https://doi.org/10.1021/acs.langmuir.7b01136.
Rizwan, S.B., Boyd, B.J., Rades, T., Hook, S., 2010. Bicontinuous cubic liquid crystals as sustained delivery systems for peptides and proteins. Expert Opin. Drug Deliv. 7, 1133–1144.
Round, A., Felisaz, F., Fodinger, L., Gobbo, A., Huet, J., Villard, C., Blanchet, C.E., Pernot, P., McSweeney, S., Roessle, M., Svergun, D.I., Cipriani, F., 2015. BioSAXS Sample Changer: a robotic sample changer for rapid and reliable high-throughput X-ray solution scattering experiments. Acta Crystallog. D Biol. Crystallogr. 71, 67–75.
Sánchez-Bautista, S., de Godos, A., Rodríguez-Alfaro, J.A., Torrecillas, A., Corbalán-García, S., Gómez-Fernández, J.C., 2007. Interaction of the C2 domain from protein kinase Cε with model membranes. Biochemistry 46, 3183–3192.
Schmiele, M., Busch, S., Morhenn, H., Schindler, T., Schmutzler, T., Schweins, R., Lindner, P., Boesecke, P., Westermann, M., Steiniger, F., Funari, S.S., Unruh, T., 2016. Structural characterization of lecithin-stabilized tetracosane lipid nanoparticles. part I: emulsions. J. Phys. Chem. B. 120, 5505–5512.
Shah, J.C., Sadhale, Y., Chilukuri, D.M., 2001. Cubic phase gels as drug delivery systems. Adv. Drug. Deliv. Rev. 47, 229–250.
Smaal, E.B., Nicolay, K., Mandersloot, J.G., de Gier, J., de Kruijff, B., 1987. ^{2}H NMR, ^{31}P-NMR and DSC characterization of a novel lipid organization in calcium-dioleoylphosphatidate membranes. Implications for the mechanism of the phosphatidate calcium transmembrane shuttle. Biochim. Biophys. Acta. 897, 453–466.
Uzqueda, M., Gonzalez-Gaitano, G., Wouessidjewe, D., Zornoza, A., Sanchez, M., Martin, C., Velaz, I., 2009. Spectroscopic characterisation of the inclusion complexes between the antifungal drugs naftifine and terbinafine and cyclodextrins. Supramol. Chem. 21, 759–769.
Wyatt, D.M., Dorschel, D., 1992. A cubic-phase delivery system composed of glyceryl monooleate and water for sustained release of water-soluble drugs. Pharm. Tech. 16, 116–130.
Yameogo, J.B.G., Geze, A., Choisnard, L., Putaux, J.-L., Gansane, A., Sirimad, S.B., Semde, R., Wouessidjewe, D., 2012. Self-assembled biotransesterified cyclodextrins as artemisinin nanocarriers – I: Formulation, lyoavailability and in vitro antimalarial activity assessment. Eur. J. Pharm. Biopharm. 80, 508–517.
Yohannes, G., Pystynen, K.-H., Riekkola, M.-L., Wiedmer, S.K., 2006. Stability of phospholipid vesicles studied by asymmetrical flow field-flow fractionation and capillary electrophoresis. Anal. Chim. Acta. 560, 50–56.
Zeng, N., Gao, X., Hu, Q., Song, Q., Xia, H., Liu, Z., Gu, G., Jiang, M., Pang, Z., Chen, H., Chen, J., Fang, L., 2012. Lipid-based liquid crystalline nanoparticles as oral drug delivery vehicles for poorly water-soluble drugs: cellular interaction and in vivo absorption. Int. J. Nanomed. 7, 3703–3718.
Zerkoune, L., Lesieur, S., Putaux, J.-L., Choisnard, L., Gèze, A., Wouessidjewe, D., Angelov, B., Vebert-Nardin, C., Doutch, J., Angelova, A., 2016. Mesoporous self-assembled nanoparticles of biotransesterified cyclodextrins and nonlamellar lipids as carriers of water-insoluble substances. Soft Matter. 12, 7539–7550.
Zhen, G., Hinton, T.M., Muir, B.W., Shi, S., Tizard, M., McLean, K.M., Hartley, P.G., Gunatillake, P., 2012. Glycerol monooleate-based nanocarriers for siRNA delivery in vitro. Mol. Pharm. 9, 2450–2457.

Supplementary Data

New nanoparticles obtained by co-assembly of amphiphilic cyclodextrins and nonlamellar single-chain lipids: Preparation and characterization.

Cảnh Hưng Nguyễn[a], Jean-Luc Putaux[b], Gianluca Santoni[c], Sana Tfaili[d], Sophie Fourmentin[e], Jean-Baptiste Coty[a], Luc Choisnard[f], Annabelle Gèze[f], Denis Wouessidjewe[f], Gillian Barratt[a], Sylviane Lesieur[a] and François-Xavier Legrand[a]

[a] Institut Galien Paris-Sud, CNRS UMR 8612, Univ. Paris-Sud, Université Paris-Saclay, 5 rue Jean-Baptiste Clément, F-92290 Châtenay-Malabry, France.

[b] Centre de Recherches sur les Macromolécules Végétales, CNRS UPR 5301, Université Grenoble Alpes, 601 rue de la chimie, F-38400 Saint-Martin-d'Hères, France

[c] European Synchrotron Radiation Facility, 71 avenue des Martyrs, F-38000 Grenoble, France.

[d] Lipides, Systèmes analytiques et Biologiques, EA 7357, Univ. Paris-Sud, Université Paris-Saclay, 5 rue Jean-Baptiste Clément, F-92290 Châtenay-Malabry, France.

[e] Unité de Chimie Environnementale et Interactions sur le Vivant, EA 4492, SFR Condorcet FR CNRS 3417, Université Littoral Côte d'Opale, 145 avenue Maurice Schumann, F-59140 Dunkerque, France.

[f] Département de Pharmacochimie Moléculaire, CNRS UMR 5063, Université Grenoble Alpes, 470 rue de la chimie, F-38400 Saint-Martin-d'Hères, France.

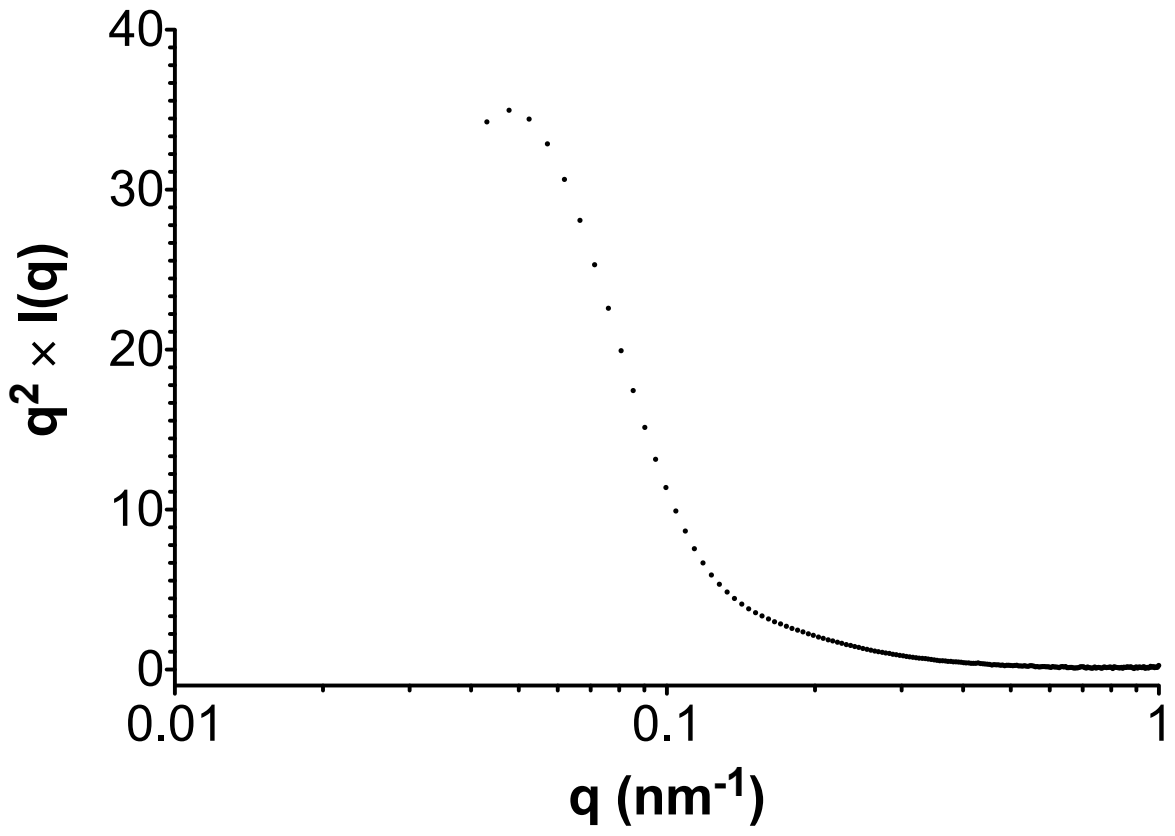

Figure S1. Kratly plot for β-CD-C_{10} nanoparticles.

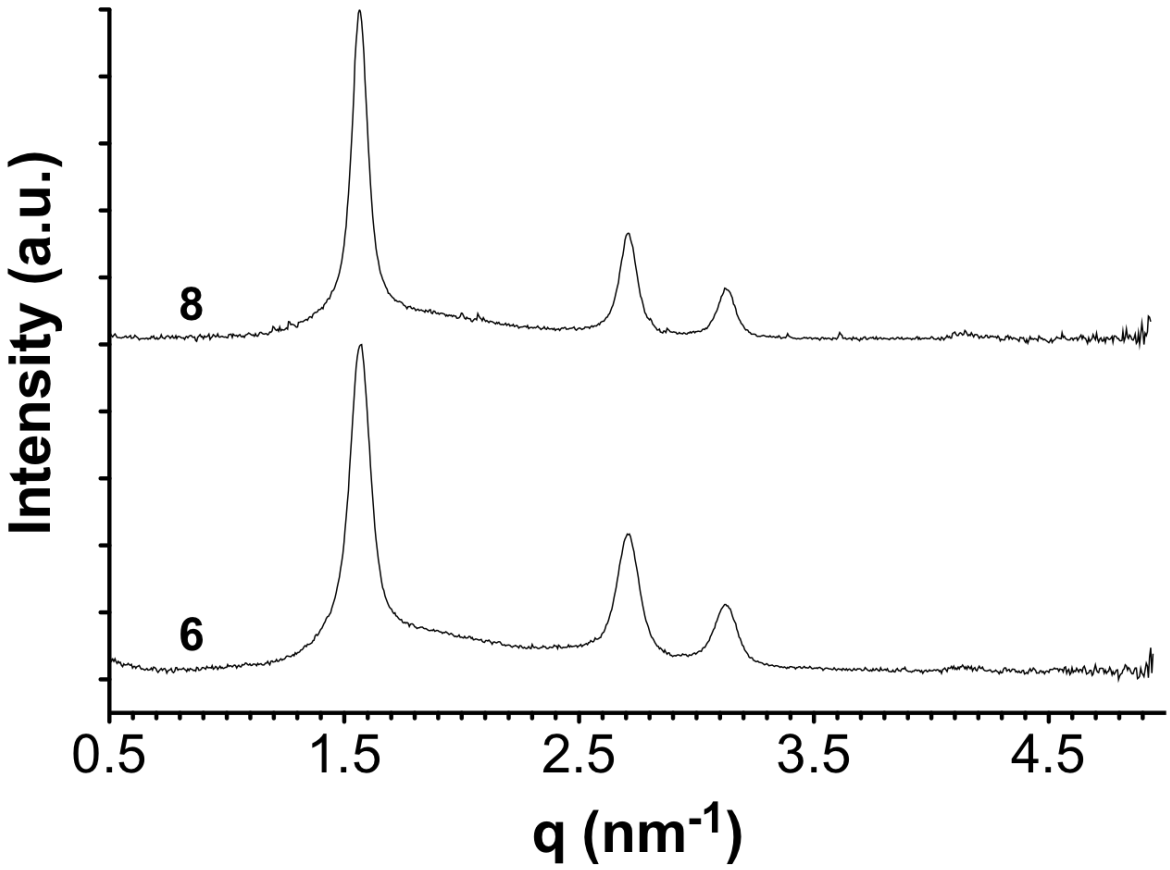

Figure S2. Comparison of SAXS profiles of β-CD-C_{10}/MO/DOPE-PEG_{2000} (49/49/2 mol%) nanoparticles prepared in pure water (6) and in 5% glucose (8).

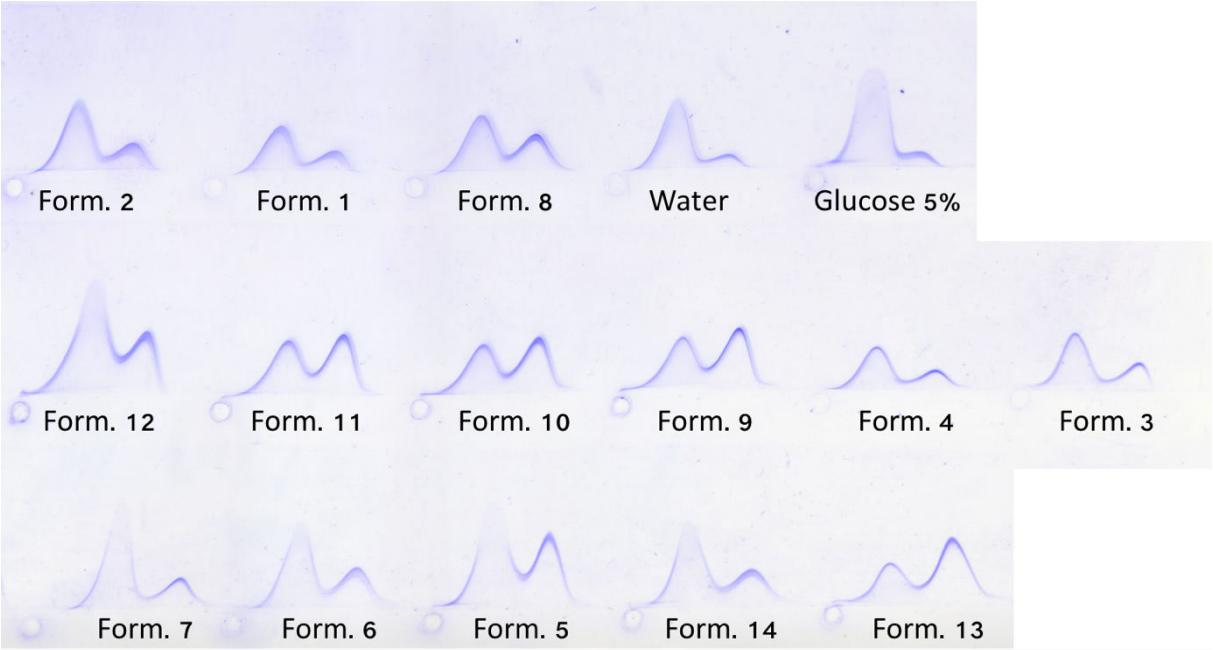

Figure S3. Electrophoregrams obtained by MultiCrossed-IE with the different formulations.

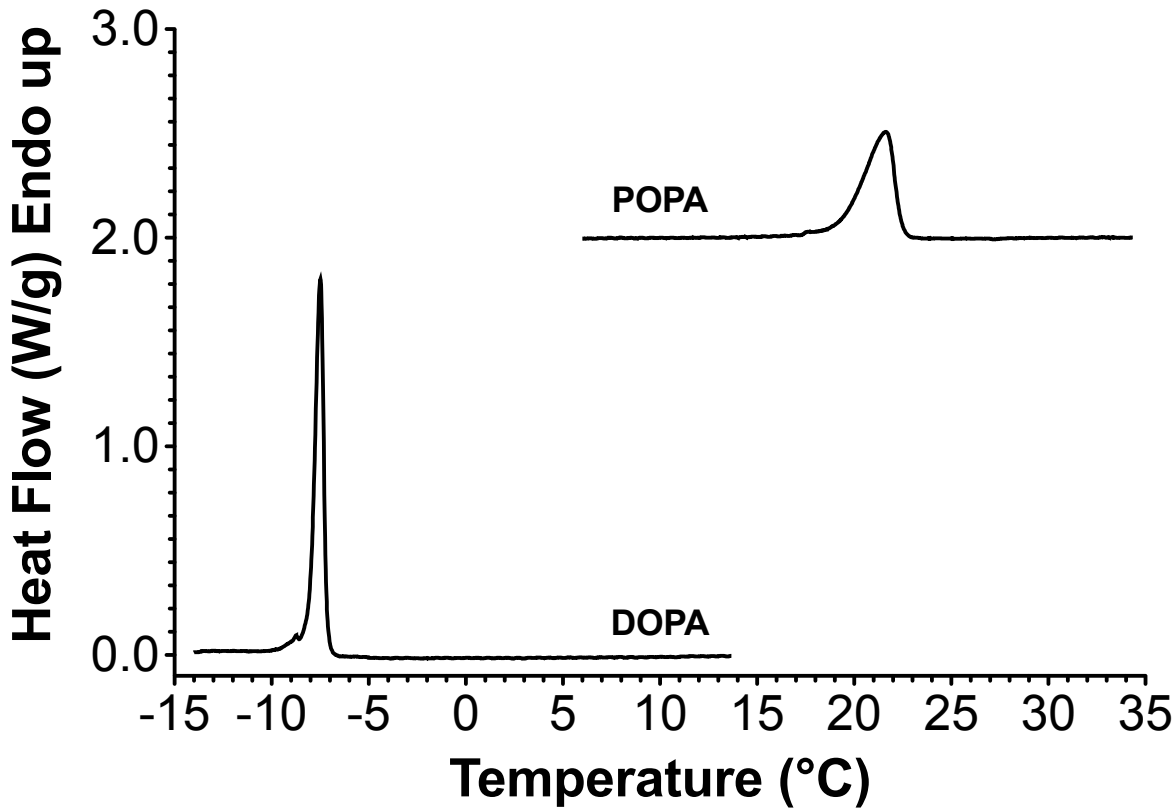

Figure S4. Differential scanning calorimetry (DSC) thermograms of hydrated DOPA and POPA (90 wt.%; heating rate of 2°C/min).

Phosphatidic Acid	T_{onset} (°C)	T_{end} (°C)	ΔH ($J.g^{-1}$)	ΔH ($kJ.mol^{-1}$)
DOPA	-8.2 ± 0.1	-7.6 ± 0.1	34.0 ± 2.0	24.6 ± 1.5
POPA	19.1 ± 0.2	22.0 ± 0.2	32.1 ± 1.8	22.4 ± 1.2

Table S1. Thermodynamic parameters of hydrated DOPA and POPA (90 wt.%).

Formulation	F1	F2	F3	F4	F5	F6	F7	F8
$d_{mean} = d_{1,0}$ (nm)	70	77	77	80	51	53	31	58
d_{median} (nm)	64	70	71	74	45	46	25	49
$d_{4,3}$ (nm)	84	91	88	89	69	77	39	105
$d_{6,5}$ (nm)	93	101	96	97	79	88	44	129
Q	0.050	0.056	0.043	0.047	0.060	0.061	0.051	0.092

Formulation	F9	F10	F11	F12	F13	F14
$d_{mean} = d_{1,0}$ (nm)	75	74	-	70	-	-
d_{median} (nm)	69	67	-	65	-	-
$d_{4,3}$ (nm)	99	91	-	95	-	-
$d_{6,5}$ (nm)	114	101	-	107	-	-
Q	0.075	0.047	-	0.059	-	-

Table S2. Diameters and polydispersity indexes deduced from TEM images.

Curriculum Vitae

Jean-Baptiste COTY

Né le 22/09/1991 (26 ans)

Nationalité : Français

Mail: coty.jb@gmail.com

Téléphone : +33 6 66 36 03 72

Langues parlées : Français (maternelle) – Anglais (courant) – Espagnol (Opérationnel)

Formation initiale :

- Oct 2014 - Présent : Thèse de doctorat à l'Institut Galien Paris Sud – UMR CNRS 8612 **– Développement de méthodes de caractérisation des interactions entre nanomédecines et protéines sanguines dans un contexte clinique (Consortium BPI France).**

- 2011- 2014 **Etudiant à l'Ecole Nationale Supérieure de Chimie Rennes (ENSCR).** Diplomé ingénieur chimiste, spécialisé en Analyse et Formulation

- 2009-2011 **: Classes préparatoires aux grandes écoles (PCSI, PC), à l'ENCPB Paris 13e.**

- Juin 2009 **: Baccalauréat Scientifique mention Bien, Lycée Condorcet de Limay (78).**

Expériences professionnelles :

- Oct 2014 - Oct 2017 : **Doctorat à l'Institut Galien Paris Sud – UMR CNRS 8612 –** Conduite de projet – Communications orales à audience internationale – Publications scientifiques – Collaborations – Interactions avec des partenaires industriels en phase clinique (Onxeo, Nanobiotix)

- Février-Août 2014 : Stage ingénieur chez **IPSEN Innovation** (Les Ulis), service Early Formulation (Réf. : Dr. Jennifer Dourlat) - *Mise au point de formulations orales/iv pour des peptides et molécules chimiques.*
Missions : proposition et étude de la stabilité de véhicules pour principes actifs, mise en place d'appareillages de caractérisation et recherche de nouvelles formulations

- Avril-Août 2013 : Stage dans le laboratoire de recherche du Pr. Molander (**University of Pennsylvania**, Philadelphie, USA) (Réf. : Pr. Gary A. Molander) - *Développement de nouvelles méthodes de synthèse.*
Missions : optimisation de conditions, HTE screening, synthèse et analyse de composés.

- Juin-Juillet 2012 : Stage ouvrier (6 semaines) chez **QUARON** (35) : *Conditionnement de produits chimiques destinés à l'industrie agroalimentaire. Aspects de sécurité(Site SEVESO II).*

Compétences :

Scientifiques : Développement pharmaceutique, Veille scientifique, Nanoparticules, Méthodes analytiques (CE, SPR, UPLC, RMN), Physico-chimie

Transversales :

Qualités de présentation (orale, écrite), Travail en équipe/collaboration, Management de projet, Capacités d'adaptation, d'organisation

Liste des publications:

Articles publiés:

- **Coty, J.-B.**, Varenne, F., Vachon, J.-J. & Vauthier, C. Serial multiple crossed immunoelectrophoresis at a microscale: A stamp-sized 2D immunoanalysis of protein C3 activation caused by nanoparticles: Proteomics and 2-DE. *ELECTROPHORESIS* **37,** 2401–2409 (2016).
- **Coty, J.-B.,** Eleamen Oliveira, E. & Vauthier, C. Tuning complement activation and pathway through controlled molecular architecture of dextran chains in nanoparticle corona. *International Journal of Pharmaceutics* **532**, 769-778 (2017).
- Nguyễn, C. H., Putaux, J.-L., Santoni, G., Tfaili, S., Fourmentin, S., **Coty, J.-B.**, Choisnard, L., Gèze, A., Wouessidjewe, D., Barratt, G., Lesieur, S. & Legrand, F.-X. New nanoparticles obtained by co-assembly of amphiphilic cyclodextrins and nonlamellar single-chain lipids: Preparation and characterization. *International Journal of Pharmaceutics* **531**, 444-456 (2017).
- Varenne, F., Rustique, E., Botton, J., **Coty, J.-B.**, Lanusse, G., Ait Lahcen, M., Rio, L., Zandanel, C., Lemarchand, C., Germain, M., Negri, L., Couffin, A.-C., Barratt, G. & Vauthier, C. Towards quality assessed characterization of nanomaterial: Transfer of validated protocols for size measurement by dynamic light scattering and evaluation of zeta potential by electrophoretic light scattering. *International Journal of Pharmaceutics* **528,** 299–311 (2017).

Articles en preparation:

- **Coty, J.-B.** & Vauthier, C. A thought about the characterization of nanomedicines: a field under construction between regulatory and methodological aspects needed to accelerate clinical developments. Article in preparation.
- **Coty, J.-B.**, Noiray, M. & Vauthier, C. Assessment of complement activation by nanoparticles as a quality requirement: development of a SPR based method and comparison with current high throughput methods. Article in preparation.
- **Coty, J.-B.**, Varenne, F., Garsaa, O., Lepotier, I., Smadja, C., Taverna, M. & Vauthier, C. Sharp characterization of nanomedicines' surface with molecular probes by capillary electrophoresis: towards understanding and evaluation of surface coverage. Article in preparation.
- Marcelino, H.R., **Coty, J.-B.**, Chéron, M., Vauthier, C., Egito, E.S.T. & Ponchel G. Amphotericin B and bovine serum albumin interactions: Physicochemical characterization and in vitro immunogenic activity. Article in preparation.
- Palácio, S.B, Taylor Sarahi, A.Y., **Coty, J.-B.**, Egidy, G., Vauthier, C. & Ponchel, G. Functionalized Poly(γ-benzyl-L-glutamate)-PEG-Bt-MART-1 nanoparticles for melanoma targeting. Article in preparation.
- Taylor Castillo, A.Y., Papagna, F., **Coty, J.-B.**, Khoubai, F.Z., Vergnaud, J., Vauthier, C., Martinez Barbosa, M.E. & Ponchel, G. Rational designed Poly(γ-benzyl-L-glutamate) nanoparticles for nanomedicine applications in cancer treatment. Article in preparation.

Liste des communications:

Communications orales:

- **Congrès SF Nano 16** (décembre 2016): Development of a high throughput immunoelectrophoresis for the characterization of complement activation by nanomedicines. **Coty, J.-B.**, Varenne, F., Vachon, J.-J. & Vauthier, C.

- **Congrès Clinam 16** (27-29 juin 2016) – Short talk: Activation of complement system by nanomedicines: Development of a multi-crossed micro-immunoelectrophoresis and application to the determination of complement activation at 50% by nanoparticles. **Coty, J.-B.**, Varenne, F., Vachon, J.-J. & Vauthier, C.

- Doc and Post-Doc day Institut Galien 2016 (juin 2016)**:** Activation of complement system by nanomedicines: Development of a high throughput method and determination of an indicator of activation. **Coty, J.-B.**, Varenne, F., Vachon, J.-J. & Vauthier, C.

Communications posters:

- **Journée de la recherche 2016 – Faculté de Pharmacie de Chatenay-Malabry** : Characterization of nanomedicine's surface via molecular probes – Development of a capillary electrophoresis method. **Coty, J.-B.**, Varenne, F., Le Potier, I., Smadja, C. & Vauthier. C.

- **Congrès Clinam 16** (27-29 juin 2016) : Development of multi-crossed micro-immunoelectrophoresis and application to the determination of complement activation at 50% by nanoparticles. **Coty, J.-B.**, Varenne, F., Vachon, J.-J. & Vauthier, C.

- **Journée de l'école doctorale 569** (17 juin 2016): Development of a serial Multi-Crossed immunoelectrophoresis: Application to the study of complement activation by nanoparticles. **Coty, J.-B.**, Varenne, F., Vachon, J.-J. & Vauthier, C.

- **Rencontres de Nanométrologie 2016:** Développement d'une méthode de caractérisation à haut débit des interactions nanomatériaux-système du complément. **Coty, J.-B.**, Varenne, F., Vachon, J.-J. & Vauthier, C.

- **Ecole d'été ULLA 2015:** Characterization of polymer nanoparticles nanomedicines: which properties and which methods? **Coty, J.-B.**, Varenne, F. & Vauthier, C.

- **Doc and Post-Doc day Institut Galien 2015** (juin 2015): Biological interactions of polymer nanomedicines with blood components – Development of methods for a routine characterization. **Coty, J.-B.**, Varenne, F., Noiray, M. & Vauthier, C.

Title : Nanomedicine characterization for the clinics: development of methods evaluating the interactions nanoparticles-plasmatic proteins for a quality control purpose

Keywords : Nanomedicine - Clinics - Characterization – Surface architecture – Blood proteins – Complement system

Abstract : Nanomedicines injected intravenously interact with surrounding biological elements in the bloodstream. Among these interactions, those with blood proteins turn out to be very important regarding the becoming of the nanovectors. They acquire a biological identity upon interaction with proteins which influence their path to target tissue and cells. The understanding and mastering of these phenomena remains a crucial issue in nanomedicine development. Methods allowing an easier study of these interactions are needed. The aim of these PhD thesis was to develop such methods, usable on a routine basis in a clinical context, allowing a fine characterization of nanomedicines and their interactions with plasmatic proteins. This PhD is part of the project "Nano Innovation for CancEr" (NICE, BPI France), gathering a consortium of industrials partners developing clinical nanomedicines.

In a first time, a bibliographic study about current methods used for such a characterization could identify two major limitations. (i) On one hand, the complexity of current available methods for which the equipment specificity and required expertise prevent their use at a large scale. (ii) On the other hand, properties today characterized on a daily basis (size, morphology, charge) are too rough compared to the sharpness of biological processes who interact and "analyze" the nanovectors introduced in biological media. These two aspects are limiting a safer development of nanomedicines as well as a good reproducibility of their action in clinics.

During this thesis, we developed methods allowing a beginning of answer to the wide problematic of nanomedicine characterization. A method for a high throughput analysis of complement activation by nanomedicines via 2D immunoelectrophoresis was developed and validated. It allows the reproducible analysis of protein C3 fragmentation. This method is applicable to the study of the impact of nanoparticles in human serum and their degree of action on the complement cascade. This method has been used for a more fundamental study on complement activation pathways activated according to the architecture of nanoparticles surface.

A second method for the study of complement activation produced by nanoparticles has been proposed using surface plasmon resonance (SPR). A chip allowing an automated screening of complement activation has been developed. This method was compared to other methods for complement activation study (2D immunoelectrophoresis, ELISA) and allowed the identification of bias during nanomedicine evaluation.

Finally, an original approach for the characterization of nanomedicine's surface architecture using proteins as molecular probes has been proposed. In this method, capillary electrophoresis has been used as analytical tool to allow a direct analysis of sample without preliminary nanoparticle removal step.

Methods developed during this work can be applied to the characterization of nanomedicines and proposed as routine methods for quality control. A development of nanomedicines characterization in this direction constitute one of the lever for a more fruitful translation of nanomedicines entering in clinical phase.

Titre : Caractérisation des nanomédecines pour la clinique : développement de méthodes évaluant les interactions nanoparticules-protéines plasmatiques pour une application en contrôle qualité

Mots clés : Nanomédecines - Clinique - Caractérisation - Conformation de surface - Protéines plasmatiques - Système du complément

Résumé : Les nanomédecines injectées par voie intraveineuse interagissent avec les éléments biologiques qui les entourent dans le compartiment sanguin. Parmi ces interactions, celles avec les protéines sanguines se révèlent être très importantes dans le devenir de ces nanovecteurs, leur conférant une identité biologique influençant leur chemin jusqu'au tissu et aux cellules cibles. La compréhension et le contrôle de ces phénomènes reste un enjeu crucial dans le développement des nanomédecines. Des méthodes permettant une étude facilitée de ces interactions sont nécessaires à cet égard. Les travaux de cette thèse ont eu pour but de développer des méthodes, utilisables en routine, permettant une caractérisation fine des nanomédecines et de leurs interactions avec les protéines plasmatiques, applicables dans un contexte clinique. Ils s'inscrivent dans un projet intitulé « Nano Innovation for CancEr » (NICE, BPI France) regroupant un consortium de partenaires industriels en développement clinique de nanomédecines.

Dans un premier temps, un travail bibliographique sur les méthodes actuellement mises en œuvre pour une telle caractérisation ont pu mettre en avant deux limitations majeures. (i) D'une part, la complexité des méthodes actuelles disponibles pour lesquelles la spécificité des équipements et l'expertise requise limitent une utilisation à large échelle. (ii) D'autre part, les propriétés aujourd'hui caractérisées en routine (taille, morphologie globale, charge) ne sont que grossières comparées à la finesse des processus biologiques qui interagissent et « analysent » les nanovecteurs une fois introduits dans le milieu biologique. Ces deux aspects limitent aujourd'hui un développement plus sûr des nanomédecines pour une bonne reproductibilité en clinique et garantir des essais de contrôle qualité fiables.
Au cours de nos travaux, nous avons développé des méthodes permettant de répondre en partie à la problématique posée par la caractérisation des nanomédecines. Une méthode d'analyse à haut débit de l'activation du système du complément par immunoélectrophorèse en deux dimensions a été développée et validée. Elle permet l'analyse reproductible de l'activation de la protéine C3. Elle est applicable à l'étude de l'effet de la présence de nanoparticules dans le sérum humain et leur degré d'action sur la cascade du complément. Cette méthode a été utilisée pour mener une étude plus fondamentale du mécanisme de l'activation du système du complément en regard de l'architecture de la surface de nanoparticules.

Une deuxième méthode d'étude de l'activation du complément produit par des nanomédecine a été proposée sur la base de la résonnance plasmonique de surface (SPR). Une puce permettant un screening automatisé de l'activation du complément a été développée. L'application de cette méthode comparée à d'autres méthodes d'études de l'activation du système du complément (Immunoélectrophorèse 2D, ELISA) a permis d'identifier des biais lors de leur application à l'évaluation des nanomédecines. Enfin, une approche originale de caractérisation de la surface de nanoparticules a été proposée utilisant des protéines pour sonder la capacité de la surface des nanoparticules à adsorber ou repousser ces dernières. Dans cette méthode, l'électrophorèse capillaire est utilisée comme outil analytique permettant une analyse directe de l'échantillon sans séparation préalable des nanomédecines.

Les méthodes développées au cours de ces travaux peuvent être appliquées à la caractérisation de nanomédecines et proposées comme des méthodes de contrôle en routine de façon plus générale. Un développement de la caractérisation dans ce sens constitue l'un des leviers pour une translation plus fructueuse des nanomédecines entrant en phase clinique.

Université Paris-Saclay
Espace Technologique / Immeuble Discovery
Route de l'Orme aux Merisiers RD 128 / 91190 Saint-Aubin, France